DISSERTATION

A METABOLOMICS APPROACH FOR EXAMINING SYNBIOTIC PROTECTION AGAINST INFECTIOUS ENTERIC PATHOGENS

Submitted by

Nora Jean Nealon

Graduate Degree Program in Cell and Molecular Biology

In partial fulfillment of the requirements

For the Degree of Doctor of Philosophy

Colorado State University

Fort Collins, Colorado

Summer 2019

Doctoral Committee:

Advisor: Elizabeth P. Ryan

Gregg Dean
Charles Henry
Stuart Tobet

ABSTRACT

A METABOLOMICS APPROACH FOR EXAMINING SYNBIOTIC PROTECTION AGAINST INFECTIOUS ENTERIC PATHOGENS

Gastrointestinal pathogens are responsible for disease in billions of people annually. *Salmonella enterica* serovar Typhimurium and human rotavirus represent two human health challenges, where escalating multidrug resistance and poor vaccine efficacy warrant the development of alternative treatments. Health-promoting probiotic microorganisms are becoming increasingly studied for their production of bioactive small molecules that confer protective effects against enteric pathogens. Among probiotics, *Lactobacilli*, *Bifidobacteria* and *E. coli* Nissle form synbiotics with rice bran, the prebiotic-rich outer coating of brown rice, to enhance animal protection against *S.* Typhimurium infection and human rotavirus diarrhea compared to probiotics or rice bran alone. Despite the beneficial interactions of probiotics and rice bran, there is a knowledge gap in understanding how synbiotic small molecules drive these protective effects, especially across probiotic species.

To test our overarching hypothesis that probiotic species would metabolize rice bran into distinct suites of small molecules that suppressed pathogen function, we first applied the cell-free supernatant from *L. paracasei*, *L. fermentum*, and *L. rhamnosus* cultured with rice bran to *S.* Typhimurium and observed magnitude-dependent growth suppression across synbiotics. Both *L. paracasei* and *L. fermentum* supernatants exhibited enhanced growth suppression compared to their probiotic-only treatments and contained differentially abundant antimicrobial lipids, amino acids, and nucleotides that have not been previously characterized for antimicrobial functions.

The cell-free supernatant of the *L. paracasei* and *L. fermentum* synbiotics were fractionated and applied to *S.* Typhimurium to identify the small molecules driving their enhanced *Salmonella* growth suppression. Metabolite profiles were also compared across synbiotics. Each synbiotic produced several bioactive fractions that suppressed *Salmonella* growth. While both *L. fermentum* and *L. paracasei* bioactive fractions contained abundant lipids, *L. fermentum* fractions were selectively-enriched in the energy metabolite fumarate and *L. paracasei* fractions were uniquely-enriched with amino acids (imidazole lactate, ornithine) suggesting that *Lactobacillus* spp. probiotics could differentially metabolize rice bran to drive *Salmonella* growth suppression with different suites of small molecules.

To examine probiotic metabolism of rice bran in mammalian systems, we compared the intestinal and blood metabolomes of healthy adult mice and gnotobiotic, neonatal pigs that were fed combinations of probiotics and rice bran to the metabolomes of animals consuming rice bran or probiotics alone. In mice, a notable difference following 15 weeks consumption of *B. longum* fermented was that the arginine metabolite N-delta-acetylornithine was significantly increased in *B. longum* fermented rice bran compared to rice bran alone and was elevated in both the colon tissue and blood of mice consuming fermented rice bran compared to rice bran alone. In gnotobiotic neonatal pigs, three weeks of prophylactic supplementation with *E. coli* Nissle and *L. rhamnosus* GG and rice bran were more effective at reducing human rotavirus diarrhea compared to pigs given these probiotics or rice bran alone. Approximately 300 colon and blood metabolites that were differentially-abundant between synbiotic-consuming pigs versus pigs consuming probiotics alone were identified, over 50% of which were lipids and amino acids.

Similar modulations lipid and amino acid metabolites (sphingolipids, diacylglycerols, arginine metabolites) were identified in the colon tissue and blood of mice and pigs consuming

the synbiotic treatments. Consequently, the association of these metabolite profiles with human rotavirus diarrhea protection, when combined with their presence in two mammalian models, provides strong rationale for these infectious enteric disease protective roles harbored by these metabolites.

The results of these studies provide a role for synbiotics in the prevention of infectious gastrointestinal diseases. For the first time, high-throughput metabolomics analyses were applied to identify differential bioactive metabolite production by *Lactobacillus* spp. + rice bran synbiotics that suppressed *S.* Typhimurium growth, as well as to compare bioactive metabolites produced by *B. longum, L. rhamnosus* GG, and *E. coli* Nissle in mice and pigs that were protective against human rotavirus diarrhea. The contributions of amino acids and lipids to the enhanced capacities of these synbiotics compared to probiotics or rice bran alone can be studied further for their mechanisms of action on pathogens. Ultimately, these bioactive synbiotic metabolites can guide the optimization and development of broad-spectrum antimicrobials and other prophylactic agents that protect against infectious enteric diseases across the human and animal lifespan.

ACKNOWLEDGEMENTS

I would like to thank my graduate adviser Dr. Elizabeth Ryan and my doctoral committee members Dr. Gregg Dean, Dr. Chuck Henry, and Dr. Stuart Tobet for their support throughout my graduate studies, including funding for this research and training provided by Dr. Elizabeth Ryan. I also wish to extend my sincerest gratitude to the Colorado State University DVM/PhD program for their financial support, including its directors Dr. Edward Hoover, Dr. Susan VandeWoulde and Dr. Justin Lee. Many thanks also go to our long-time collaborators Dr. Lijuan Yuan, Dr. Samuel Vilchez, Dr. Joy Scaria, and Dr. Linto Antony for their constructive feedback across projects. This thesis was made successful also due to Dr. Genevieve Forster, Amethyst Holder, Colette Worcester, Hannah Haberecht, Shea Boyer, and Paige Lahaie for their patience, infectiously positive energy, and enthusiasm while working alongside me on research projects and publications, and for the many happy memories we have made while growing as future scientists, medical doctors, and health professionals. Most importantly, I would also like to thank my family including my parents Nora and Donald Nealon, my sister Tara Hodson, my brother-in-law Thomas Hodson, my Grandmother Jean Nealon, and my Aunts Anne Grande and Susie Nealon for their constant love and encouragement, and their confidence in my ability to succeed. Finally, I want to recognize my multiple pets including my west-highland white terriers Mr. McDuff and Sir Winston, my incredibly large goldfish Goldie, my painted turtles Squirt, Crush, and Pancake, and of course the many cats who have “adopted” me over the years and provided company as I applied for veterinary school, spent long nights studying, and sat patiently purring nearby as I wrote my dissertation: Jellybean, Squeaker, Gunner, Richard Parker, John Dorian, Denise and Garfunkel.

TABLE OF CONTENTS

LIST OF TABLES

Chapter 1:

No Tables

Chapter 2:

Chapter 3:

Chapter 4:

Chapter 5:

Chapter 6:

Chapter 7:

No Tables

Appendix:

LIST OF FIGURES

Chapter 1:

Chapter 2:

Chapter 3:

Chapter 4:

Chapter 5:

Chapter 6:

Appendix:

LIST OF PUBLICATIONS

Articles:

1. Forster, G.M.*, **Nealon, N.J.***, Hill, D., Jensen, T.D., Stone, T.L., Bauer, J.E., and Ryan, E.P. *Navy bean and black bean-based dog foods are digestible during weight loss in overweight and obese companion dogs*. Journal of Applied Animal Nutrition. 4:e4. April 2016. ***Co-first authors.**

2. Nealon, N.J., Yuan, L., Yang, X., and Ryan, E.P. *Rice Bran and Probiotics Alter the Porcine Large Intestine and Serum Metabolomes for Protection against Human Rotavirus Diarrhea*. Frontiers in Microbiology. 8(653):eCollection. April 2017.

3. Nealon, N.J.*, Worcester, C.R.*, and Ryan, E.P. *Lactobacillus paracasei metabolism of rice bran reveals metabolome associated with Salmonella Typhimurium growth production*. Journal of Applied Microbiology. 122:1639-1656. June 2017. ***Co-first authors**

4. Rubinelli, P.M., Kim, S.A., Park, S.H., Roto, S.M., **Nealon, N.J.**, Ryan, E.P., Ricke, S.C. *Differential effects of rice bran cultivars to limit Salmonella Typhimurium in chicken cecal in vitro incubations and impact on the cecal microbiome and metabolome*. PLoS One. 12(9):e0185002. September 2017.

5. Borresen, E.C., Zhang, L., Trehan, I., **Nealon, N.J.**, Maleta, K.M., Manary, M.J., and Ryan, E.P. *The Nutrient and Metabolite Profile of 3 Complementary Legume Foods with Potential to Improve Gut Health in Rural Malawian Children*. Current Developments in Nutrition. 1(10):e001610. September 2017.

6. Zarei, I., Brown, D.G., **Nealon, N.J.**, and Ryan, E.P. *Rice Bran Metabolome Contains Amino Acids, Vitamins & Cofactors, and Phytochemicals with Medicinal and Nutritional Properties*. Rice. 10(1):24. December 2017.

8. Haberecht, H.B.*, **Nealon, N.J**.*, Gilliand, J., Holder, A., Runyan, C., Oppel, R., Ibrahim, H., Mueller, L., Schrupp, F., Vilchez, S., Antony, L., Scaria, J., and Ryan, E.P. *Antimicrobial Resistant Escherichia coli from Environmental Waters in Northern Colorado*. Journal of Environmental and Public Health. January 2019. ***Co-first authors**

9. Schwertfedger, L.A., **Nealon, N.J.**, Ryan, E.P., and Tobet, S.A. *Human Colon Function Ex Vivo: Dependence on Oxygen and Sensitivity to Antibiotic*. PLoS One. May 2019.

Book chapter:

1. Nealon, N.J. and Ryan, E.P. Rice Bran. Chapter 4. *Rice*. In: *Whole Grains and Their Bioactives.* Edition 1. Hoboken, N.J.: Wiley, 2019. Edited by: Johnson, J. and Wallace, T. C.

Abstracts:

National:

1. Nealon, N.J., Trébillod, G., Stockman, J., and Ryan, E.P. *Dietary intervention with rice bran and navy beans for modulation of apparent total-tract digestibility and the gut microbiome during chemotherapy: A pilot study in client-owned dogs*. 18th Annual American Academy of Veterinary Nutrition Clinical Nutrition and Research Symposium. Seattle, WA. June 6, 2018. (Poster).

2. Nealon, N.J., Haberecht, H.B., and Ryan, E.P. *A role for synbiotics in the protection against enteric diseases. Keystone Symposium on Antimicrobials and Resistance: Opportunities and Challenges*. Santa Fe, NM. October 31, 2017. (Poster).

3. Nora Jean Nealon, Colette R. Worcester, & Elizabeth P. Ryan. *The Lactobacillus metabolome reveals species-level differences in the production of bioactive molecules important to animal and human gastrointestinal health.* American Academy of Veterinary Nutrition: 17th Annual Clinic Nutrition and Research Symposium. National Harbor, MD, June 7, 2017. (Oral Presentation).

4. Nealon NJ, Yuan L, and Ryan EP. *Rice bran and probiotics alter the porcine metabolome for enhanced protection against Human Rotavirus diarrhea.* 16th Annual AAVN Clinical Nutrition and Research Symposium. Denver, CO. June 8, 2016. (Poster).

5. Nealon NJ, Yuan L, and Ryan EP. *Probiotic metabolism of rice bran promotes novel metabolite profiles for antimicrobial activity.* 55th Annual Meeting of the Society of Toxicology. New Orleans, LA. March 16, 2016. (Poster).

Regional:

1. N.J. Nealon, K.D. Parker, P. Lahaie, H. Ibrahim, A.K. Maurya, K. Raina, and E.P. Ryan. *Host and gut microbial metabolism of Bifidobacterium longum-fermented rice bran in healthy mice and bioavailability of and cancer-protective compounds*. Front Range Microbiome Symposium. Fort Collins, CO. April 19, 2019. (Oral Presentation).

2. N.J. Nealon, K.D. Parker, P. Lahaie, H. Ibrahim, A.K. Maurya, K. Raina, and E.P. Ryan. *Host and gut microbial metabolism of Bifidobacterium longum-fermented rice and rice bran in healthy mice for identification of colorectal cancer-protective metabolites*. Cellular and Molecular Oncology Conference. Colorado University. Boulder, CO. March 4, 2019. (Poster).

3. Nora Jean Nealon, Shea M. Boyer, Hannah B. Haberecht, and Elizabeth P. Ryan. *A Metabolomics Approach for Understanding Synbiotic Growth Suppression of Antimicrobial Resistant Salmonella Typhimurium*. American Society of Microbiology. Fort Collins, CO. November 10, 2018. (Oral Presentation).

4. Nora Jean Nealon, Shea M. Boyer, Hannah B. Haberecht, and Elizabeth P. Ryan. A *Metabolomics Approach for Understanding Synbiotic Growth Suppression of Antimicrobial Resistant Salmonella Typhimurium*. Colorado Biological Mass Spectrometry Society. Aurora, CO. July 19, 2018. (Oral Presentation).

5. Nealon NJ, Yuan L, and Ryan EP. *Rice bran and probiotics alter the porcine metabolome for enhanced protection against Human Rotavirus diarrhea.* 2016 Second Annual Front Range Computational and Systems Biology Symposium. Fort Collins, CO. July 25, 2016. (Poster).

Local/Intra-University:

1. N.J. Nealon, K.D. Parker, P. Lahaie, H. Ibrahim, A.K. Maurya, K. Raina, and E.P. Ryan. *Host and gut microbial metabolism of Bifidobacterium longum-fermented rice and rice bran in healthy mice for identification of colorectal cancer-protective metabolites*. CMB-BMB-MCIN Poster Symposium. Colorado State University. Fort Collins, CO. February 22, 2019 (Poster).

2. Nora Jean Nealon, Shea M. Boyer, Hannah B. Haberecht, and Elizabeth P. Ryan. *Lactobacillus spp. Differentially Metabolize Rice Bran to Suppress Antimicrobial Resistant Salmonella Growth*. College of Veterinary Medicine and Biomedical Science Annual Research Day, CSU. Fort Collins, CO. January 26, 2019. (Oral Presentation).

3. Nora Jean Nealon, Shea M. Boyer, Hannah B. Haberecht, and Elizabeth P. Ryan. *Rice bran differentially modulates Lactobacillus spp. growth suppression of antimicrobial resistant Salmonella Typhimurium*. Graduate Student Showcase, CSU. Fort Collins, CO, November 13, 2018. (Poster).

4. Nealon, N.J., Trébillod, G., Stockman, J., and Ryan, E.P. *Dietary intervention with rice bran and navy beans for modulation of apparent total-tract digestibility and the gut microbiome during chemotherapy: A pilot study in client-owned dogs*. CMB-BMB-MCIN Poster Symposium. Fort Collins, CO. February 23, 2018. (Poster).

5. Nora Jean Nealon, Hannah Haberecht, and Elizabeth P. Ryan. *Fractionation of probiotic-fermented rice bran to identify salmonella-growth inhibitory compounds*. College of Veterinary Medicine and Biomedical Science Annual Research Day, CSU. Fort Collins, CO, January 20, 2018. (Oral Presentation).

6. Nora Jean Nealon, Colette R. Worcester, & Elizabeth P. Ryan. "*The Lactobacillus metabolome reveals species-level differences in the production of bioactive molecules*". Graduate Student Showcase, CSU. Fort Collins, CO, November 9, 2017. (Poster).

7. Nora Jean Nealon. *You are what your probiotics eat: Using rice bran to improve gut protection against infectious diseases*. Colorado State University Vice President for Research Three Minute Thesis Challenge, CSU. Fort Collins, CO, February 13, 2017. (Oral Presentation).

8. Nora Jean Nealon, Colette R. Worcester, & Elizabeth P. Ryan. *The Lactobacillus metabolome reveals species-level differences in the production of bioactive molecules*. College of Veterinary Medicine and Biomedical Science Annual Research Day, CSU. Fort Collins, CO, January 28, 2017. (Poster).

9. Nora Jean Nealon, Colette R. Worcester, and Elizabeth P. Ryan. *The Lactobacillus metabolome reveals species-level differences in the production of bioactive molecules.* Colorado State University Graduate Student Showcase, CSU. Fort Collins, CO, November 15, 2016. (Poster).

10. Nealon NJ, Worcester CW, and Ryan EP. *Probiotic Metabolism of Rice Bran Promotes Novel Metabolite Profiles for Antimicrobial Activity against Salmonella enterica serovar Typhimurium.* CSU Ventures Innovation Symposium, CSU. Fort Collins, CO, April 27, 2016. (Poster).

11. Nealon NJ, Yuan L, Brown DG, and Ryan EP. *Rice bran in the presence and absence of probiotics differentially alters the porcine large intestinal and serum metabolome for enhanced protection against human rotavirus infection.* CMB/MCIN/BMB Spring Poster Symposium, CSU. Fort Collins, CO, February 2016. (Poster).

12. Nealon NJ, Yuan L, Brown DG, and Ryan EP. *Rice bran in the presence and absence of probiotics differentially alters the porcine large intestinal and serum metabolome for enhanced protection against human rotavirus infection.* CVMBS Annual Research Day, CSU. Fort Collins, CO, January 30, 2016. (Poster).

13. Nealon NJ, Worcester C, & Ryan EP. *Rice bran extracts enhance the antimicrobial activity of Lactobacillus spp. against Salmonella typhimurium in-vitro.* Graduate Student Showcase, CSU. Fort Collins, CO, November 11, 2015. (Poster).

14. Nealon NJ, Forster GM, & Ryan EP. *Dry bean (Phaseolus vulgaris) consumption supports long-term weight loss in companion dogs.* American Animal Hospital Association (AAHA) Accreditation Research Mixer. CSU. Fort Collins, CO, April 11, 2015. (Poster).

15. Nealon NJ, Forster GM, & Ryan EP. *Dry bean (Phaseolus vulgaris) consumption supports long-term weight loss in companion dogs.* CVMBS Annual Research Day, CSU. Fort Collins, CO, January 31, 2015. (Poster).

CHAPTER ONE

INTRODUCTION[1]

1.1. Overview of the global burden of infectious gastrointestinal diseases:

Infectious gastrointestinal diseases of bacterial and viral origin cause an estimated one billion diarrheal episodes in people annually and are additionally responsible for 760,000 deaths in children under five (WHO, 2013). Among pathogenic bacteria, the World Health Organization reports non-typhoidal *Salmonella* as one of the leading global causes of foodborne diarrhea (WHO, 2016). The serotype most commonly identified in these outbreaks is *Salmonella enterica* serovar Typhimurium, a highly transmissible zoonotic agent that causes severe gastroenteritis in humans and animals and which is frequently implicated in spreading through food systems (Donado-Godoy *et al.*, 2014; Iannino *et al.*, 2015; Kemppainen *et al.*, 2017; Peng *et al.*, 2016). Escalating antimicrobial resistance makes preventing and containing *S.* Typhimurium outbreaks increasingly difficult due to the healthcare risks it poses (Adler *et al.*, 2016). In a 2013 analysis conducted by the Center for Disease Control, approximately 100,000 Americans presenting for hospitalization with *S.* Typhimurium were infected with a multidrug resistant strain, and 5% of these strains were resistant to five or more drugs (CDC, 2018a). Antimicrobial-resistant infections, especially in Gram-negative bacteria like *S.* Typhimurium, lead to an increased risk of prolonged disease and pathogen transmission to others, long-term health complications to infected individuals, and potential septic shock due to the lipopolysaccharide constituents present

[1]**Section 1.3. is an excerpt from: Nealon, N.J.** and Ryan, E.P. Rice Bran. Chapter 4. *Rice*. In: *Whole Grains and Their Bioactives.* Edition 1. Hoboken, N.J.: Wiley, 2019. Edited by: Johnson, J. and Wallace, T. C

in the cell walls of Gram-negative bacteria (Chlebicz and Slizewska, 2018; He *et al.*, 2013; Michael and Schwarz, 2016; Muller-Loennies *et al.*, 2007). These factors in turn can increase healthcare associated costs associated with Salmonellosis, impair efforts to contain the outbreak, and can contribute to food insecurity if it spreads through agricultural, poultry, and livestock markets (Diarra *et al.*, 2014; Florez-Cuadrado *et al.*, 2018; Founou *et al.*, 2018; He *et al.*, 2013; Holschbach and Peek, 2018; Mhongole *et al.*, 2017; Peng *et al.*, 2016; Schwartz and Morris, 2018).

Along with infectious bacteria, human rotavirus is the leading cause of severe childhood diarrhea in developing countries (Yang *et al.*, 2014). To date, two attenuated multivalent oral vaccines, Rotarix and Rotateq, have been tested in human clinical trials (Sadiq *et al.*, 2018). Although these vaccines successfully attenuated human rotavirus diarrheal severity and disease duration, they exhibited decreased efficacy in developing countries where they are coincidentally the most needed (Willame *et al.*, 2018). Given the global burden of infectious enteric pathogens, there is a need for broad-spectrum preventive and treatment strategies that are effective at preventing and treating disease caused by antimicrobial-resistant bacteria and viruses.

1.2. Probiotics for gastrointestinal health promotion and infectious disease treatment:

Probiotics are becoming increasingly explored as alternative and adjunctive treatments to infectious and chronic gastrointestinal diseases. As defined by the Food and Agriculture Organization (**FAO**), probiotics are microorganisms, either supplemented or endogenous, that confer a health benefit to the host (FAO, 2006). Many of the most conventionally studied gut native probiotics are members of the genus *Lactobacillus* or *Bifidobacteria* or derive from the strain *E. coli* Nissle. *Lactobacillus* and *Bifidobacteria*, which collectively contain approximately

221 established probiotic species (Goldstein *et al.*, 2015), are common to the intestinal tract of healthy infants and adults (Dieterich *et al.*, 2018; Hidalgo-Cantabrana *et al.*, 2017; Turroni *et al.*, 2018). *E. coli* Nissle is one of the few Gram-negative bacteria identified as a probiotic (Sonnenborn, 2016), where its distinct cell wall composition and physiology allows it to interact with the host through mechanisms different from Gram-positive probiotics (Kandasamy *et al.*, 2017; van der Hooft *et al.*, 2019). As a group, probiotic microorganisms exhibit wide diversity in the mechanisms they use to promote host health which is evident in their differential immune modulation of cytokines and lymphocytes, their species-dependent capacities to induce the expression of mucosal tight junction proteins, and in the diversity of small molecules that they produce that directly or indirectly antagonizes pathogen function (Engevik and Versalovic, 2017; Hidalgo-Cantabrana *et al.*, 2017; Hiippala *et al.*, 2018; Yousefi *et al.*, 2019).

1.3. Rice bran gastrointestinal health benefits for infectious disease prevention:

Domesticated rice (Agarrwal *et al.*) is a major staple crop in human food systems and is grown in over 114 countries (Sharif *et al.*, 2014). Whole grain or "brown" rice, which consists of the germ, endosperm, and bran, is becoming increasingly recognized for its human health benefits even though most of the world consumes polished white rice. The whole grain rice parts and types are displayed in **Figure 1.1**. Rice bran is abundant in lipids, proteins, and fibers and it additionally contains a unique and robust suite of bioactive amino acids, vitamins, and phytochemicals that have many established roles in human health promotion and enteric disease prevention (Borresen and Ryan, 2014; Sharif *et al.*, 2014; Zarei *et al.*, 2017). The bran component of whole grain rice is the major fraction contributing to the overall nutritive value of the whole grain (Borresen *et al.*, 2014).

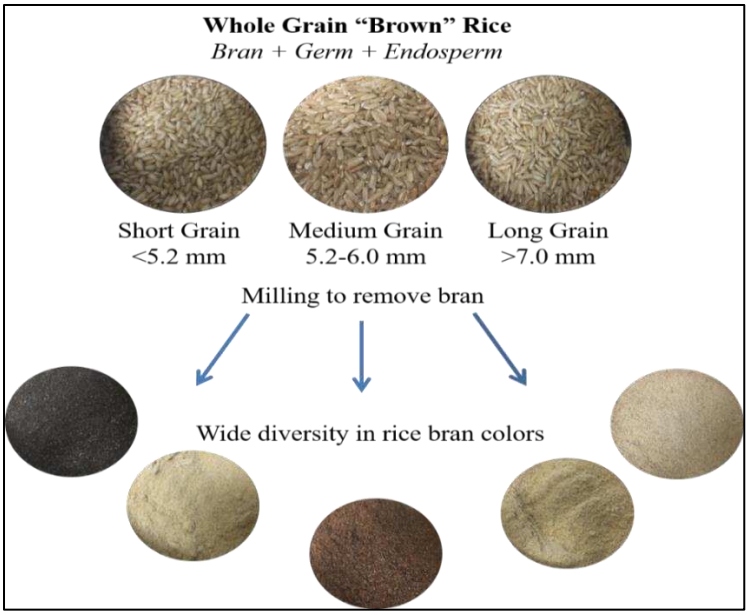

Figure 1.1. Brown rice milling produces rice bran, the outer coating of the rice grain.

Emerging research exists for the ability of whole grain rice, particularly the rice bran fraction, to prevent infectious diseases affecting the gut. A primary focus has been on antidiarrheal properties of rice bran to combat human rotavirus and norovirus infections, which are the leading global causes of childhood diarrhea (Lei *et al.*, 2016; Yang, 2015; Yang *et al.*, 2014). Currently, limited vaccine efficacy against human rotavirus and the lack of a human norovirus vaccine support the demand for alternative enteric disease prevention and management strategies (Cortes-Penfield *et al.*, 2017; Sadiq *et al.*, 2018). Prophylactic feeding studies in germ-free pigs suggested that rice bran can reduce human rotavirus and norovirus diarrhea via direct antiviral, immunomodulatory, and gut barrier protective actions on the intestinal tract (Lei *et al.*, 2016; Yang *et al.*, 2015; Yang *et al.*, 2014). These activities include increased production of mucosal-protective immunoglobulin-A (**IgA**) antibodies, improved mucosal integrity during viral infections and production of anti-inflammatory cytokines at the gut barrier (Lei *et al.*, 2016; Yang *et al.*, 2015; Yang *et al.*, 2014).

In a bacterial pathogen context, whole grain rice components, particularly rice bran, have been examined for protective effects against *Salmonella*. Investigations by Kumar *et al.*, Ghazi *et al*., and Goodyear *et al.* support the ability of rice bran to reduce *Salmonella* Typhimurium growth and pathogenicity in murine and porcine models (Ghazi *et al.*, 2016; Goodyear *et al.*, 2015; Henderson *et al.*, 2012a). Goodyear *et al*. and Ghazi *et al*. observed the differential ability of rice bran varieties in reducing *Salmonella* invasion and replication and concluded that these differences could be explained in part by the distinct profiles of bioactive compounds found in each rice variety (Goodyear *et al.*, 2015). Specifically, Lijiangxintuanheigu (**LTH**) a pigmented rice bran, was found to more effectively suppress *Salmonella* infection into and intracellular replication within cells compared to Sanhuangzhan (**SHZ**), a brown rice bran (Ghazi *et al.*, 2016). These enhanced effects of LTH were associated with higher levels of galactolipids, phospholipids, and flavonoids when compared to SHZ (Ghazi *et al.*, 2016). Collectively, these studies indicate that whole grain rice could potentially help to treat and prevent disease outbreaks caused by human enteric pathogens.

1.4. Rice bran-based synbiotics for improved protection against infectious gastrointestinal disease:

Rice bran's bioactivity can be enhanced when it is fermented with probiotics. The combination of a probiotic and a prebiotic is called a synbiotic, and these biological and dietary components are believed to work synergistically to enhance the health benefits each delivers to the host (Markowiak and Slizewska, 2017). Synbiotic interactions of probiotics and rice bran have been shown to increase *Lactobacillus* spp. in mice while simultaneously reducing *S.* Typhimurium fecal shedding (Henderson *et al.*, 2012a). Rice bran synbiotics have also been

demonstrated increase *L. rhamnosus* GG and *E. coli* Nissle in gnotobiotic pigs while enhancing their capacity to suppress human rotavirus and norovirus diarrhea (Lei *et al.*, 2016; Yang, 2015). In healthy adults, rice bran consumption increased *Bifidobacterium longum* levels and was associated with increased colonic production of short chain fatty acids and aromatic phytochemicals that had reported roles in supporting colonocyte metabolism, enhancing immunity, and protecting the gut barrier (Sheflin *et al.*, 2015), all of which are factors contributing to prophylactic protection against infectious enteric agents. Despite the probiotic diversity in creating these and other synbiotics, there is currently a lack of research exploring how probiotic species diversity influences the functions of synbiotics on the host.

Understanding and comparing the metabolic strategies that probiotics use to break down prebiotics represents one way that synbiotics can be screened and optimized as treatments for infectious gastrointestinal diseases. A high-throughput assessment of probiotic metabolism is made possible through the expansion of metabolomics technologies, a series of chromatographic and mass spectral platforms that separates and detects small molecules within a sample (O'Gorman and Brennan, 2015; Ryan *et al.*, 2013). In rice bran, metabolomics analyses have been completed and identified multiple fatty acid, vitamin-E metabolites that contributed to intestinal health and decreased *S*. Typhimurium shedding (Forster *et al.*, 2013; Henderson *et al.*, 2012b; Heuberger *et al.*, 2010; Kumar *et al.*, 2012), established the global, non-targeted metabolite profiles of 17 global rice bran varieties (Zarei *et al.*, 2018), and in three American varieties metabolomics platforms identified 65 amino acids, cofactors, vitamins and phytochemicals with previously-reported bioactivity, including antimicrobial and immune-modulatory functions important to pathogen protection (Zarei *et al.*, 2017). Fewer characterizations of probiotic metabolomes have been completed. While multiple previous

studies have examined the gut microbiomes of animals and people to indirectly understand probiotic metabolism of dietary components (Ahmed *et al.*, 2016; Chen *et al.*, 2018; Engevik and Versalovic, 2017; Lazar *et al.*, 2019; Pimentel *et al.*, 2018; Spinler *et al.*, 2017; Whittemore *et al.*, 2018; Zheng *et al.*, 2018), they have neither established nor compared the global metabolomes of individual probiotic as they interacted with dietary prebiotics. A metabolomic characterization of probiotic and rice bran combinations will help to address major knowledge gaps in understanding probiotic mechanisms of action and will provide a framework for predicting and optimizing the disease-fighting capacities of synbiotics.

1.5. Hypothesis and Specific Aims:

Given the demonstrated capacities of rice bran synbiotics to treat infectious enteric diseases, and when considering the need to better understand synbiotic mechanisms of disease prevention, the overarching objective of this thesis was to characterize the synbiotic metabolomes of six different probiotic and rice bran combinations, examine their effects on *Salmonella* Typhimurium and human rotavirus function, and identify potential metabolites and mechanisms of action driving synbiotic infectious disease prevention. The central hypothesis, which is described in **Figure 1.2**, is that rice bran will differentially enhance bioactive compound production across six probiotic species to increase *S.* Typhimurium growth suppression and decrease human rotavirus diarrhea when compared to either probiotic or rice bran alone, as measured with *in vitro*, adult mouse, and gnotobiotic neonatal pig systems. To examine this hypothesis, the following thesis chapters will explore rice bran metabolism by one *Lactobacillus* spp. for its effects on *S*. Typhimurium growth, compare three *Lactobacillus* and rice bran synbiotics for differential production of bioactive compounds and capacity to suppress

antimicrobial resistant *S.* Typhimurium growth, apply chromatographic methods to identify and compare major bioactive components of these *Lactobacillus* synbiotics, and finally examine two rice bran synbiotics (*B. longum*, *L. rhamnosus* GG + *E. coli* Nissle) in mice and pigs to understand their metabolism of bioactive compounds in complex mammalian systems as related to infectious gastrointestinal disease protection. The specific aims (**Chapters 2**, **3**, **4**, **5** and **6**) designed to examine this hypothesis are stated below.

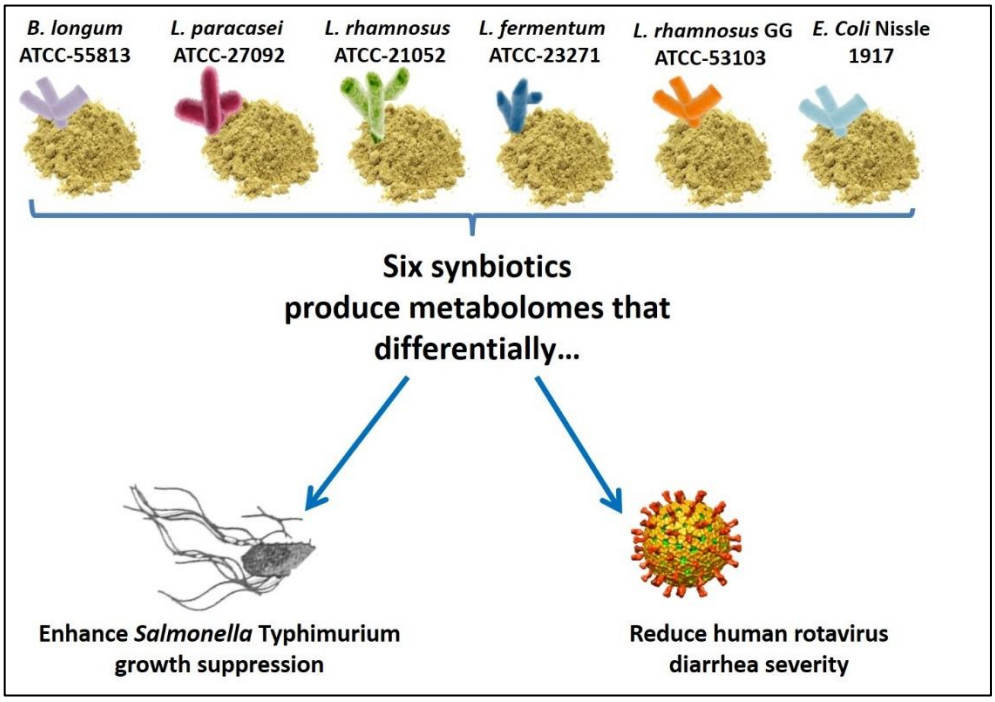

Figure 1.2. Overarching hypothesis for examining synbiotic differential metabolism of bioactive compounds that enhance protection against infectious enteric diseases compared to probiotic or rice bran alone.

Specific Aim 1: Evaluate synbiotics for antimicrobial-resistant *Salmonella* growth suppression and screen metabolite profiles for differential production of bioactive compounds.

Experiment 1.1: Establish a cell-free supernatant model for examining small molecule contributors to *Lactobacillus* + rice bran synbiotic suppression of *S.* Typhimurium growth.

Hypothesis 1.1: Rice bran will enhance *Salmonella* growth suppression by *L. paracasei* cell-free supernatant and will modulate *L. paracasei* metabolism of bioactive compounds.

Experiment 1.2: Compare antimicrobial-resistant *Salmonella* growth suppression across supernatants collected from three *Lactobacillus* + rice bran synbiotics.

Hypothesis 1.2: *The cell-free supernatant from three Lactobacillus spp. + rice bran synbiotics will differentially enhance growth-inhibition of Salmonella when compared to either a Lactobacillus spp. or rice bran alone in time, dose, and magnitude-dependent manners.*

Experiment 1.3: Examine the non-targeted metabolome of three *Lactobacillus* + rice bran synbiotics and screen supernatants for differential production of bioactive compounds.

Hypothesis 1.3: *The cell-free supernatant from three Lactobacillus spp. + rice bran synbiotics will produce metabolomes differentially abundant in metabolites with antimicrobial functions.*

Experiment 1.4: Apply bioactivity-guided fractionation to *Lactobacillus* + rice bran synbiotic supernatants to identify key metabolites driving *Salmonella* growth suppression.

Hypothesis 1.4: *Chromatographic separation of Lactobacillus spp. + rice bran synbiotics will identify fractions that suppress Salmonella growth and will reveal Lactobacillus species differences in metabolites driving Salmonella growth suppression.*

Specific Aim 2: Evaluate synbiotic metabolism in healthy mice for production of metabolites conferring infectious enteric disease protection.

Experiment 2.1: Compare the non-targeted metabolome of rice bran and *Bifidobacterium longum*-fermented rice bran prepared as laboratory rodent diets.

Hypothesis 2.1: *Rice bran fermentation with Bifidobacterium longum will modulate the lipid and amino acid composition of rice bran in laboratory rodent diets.*

Experiment 2.2: Compare the colon tissue and whole blood metabolomes of mice consuming rice bran versus *Bifidobacterium longum*-fermented rice bran.

Hypothesis 2.2: *Consumption of rice bran versus fermented rice bran by healthy mice will modulate the abundance and distribution of gastrointestinal disease-protective metabolites in the colon and blood of healthy mice.*

Specific Aim 3: Identify synbiotic metabolites that are protective against human rotavirus diarrhea in gnotobiotic neonatal pigs.

Experiment 3.1: Compare the non-targeted large intestinal and plasma metabolomes of gnotobiotic neonatal pigs fed probiotics + rice bran or probiotics-only.

Hypothesis 3.1: *Prophylactic consumption of probiotic L. rhamnosus GG/E. coli Nissle + rice bran synbiotics versus probiotics-only will modulate large intestinal and plasma profiles of amino acids and lipids in gnotobiotic neonatal pigs.*

Experiment 3.2: Examine large intestinal and plasma metabolomes of synbiotic versus probiotic-only consuming pigs for synbiotic enhancement of metabolites conferring human rotavirus diarrheal protection.

Hypothesis 3.2: *Prophylactic synbiotic consumption will enhance large intestinal and plasma abundances of antidiarrheal, gut barrier protective, immune-modulatory, and antiviral metabolites in gnotobiotic neonatal pigs.*

REFERENCES

Adler, A., N.D. Friedman, and D. Marchaim, Multidrug-Resistant Gram-Negative Bacilli: Infection Control Implications. Infect Dis Clin North Am, 2016. 30(4): p. 967-997.

Ahmed, I., et al., Microbiome, Metabolome and Inflammatory Bowel Disease. Microorganisms, 2016. 4(2).

Antibiotic Resistant Threats in the United States, U.S.D.o.H.a.H. Services, Editor. 2013: Atlanta, Georgia.

Antibiotic/Antimicrobial Resistance (CDC): Biggest Threats and Data, D.o.H.Q.P. (CDC), Editor. 2018: Atlanta, Georgia.

Borresen, E.C. and E.P. Ryan, Chapter 22 - Rice Bran: A Food Ingredient with Global Public Health Opportunities, in Wheat and Rice in Disease Prevention and Health, R.R. Watson, V.R. Preedy, and S. Zibadi, Editors. 2014, Academic Press: San Diego. p. 301-310.

Chen, Y.T., et al., A combination of Lactobacillus mali APS1 and dieting improved the efficacy of obesity treatment via manipulating gut microbiome in mice. Sci Rep, 2018. 8(1): p. 6153.

Chlebicz, A. and K. Slizewska, Campylobacteriosis, Salmonellosis, Yersiniosis, and Listeriosis as Zoonotic Foodborne Diseases: A Review. Int J Environ Res Public Health, 2018. 15(5).

Cortes-Penfield, N.W., et al., Prospects and Challenges in the Development of a Norovirus Vaccine. Clin Ther, 2017. 39(8): p. 1537-1549.

Diarra, M.S., et al., Antibiotic resistance and diversity of Salmonella enterica serovars associated with broiler chickens. J Food Prot, 2014. 77(1): p. 40-9.

Diarrhoeal disease. [internet] 2013 Apr. 2013 [cited 2016 Dec. 3]; Available from: http://www.who.int/mediacentre/factsheets/fs330/en/.

Dieterich, W., M. Schink, and Y. Zopf, Microbiota in the Gastrointestinal Tract. Med Sci, 2018. 6(4).

Donado-Godoy, P., et al., Counts, serovars, and antimicrobial resistance phenotypes of Salmonella on raw chicken meat at retail in Colombia. J Food Prot, 2014. 77(2): p. 227-35.

Engevik, M.A. and J. Versalovic, Biochemical Features of Beneficial Microbes: Foundations for Therapeutic Microbiology. Microbiol Spectr, 2017. 5(5).

FAO, Probiotics in food: Health and nutritional properties and guidelines for evaluation. 2006, Food and Agriculture Organization: Viale delle Terme di Caracalla, Rome.

Florez-Cuadrado, D., et al., Antimicrobial Resistance in the Food Chain in the European Union. Adv Food Nutr Res, 2018. 86: p. 115-136.

Forster, G.M., et al., Rice varietal differences in bioactive bran components for inhibition of colorectal cancer cell growth. Food Chem, 2013. 141(2): p. 1545-52.

Founou, L.L., et al., Antibiotic Resistance in Food Animals in Africa: A Systematic Review and Meta-Analysis. Microb Drug Resist, 2018. 24(5): p. 648-665.

Ghazi, I.A., et al., Rice Bran Extracts Inhibit Invasion and Intracellular Replication of Salmonella typhimurium in Mouse and Porcine Intestinal Epithelial Cells. Medicinal and Aromatic Plants, 2016. 271(5).

Goldstein, E.J., K.L. Tyrrell, and D.M. Citron, Lactobacillus species: taxonomic complexity and controversial susceptibilities. Clin Infect Dis, 2015. 60 Suppl 2: p. S98-107.

Goodyear, A., et al., Dietary rice bran supplementation prevents Salmonella colonization differentially across varieties and by priming intestinal immunity. Journal of Functional Foods, 2015. 18: p. 653-664.

Henderson, A.J., et al., Consumption of rice bran increases mucosal immunoglobulin A concentrations and numbers of intestinal Lactobacillus spp. J Med Food, 2012. 15(5): p. 469-75.

Heuberger, A.L., et al., Metabolomic and functional genomic analyses reveal varietal differences in bioactive compounds of cooked rice. PLoS One, 2010. 5(9): p. e12915.

Hidalgo-Cantabrana, C., et al., Bifidobacteria and Their Health-Promoting Effects. Microbiol Spectr, 2017. 5(3).

Hiippala, K., et al., The Potential of Gut Commensals in Reinforcing Intestinal Barrier Function and Alleviating Inflammation. Nutrients, 2018. 10(8).

Holschbach, C.L. and S.F. Peek, Salmonella in Dairy Cattle. Vet Clin North Am Food Anim Pract, 2018. 34(1): p. 133-154.

Iannino, F., et al., Development of a dual vaccine for prevention of Brucella abortus infection and Escherichia coli O157:H7 intestinal colonization. Vaccine, 2015. 33(19): p. 2248-53.

Kandasamy, S., et al., Unraveling the Differences between Gram-Positive and Gram-Negative Probiotics in Modulating Protective Immunity to Enteric Infections. Front Immunol, 2017. 8: p. 334.

Kemppainen, K.M., et al., Factors that Increase Risk of Celiac Disease Autoimmunity Following a Gastrointestinal Infection in Early Life. Clinical Gastroenterology and Hepatology.

Kumar, A., et al., Dietary rice bran promotes resistance to Salmonella enterica serovar Typhimurium colonization in mice. BMC Microbiol, 2012. 12: p. 71.

Lazar, V., et al., Gut Microbiota, Host Organism, and Diet Trialogue in Diabetes and Obesity. Front Nutr, 2019. 6: p. 21.

Lei, S., et al., High Protective Efficacy of Probiotics and Rice Bran against Human Norovirus Infection and Diarrhea in Gnotobiotic Pigs. Front Microbiol, 2016. 7: p. 1699.

Markowiak, P. and K. Slizewska, Effects of Probiotics, Prebiotics, and Synbiotics on Human Health. Nutrients, 2017. 9(9).

Mhongole, O.J., et al., Characterization of Salmonella spp. from wastewater used for food production in Morogoro, Tanzania. World J Microbiol Biotechnol, 2017. 33(3): p. 42.

Michael, G.B. and S. Schwarz, Antimicrobial resistance in zoonotic nontyphoidal Salmonella: an alarming trend? Clin Microbiol Infect, 2016. 22(12): p. 968-974.

Muller-Loennies, S., L. Brade, and H. Brade, Neutralizing and cross-reactive antibodies against enterobacterial lipopolysaccharide. Int J Med Microbiol, 2007. 297(5): p. 321-40.

O'Gorman, A. and L. Brennan, Metabolomic applications in nutritional research: a perspective. J Sci Food Agric, 2015. 95(13): p. 2567-70.

Peng, M., et al., Prevalence and antibiotic resistance pattern of Salmonella serovars in integrated crop-livestock farms and their products sold in local markets. Environ Microbiol, 2016. 18(5): p. 1654-65.

Pimentel, G., et al., Metabolic Footprinting of Fermented Milk Consumption in Serum of Healthy Men. J Nutr, 2018. 148: p. 851-860.

Ryan, E.P., et al., Advances in Nutritional Metabolomics. Curr Metabolomics, 2013. 1(2): p. 109-120.

Sadiq, A., et al., Rotavirus: Genetics, pathogenesis and vaccine advances. Rev Med Virol, 2018. 28: p. e2003.

Schwartz, K.L. and S.K. Morris, Travel and the Spread of Drug-Resistant Bacteria. Curr Infect Dis Rep, 2018. 20(9): p. 29.

Sharif, M.K., et al., Rice bran: a novel functional ingredient. Crit Rev Food Sci Nutr, 2014. 54: p. 807-16.

Sheflin, A.M., et al., Pilot dietary intervention with heat-stabilized rice bran modulates stool microbiota and metabolites in healthy adults. Nutrients, 2015. 7(2): p. 1282-300.

Sonnenborn, U., Escherichia coli strain Nissle 1917-from bench to bedside and back: history of a special Escherichia coli strain with probiotic properties. FEMS Microbiol Lett, 2016. 363(19).

Spinler, J.K., et al., Next-Generation Probiotics Targeting Clostridium difficile through Precursor-Directed Antimicrobial Biosynthesis. Infect Immun, 2017. 85(10).

Turroni, F., et al., Bifidobacteria and the infant gut: an example of co-evolution and natural selection. Cell Mol Life Sci, 2018. 75(1): p. 103-118.

van der Hooft, J.J.J., et al., Substantial Extracellular Metabolic Differences Found Between Phylogenetically Closely Related Probiotic and Pathogenic Strains of Escherichia coli. Front Microbiol, 2019. 10: p. 252.

Whittemore, J.C., et al., Short and long-term effects of a synbiotic on clinical signs, the fecal microbiome, and metabolomic profiles in healthy research cats receiving clindamycin: a randomized, controlled trial. PeerJ, 2018. 6: p. e5130.

Willame, C., et al., Effectiveness of the Oral Human Attenuated Rotavirus Vaccine: A Systematic Review and Meta-analysis-2006-2016. Open Forum Infect Dis, 2018. 5(11): p. 292.

WHO, Salmonella (non-typhoidal). [Internet] 2016 December 2016 [cited 2017 July 30]; Available from: http://www.who.int/mediacentre/factsheets/fs139/en/.

Yang, X., et al., Dietary rice bran protects against rotavirus diarrhea and promotes Th1-type immune responses to human rotavirus vaccine in gnotobiotic pigs. Clin Vaccine Immunol, 2014. 21(10): p. 1396-403.

Yang, X., et al., High protective efficacy of rice bran against human rotavirus diarrhea via enhancing probiotic growth, gut barrier function, and innate immunity. Sci Rep, 2015. 5: p. 15004.

Yousefi, B., et al., Probiotics importance and their immunomodulatory properties. J Cell Physiol, 2019. 234: p. 8008-8018.

Zarei, I., et al., Comparative Rice Bran Metabolomics across Diverse Cultivars and Functional Rice Gene(-)Bran Metabolite Relationships. Metabolites, 2018. 8(4).

Zarei, I., et al., Rice Bran Metabolome Contains Amino Acids, Vitamins & Cofactors, and Phytochemicals with Medicinal and Nutritional Properties. Rice (N Y), 2017. 10(1): p. 24.

Zheng, X., S. Wang, and W. Jia, Calorie restriction and its impact on gut microbial composition and global metabolism. Front Med, 2018. 12: p. 634-644.

CHAPTER TWO

LACTOBACILLUS PARACASEI METABOLISM OF RICE BRAN REVEALS METABOLOME ASSOCIATED WITH *SALMONELLA* TYPHIMURIUM GROWTH REDUCTION[2]

2.1. Summary:

2.1.1. Aims:

This study aimed to determine the effect of a cell-free supernatant of *Lactobacillus paracasei* ATCC27092 with and without rice bran extract **(RBE)** on *Salmonella* Typhimurium 14028s growth, and to identify a metabolite profile with antimicrobial functions.

2.1.2. Methods and Results:

Supernatant was collected from overnight cultures of *L. paracasei* incubated in the presence **(LP+RBE)** or absence **(LP)** of RBE and applied to *S.* Typhimurium. LP+RBE reduced 13.1% more *S.* Typhimurium growth than LP after 16 h ($P<0.05$). Metabolite profiles of LP and LP+RBE were examined using non-targeted global metabolomics consisting of ultra-high-performance liquid chromatography coupled with tandem mass-spectrometry. A comparison of LP and LP+RBE revealed 84 statistically significant metabolites ($P<0.05$), where 20 were classified with antimicrobial functions.

---

[2] **Nealon, N.J.***, Worcester, C.R.*, and Ryan, E.P. *Lactobacillus paracasei metabolism of rice bran reveals metabolome associated with Salmonella Typhimurium growth production*. Journal of Applied Microbiology. 122:1639-1656. June 2017. ***Co-first authors**

2.1.3. Conclusions:

LP+RBE reduced *S.* Typhimurium growth to a greater extent than LP, and the metabolite profile distinctions suggested that RBE favorably modulates the metabolism of *L. paracasei*. These findings warrant continued investigation of probiotic and RBE antimicrobial activities across microenvironments and matrices where *S.* Typhimurium exposure is problematic.

2.1.4. Significance and Impact of Study:

This study showed a novel metabolite profile of probiotic *L. paracasei* and prebiotic rice bran that increased antimicrobial activity against *S.* Typhimurium.

2.2. Introduction:

Globally, *Salmonella enterica* serovar Typhimurium accounts for the majority of human Salmonellosis cases each year. *S.* Typhimurium causes widespread disease because of zoonotic transmission from cattle, poultry, swine, sheep, rodents, and horses (Tsolis *et al.*, 1999). An emerging strategy against *S.* Typhimurium involves the use of probiotics and prebiotics. As defined by the World Health Organization (**WHO**) and Food and Drug Administration (**FDA**), probiotics are live microorganisms that, when administered in adequate amounts, confer a health benefit to the host (FAO, 2006). Many widely investigated probiotic species belong to the bacterial genus *Lactobacillus*, which has a natural ability to reduce the growth of *S.* Typhimurium (Heredia-Castro *et al.*, 2015). In particular, *Lactobacillus paracasei* strains have been shown to effectively reduce the growth of enteric pathogens including *S.* Typhimurium, *Listeria monocytogenes* and *Escherichia coli* O157:H7 (Caridi, 2002; Chiang and Pan, 2012; Valerio *et al.*, 2013).

Rice bran, the outer layer of the rice grain, is a natural and rich source of prebiotics that can be metabolized by the gut microbiome to modulate mucosal immune responses, reduce intestinal colonization of enteric pathogens (Kumar *et al.*, 2012), and increase numbers of native probiotic lactobacilli (Goodyear *et al.*, 2015; Henderson *et al.*, 2012a). Rice bran was also shown to support probiotic *E. coli* Nissle and *Lactobacillus rhamnosus* GG growth in gnotobiotic piglets (Yang *et al.*, 2015). Molecular mechanisms by which *Lactobacillus* spp. utilize and metabolize prebiotics are not well understood. Metabolomics has been minimally used to elucidate the functional significance of synbiotics via identification and quantification of small molecules (Ryan *et al.*, 2011). Past investigations evaluated small molecule profiles produced by the microbiome *in-vitro* and *in-vivo*, including probiotics (Mozzi *et al.*, 2013; Vitali *et al.*, 2010; Weir *et al.*, 2013). Metabolite profiles have been determined for an increasing number of foods fermented by lactic acid bacteria including rye, yogurt, and wine (Arbulu *et al.*, 2015; Koistinen *et al.*; Settachaimongkon *et al.*, 2014).

It was hypothesized that a combination of *L. paracasei* and rice bran extract would result in a unique profile of metabolites with antimicrobial activity that more effectively reduce the growth of *S.* Typhimurium compared to *L. paracasei* alone. This study aimed to compare the effectiveness of *L. paracasei* alone and *L. paracasei* with rice bran extract supernatants at reducing *S.* Typhimurium growth and to evaluate their metabolomic profiles. The small molecule changes that occur in the presence and absence of rice bran extract illustrate how *L. paracasei* and rice bran synergistically promote *S.* Typhimurium growth reduction.

2.3. Materials and Methods:

2.3.1. Bacterial Strains and Culture Reagents:

Lactobacillus paracasei ATCC27092 was purchased from ATCC (Manassas, VA), and *Salmonella enterica* subsp. *enterica* serovar Typhimurium 14028s Kan^r (rPSM::GFP) was a generous gift from Dr. Andres Vazquez-Torres (University of Colorado). All bacterial cultures were stored at -80°C as one ml aliquots supplemented with 20% glycerol in Luria Bertani **(LB)** broth (MO BIO Laboratories, Inc. Carlsbad, CA, USA) for *S.* Typhimurium, and deMan Rogasa Sharpe broth **(MRS)** (Becton, Dickinson, and Company Difco Laboratories, Franklin Lakes, NJ, USA) for *L. paracasei*. MRS broth and agar, LB broth, and MacConkey agar (Becton, Dickinson, and Company Difco Laboratories, Franklin Lakes, NJ) were prepared and sterilized according to the manufacturer. To prepare MRS broth supplemented with rice bran extract **(RBE)**, 100 $\mu g\ ml^{-1}$ RBE was added to the broth. The media was autoclaved with an 18 min sterilization time, then stored at 4°C until use.

2.3.2. Rice Bran Extraction:

RBE was prepared as described previously (Kumar *et al.*, 2012). Briefly, 4 g finely-ground, heat-stabilized Calrose rice bran (USDA-ARS Rice Research Unit, Stuttgart, AK) was extracted in 42.6 ml of 80% methanol. The mixture was vortexed (232 Vortexer Fischer Scientific) on a high-power setting for 5 min, incubated at -80°C overnight, and centrifuged (Beckman Coulter Allegra X-14R) at 3,724 g for 5 min. The supernatant was collected and kept at -80°C until it could be dried in a speedvac concentrator (SPD1010, Thermo Scientific) at 45°C, with the heating time for 5 min, and a vacuum pressure of 7.5 torrs.

2.3.3. L. paracasei Cell-Free Supernatant Preparation:

The CFS preparation was modified from a published procedure (Wang *et al.*, 2012). Briefly, *L. paracasei* isolates were thawed from storage in -80°C, suspended in MRS broth and grown at 37°C until mid/late logarithmic phase. Approx. $1X10^7$ cells were inoculated into 15 ml of MRS or MRS + 100 µg ml^{-1} RBE. The RBE concentration was determined based on dose-response experiments that observed 100 µg ml^{-1} of RBE, when added to fixed amounts of *S.* Typhimurium, reduced growth compared to a RBE-free control culture of *S.* Typhimurium, as evidenced by differences in optical density at 600 nm **(OD600)** over 12 h (**Figure 2.1A**). Each treatment was incubated at 37°C for 24 h. *L. paracasei* supernatant **(LP)** and *L. paracasei* supernatant with rice bran extract **(LP+RBE)** was collected by centrifuging two times at 3,724 g for 10 min. The pH of the supernatant was adjusted using a pH meter (Corning Pinnacle 530) with one mol l^{-1} NaOH (Sigma Aldrich) until a pH of 4.5 was reached. CFS was filter-sterilized through a 0.2µm pore (Pall Corporation LifeSciences Acrodisc syringe filters) into one ml aliquots before being stored at -80°C. Sterility of all CFS was confirmed by plating the treatment on MRS agar and confirming the absence of any bacterial growth after 48 h. Three independent batches of CFS were used in this study.

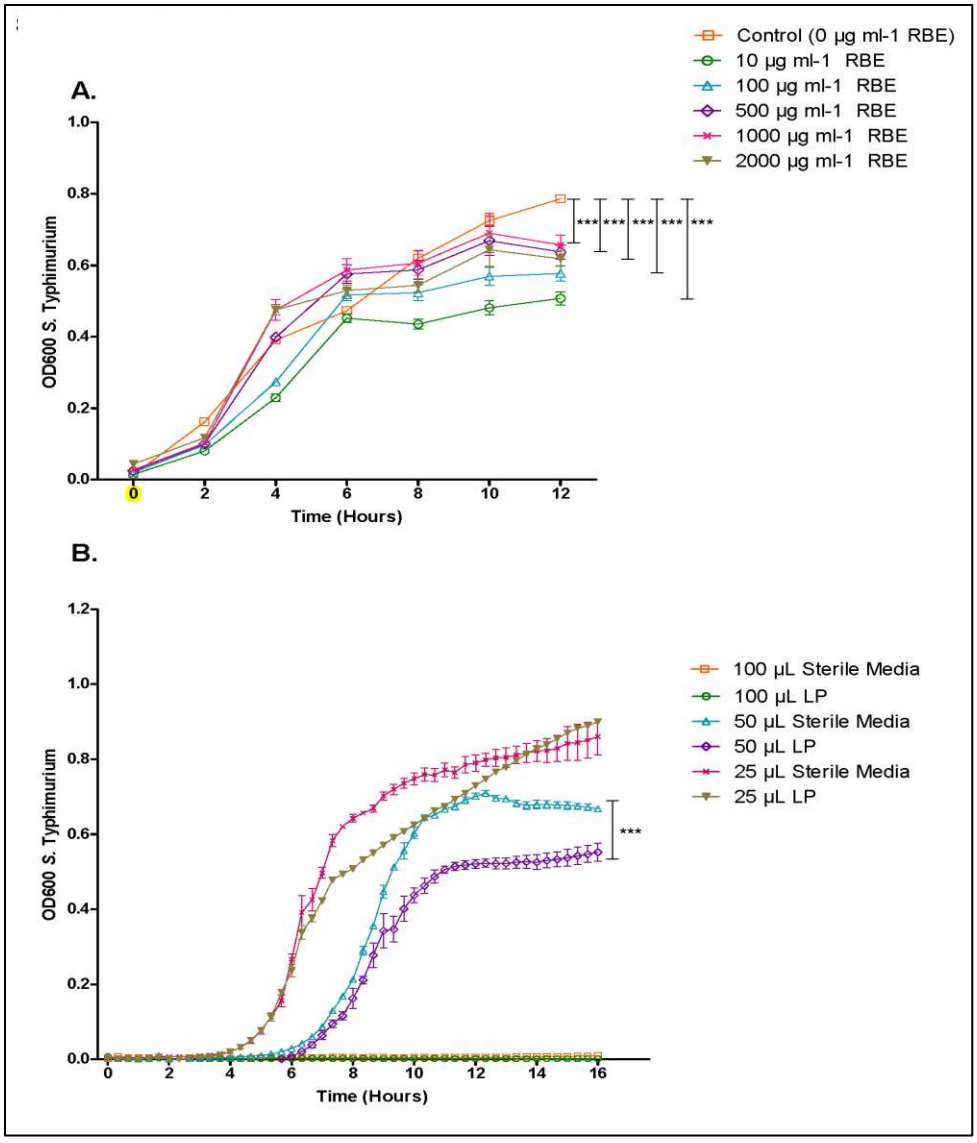

Figure 2.1. Dose–response studies were performed for selection of (A) rice bran concentration and (B) vehicle control volume to use in the *S.* Typhimurium growth reduction assay.
***RBE**: Rice bran extract; **LP**: Lactobacillus paracasei; **OD600**: Optical density at 600 nanometers.*

2.3.4. S. Typhimurium Growth Reduction Assay:

S. Typhimurium was thawed from storage in -80°C and suspended in sterile LB. Stocks were grown in a 24-well plate at 37°C until early/mid logarithmic phase and were assessed using the Cytation3 plate reader. In a 96 well plate, 20 µl of *S.* Typhimurium (approx. $2X10^6$ cells) was diluted 10-fold into 180 µl of sterile LB. To determine an appropriate treatment volume for

the growth reduction assay, a dose curve analysis using LP was performed on *S.* Typhimurium (**Figure 2.1B**). In brief, 100 µl, 50 µl and 25 µl doses of 100% LP were added to approx. $2X10^5$ *S.* Typhimurium cells, and growth was evaluated for 24 h at OD600. 50 µl of treatment was the lowest dose at which a difference was observed in the inhibitory capacity of LP compared to a volume-adjusted control.

To evaluate the effect of CFS on *S.* Typhimurium growth, a 50 µl of treatment with different percentages of CFS were added to each well: 0% Vehicle Control, 20%, 40%, 60%, 80% and 100%. A negative control of *S.* Typhimurium inoculated with 50 µl LB broth was included on each well plate. To control for pH differences between treatments, all media was adjusted to a pH of 4.5 using 1N of NaOH or HCl before use. The plate was read on an automatic plate reader, incubated at 37°C for approx. 16 h, and individual wells were read atOD600 every 20 min. To evaluate differences between all treatments, OD600 was plotted over time. To further quantify growth reduction by LP and LP+RBE, percent growth reduction was calculated from OD600 values using the following equation:

$$\frac{|100\%\ \text{supernatant} - \text{Vehicle Control}|}{\text{Vehicle Control}}\ \text{X}\ 100\%$$

Experiments were repeated four times for all CFS concentrations, eight times for 100% LP, and nine times for 100% LP+RBE using the same three batches of supernatant previously described.

2.3.5. Probiotic Supernatant Agar Well Diffusion Assay:

The agar well diffusion assay was modified from a published procedure (Aminnezhad *et. al* 2015). Briefly, Mueller Hinton agar (Hardy Diagnostics, Santa Maria, CA) was inoculated with *S.* Typhimurium suspended in normal saline (0.89% grams NaCl ml^{-1}), equivalent to a 0.5 McFarland Standard (Hardy Diagnostics, Santa Maria, CA). Eight-millimeter wells were

punched into the agar and filled with 100 µl of the following treatments adjusted to a final pH of 4.5: Vehicle Control, Vehicle Control+RBE, LP, and LP+RBE. Non-pH-adjusted normal saline was included as a negative control on each plate. Plates were incubated at 37°C overnight, and inhibition zone diameters were measured in millimeters. Measurements were collected from seven different plates and included supernatant collected from three independent cultures of LP and LP+RBE.

2.3.6. Supernatant Extract Preparation for Metabolomics:

Metabolomics was performed by Metabolon Inc © (Durham, NC). Briefly, one ml supernatant samples were stored at -80°C in microcentrifuge tubes and sent on dry ice to Metabolon in triplicate. The samples sent for analysis included Vehicle Control, Vehicle Control+RBE, LP and LP+RBE. Upon arrival, samples were stored at -80°C in liquid nitrogen until processing. To improve recovery of small molecules prior to detection, the protein fraction was removed by extracting the sample with a 5:1 methanol:water solution, using vigorous shaking at room temperature for two min followed by centrifugation at 680xg for three min. The extracted samples were split into four parts for analysis via ultra-high-performance liquid chromatography-tandem mass spectrometry **(UPLC-MS/MS)** including two separate reverse phase UPLC-MS/MS with positive ion mode electrospray ionization **(ESI)**, reverse phase UPLC-MS/MS with negative ion mode ESI, and one sample for high liquid chromatography UPLC-MS/MS negative ion mode ESI.

2.3.7. UPLC-MS/MS analysis:

Metabolite profiling was performed using a Waters ACQUITY UPLC, a Thermo Scientific Q-Exactive heated electrospray ionization **(HESI-II)** source, and an Orbitrap mass analyzer operated at 35,000 mass resolution. For UPLC analysis, the sample extracts were dried and reconstituted in solvents appropriate for each of the four detection methods, and standards were included to ensure experimental consistency. Acidic positive ion conditions were optimized for either hydrophobic or hydrophilic compounds and were eluted from a C18 column (Waters UPLC BEH C18-2.1x100 mm, 1.7 um) using water and methanol (hydrophilic optimization) or methanol, acetonitrile and water (hydrophobic optimization) containing 0.05% perfluoropentanoic acid **(PFPA)** (hydrophilic optimization) or 0.5% PFPA (hydrophobic optimization) and 0.1% formic acid. Two aliquots were analyzed using basic negative ion conditions; one was eluted on a separate C18 column using methanol and water with 6.5 mM of Ammonium Bicarbonate at pH 8, and the other was eluted from a HILC column (Waters UPLC BEH Amide 2.1x150 mm, 1.7 µm) using a water-acetonitrile gradient with 10 mM of Ammonium Formate, pH 10.8. The total scan range covered a 70-1000 mass-to-charge ratio (**m/z**).

2.3.8. Data extraction and compound identification:

Raw data was extracted, peak-identified, and quality-control processed as previously described (Brown *et al.*, 2016) and compounds were then identified by comparison to library entities of purified standards or recurrent unknown entities, including over 3300 commercially available purified standard compounds. Identifications were made based on retention time/index **(RI)** with a narrow window of identification, m/z +/- 10 parts per million, and chromatographic

data including MS/MS forward and reverse scores between the experimental data and authentic standards. The raw counts of both supernatant profiles were converted into relative abundances and then median-scaled to one. For each metabolite, fold difference was calculated by dividing the scaled relative abundance of LP+RBE by LP.

2.3.9. Metabolic Pathway Analysis:

Pathway analysis was conducted as described previously (Brown *et al.*). For selected lipids and amino acids/peptides, metabolite fold differences between LP+RBE and LP were visualized using Cytoscape 2.8.3 software. For each metabolite, node color was determined by the direction of fold difference when comparing LP+RBE to LP, and node diameter was determined by the magnitude of the fold difference. The value on each node represents a pathway enrichment score, which was calculated by dividing the number of significant metabolites in pathway (*k*) by the total number of detected metabolites in pathway (*m*). This value was then divided by the fraction of the total number of significant metabolites in the dataset (*n*) over the total number of detected metabolites in the complete dataset (*N*):

$$\frac{k/m}{n/N}$$

Pathway enrichment scores greater than one indicated that a given pathway contained more metabolites with statistically significant fold differences between LP+RBE and LP compared to all pathways in the study.

2.3.10. Statistical analysis:

All statistical analyses for the *S.* Typhimurium growth reduction and well diffusion assays were performed using GraphPad Prism 6.07 (San Diego, CA). For the *S.* Typhimurium growth

reduction assays, treatments were analyzed using a two-way repeated measures analysis of variance with a Bonferroni post-test to compare treatment means. For the agar well diffusion assay, treatments were compared using a one-way ANOVA with a Tukey post-test to compare treatment means. Significance was determined at the level of $P<0.05$. For metabolomic data, statistical analysis was performed by Metabolon Inc © using ArrayStudio (Omnicsoft, Cary, NC) R version 2.142 and/pr SAS v9.4. The relative abundance of each metabolite from LP and LP+RBE was scaled to that metabolite's median relative abundance and each scaled relative abundance was compared between LP and LP+RBE using a Welch's two-sample t test. Statistical significance was determined at the level of $P<0.05$.

2.4 Results:

2.4.1. S. Typhimurium growth reduction by L. paracasei and rice bran extract:

The dose dependent effects of LP and LP+RBE on *S.* Typhimurium growth were determined with increasing percentages of supernatant that were added and compared to a fixed volume of a vehicle control or vehicle control+RBE respectively. In both the LP and LP+RBE treatments, *S.* Typhimurium growth was reduced in a dose-dependent manner **(Figure 2.2).** By 5.0 h, all LP doses (20-100%) significantly reduced *S.* Typhimurium growth compared to the vehicle control. The average percent difference between LP and the vehicle control included: 22.2% for the 20% LP dose, 35.9% for 40% LP, 47.4% for 60% LP, 55.3% for 80% LP, and 60.6% for the 100% LP **(Figure 2.2A).** By the study endpoint of 16 h, two LP concentrations continued to show increased growth reduction compared to the vehicle control and included: 40% LP (41.7%), and 100% LP (68.4%) **(Figure 2.2A).**

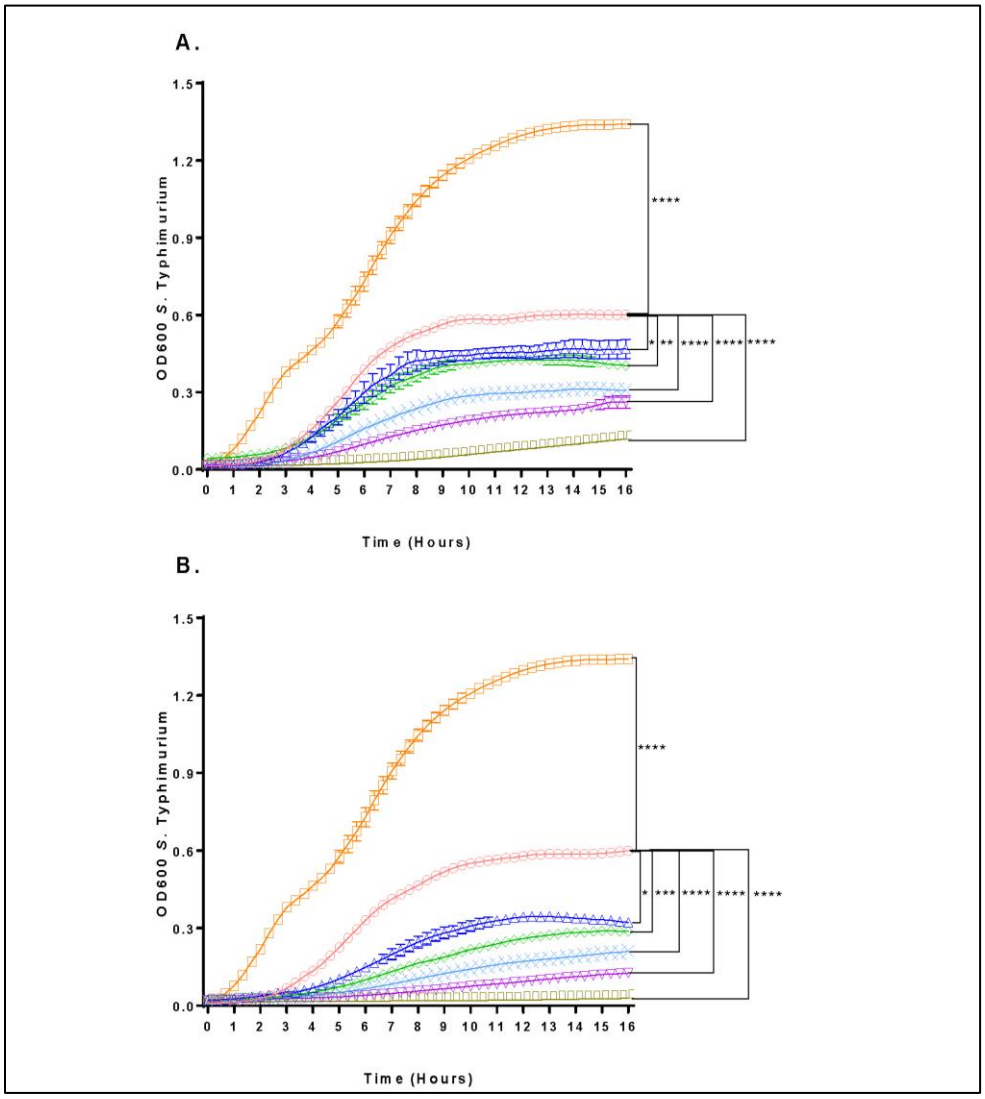

Figure 2.2: *L. paracasei* supernatant in the presence and absence of rice bran extract reduces *S.* Typhimurium growth in a dose-dependent manner.

*The dose-dependent effects of (**A**) LP and (**B**) LP+RBE on S. Typhimurium growth were evaluated. Optical density at a wavelength of 600 nm was plotted on the y-axis and time on the x-axis. Each point represents the mean of four independent experiments and error bars indicate standard error. □ indicates Negative Control, ○ indicates Vehicle Control or Vehicle Control + RBE, ∆ indicates 20% LP or LP+RBE, ◊ indicates 40% LP or LP+RBE, **X** indicates 60% LP or LP+RBE, Downwards-pointing triangle indicates 80% LP or LP+RBE, and Rectangle indicates 100% LP or LP+RBE. Statistical significance between all treatments compared to the Vehicle Control occurred at **(A)** 5.0 h in LP and **(B)** 3.7 h in LP+RBE where *P <0.05, ** P<0.01, *** P<0.001 and **** P<0.0001. In **(A)** and **(B)**, results represent four independent experiments.*

LP+RBE treatments significantly reduced *S.* Typhimurium growth by 3.7 h. The average percent difference for LP+RBE over RBE alone was 8.9% for the 20% LP+RBE dose, 16.1% for 40% LP+RBE, 21.6% for 60% LP+RBE, 25.5% for 80% LP+RBE, and 37.0% for 100% LP+RBE **(Figure 2.2B).** At 16 h, all LP+RBE doses showed increasing growth reduction: 38.8% for 20% LP+RBE, 43.9% for 40% LP+RBE, 55.2% for 60% LP+RBE, 67.6% for 80% LP+RBE, and 82.0% for 100% LP+RBE **(Figure 2.2B).** At 16 h, the 100% CFS dose showed highest *S.* Typhimurium growth reduction compared to the vehicle control: 68.4% for 100% LP and 82.0% for 100% LP+RBE **(Figure 2.2).**

Next, 100% LP and 100% LP+RBE were compared to each other. At 9.0 h, LP+RBE was more effective than LP at reducing *S.* Typhimurium growth ($P<0.05$) and became increasingly effective through 16 h ($P<0.0001$) **(Figure 2.3A)**. The 100% LP+RBE reduced *S.* Typhimurium growth 13.1% more than 100% LP at 16 h ($P<0.05$) **(Figure 2.3B)**. All LP+RBE doses (20%, 40%, 60%, 80%) were more effective than LP at reducing *S*. Typhimurium growth by 16h (data not shown).

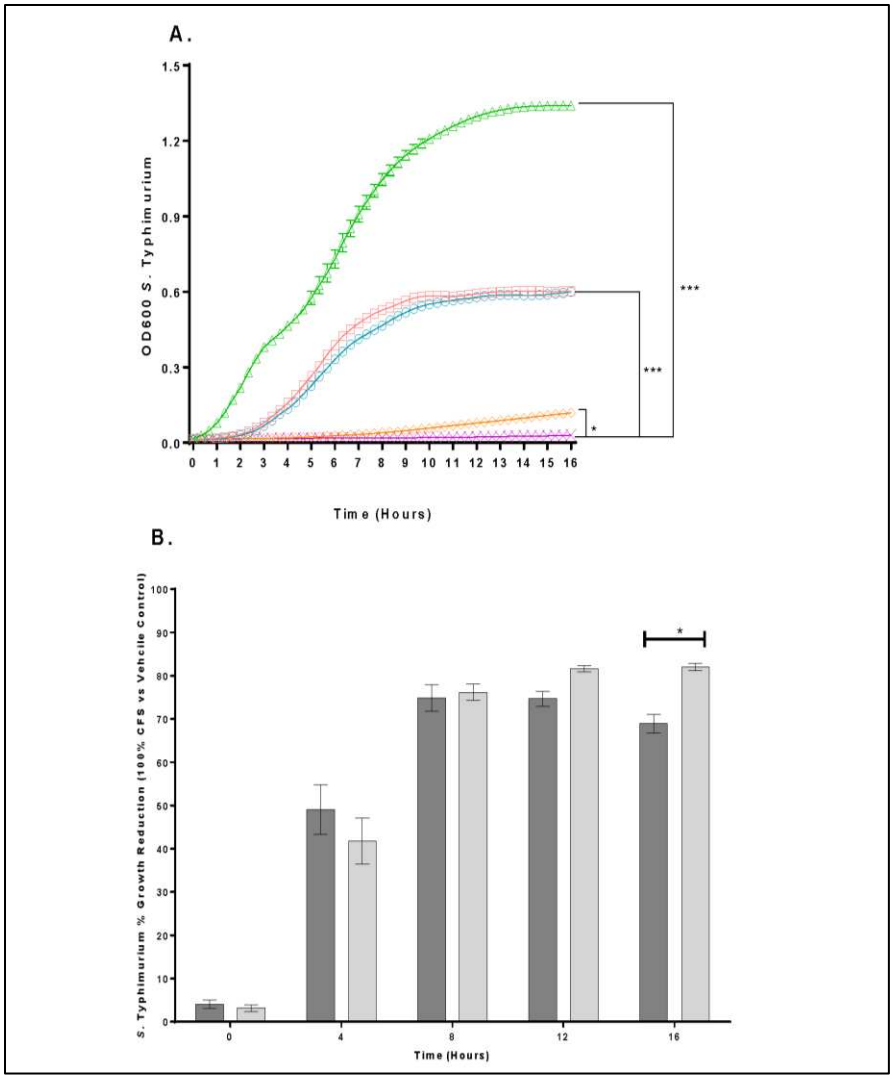

Figure 2.3. Rice bran extract enhances the ability of *L. paracasei* supernatant to reduce *S.* Typhimurium growth.

(A) *The effectiveness of 100% LP and 100% LP+RBE at reducing S. Typhimurium growth were compared. The optical density at 600 nm is plotted on the y-axis, and time on the x-axis. Each point represents the mean of eight (**LP**) or nine independent experiments (**LP+RBE**) treatments and error bars show standard error. ⊿ indicates Negative Control, □ indicates Vehicle Control, ○ indicates Vehicle Control+RBE, ◊ indicates LP and X indicates LP+RBE. By 9.0 h, LP+RBE reduced S. Typhimurium growth more than LP, Vehicle Control, Vehicle Control+RBE and the Negative Control, where*P<0.05, ***P<0.001 and **** P<0.0001.* ***(B)*** *For the 100% CFS treatments, percent S. Typhimurium growth inhibition of LP and LP+RBE treatments media was compared at 0, 4.0, 8.0, 12.0 and 16.0 h. At 16.0 h, LP+RBE reduced growth 13.1% more than LP *P<0.05. Each bar represents the mean percent difference of eight (**LP**) or nine (**LP+RBE**) independent experiments and error bars indicate standard error. Light grey bars represent LP and dark grey bars represent LP+RBE.*

2.4.2. Probiotic supernatant agar well diffusion assay against S. Typhimurium:

To further assess the ability of CFS to reduce *S.* Typhimurium growth, the inhibitory zone diameters of LP, LP+RBE, Vehicle Control, Vehicle Control+RBE and Normal Saline (Negative Control) treatments were compared in an agar well diffusion assay where all treatments were pH-adjusted to 4.5 prior to use. The mean inhibitory zone diameter (millimeters) and standard error are displayed for each treatment in **Table 2.1** and represent seven independent experiments: Normal saline (8.00 +/- 0.00), Vehicle Control (8.93 +/- 0.468), Vehicle Control+RBE (9.43 +/- 0.517), LP (10.86 +/- 0.261), and LP+RBE (12.07 +/- 0.277). The diameters of the wells themselves were 8.0 millimeters, and normal saline did not create an inhibitory zone in any replicate. LP+RBE had a larger inhibitory zone diameter than all treatments: LP+RBE vs Normal Saline, Vehicle Control and Vehicle Control+RBE ($P<0.001$), LP+RBE vs LP ($P<0.05$).

Table 2.1. Agar well diffusion of *L. paracasei* supernatant against *S.* Typhimurium in the presence and absence of rice bran extract

Treatment	**Zone of Inhibition (mm)***
Normal Saline (Negative Control)	(8.00 +/- 0.00)
Vehicle Control	(8.93 +/- 0.468)
Vehicle Control+RBE	(9.43 +/- 0.517)
LP	(10.86 +/- 0.261)
LP+RBE	(12.07 +/- 0.277)

***** Inhibitory zone diameters (millimeters) against *S.* Typhimurium were determined for supernatants and control media. Results are reported as (mean +/-standard error) and were collected from seven independently-measured plates. Measurements were analyzed using a 1-way ANOVA, and pairs of treatments were compared using a Tukey post-test, where statistical significance was determined as $P<0.05$. LP+RBE had a significantly larger zone of inhibition compared to all other treatments: Normal Saline ($P<0.0001$), Vehicle Control ($P<0.0001$), Vehicle Control+ RBE ($P<0.0001$), LP ($P<0.05$).

2.4.3. Metabolomics of probiotic L. paracasei supernatant and rice bran extract:

Metabolome analysis of LP and LP+RBE led to identification of 362 metabolites that were organized by chemical class and summarized in **Table 2.2**. Of the 362 metabolites, 138 were classified as amino acids, 29 peptides, 29 carbohydrates, 11 tricarboxylic acid cycle, 54 lipids, 54 nucleotides, 20 cofactors and vitamins, and 27 phytochemicals. There was a total of 84

metabolites with a fold difference that significantly differed between LP+RBE and LP **(Table 2.3)**. Of these, 58 metabolites that had a higher and 26 had a lower relative abundance in LP+RBE compared to LP. Amino acid and lipid metabolite classes represented ~55% of metabolites differentially expressed between LP and LP+RBE. The relative abundance distributions for lipids and amino acids/small peptides across groups are depicted in **Figure 2.4A** and **Figure 2.4B**.

Table 2.2. Number of metabolites across classes that show a higher or lower fold change in *L. paracasei* supernatant cultured in the presence or absence of rice bran extract

Metabolite Classification	Number of Metabolites (**P<0.05**)
Amino Acids	138 **(19↑, 9↓)**
Peptides	29 **(2↑)**
Carbohydrates	29 **(7↑)**
Tricarboxylic Acid Cycle	11 **(2↑, 1↓)**
Lipids	54 **(8↑, 9↓)**
Nucleotides	54 **(12↑, 3↓)**
Cofactor and Vitamins	20 **(1↑, 1↓)**
Other Phytochemicals	27 **(7↑, 3↓)**
Total Number of Identified Metabolites	*362* ***(58↑, 26↓)***

Metabolite profiles of *L. paracasei* (LP) and *L. paracasei* + rice bran extract (LP+RBE) supernatant. For each metabolite, fold difference was calculated by dividing the scaled relative abundance in LP+RBE by LP. Fold differences were analyzed using a Welch's Two-Sample t-test, and metabolites with a fold difference at statistically different (P<0.05) levels between LP+RBE and LP are marked with ↑ or ↓ to denote the direction of change when comparing LP+RBE to LP.

A. Lipids

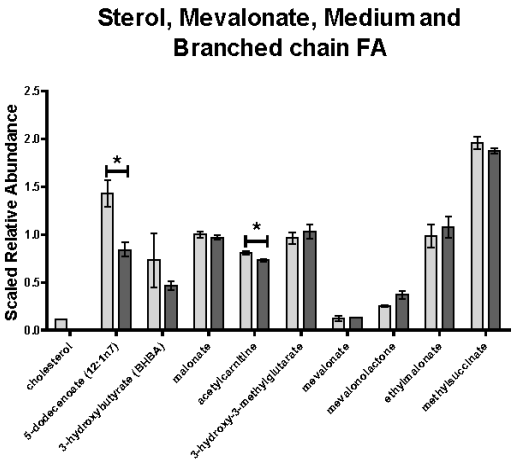
Sterol, Mevalonate, Medium and Branched chain FA
Scaled Relative Abundance
cholesterol
5-dodecenoate (12:1n7)
3-hydroxybutyrate (BHBA)
malonate
acetylcarnitine
3-hydroxy-3-methylglutarate
mevalonate
mevalonolactone
ethylmalonate
methylsuccinate

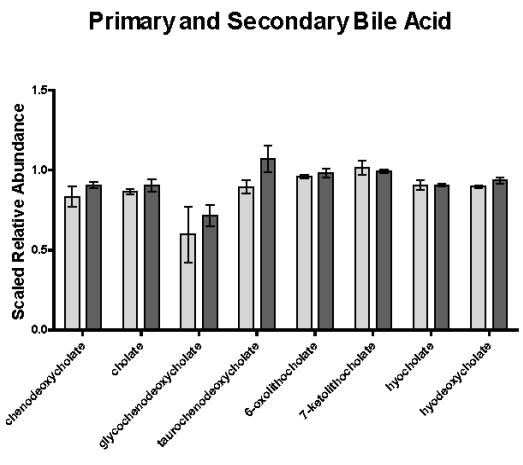
Primary and Secondary Bile Acid
Scaled Relative Abundance
chenodeoxycholate
cholate
glycochenodeoxycholate
taurochenodeoxycholate
6-oxolithocholate
7-ketolithocholate
hyocholate
hyodeoxycholate

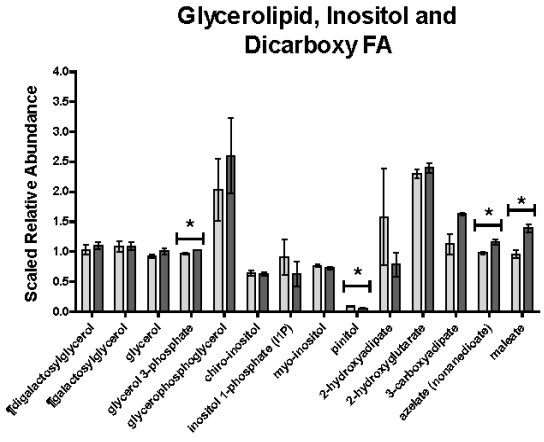
Glycerolipid, Inositol and Dicarboxy FA
Scaled Relative Abundance
digalactosylglycerol
galactosylglycerol
glycerol
glycerol 3-phosphate
glycerophosphoglycerol
chiro-inositol
inositol 1-phosphate (1P)
myo-inositol
pinitol
2-hydroxyadipate
2-hydroxyglutarate
3-carboxyadipate
azelate (nonanedioate)
malate

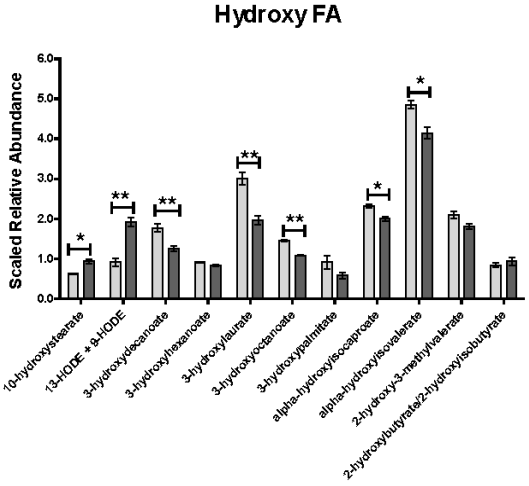
Hydroxy FA
Scaled Relative Abundance
10-hydroxystearate
13-HODE + 9-HODE
3-hydroxydecanoate
3-hydroxyhexanoate
3-hydroxylaurate
3-hydroxyoctanoate
3-hydroxypalmitate
alpha-hydroxyisocaproate
alpha-hydroxyisovalerate
2-hydroxy-3-methylvalerate
2-hydroxybutyrate/2-hydroxyisobutyrate

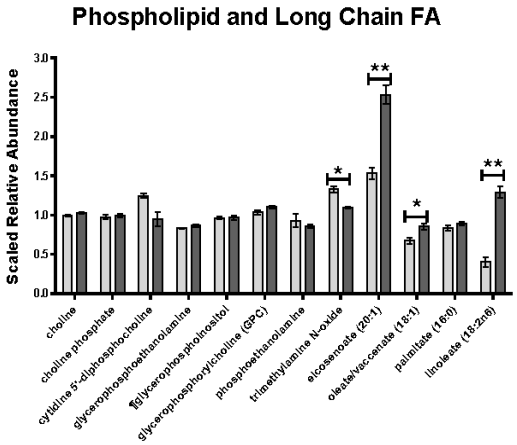
Phospholipid and Long Chain FA
Scaled Relative Abundance
choline
choline phosphate
cytidine 5'-diphosphocholine
glycerophosphoethanolamine
glycerophosphoinositol
glycerophosphorylcholine (GPC)
phosphoethanolamine
trimethylamine N-oxide
eicosenoate (20:1)
oleate/vaccenate (18:1)
palmitate (16:0)
linoleate (18:2n6)

Continued: Figure 2.4B

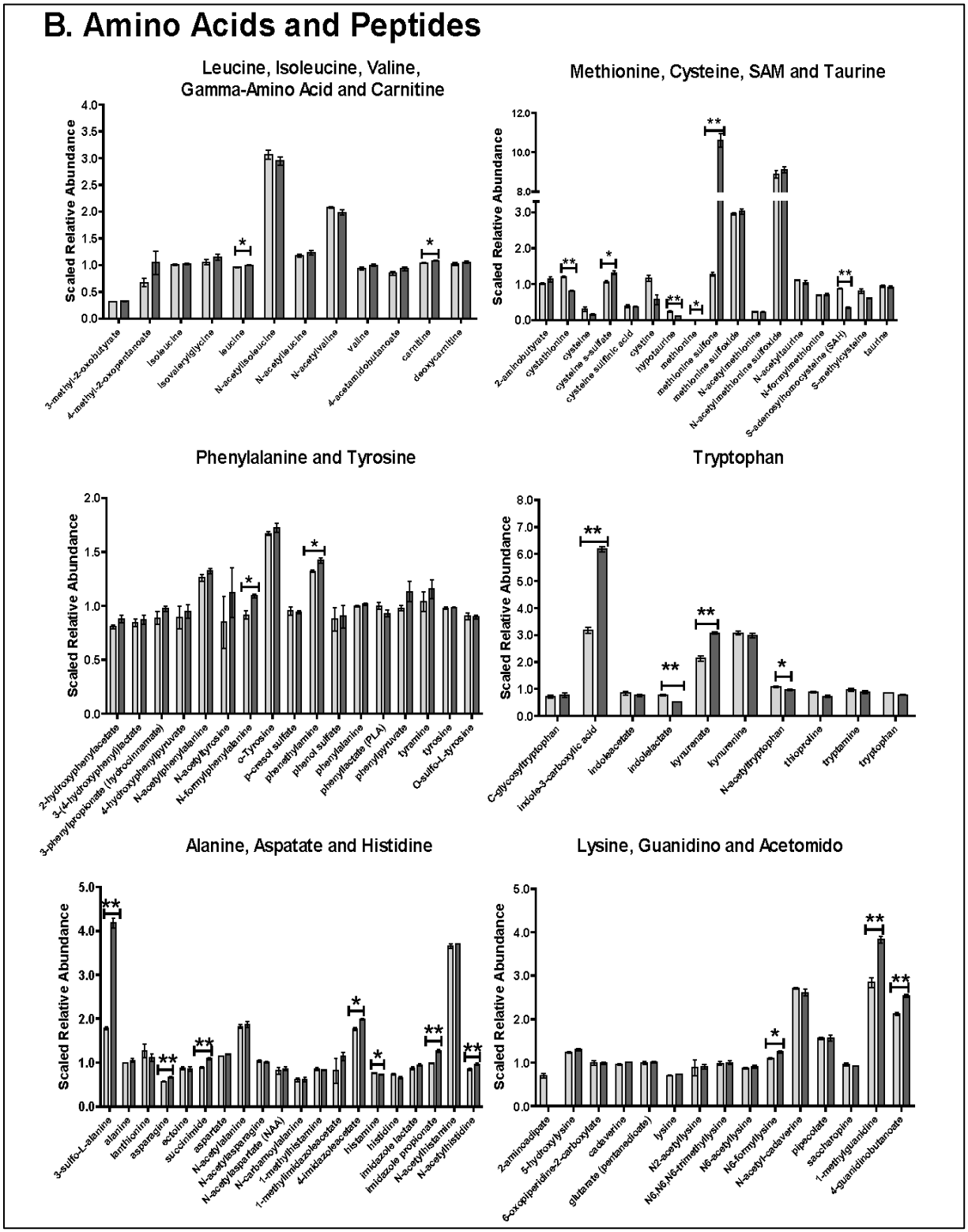

Figure 2.4. Rice bran extract alters the lipid, amino acid, and peptide metabolite profiles of *L. paracasei* supernatant.

*LP and LP+RBE were profiled using UPLC-MS/MS. Each bar represents three independent samples and depicts the metabolite scaled relative abundance. Error bars depict standard error of the mean, *P<0.05, and **P<0.01. Metabolites were classified into metabolic pathways of (**A**) lipids and (**B**) amino acids/peptides based on their biochemical properties and/or physiological functions.Light grey bars represent LP and dark grey bars represent LP+RBE. **FA** indicates fatty acid and **SAM** indicates S-adenosyl methione.*

Table 2.3. Statistically-significant metabolites from *L. paracasei* supernatant prepared in the presence and absence of rice bran extract

Metabolite	HMDB*	Fold Difference†	p-value‡
Amino Acid			
methionine sulfone	-	↑ 8.29	3.16E-06
3-sulfo-L-alanine	02757	↑ 2.34	3.13E-05
indole-3-carboxylic acid	03320	↑ 1.94	0.00065
kynurenate	00715	↑ 1.44	0.0086
1-methylguanidine	01522	↑ 1.34	0.0063
imidazole propionate	02271	↑ 1.28	0.0047
cysteine s-sulfate	00731	↑ 1.24	0.013
succinimide	-	↑ 1.22	0.0075
beta-alanine	00056	↑ 1.22	0.0089
4-guanidinobutanoate	03464	↑ 1.19	0.0024
N-formylphenylalanine	-	↑ 1.18	0.048
asparagine	00168	↑ 1.17	0.0015
N-acetylhistidine	32055	↑ 1.13	0.020
N6-formyllysine	-	↑ 1.13	0.013
4-imidazoleacetate	02024	↑ 1.12	0.024
phenethylamine	02017	↑ 1.07	0.030
creatinine	00562	↑ 1.08	0.037
carnitine	00062	↑ 1.03	0.034
proline	00162	↑ 1.03	0.040
leucine	00687	↑ 1.03	0.042
histamine	00870	↓ 0.94	0.042
acetylcarnitine	00201	↓ 0.90	0.042
N-acetyltryptophan	13713	↓ 0.88	0.030
N-acetylserine	02931	↓ 0.87	0.037
spermine	01256	↓ 0.70	0.044
indolelactate	00671	↓ 0.68	0.0040
cystathionine	00099	↓ 0.67	0.00019
methionine	00696	↓ 0.64	0.023
hypotaurine	00965	↓ 0.46	0.0037
S-adenosylhomocysteine	00939	↓ 0.39	0.0010
Peptide			
§gamma-glutamylisoleucine	11170	↑ 1.19	0.024
tyrosylglycine	-	↑ 1.17	0.017
Carbohydrate			
sucrose	00258	↑ 7.39	5.76E-07
arabonate/xylonate	-	↑ 1.87	0.0059
ribonate	00867	↑ 1.86	0.0015
erythrulose	06293	↑ 1.46	0.029
erythronate	00613	↑ 1.24	0.016

Table 2.3. Statistically-significant metabolites from *L. paracasei* supernatant prepared in the presence and absence of rice bran extract

Metabolite	HMDB*	Fold Difference†	p-value‡
N-acetylglucosamine/ N-acetylgalactosamine	-	↑ 1.12	0.018
glycerate	00139	↑ 1.07	0.0026
Tricarboxylic Acid Cycle			
tricarballylate	31193	↑ 1.79	6.83E-05
citraconate/glutaconate	-	↑ 1.16	0.017
alpha-ketoglutarate	00208	↓ 0.76	0.031
Lipid			
linoleate (18:2n6)	00673	↑ 3.18	0.0075
13-HODE + 9-HODE	-	↑ 2.11	0.0082
eicosenoate (20:1)	02231	↑ 1.65	0.0017
10-hydroxystearate	-	↑ 1.49	0.014
maleate	00176	↑ 1.44	0.017
oleate/vaccenate (18:1)	-	↑ 1.26	0.041
azelate (nonanedioate)	00784	↑ 1.18	0.024
glycerol 3-phosphate	00126	↑ 1.05	0.031
alpha-hydroxyisocaproate	00746	↓ 0.86	0.016
alpha-hydroxyisovalerate	00407	↓ 0.85	0.025
trimethylamine N-oxide	00925	↓ 0.82	0.014
3-hydroxyoctanoate	01954	↓ 0.74	0.0015
3-hydroxydecanoate	02203	↓ 0.70	0.0085
3-hydroxylaurate	00387	↓ 0.65	0.0055
pinitol	34219	↓ 0.61	0.015
5-dodecenoate (12:1n7)	00529	↓ 0.58	0.015
Nucleotide			
2'-deoxycytidine	00014	↑ 1.60	0.0034
N6-succinyladenosine	00912	↑ 1.51	0.0032
2'-deoxyadenosine	00101	↑ 1.31	0.0015
orotate	00226	↑ 1.21	0.023
guanine	00132	↑ 1.16	0.0026
guanosine	00133	↑ 1.12	0.015
guanosine-2',3'-cyclic monophosphate	11629	↑ 1.11	0.046
hypoxanthine	00157	↑ 1.08	0.046
cytidine	00089	↑ 1.06	0.035
§guanosine 2'-monophosphate (2'-GMP)	-	↑ 1.06	0.036
2'-deoxyuridine	00012	↑ 1.05	0.043
cytidine 3'-monophosphate (3'-CMP)	-	↓ 0.94	0.015
cytidine 5'-monophosphate (5'-CMP)	00095	↓ 0.91	0.0071
adenosine	00050	↓ 0.89	0.0015
Cofactor and Vitamin			
pyridoxate	00017	↑ 1.19	0.020
pyridoxamine	01431	↓ 0.80	0.026
Phytochemicals/Other			
beta-guanidinopropanoate	13222	↑ 1.74	0.00042
harmane	-	↑ 1.62	7.51E-05
nicotianamine	-	↑ 1.52	0.029
4-hydroxybenzoate	00500	↑ 1.40	0.00062
salicylate	01895	↑ 1.25	0.019
pyrraline	-	↑ 1.24	0.0057
2-oxindole-3-acetate	-	↑ 1.22	0.019
daidzein	03312	↓ 0.86	0.040

Table 2.3. Statistically-significant metabolites from *L. paracasei* supernatant prepared in the presence and absence of rice bran extract

Metabolite	HMDB*	Fold Difference†	p-value‡
2-ketogluconate	-	↓ 0.68	0.0066
N-glycolylneuraminate	00833	↓ 0.61	0.011

* Human metabolome database (**HMDB**) numbers are given when available.
† For each metabolite, fold difference is expressed as the scaled relative abundance in LP+RBE over LP; Arrows indicate the direction of change between treatments.
‡ Each metabolite presented has a statistically-significant ($P<0.05$) fold difference, as determined by a Welch's Two-Sample t-Test.
§Indicates compounds that have not been officially confirmed based on a standard, but second-order identity in Metabolon Inc. library.

The lipid metabolite changes included, but were not limited to medium-chain, branched chain, long-chain and other fatty acids **(Figure 2.5A)**. Fold differences **(FD)** between lipids, when comparing LP+RBE to LP included: linoleate (3.18 FD), 13-HODE + 9-HODE (2.11 FD), eicosenoate (1.65 FD), 10-hydroxystearate (1.49 FD), maleate (1.44 FD), oleate/vaccenate (1.26 FD), azelate (1.18 FD), glycerol 3-phosphate (1.05 FD), alpha-hydroxyisocaproate (0.86 FD), alpha-hydroxyisovalerate (0.85 FD), trimethylamine N-oxide (0.82 FD), 3-hydroxyoctanoate (0.74 FD), 3-hydroxydecanoate (0.70 FD), 3-hydroxylaurate (0.65 FD), pinitol (0.61 FD), and 5-dodecenoate (0.58 FD).

Fold differences between amino acids/peptides when comparing LP+RBE to LP included: methionine sulfone (8.29 FD), 3-sulfo-L-alanine (2.34 FD), indole-3-carboxylic acid (1.94 FD), kynurenate (1.44 FD), 1-methylguanidine (1.34 FD), imidazole propionate (1.28 FD), cysteine s-sulfate (1.24 FD), succinimide (1.22 FD), 4-guanidinobutanoate (1.19 FD), N-formylphenylalanine (1.18 FD), asparagine (1.17 FD), N-acetylhistidine (1.13 FD), N6-formyllysine (1.13 FD), 4-imidazoleacetate (1.12 FD), phenethylamine (1.07 FD), creatinine (1.08 FD), carnitine (1.03 FD), proline (1.03 FD), leucine (1.03 FD), histamine (0.94 FD), acetylcarnitine (0.90 FD), N-acetyltryptophan (0.88 FD), N-acetylserine (0.87 FD), spermine (0.70 FD), indolelactate (0.68 FD), cystathionine (0.67 FD), methionine (0.64 FD), hypotaurine

(0.46 FD), and S-adenosylhomocysteine (0.39 FD) **(Figure 2.5B).** A literature search of the significant metabolites in the comparison of LP+RBE to LP revealed metabolites with established antimicrobial activities, many of which included the above lipids and amino acids/peptides **(Table 2.4)**.

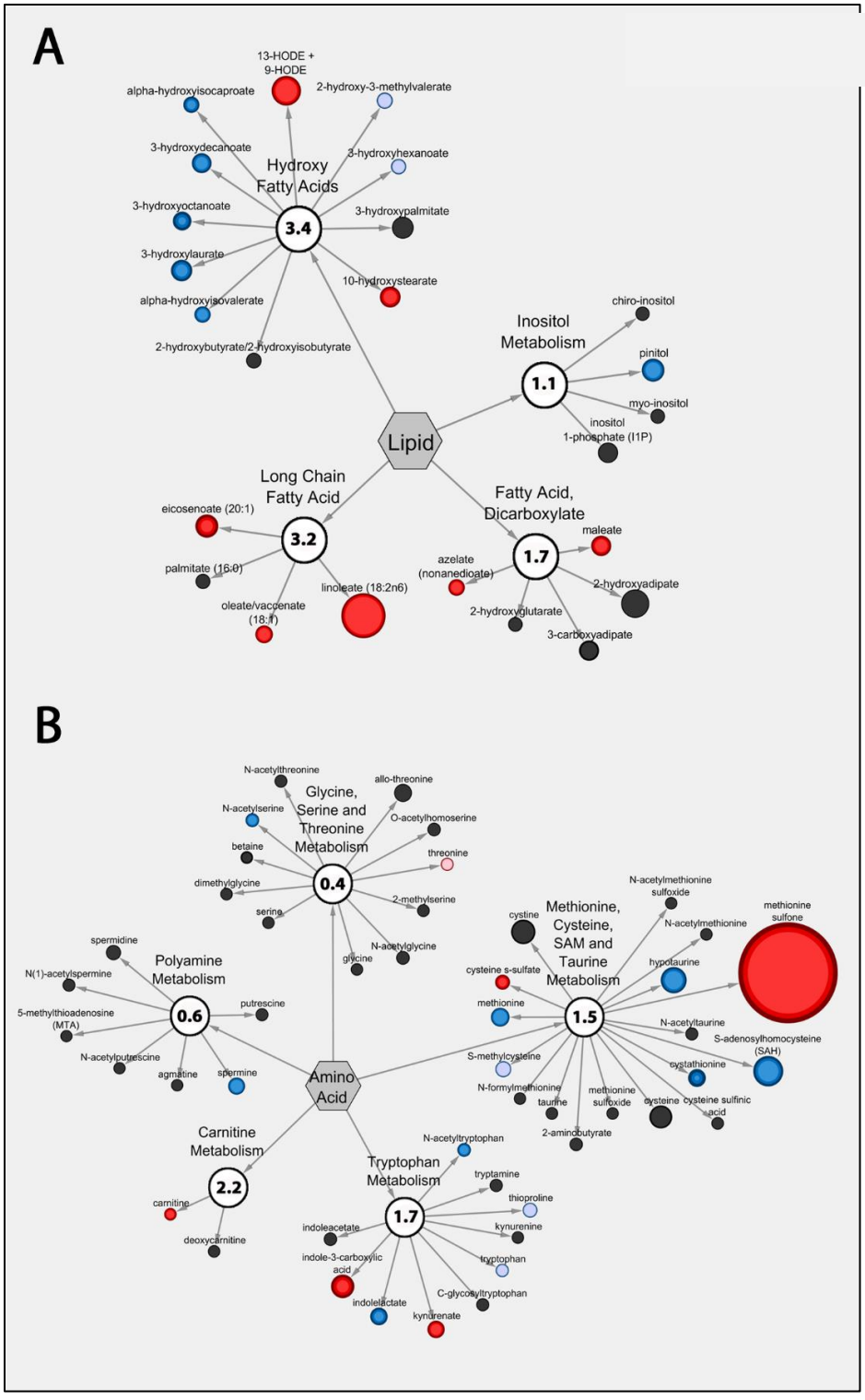

Figure 2.5. Cytoscape visualization illustrates the metabolic pathways most differentially regulated between treatments.

Cytoscape visualization of ***(A)*** *lipid and* ***(B)*** *amino acid metabolic pathways that differ between LP and LP+RBE. For each metabolite, node diameter is proportional to the fold*

difference in LP+RBE compared to LP. Node colors indicate the direction of a metabolite's fold difference, where red indicates metabolites with a higher scaled abundance in LP+RBE ($P<0.05$), blue indicates lower abundance in LP+RBE ($P<0.05$), pink indicates trending higher in LP+RBE ($0.05<P<0.10$), and light blue indicates trending lower in LP+RBE ($0.05<P<0.10$). Black nodes indicate metabolites with fold differences that were not significantly altered between treatments. The pathway enrichment score is the number in the circles for each sub-classification.

2.4.4. Visualization of metabolic pathways between LP+RBE and LP supernatant treatments:

The Cytoscape software visualization tool in MetaboLync © was used to highlight lipids **(Figure 2.5A)** and amino acids/peptides **(Figure 2.5B)** in LP+RBE and LP that contained metabolites with reported antimicrobial functions from **Table 2.4**. For a given metabolite, node color indicated the direction and statistical significance, and node diameter indicated the magnitude of the fold difference. A pathway enrichment score was calculated for each metabolic pathway as described in the methods. Lipid metabolic pathways visualized, in descending order of pathway enrichment score were: hydroxy fatty acids (3.4), long chain fatty acids (3.2), dicarboxylate fatty acid (1.7), and inositol (1.1) **(Figure 2.5A)**. Amino acid/peptide metabolic pathways visualized, in descending order of pathway enrichment score were: carnitine (2.2), tryptophan (1.7), methionine, cysteine, S-adenosyl methionine and taurine (1.5), polyamine (0.6), and glycine, serine, and threonine (0.4) **(Figure 2.5B)**.

Table 2.4. Metabolites from *L. paracasei* supernatant prepared in the presence and absence of rice bran extract with reported antimicrobial activities

	Fold Difference*	p value†	Functions	References
Amino Acids/Peptides				
methionine sulfone	↑ 8.29	3.16E-06	Inhibits *S.* Typhimurium growth by blocking glutamate synthesis.	(Hentchel and Escalante-Semerena, 2015)
indole-3-carboxylic acid	↑ 1.94	0.00065	Inhibited the growth of *Staphylococcus aureus*, *Pseudomonas aeruginosa*, *Candida albicans*, *Escherichia coli*, *Klebsiella pneumoniae*, and multidrug resistant strains of these species.	(Hinton and Ingram (2000)
carnitine	↑ 1.03	0.034	Inhibited the growth of *Streptococcus agalactiae in-vitro*.	(Atroshi *et al.*, 1998)
N-acetylserine	↓ 0.87	0.037	May increase the susceptibility of *S.* Typhimurium to methicillin *in-vitro* by modifying cysteine metabolism.	(Oppezzo and Anton, 1995)
spermine	↓ 0.70	0.044	May increase susceptibility of *S.* Typhimurium and other bacteria to Beta-lactam antibiotics.	(Kwon and Lu, 2007)
S-adenosyl-homocysteine	↓ 0.39	0.001	In high enough concentrations it can inhibit bacterial S-adenosyl methionine metabolism, which is important for quorum sensing and polyamine synthesis.	(Parveen and Cornell, 2011; Simms and Subbaramaiah, 1991)
Tricarboxylic Acid Cycle				
tricarballylate	↑ 1.79	6.83E-05	Toxic to *S. enterica* if accumulated to high levels.	(Boyd *et al.*, 2012)
Lipids				
3-hydroxyoctanoate	↓ 0.74	0.0015	3-hydroxyoctanoate and its derivatives inhibited the growth of *S.* Typhimurium, *E. coli*, *S. aureus*, *L. monocytogenes*, *P. aeruginosa*, *C. albicans* and *Microsporum gypseum*.	(Radivojevic *et al.*, 2016)
linoleate (18:2n6)	↑ 3.18	0.0075	Bactericidal and bacteriostatic against *S. aureus*, *Streptococcus pyogenes*, and *E. coli* by inhibiting fatty acid synthesis.	(Zheng *et al.*, 2005)
13-Hydroxy-octadecadienoate/ 9-Hydroxy-10,12-octadecadienoate	↑ 2.11	0.0082	Detected in an oxylipin extract that inhibited growth of *Penicillium funiculosum* and *Enterococcus hirae in-vitro*.	(Martin-Arjol *et al.*, 2010)

Table 2.4. Metabolites from *L. paracasei* supernatant prepared in the presence and absence of rice bran extract with reported antimicrobial activities

	Fold Difference*	p value†	Functions	References
maleate	↑ 1.44	0.017	Reduced the growth of *S.* Typhimurium on refrigerated turkey frankfurters.	(Gadang *et al*., 2008)
‡oleate/vaccenate (18:1)	↑ 1.26	0.041	Reduced growth of pathogens on poultry skin, including *S.* Typhimurium and prevented fatty acid elongation in a variety of pathogens.	(Hinton and Ingram, 2000; Zheng *et al.*, 2005)
azelate (nonanedioate)	↑ 1.18	0.024	Reduced growth of *S. aureus*, *Staphylococcus epidermidis*, and *Propionibacterium acnes* in *vitro*.	(Charnock *et al*., 2004)
alpha-hydroxyisocaproate	↓ 0.86	0.016	Bactericidal against several strains of both gram-negative and gram-positive bacteria in *vitro*.	(Sakko *et al.*, 2012)
pinitol	↓ 0.61	0.015	Synergistically enhances the potency of beta-lactam antimicrobials by lowering the effective dose 8-fold. As part of an *Ademsia aegiceras* extract, it had bacteriostatic and/or bactericidal effects against *S. aureus*, *E. coli*, *Proteus mirabilis*, and *Pseudomonas aeruginosa*.	(Ahmad *et al.*, 2016)
Nucleotides				
‡hypo-xanthine	↑ 1.08	0.046	Inhibits *Salmonella enteriditis* and *Escherichia coli* growth when added to breast milk.	(Al-Shehri *et al.*, 2015)
Other Phytochemicals				
harmane	↑ 1.62	7.51E-05	Inhibits the growth of and functions as a bactericidal agent against *Salmonella* spp. and other pathogens in *vitro* by intercalating with DNA.	(Arshad *et al.*, 2008; Cowan, 1999)
4-hydroxybenzoate	↑ 1.40	0.00062	Inhibited the growth of *S. aureus*, *E. coli*, *Saccharomyces cerevisiae*, and *Fusarium culmorum* in *vitro*.	(Kosová *et al.*, 2015)
daidzein	↓ 0.86	0.040	Extracted from soy milk, where it inhibited the growth of *S.* Typhimurium, and a variety of enteric pathogens.	(Chin *et al.*, 2012)
2-keto-gluconate	↓ 0.68	0.0066	Reduced the growth of a variety of microorganisms in studies evaluating secondary metabolites produced by *Pseudomonas fluorescens*.	(Cheng *et al.*, 2015)

Table 2.4. Metabolites from *L. paracasei* supernatant prepared in the presence and absence of rice bran extract with reported antimicrobial activities

	Fold Difference*	p value†	Functions	References

*For each metabolite, fold difference is expressed as the scaled relative abundance in LP+RBE over LP. Arrows indicate the direction of change between treatments.
†All metabolites presented have a statistically-significant ($p<0.05$) fold difference as determined by a Welch's Two-Sample t-Test.
‡ Indicates compounds that have not been officially confirmed based on a standard, but second-order identity in Metabolon Inc. library.

2.5. Discussion:

This study demonstrated that a synbiotic of *L. paracasei* and RBE contains small molecules with the capacity to reduce *S.* Typhimurium growth and appeared to function through pH-independent mechanisms (**Figure 2.2 and 2.3**). The metabolome of LP and LP+RBE identified 84 small molecules that could explain how LP+RBE reduced *S.* Typhimurium growth more effectively than LP **(Table 2.3)**. The presence of MRS components did not contribute to treatment differences between LP and LP+RBE because each treatment contained identical amounts of MRS media. The MRS and MRS+RBE media had similar compounds identified from both LP and LP+RBE treatments respectively, and therefore the differential effects of LP and LP+RBE were distinguished by fold differences in the compounds measured between the two treatment groups. The metabolite differences were measured by the relative abundances for each metabolite and were attributed to *L. paracasei* metabolism of RBE. Given that these metabolites identified had antimicrobial activities against a variety of pathogens **(Table 2.4),** there is promising potential for these supernatants to be used with a broad spectrum of pathogen protection applications relevant to food safety as well as human and animal health.

RBE-mediated alterations to *L. paracasei* lipid metabolism, primarily fatty acid production, may explain how LP+RBE can reduce *S.* Typhimurium growth more than *L. paracasei* alone. Bacterial production of fatty acids may occur through fermentation of complex carbohydrates,

catabolism of complex lipids with fatty acid moieties, de-novo fatty acid synthesis, or via the bioconversion of amino acids into fatty acids (Buccioni *et al.*, 2012). Maleate, azelate, alpha-hydroxyisocaproate, lineolate, oleate/vaccenate and 13-hydroxyoctadecadienoate (**HODE**) were abundant in LP+RBE compared to LP and had reported antimicrobial activity. Maleate is commonly used as a bacteriostatic agent against *S.* Typhimurium on frankfurters (Gadang *et al.*, 2008). Azelate is used as a topical dermatosis agent to reduce the growth of *S. aureus*, *S. epidermidis*, and *P. acnes* (Charnock *et al.*, 2004). Both maleate and azelate are present in the rice plant (Cheng *et al.*, 2015; Ryan *et al.*, 2011), and *L. paracasei* metabolism increases their bioavailability. Linoleate is also detected at high levels in rice bran (Aminnezhad *et al.*, 2015). Multiple species of lactobacilli have the capability to produce linoleic acid, as well as catabolize linoleic acid into oleate/vaccenate and 13-HODE (Black *et al.*, 2013; Druart *et al.*, 2014). Collectively, these fatty acids in LP+RBE demonstrated to have bacteriostatic functions against multiple pathogenic microorganisms, including *S.* Typhimurium, and this may be mediated in part due to interference with bacterial fatty acid synthesis (Hinton and Ingram, 2000; Martin-Arjol *et al.*, 2010; Zheng *et al.*, 2005).

In addition to lipids, RBE amino acids and small peptides serve as another metabolite source that *L. paracasei* can bio-convert into different compounds or catabolize into free amino acids with antimicrobial functions (Neis *et al.*, 2015). Alterations to methionine and tryptophan metabolism may serve as major mechanisms by which RBE enhances the antimicrobial activity of *L. paracasei* against *S.* Typhimurium. Methionine sulfone (8.29-fold increase in LP+RBE), which forms during methionine oxidation, has been shown to inhibit *S.* Typhimurium growth by blocking glutamate synthesis (Hentchel and Escalante-Semerena, 2015). Lactobacilli modulate the oxidative state of their environment by producing hydrogen peroxide (Pessione, 2012). The

supernatant environment created by LP+RBE, coupled with normal hydrogen peroxide production by *L. paracasei* may facilitate methionine oxidation into methionine sulfone. Although methionine sulfone is typically considered a marker of oxidative damage (Hoshi and Heinemann, 2001), its presence in controlled amounts may be beneficial as an antimicrobial defense. Multiple studies have investigated the roles of *Lactobacillus* spp. in tryptophan metabolism, which have linked the production of tryptophan-derived metabolites to modulations of the mucosal immune and enteric nervous systems (Clarke *et al.*, 2014; Zelante *et al.*, 2013). Indole-3-carboxylic acid was increased and is synthesized from tryptophan by both plant and microbial species (Böttcher *et al.*, 2014; Kavitha *et al.*, 2010). As an antimicrobial agent, indole-3-carboxylic acid has been shown to inhibit the growth of a variety of bacterial and fungal pathogens, including multi-drug resistant bacteria (Zutz *et al.*, 2016). In the presence of RBE, *L. paracasei* may increase its production or the bioavailability of indole-3-carboxylic acid during tryptophan metabolism.

Metabolism of RBE by *L. paracasei* may have increased the bioavailability of other rice bran phytochemicals, including harmane and 4-hydroxybenzoate **(Table 2.3)**. Harmane is a beta-carboline alkaloid present in plants and has been shown to have growth inhibitory and bactericidal effects against some *Salmonella* spp. (Arshad *et al.*, 2008) and works mechanistically to intercalate DNA (Cowan, 1999). Four-hydroxybenzoate, a derivative of benzoic acid produced by plants and some species of bacteria, has been demonstrated to reduce the growth of a variety of gram positive and negative bacteria, yeasts, and molds (Kosová *et al.*, 2015; Peng *et al.*, 2006). Increased expression of both hypoxanthine and tricarballylate in LP+RBE suggested that RBE modulations to *L. paracasei* nucleotide and TCA cycle metabolism are important to its *S.* Typhimurium growth-inhibitory properties **(Table 2.3)**. Tricarballylate

was reported to inhibit citric acid cycle enzymes and was reported to have toxic effects on *S. enterica* when it was accumulated intracellularly at high levels (Boyd *et al.*, 2012). Past investigations have associated tricarballylate production with the metabolic activity of healthy intestinal and rumen flora (Cook *et al.*, 1994; McDevitt and Goldman, 1991) suggesting that in the presence of RBE, *L. paracasei* may increase the production of tricarballylate to levels that *S.* Typhimurium cannot tolerate so that it has a decreased ability to replicate and/or invade host cells.

Four of the lipid groups and three of the amino acid groups had pathway enrichment scores greater than one, indicating these pathways contribute to LP+RBE effects on growth inhibition. For example, spermine and pinitol decreased 0.70-fold and 0.61-fold in LP+RBE, yet in past investigations they increased the function of methicillin and beta-lactam antimicrobials respectively (Ahmad *et al.*, 2016; Kwon and Lu, 2007). These studies suggest that regardless of absolute or relative metabolite abundance, the mere presence or absence of metabolites within the supernatant influence the functions of other metabolites present in the supernatant. The level of inhibition, antagonism, additive or synergistic functions for a given combination of metabolites in the supernatant is complex to investigate as a bioactive mixture, and the reductionist approaches needed may yield conflicting results. Thus, the relationships between metabolites, for inhibition of pathogen growth, remains an area of ongoing investigation that can be further explored with targeted metabolite profile analyses and merits consideration of bioactivity-guided fractionation methods. The metabolomics investigation conducted herein compared the mechanisms of LP+RBE and LP alone by looking at levels of metabolite abundance and metabolic pathway activity. In order to distinguish the unique mechanisms by which RBE modulates *L. paracasei* metabolism, the metabolome could be compared with gene

expression levels obtained from meta-transcriptomics and genomics analyses of LP+RBE and LP. This approach would seek to determine direct changes to *L. paracasei* gene expression of metabolic enzymes in the presence of RBE. Evaluating the small molecule profiles of a symbiotic should integrate information from metabolites, overlapping pathways, and metabolic networks to provide a comprehensive understanding of overall function.

The experiments described herein illustrated the *in-vitro* efficacy of Pro+RBE over Pro alone in reducing *S.* Typhimurium growth, and warrant investigation for the efficacy of Pro+RBE against other enteric pathogens. These data, demonstrating enhanced antimicrobial activity of Pro+RBE, support results from various animal models (Kumar *et al.*, 2012; Yang *et al.*, 2015). In mice, rice bran simultaneously reduced *S.* Typhimurium shedding and promoted *Lactobacillus* growth (Kumar *et al.*, 2012), and in pigs, there was less diarrhea from Rotavirus (Yang *et al.*, 2015), suggesting that Pro+RBE may benefit the host for prevention of pathogen colonization, and for the host immune system to mount a protective response before the onset of extensive disease. The dose of RBE used in these studies has influenced the observable levels of pathogen inhibition, and future investigations merit attention to RBE dose with an intact and varied microbiome composition and structure for demonstrating antimicrobial activities with *L. paracasei*. Given the growing concern for antimicrobial resistance in *S.* Typhimurium, alternative treatments and preventive measures are needed. Understanding the metabolite profile of a synbiotic can lead to a comprehensive understanding for how food components enhance the natural antimicrobial activity of *L. paracasei*. In an era of multidrug resistance, synbiotics of *Lactobacillus* and rice bran have strong potential to provide broad-spectrum protection against many pathogens by serving as viable, natural alternatives, or by applications in combination with standard antimicrobial drugs to reduce the dosages needed to be efficacious.

REFERENCES

Agarrwal, R., et al., (2016) Metabolic and transcriptomic changes induced in host during hypersensitive response mediated resistance in rice against the Asian rice gall midge. *Rice* 9, 5.

Ahmad, F., et al., (2016) Synergistic effect of (+)-pinitol from *Saraca asoca* with beta-lactam antibiotics and studies on the in silico possible mechanism. *J Asian Nat Prod Res* 18, 172-83.

Al-Shehri, S., et al., (2015) Breastmilk-saliva interactions boost innate immunity by regulating the oral microbiome in early infancy. *PLoS ONE* 10.

Aminnezhad, S., Kermanshahi, R. K. and Ranjbar, R. (2015) Evaluation of synergistic interactions between cell-free supernatant of lactobacillus strains and amikacin and genetamicin against *Pseudomonas aeruginosa*. *Jundishapur J Microbiol,* 8.

Arbulu, M., et al., (2015) Untargeted metabolomic analysis using liquid chromatography quadrupole time-of-flight mass spectrometry for non-volatile profiling of wines. *Analytica Chimica Acta* 858, 32-41.

Arshad, N., et al., (2008) Effect of *Peganum harmala* or its beta-carboline alkaloids on certain antibiotic resistant strains of bacteria and protozoa from poultry. *Phytother Res* 22, 1533-8.

Atroshi F., Rizzo A., Westermarck T. and Ali-vehmas T. (1998) Effects of tamoxifen, melatonin, coenzyme Q10, and L-carnitine supplementation on bacterial growth in the presence of mycotoxins. Pharmacol Res 38, 289–295.

Black, B. A., et al., (2013) Antifungal hydroxy fatty acids produced during sourdough fermentation: microbial and enzymatic pathways, and antifungal activity in bread. *Appl Environ Microbiol* 79, 1866-1873.

Böttcher, C., et al., (2014) The biosynthetic pathway of indole-3-carbaldehyde and indole-3-carboxylic acid derivatives in *Arabidopsis*. *Plant Physiol* 165, 841-853.

Boyd, J. M., Teoh, W. P. and Downs, D. M. (2012). Decreased transport restores growth of a *Salmonella enterica* apbC mutant on tricarballylate. *J Bacteriol* 194, 576-583.

Brown, D. G., et al., (2016) Metabolomics and metabolic pathway networks from human colorectal cancers, adjacent mucosa, and stool. *Cancer Metab* 4, 11.

Buccioni, A., et al., (2012) Lipid metabolism in the rumen: New insights on lipolysis and biohydrogenation with an emphasis on the role of endogenous plant factors. *Anim Feed Sci and Technol* 174, 1-25.

Caridi, A. (2002) Selection of *Escherichia coli*-inhibiting strains of *Lactobacillus paracasei subsp. paracasei*. *J Ind Microbiol Biotechnol* 29, 303-8.

Charnock, C., Brudeli, B. and Klaveness, J. (2004) Evaluation of the antibacterial efficacy of diesters of azelaic acid. *Eur J Pharm Sci* 21, 589-96.

Cheng X. and van deer Vort M. and Raaijmakers J.M., (2015) Gac-mediated changes in pyrroquinoline quinone biosynthesis enhance the antimicrobial activity of Pseudomonas fluorescens SBW25. Environ Microbiol Rep 7, 139–147.

Chiang, S.S. and Pan, T.M. (2012) Beneficial effects of *Lactobacillus paracasei subsp. paracasei* NTU 101 and its fermented products. *J Appl Microbiol and Biotechnol* 93, 903-916.

Chin, Y.P., et al., (2012) Bactericidal activity of soymilk fermentation broth by in vitro and animal models. *J Med Food* 15, 520-526.

Clarke, G., et al., (2014) Minireview: Gut microbiota: the neglected endocrine organ. *Mol Endocrinol* 28, 1221-38.

Cook, G. M., Wells, J. E. and Russell, J. B. (1994) Ability of *Acidaminococcus fermentans* to oxidize trans-aconitate and decrease the accumulation of tricarballylate, a toxic end product of ruminal fermentation. *Appl Environ Microbiol* 60, 2533-7.

Cowan, M. M. (1999) Plant products as antimicrobial agents. *Clin Microbiol Rev* 12, 564-582.

Druart, C., et al., (2014) Modulation of the gut microbiota by nutrients with prebiotic and probiotic properties. *Adv Nutr* 5, 624S-633S.

FAO, (2006) Probiotics in food: Health and nutritional properties and guidelines for evaluation. *FAO Food Nutr Pap* 85, 50.

Gadang, V. P., et al., (2008) Evaluation of antibacterial activity of whey protein isolate coating incorporated with nisin, grape seed extract, malic acid, and EDTA on a turkey frankfurter system. *J Food Sci* 73, M389-94.

Goodyear, A., et al., (2015) Dietary rice bran supplementation prevents *Salmonella* colonization differentially across varieties and by priming intestinal immunity. *J Funct Foods* 18, Part A, 653-664.

Henderson, A. J., et al., (2012) Consumption of rice bran increases mucosal immunoglobulin A concentrations and numbers of intestinal *Lactobacillus* spp. *J Med Food* 15.

Hentchel, K. L. and Escalante-Semerena, J. C. (2015) In *Salmonella enterica*, the Gcn5-related acetyltransferase MddA (formerly YncA) acetylates methionine sulfoximine and methionine sulfone, blocking their toxic effects. *J Bacteriol* 197, 314-25.

Heredia-Castro, P. Y., et al., (2015) Antimicrobial activity and partial characterization of bacteriocin-like inhibitory substances produced by *Lactobacillus* spp. isolated from artisanal mexican cheese. *J Dairy Sci* 98, 8285-93.

Hinton, A., Jr. and Ingram, K. D. (2000) Use of oleic acid to reduce the population of the bacterial flora of poultry skin. *J Food Prot* 63, 1282-6.

Hoshi, T. and Heinemann, S. H. (2001) Regulation of cell function by methionine oxidation and reduction. *J Physiol (Khanna et al.)* 531, 1-11.

Kaur, A., Jassal, V., Thind, S. S. and Aggarwal, P. (2012) Rice bran oil an alternate bakery shortening. *J Food Sci Technol* 49, 110-4.

Kavitha, A., Prabhakar, P., Vijayalakshmi, M. and Venkateswarlu, Y. (2010) Purification and biological evaluation of the metabolites produced by *Streptomyces* sp. TK-VL_333. *Res Microbiol* 161, 335-45.

Kim, G. R., et al., (2014) Combined mass spectrometry-based metabolite profiling of different pigmented rice (*Oryza sativa L.*) seeds and correlation with antioxidant activities. *Molecules* 19, 15673-86.

Koistinen, V. M., et al., (2016) Changes in the phytochemical profile of rye bran induced by enzymatic bioprocessing and sourdough fermentation. *Food Res Int* [no pagination].

Kosová, M., et al., (2015) Antimicrobial effect of 4-hydroxybenzoic acid ester with glycerol. *J Clin Pharm Ther* 40, 436-440.

Kumar, A., et al., (2012) Dietary rice bran promotes resistance to *Salmonella enterica* serovar Typhimurium colonization in mice. *BMC Microbiol* 12, 1-9.

Kwon, D.H. and Lu, C. D. (2007) Polyamine Effects on antibiotic susceptibility in bacteria. *Antimicrob Agents Chemother* 51, 2070-2077.

Lievin-Le Moal, V., Amsellem, R. and Servin, A. L. (2011). Impairment of swimming motility by antidiarrheic *Lactobacillus acidophilus* strain LB retards internalization *of Salmonella enterica* serovar Typhimurium within human enterocyte-like cells. *Antimicrob Agents Chemother* 55, 4810-20.

Martin-Arjol, I., et al., (2010) Identification of oxylipins with antifungal activity by LC-MS/MS from the supernatant of *Pseudomonas* 42A2. *Chem Phys Lipids* 163, 341-6.

Mcdevitt, J. and Goldman, P. (1991) Effect of the intestinal flora on the urinary organic acid profile of rats ingesting a chemically simplified diet. *Food Chem Toxicol* 29, 107-13.

Mozzi, F., et al., (2013) Metabolomics as a tool for the comprehensive understanding of fermented and functional foods with lactic acid bacteria. *Food Res Int* 54, 1152-1161.

Neis, E. P. J. G., Dejong, C. H. C. and Rensen, S. S. (2015) The role of microbial amino acid metabolism in host metabolism. *Nutrients* 7, 2930-2946.

Oppezzo, O. J. and Anton, D. N. (1995) Involvement of cysB and cysE genes in the sensitivity of *Salmonella* Typhimurium to mecillinam. *J Bacteriol* 177, 4524-7.

Parveen, N. and Cornell, K. A. (2011) Methylthioadenosine/S-adenosylhomocysteine nucleosidase, a critical enzyme for bacterial metabolism. *Mol Microbiol* 79, 7-20.

Peng, X., et al., (2006) Discovery of a marine bacterium producing 4-Hydroxybenzoate and its alkyl esters, parabens. *Appl Environ Microbiol* 72, 5556-5561.

Pessione, E. (2012) Lactic acid bacteria contribution to gut microbiota complexity: lights and shadows. *Front Cell Infect Microbiol* 2, 86.

Radivojevic, J., et al., (2016) Polyhydroxyalkanoate-based 3-hydroxyoctanoic acid and its derivatives as a platform of bioactive compounds. *Appl Microbiol Biotechnol* 100, 161-72.

Ryan, E. P., et al., (2011) Rice bran fermented with *Saccharomyces boulardii* generates novel metabolite profiles with bioactivity. *J Agric Food Chem* 59, 1862-70.

Sakko, M., et al., (2012) 2-Hydroxyisocaproic acid (HICA): a new potential topical antibacterial agent. *Int J Antimicrob Agents* 39, 539-540.

Settachaimongkon, S., et al., (2014) Influence of different proteolytic strains of *Streptococcus thermophilus* in co-culture with *Lactobacillus delbrueckii* subsp. bulgaricus on the metabolite profile of set-yoghurt. *Int J Food Microbiol,* 177, 29-36.

Simms, S. A. and Subbaramaiah, K. (1991) The kinetic mechanism of S-adenosyl-L-methionine: glutamylmethyltransferase from *Salmonella* Typhimurium. *J Biol Chem* 266, 12741-6.

Tsolis, R. M., et al., (1999) Identification of a putative *Salmonella enterica* serotype Typhimurium host range factor with homology to IpaH and YopM by signature-tagged mutagenesis. *Infect Immun* 67, 6385-93.

Valerio, F., et al., (2013) Bioprotection of ready-to-eat probiotic artichokes processed with *Lactobacillus paracasei* LMGP22043 against foodborne pathogens. *J Food Sci* 78, M1757-63.

Vitali, B., et al., (2010) Impact of a synbiotic food on the gut microbial ecology and metabolic profiles. *BMC Microbiol* 10, 4.

Wang, Y., et al., (2012) *Lactobacillus rhamnosus* GG culture supernatant ameliorates acute alcohol-induced intestinal permeability and liver injury. *Am J Physiol-Gastrointes Liver Physiol* 303, G32-G41.

Weir, T. L., et al., (2013). Stool Microbiome and metabolome differences between colorectal cancer patients and healthy adults. *PLoS ONE* 8.

Yang, X., et al., (2015) High protective efficacy of rice bran against human rotavirus diarrhea via enhancing probiotic growth, gut barrier function, and innate immunity. *Sci Rep* 5, 15004.

Zelante, T., et al., (2013) Tryptophan catabolites from microbiota engage aryl hydrocarbon receptor and balance mucosal reactivity via interleukin-22. *Immunity* 39, 372-85.

Zheng, C. J., et al., (2005) Fatty acid synthesis is a target for antibacterial activity of unsaturated fatty acids. *FEBS Lett* 579, 5157-62.

Zutz, C., et al., (2016) Valproic acid induces antimicrobial compound production in doratomyces microspores. *Front Microbiol* 7, 510.

CHAPTER THREE

CELL-FREE SUPERNATANT METABOLOMES FROM *LACTOBACILLUS* SPP. AND RICE BRAN SYNBIOTICS ARE ASSOCIATED WITH DIFFERENTIAL GROWTH SUPPRESSION OF ANTIMICROBIAL RESISTANT *SALMONELLA* TYPHIMURIUM

3.1. Summary:

3.1.1 BACKGROUND:

Increasing antimicrobial resistance in *Salmonella* Typhimurium complicates salmonellosis treatment. Rice bran was shown to reduce *S.* Typhimurium shedding in mice while simultaneously increasing *Lactobacillus* spp. In a follow-up study, rice bran enhanced *L. paracasei* growth suppression of *S.* Typhimurium by increasing antimicrobial metabolite production. Given their inherent metabolic diversity, the current study examined three *Lactobacillus* spp. (*L. fermentum*, *L. paracasei*, *L rhamnosus*) in the presence and absence of rice bran for growth suppression of two *S.* Typhimurium isolates with and without phenotypic multidrug resistance. The global, non-targeted metabolomic profiles of cell-free supernatants were profiled to compare *Lactobacillus* spp. metabolism of rice bran and antimicrobial compound production.

3.1.2. RESULTS:

While rice bran did not increase the growth of any *Lactobacillus* spp., the *L. fermentum* + rice bran and *L. paracasei* + rice bran treatments exhibited 9.04%-11.53% and 42.47%-55.21% enhanced growth suppression respectively against phenotypically non-resistant

Salmonella and multidrug-resistant *Salmonella* when compared to their *Lactobacillus*-only treatments. A lower concentration of cell-free supernatant + rice bran was needed to maximally suppress growth of the antimicrobial-resistant *Salmonella* isolate (18% v/v) compared to non-resistant *Salmonella* (22% v/v). The global, non-targeted metabolome identified 23 metabolic pathways containing 87 metabolites that distinguished the two effective *L. fermentum* + rice bran and *L. paracasei* + rice bran treatments, most notably across amino acid, lipid, carbohydrate and nucleotide metabolism. Forty-two of these metabolites had previously-reported antimicrobial functions.

3.1.3. CONCLUSIONS:

Rice bran modulates *Lactobacillus* suppression of *Salmonella* in a species-dependent manner and drives distinct differences in antimicrobial compound production in their cell-free supernatant metabolomes, suggesting that synbiotics prepared with different *Lactobacillus* spp. suppress *Salmonella* growth via species-specific small molecule mechanisms. These results emphasize that probiotic species metabolic differences should be considered when preparing synbiotics to treat salmonellosis. Furthermore, this study illustrates that different synbiotics doses may be needed to treat multidrug resistant pathogens compared to non-resistant pathogens. The metabolites identified in this study warrant further mechanistic action for their effects on *Salmonella* growth suppression and highlight the potential of *Lactobacillus* + rice bran synbiotics to be evaluated as a sustainable alternative or adjunctive treatment to conventional antimicrobial agents.

3.2 Introduction:

Globally, *Salmonella enterica* serovar Typhimurium is a leading cause of human foodborne diarrhea that causes over 1 million disease outbreaks annually (CDC, 2018c), and escalating antimicrobial resistance accounts for an estimated 100,000 cases of salmonellosis each year. Antimicrobial resistance across *Salmonella* Typhimurium isolates spans multiple drug classes including penicillin, sulfonamides, tetracyclines, fluoroquinolones, aminoglycosides, cephalosporins, and carbapenems, which are frequently used to treat *Salmonella* and many other human and animal pathogens (Fernandez *et al.*, 2018; Lamas *et al.*, 2018). Current approaches to combat antimicrobial resistance focus on developing new antimicrobial agents by modifying compounds from existing drug classes (Aminov, 2017). However, there has been a marked decline in the discovery of new antimicrobial agents (Aminov, 2017), and alternative approaches for preventing and treating salmonellosis are warranted.

A growing body of research examines of probiotic health-promoting microorganisms and as an alternative means of preventing and reducing *Salmonella* outbreaks (Distrutti *et al.*, 2016; Luoma *et al.*, 2017; Markowiak and Slizewska, 2017; Nealon *et al.*, 2017a). Among probiotic bacteria, the genetically and metabolically-diverse *Lactobacillus* spp. have been routinely shown to suppress the growth of *Salmonella* Typhimurium, and they exhibit species differences in these growth suppressive capacities (Marianelli *et al.*, 2010). Emerging evidence supports that combining *Lactobacillus* spp. probiotics with prebiotic nutrient sources can produce synbiotics that enhance the antimicrobial activity of *Lactobacillus* spp. (Piatek *et al.*, 2019). While many synbiotics use purified carbohydrates as prebiotics, whole foods have promising synbiotic functions and include whole grain wheat, cooked beans, and the rice bran milled from brown rice (Han *et al.*, 2018; Sheflin *et al.*, 2017; Vitaglione *et al.*, 2015; Zarei *et al.*, 2017). Among these,

rice bran is a rich and diverse source of carbohydrates, lipids, amino acids and vitamins/cofactors (Zarei *et al.*, 2017) and as a prebiotic, rice bran has been shown to enhance *Lactobacillus* growth in people, mice, pigs, and broiler chickens (Nealon *et al.*, 2017b; Rubinelli *et al.*, 2017; Sheflin *et al.*, 2017; Zarei *et al.*, 2017).

During rice bran fermentation, *Lactobacillus* spp. secrete short and long-chain fatty acids, amino acids, and many other compounds including those that they release from the rice bran food matrix that have previously-reported antimicrobial functions (Nealon *et al.*, 2017a). In wild-type mice orally-challenged with *Salmonella* Typhimurium, prophylactic consumption of 10% w/w rice bran daily for 4 weeks simultaneously increased intestinal *Lactobacillus spp*. and decreased *Salmonella* shedding (Henderson *et al.*, 2012a; Kumar *et al.*, 2012), suggesting that rice bran functioned as a prebiotic by enhancing the natural *Salmonella*-suppressive capacities of *Lactobacillus*. However, despite the established genetic and metabolic diversity across *Lactobacillus* spp., little research has been done to explore *Lactobacillus* spp. differences in antimicrobial compound secretion, and how these *Lactobacillus* spp. differences in pathogen suppression may be reflected in the synbiotic metabolites they produce.

Metabolomic platforms, including chromatography and mass spectrometry, can detect hundreds of small molecules produced in microbial systems (Shaffer *et al.*, 2017) and can be used to understand and systematically-organize the small molecules present in rice bran synbiotics. Previous studies have characterized the global, non-targeted metabolomes of probiotic spp., rice bran and other dietary prebiotics, and have been used to elucidate metabolites found in a synbiotic supernatant (Nealon *et al.*, 2017a; Nealon *et al.*, 2017b; Rubinelli *et al.*, 2017; Zarei *et al.*, 2017), which is defined as the small molecules secreted by probiotic bacteria and released from prebiotics during digestion that are present in the cell-free supernatant of a

synbiotic culture. Comparing the supernatant metabolite profiles of synbiotics prepared with different *Lactobacillus* spp. represents a novel application of metabolomics platforms that can be used to discover and optimize novel, synbiotic-derived antimicrobial compounds that effectively suppress the growth of antimicrobial-resistant *Salmonella* Typhimurium.

The objective of this study was to screen the cell-free supernatant collected from three *Lactobacillus* spp. + rice bran synbiotics for growth of antimicrobial-resistant *Salmonella* Typhimurium. The cell free supernatants were then examined for differences in antimicrobial metabolite production. The overarching hypothesis was that the cell-free supernatant collected from *Lactobacillus* spp. and rice bran synbiotics would differentially suppress the growth of multidrug resistant *Salmonella* Typhimurium and that the metabolite profiles of synbiotic supernatants from different *Lactobacillus* spp. would produce distinct profiles of antimicrobial compounds.

3.3. Materials and Methods:

3.3.1. Bacterial strains and culture preparation:

Three *Lactobacillus* spp. isolated from human fecal and colon tissue samples were purchased from ATCC (Manassas, VA): *Lactobacillus fermentum* ATCC 23271, *Lactobacillus paracasei* ATCC 27092, and *Lactobacillus rhamnosus* ATCC 21052. These were selected for differences in metabolism and growth phenotypes. Prior to use, all bacteria were stored at -80°C as 1mL aliquots with 20% glycerol (Avantor, Radnor, PA) with deMan Rogasa Sharpe (MRS) broth (Becton, Dickinson and Company, Difco Laboratories, Franklin Lakes, NJ) for *Lactobacillus* spp., or Luria-Bertani (**LB**) broth (MOBIO Laboratories Inc., Carlsbad, CA) for *S.* Typhimurium isolates. Broth was prepared and autoclaved according to manufacturer protocols.

Two *Salmonella enterica* subsp. *enterica* serovar Typhimurium isolates were used in this study: *Salmonella* Typhimurium Kan^r 14028s (rPSM::GFP) (**ST-14028s**), was generously donated by Dr. Andres Vazquez-Torres from the University of Colorado, and *Salmonella enterica* subsp. *enterica* serovar Typhimurium AMR-11 (**ST-AMR-11**) was donated by Dr. Sangeeta Rao from Colorado State University. These *Salmonella* isolates were selected for phenotypic differences in antimicrobial resistance and genotypes confirming distinct antimicrobial resistance profiles. These antimicrobial resistance phenotypes and genotypes and growth kinetics of both *Salmonella* isolates are resistance profiles are provided in **Figures 3.1**.

3.3.2. Salmonella DNA extraction, genome assembly and genome analysis:

Salmonella isolates were cultured for 24h at 37°C in tryptic soy broth (**TSB**) prior to DNA extraction (Remel, Lenexa, KS). Cultures were then centrifuged at 4000Xg for 10 minutes and re-constituted in 250 µl of sterile TSB or MRS. DNA was extracted with a DNeasy Powersoil kit (Qiagen, Valencia, CA) following manufacturer protocols. Extractions from each microbial isolate were quality-checked and DNA quantified using a NanoDrop 2000 (Thermo Scientific, Lafayette, CO), and then stored at -20°C until use. Whole genome sequencing was performed at the South Dakota State University: Animal Disease and Diagnostic Laboratory as previously described by Dr. Joy Scaria and Dr. Linto Antony (Thomas *et al.*, 2017). Briefly, 0.3 ng/µL of DNA from each *Salmonella* isolate was processed with a Nextera XT DNA Sample Prep Kit (Illumina Inc., San Diego, CA), pooled together in equimolar amounts, and sequenced on an Illumina Miseq platform (Illumina Inc., San Diego, CA) with a 2X250 paired end approach and V2 chemistry. Following sequencing, pooled files were demultiplexed and converted into FASTQ files (Casava version 1.8.2 (Illumina Inc., San Diego, CA). Genious Version 11.4

(Biomatters Inc., Newark, NJ) was used to trim and assemble each *Salmonella* genome de-novo. The assembled *Salmonella* genomes were **BLAST** (basic local alignment search tool)-searched using the MEGARes database (Lakin *et al.*, 2017). *Salmonella* gene identities were confirmed based on an 85% minimum sequence match to database gene entries.

3.3.3. Salmonella antimicrobial susceptibility testing:

Antimicrobial susceptibility testing of ST-AMR-11 and ST-14028s was performed at the Colorado State University Veterinary Teaching Hospital using protocols developed by the National Antimicrobial Resistance Monitoring System for Enteric Bacteria (**NARMS**) (CLSI, 2010). Briefly, *Salmonella* isolates were cultured overnight onto tryptic soy agar plates and sub-cultured into cation-adjusted Mueller Hinton broth. Approximately 1 x 10^8 CFU/mL was added to broth cultures containing each of the following antimicrobial treatments: Amoxicillin-Clavulanate, Ampicillin, Azithromycin, Ceftiofur, Chloramphenicol, Ciprofloxacin, Sulfisoxazole, Tetracycline, and Trimethoprim-Sulfamethoxazole. After 16-20 hours of incubation, designations of "susceptible" and "resistant" were assigned according to standard minimum inhibitory concentrations reported for each drug (CDC, 2018b; CLSI, 2010).

3.3.4. Evaluation of Salmonella Typhimurium isolates growth kinetics:

Approximately 1X10^6 CFU/mL of ST-14028s and ST-AMR-11 were added to 180 µL of LB broth. Growth was measured on a 96-well plate over 24h using a Cytation3 plate reader (BioTek Instruments Inc., Winooski, VT) that measured culture optical density at 600 nanometers (**OD600**) every 20 minutes. For each *Salmonella* isolate, three independent experiments were performed, and each plate contained 12 technical replicates. A repeated

measures two-way analysis of variance with a Tukey post-test compared the OD600 of *Salmonella* isolates over time, and statistical significance was defined as a $p<0.05$.

3.3.5. Rice bran extraction and media preparation:

Rice bran extract was prepared using heat-stabilized Calrose rice bran (USDA-ARS Rice Research Unit, Stuttgart, AK) and previously-published methods (Ryan *et al.*, 2011). Briefly, 4-grams of heat-stabilized rice bran was extracted in 42.6 mL of 80% ice-cold methanol and vortexed on a high-power setting for 5 minutes (232 Vortexer Fisher Scientific, Pittsburgh, PA, USA), incubated overnight at -80°C, and centrifuged at 4,000g for 5 minutes (Beckman Coulter Allegra X-14R). Supernatant was collected and dried in a speedvac concentrator (SPD1010, Thermo Scientific, Pittsburgh, PA) at 45°C for approximately 48h until dried. To prepare MRS + rice bran extract, 100 µg of rice bran extract was added to 1 ml of MRS broth and autoclaved using a 45-minute sterilization time. Broth was stored at 4°C until use for *Salmonella* growth suppression assays.

3.3.6. Preparation of cell-free supernatant from Lactobacillus spp. in the presence and absence of rice bran extract:

Cell-free supernatant (**CFS**) was prepared as described previously (Nealon *et al.*, 2017a). Briefly, $1x10^6$ CFU/mL of *L. fermentum*, *L. paracasei*, or *L. rhamnosus* were grown for 24h to mid/late logarithmic phase, added to 15 mL of MRS broth or 15 mL of MRS broth + 100 µg/mL rice bran extract, and incubated at 37°C for 24h. The 100 µg/mL dose of rice bran extract was chosen from previous studies, whereby 100 µg/mL rice bran extract significantly suppressed *S.* Typhimurium growth compared to a rice bran extract-free control (Nealon *et al.*, 2017a).

Following the 24h incubation, where all cultures were determined to be in stationary phase (data not shown), cultures underwent two rounds of centrifugation at 4000g for 10 minutes to separate out the supernatant from the remaining bacterial pellet, and approximately 14 mL of CFS were collected each time. Supernatant was adjusted to a pH of 4.5, filter-sterilized through a 0.22-µm pore (Pall Corporation LifeSciences Acrodisc syringe filters, Port Washington, NY) and stored as 1 mL aliquots at -80°C until use. Supernatant sterility was confirmed prior to use by screening it for absence of any growth at 37°C with repeated OD600 reads every 20 minutes for 24h. A minimum of three biological replicates of each supernatant with and without rice bran extract were used to conduct each experiment described herein.

3.3.7. Salmonella growth suppression assay with Lactobacillus and synbiotic supernatants:

The assay for *Salmonella* growth suppression with *Lactobacillus* +/- rice bran extract supernatants was adapted from previously-reported methods (Nealon *et al.*, 2017a). Each *Salmonella* isolate was grown in LB broth at 37°C, until it reached early/mid logarithmic growth phase as determined by repeated optical density reads at an OD600. The supernatants of *Lactobacillus*-only and *Lactobacillu*s + rice bran extracts were tested for dose-dependent effects on *Salmonella* growth. Approximately $2x10^6$ *Salmonella* were added to sterile LB in a 96-well plate, and different concentrations of supernatant (12% to 25% for CFS per volume of LB were added to each well. For each CFS dose, the vehicle control was either MRS (*Lactobacillus*-only) or MRS + 100 µg/mL rice bran extract (*Lactobacillus* + rice bran extract CFS). The negative controls were *Salmonella* inoculated into equivalent volumes of LB-only. All controls were adjusted to a pH of 4.5. To measure *Salmonella* growth over time in response to supernatant treatments, OD600 was measured at 37°C every 20 minutes for 16h. To quantify *Salmonella*

growth suppression differences between treatments, the percent difference in growth suppression was calculated between pairs of treatments at each time point using the following formula:

$$\frac{(OD600\ Treatment\ 1 - OD600\ Treatment\ 2)}{(OD600\ Treatment\ 2)} * 100\%$$

Each experiment contained a minimum of two technical replicates per treatment dose, and each experiment was repeated a minimum of three times. For each *Salmonella* isolate, a repeated-measures 2-way analysis of variance with a Tukey post-test was used to examine treatment and time-dependent differences in supernatant growth suppression, and significance was defined as $p<0.05$. Statistical analysis was performed using GraphPad Prism Version 8.00 (La Jolla, CA).

3.3.8. Lactobacillus and Lactobacillus + Rice Bran Extract supernatant metabolome processing and analysis:

The global, non-targeted metabolite profiles of each *Lactobacillus*-only supernatant, *Lactobacillus* + rice bran extract supernatant, vehicle control, and vehicle control + rice bran extract was performed by Metabolon Inc© (Durham, NC), and each treatment was processed in triplicate (Nealon *et al.*, 2017a). Prior to analysis, each sample was extracted in ice-cold 80% methanol to remove protein. Extracted samples were split into four parts for global, non-targeted metabolomics analysis with ultra-high performance liquid chromatography-tandem mass spectrometry (**UPLC-MS/MS**) on a Waters ACQUITY UPLC C18 column (Waters UPLC BEH C18-2 1 x 100 mm, 1.7 1m) and a Thermo Scientific Q-exactive heated electrospray ionization mass spectrometer with an Orbitrap mass analyzer (Waltham, MA, USA): Reverse-phase chromatography with a water:methanol gradient + positive ion mode electrospray ionization (**ESI**), reverse-phase chromatography with a water:methanol:acetonitrile gradient + positive ion mode ESI, reverse-phase chromatography with a water:methanol:ammonium bicarbonate

gradient + negative ion mode ESI, and normal-phase chromatography with a water:acetonitrile gradient + negative ion mode ESI. The mass analyzed was operated at 35,000 mass resolution and the mass:charge (m/z) scan range covered 70-1000 m/z.

Raw data files were processed by peak-aligning sample spectral files across m/z and retention times. Metabolite identifications were made based on annotating aligned peaks to an internal Metabolon library of over 3300 standards where an m/z ratio of +/- 10 parts per million was the tolerated error alignment. Additional considerations for compound identification were made based on retention index matches of peaks to standards and by comparing MS/MS forward and reverse scores between the experimental data and authentic standards. For each metabolite, spectral raw abundances were converted into median-scaled relative abundances by dividing metabolite raw abundance by the median raw abundance for that metabolite across the entire dataset.

To examine differences in metabolite abundance across *Lactobacillus*-only and synbiotic supernatants, median-scaled relative abundances were compared using one-way analysis of variance with a Welch's post-test at Metabolon Inc. using ArrayStudio (Omnic-soft, Cary, NC), R version 2.142, and SAS version 9.4. Significance was defined as $p<0.05$. Metabolite abundance differences were displayed as fold differences, which were calculated by dividing the average median-scaled abundance of one treatment by another treatment, where metabolite median-scaled abundance averages represented the mean value of the three technical replicates of each treatment. Fold difference was calculated for the following contrasts*: L. paracasei* / *L. fermentum*; *L. rhamnosus* / *L. fermentum*; *L. rhamnosus* / *L. paracasei*; *L. paracasei* + rice bran extract/ *L. fermentum* + rice bran extract; *L. rhamnosus* + rice bran extract / *L. fermentum* + rice bran extract, *L. rhamnosus* + rice bran extract / *L. paracasei* + rice bran extract. To identify the

major metabolic pathways contributing to treatment differences, pathway enrichment scores were calculated for each contrast by dividing the number of statistically-significant metabolites in a given metabolic pathway (*k*) by the total number of metabolites in the pathway (*m*), and dividing this resultant value by the ratio of the total number of statistically-significant metabolites in the contrast (*n*) by the total number of metabolites in the dataset (*N*). A pathway enrichment score of ≥1.00 indicated that the pathway contained more statistically-significant metabolites on average when compared to all other pathways in the dataset, and a score of ≥1.50 was defined as a major metabolic pathway contributor to supernatant differences.

3.4. Results:

3.4.1. Salmonella Typhimurium isolates had distinct genotypic and phenotypic profiles of antimicrobial resistance and exhibited different growth kinetics:

BLAST-search identified 59 total antimicrobial resistance genes, including 34 genes in ST-14028s and 46 genes in ST-AMR-11. A complete list of genes are listed by drug class in **Figure 3.1A**. The genes identified in ST-14028s included: 3 aminoglycosides, 1 bacitracin, 6 beta-lactams, 2 cationic peptides, 1 chloramphenicol, 8 efflux pumps, 6 multi-drug resistance regulators, 1 elfamycin, 3 fluoroquinolones, 1 rifampin, 1 sulfonamide, and 1 tetracycline resistance gene. In ST-AMR-11, the genes included: 4 aminoglycosides, 7 beta-lactams, 1 bleomycin, 1 cationic antimicrobial peptide, 2 phenicols, 12 efflux pumps, 9 multi-drug resistance regulators, 1 elfamycin, 1 macrolide, 3 fluoroquinolones, 1 rifampin, 3 sulfonamides, and 1 tetracycline resistance gene. Efflux pumps were the most abundant resistance class identified in both ST-14028s (~23% of antimicrobial resistance genes) and in ST-AMR11 (~26% of antimicrobial resistance genes).

Twenty-one antimicrobial resistance genes were identified in both *Salmonella* isolates. Beta lactams and multidrug resistance regulators comprised ~47% of these conserved genes and included the beta-lactamase genes *blaCTX*, *blaOXA*, and *blaTEM*, the outer membrane proteins *omp36*, and *ompF*, and the drug resistance regulators *asmA*, *golS*, *ramR*, *sdiA*, and *soxS*. Thirty-eight genes were unique to either *Salmonella* isolate, including 13 genes in ST-14028s and 25 in ST-AMR-11. For ST-14028s efflux pumps and cationic antimicrobial peptides (~53% of the unique genes) most distinguished it from ST-AMR11 and included the cationic peptides *phoP* and *pmrC*, and the efflux pumps *mdtB*, *mdtC*, *mdtH*, *mdtK*, and *mdtP*. In ST-AMR-11, efflux pumps and multidrug resistance regulator genes (~44% of the uniquely-harbored genes) contributed to the largest distinctions from ST-14028s and included the efflux pumps *adeB*, *gyrA*, *mdtF*, *mexB*, *oqxA*, *oqxB*, and *tolC*, as well as the multidrug resistance regulators *cpxA*, *cpxAR*, *emrR*, and *hns*.

ST-AMR-11 was resistant to 7 of the 9 antimicrobials examined during broth microdilution including amoxicillin-clavulanate, ampicillin, azithromycin, ceftiofur, chloramphenicol, sulfisoxazole, tetracycline, and trimethoprim-sulfamethoxazole, and was susceptible to azithromycin and ciprofloxacin. ST-14028s did not exhibit resistance to any drugs. The phenotypic resistance pattern observed for ST-AMR-11 was validated by the presence of genes in the ST-AMR-11 genome including beta-lactam resistance genes *blaCMY*, *blaCTX*, *blaOXA*, *blaTEM*, *carB*, and *ompF* contributing to amoxicillin-clavulanate, ampicillin, and ceftiofur resistance, the phenicol resistance genes *catB* and *florR* contributing to chloramphenicol resistance, the sulfonamide genes *folP*, *sul2* and *sul3* contributing to sulfisoxazole and trimethoprim-sulfamethoxazole resistance, and the genes *tetA* and *tetR* contributing to tetracycline resistance. Multiple efflux pumps and multidrug resistance regulator genes were also

believed to contribute to antimicrobial resistance across all of the drug classes screened against ST-AMR-11.

In addition to genotypic and phenotypic differences in antimicrobial resistance, the *Salmonella* isolates showed differences in growth kinetics (**Figure 3.1C**). Between 5.67h and 11.00h, which was approximately during the mid to late logarithmic growth phase, ST-AMR-11 grew at a significantly higher rate than ST-14028s ($p<0.05$). Both isolates exhibited minimal differences in their stationary phase length (0h-2h), their rate of early logarithmic phase growth (2h-5.33h), and their stationary phase growth rate (11h-16h).

A.

Salmonella Typhimurium Isolate	Amoxicillin-Clavulanate	Ampicillin	Azithromycin	Ceftiofur	Chloramphenicol	Ciprofloxacin	Sulfisoxazole	Tetracycline	Trimethoprim-	Sulfamethoxazole
ST-14028s	S	S	S	S	S	S	S	S	S	
ST-AMR-11	R	R	S	R	R	S	R	R	R	

B.

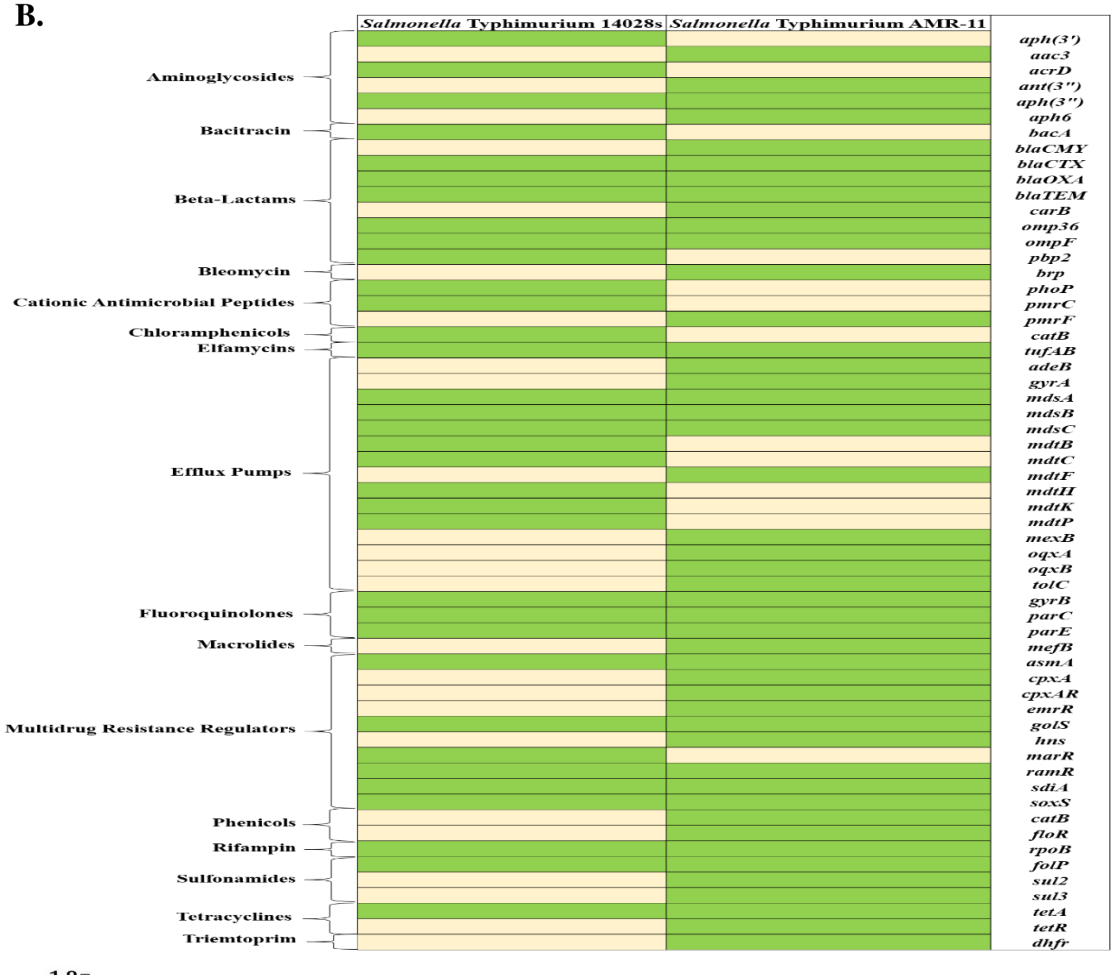

C.

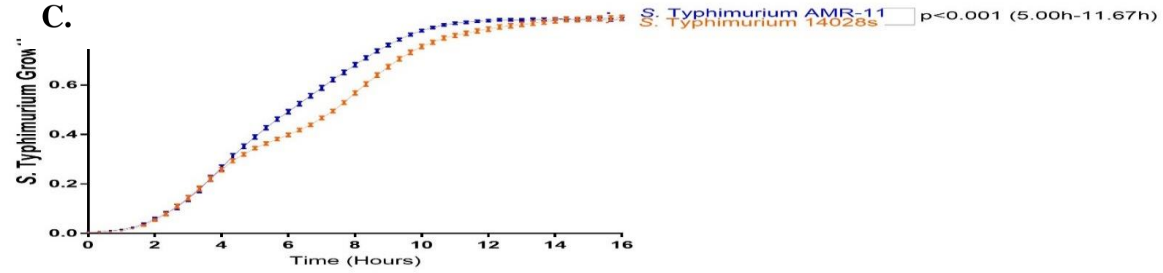

Figure 3.1. *S.* Typhimurium isolates have distinct genotypic and phenotypic antimicrobial resistance profiles and exhibit distinct growth kinetics.

3.1A: *For each antimicrobial drug, "**S**" indicates susceptible; "**R**" indicates resistant.* ***3.1B:*** *Antimicrobial genes classified by drug resistance class. Green cells indicate a gene match of ≥85% between the MEGARes database entry and the gene present in each genome. Beige cells indicate gene either matched ≤85% to all associated database entries or was not present in the given isolate.* ***3.1C****: S. Typhimurium isolate relative growth as measured by optical density where each time point plotted represents the mean of three independent experiments and bars depict standard error of the mean.*

3.4.2. Cell-free supernatant from synbiotics suppresses the growth of antimicrobial resistant Salmonella Typhimurium.

The cell-free supernatant from *Lactobacillus* spp. and *Lactobacillus spp.*+ rice bran extract exhibited concentration-dependent growth suppression of two *Salmonella* strains (ST-14028s and ST-AMR-11. At 16h (late exponential phase), the *Salmonella* isolates did not show intrinsic differences in growth rates (**Figure 3.1**), and this time point was consequently used to compare *Salmonella* growth suppression efficacy between cell-free supernatant treatments. **Figure 3.2** compares *Salmonella* isolate growth suppression with each *Lactobacillus* and *Lactobacillus* + rice bran extract supernatant for ST-14028s (**3.2A**) and ST-AMR-11 (**3.2B**). Furthermore, to quantitatively levels of *Salmonella* growth suppression across each supernatant, percent growth suppression difference was calculated for cell-free supernatants of *Lactobacillus* spp. compared to each other, for *Lactobacillus* spp. supernatant compared to their *Lactobacillus* + rice bran extract supernatant, and between *Lactobacillus* + rice bran extract cell-free supernatants. **Table 3.1** summarizes these relative percent *Salmonella* growth suppression values for these comparisons.

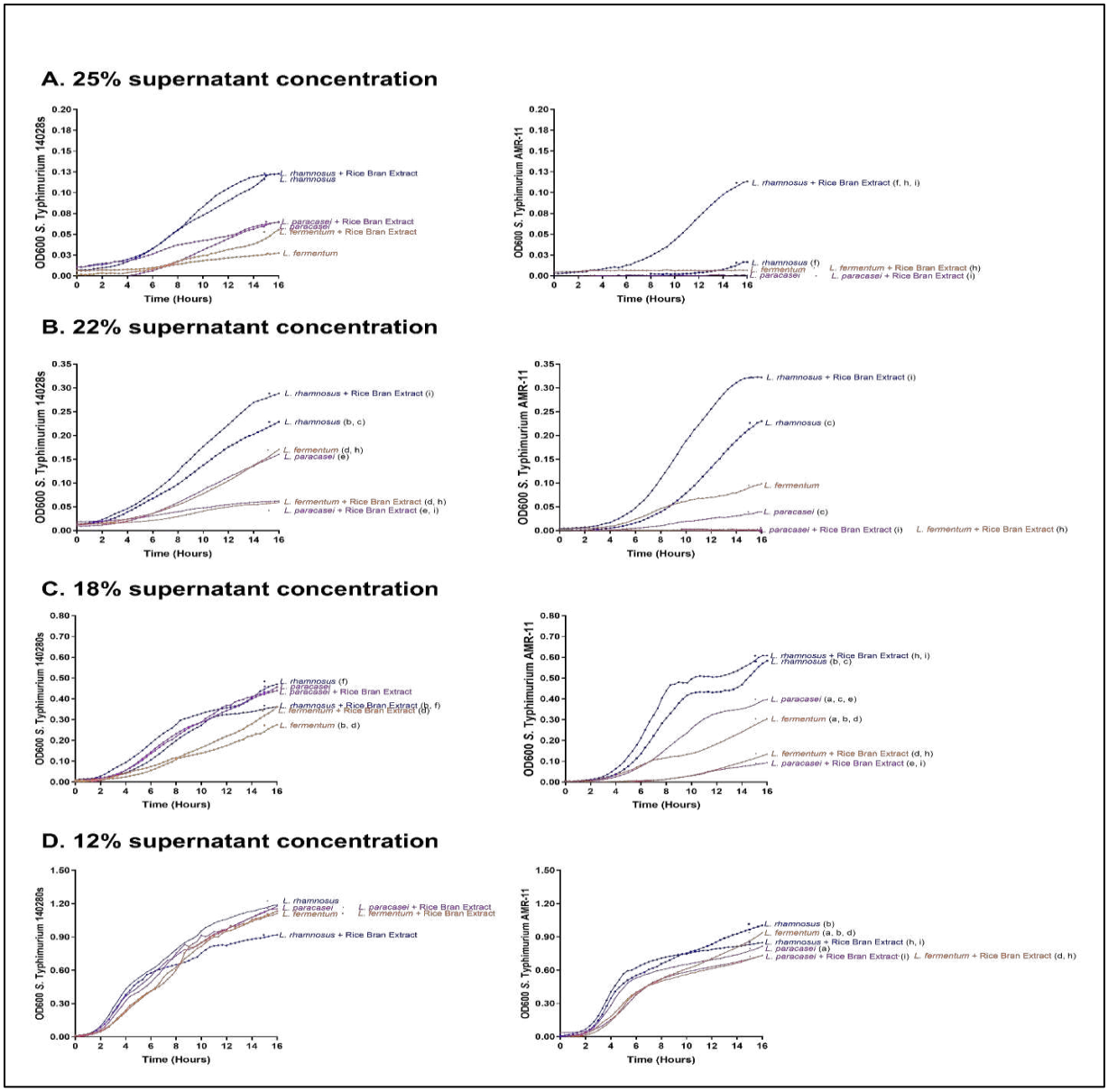

Figure 3.2. *Lactobacillus*-only and synbiotic supernatants differentially suppresses the growth of non-resistant and multidrug resistant *S.* Typhimurium in a dose-dependent manner.

*For each Salmonella isolate, growth suppression by different probiotic versus synbiotic supernatants are depicted at a 25% v/v supernatant concentration (**3.2A**), 22% (**3.2B**), 18% (**3.2C**), and 12% (**3.2D**). Optical density (**OD600**) at each time point represents the mean of at least three independent experiments. Letters denote supernatant treatments that are statistically-different ($p<0.05$) at 16h: **a**: L. paracasei/L. fermentum, **b**: L. rhamnosus/L. fermentum, **c**: L. rhamnosus/L. paracasei, **d**: L. fermentum + rice bran extract/L. fermentum; **e**: L. paracasei + rice bran extract/L. paracasei; **f**: L. rhamnosus + rice bran extract/L. rhamnosus; **g**: L. paracasei + rice bran extract/L. fermentum + rice bran extract; **h**: L. rhamnosus + rice bran extract/L. fermentum + rice bran extract; **i**: L. rhamnosus + rice bran extract/L. paracasei + rice bran extract.*

Table 3.1. Percent difference in of *Salmonella* Typhimurium growth suppression at 16 hours by *Lactobacillus* and *Lactobacillus* + Rice Bran Extract cell-free supernatants

Isolate	***S.* Typhimurium 14028s**				***S.* Typhimurium AMR-11**			
Cell-Free Supernatant Concentration (% Volume)[1]	**12% CFS[2]**	**18% CFS**	**22% CFS**	**25% CFS**	**12% CFS**	**18% CFS**	**22% CFS**	**25% CFS**
L. paracasei / *L. fermentum*	-	-	-	-	↑18.85% ± 5.27%	↑52.27 ± 9.23%	-	-
L. rhamnosus / *L. fermentum*	↓9.55% ± 7.39%	-	-	-	↓21.97% ± 7.56%	↓56.31% ± 28.04%	-	-
L. rhamnosus / *L. paracasei*	-	-	-	-	-	↓95.55% ± 40.53%	↓110.22% ± 21.06%	-
L. fermentum + Rice Bran Extract/ *L. fermentum*	-	-	↑46.95% ± 27.10%	-	↑23.82% ± 7.71%	↑42.47% ± 10.93%	-	-
L. paracasei + Rice Bran Extract / *L. paracasei*	-	-	↑34.97% ± 13.96%	-	-	↑55.21% ± 9.72%	-	-
L. rhamnosus + Rice Bran Extract / *L. rhamnosus*	↑12.18% ±5.44%	-	-	-	-	-	-	↓65.45% ± 72.95
L. paracasei + Rice Bran Extract / *L. fermentum* + Rice Bran Extract	-	-	-	-	-	-	-	↑5.98% ± 7.43%
L. rhamnosus + Rice Bran Extract / *L. fermentum* + Rice Bran Extract	↑20.20% ± 7.08%	-	↓121.57% ± 19.76%	-	↓11.67% ± 2.03%	↓165.62% ± 101.98%	↓212.07% ± 3.37%	↓53.59% ± 77.88%
L. rhamnosus + Rice Bran Extract / *L. paracasei* + Rice Bran Extract	-	-	↓137.92% ± 30.59%	-	↓20.59% ± 2.53%	↓193.65% ± 50.88%	↓190.86% ± 21.05%	↓55.02% ± 82.01%

1. Growth suppression values for each supernatant dose represent the average value for a minimum of three independent experiments ± standard error of the mean.
2. **CFS:** Cell-free supernatant
3. ↑ indicates treatment in the numerator exhibited increased ($p<0.05$) growth suppression compared to the treatment in the denominator; ↓ indicates treatment in the numerator exhibited decreased growth suppression compared to the treatment in the denominator.
4. Dash indicates that treatments did not have statistically-different levels of growth suppression at 16 hours.

For ST-14028s, all cell-free supernatants treatments were compared using the 22% supernatant concentration because this was the lowest concentration at which each supernatant achieved *Salmonella* growth suppression compared to the negative control at 16h ($p<0.05$). When comparing ST-14028s growth suppression from the synbiotic-derived cell-free supernatants to those from the probiotic-only cell-free supernatants, the *L. fermentum* + rice bran

extract supernatant was 9.04% more effective at suppressing *Salmonella* growth than *L. fermentum* alone, and the *L. paracasei* + rice bran extract supernatant was 11.53% more effective than the *L. paracasei* supernatant alone ($p<0.0001$). At 16.00h, no differences in ST-14028s growth suppression were observed between *L. rhamnosus* + rice bran extract and *L. rhamnosus* growth suppression.

For ST-AMR-11, the 18% concentration was the lowest that demonstrated growth suppression for all treatments compared to the negative control ($p<0.05$). At 16.00h, the *L. paracasei* + rice bran extract cell-free supernatant was 55.21% more effectively than the *L. paracasei*-only cell-free supernatant ($p<0.0001$), and the *L. fermentum* + rice bran extract was 42.47% more effective when compared to the *L. fermentum*-only supernatant ($p<0.0001$). No difference in ST-AMR-11 growth suppression was observed between the *L. rhamnosus* and *L. rhamnosus* + rice bran extract cell-free supernatants at 16.00h.

3.4.3 Lactobacillus spp. have distinct metabolite profiles in the cell-free supernatant following rice bran extract fermentation.

The global, non-targeted metabolomics analysis identified 348 total metabolites across all *Lactobacillus*-only and *Lactobacillus* + rice bran extract cell-free supernatants. An overview of these metabolome differences between all supernatant treatments was visualized using principal components analysis (**PCA**) (**Figure 3.3**). PCA analysis revealed that the largest variation in metabolite profiles (Component 1, 33.04% of the variation) was explained by separation of *Lactobacillus* species from each other in either the presence or absence of rice bran extract (**Figure 3.3**). Component 2 (22.56% of the variation) primarily separated the vehicle control

treatments from all *Lactobacillus* spp. and *Lactobacillus* + rice bran extract cell-free supernatants (**Figure 3.3**).

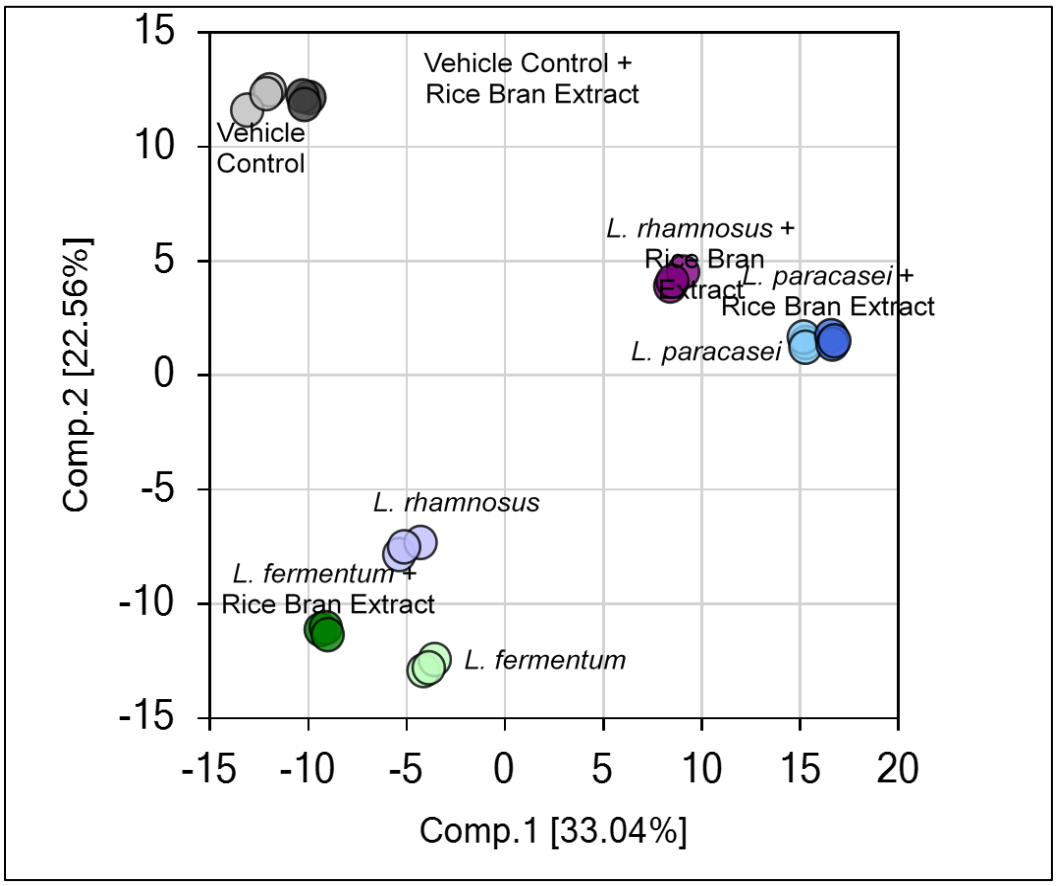

Figure 3.3. *Lactobacillus* spp. supernatants are modulated during rice bran extract fermentation.

Principal components analysis of supernatants from Lactobacillus spp. alone and each synbiotic. Values on each axis refer to the percent variance contributed by each component to the overall metabolite abundance variance between treatments.

To identify metabolites contributing to the differences between *Lactobacillus* spp. and *Lactobacillus* spp. + rice bran extract cell-free supernatants, compounds were organized by their chemical class and associated metabolic pathway. Of the 348 total metabolites identified, there were 139 amino acids, 31 carbohydrates, 18 cofactors and vitamins, 10 energy metabolites (tricarboxylic acid cycle and oxidative phosphorylation), 51 lipids, 57 nucleotides, 35 peptides,

and 35 phytochemicals/other metabolites were identified. Major chemical classes contributing to *Lactobacillus*-only cell-free supernatant differences included amino acids (112 metabolites with significantly-different abundances across two or three *Lactobacillus* spp.), nucleotides (45 metabolites), and lipids (40 metabolites) (**Figure 3.4A**). These chemical classes were also major contributors to the observed differences between *Lactobacillus* + rice bran extract supernatants and included 104 amino acids, 49 nucleotides, and 39 lipids with significantly-different abundances across two or three *Lactobacillus* spp. + rice bran extract (**Figure 3.4B**).

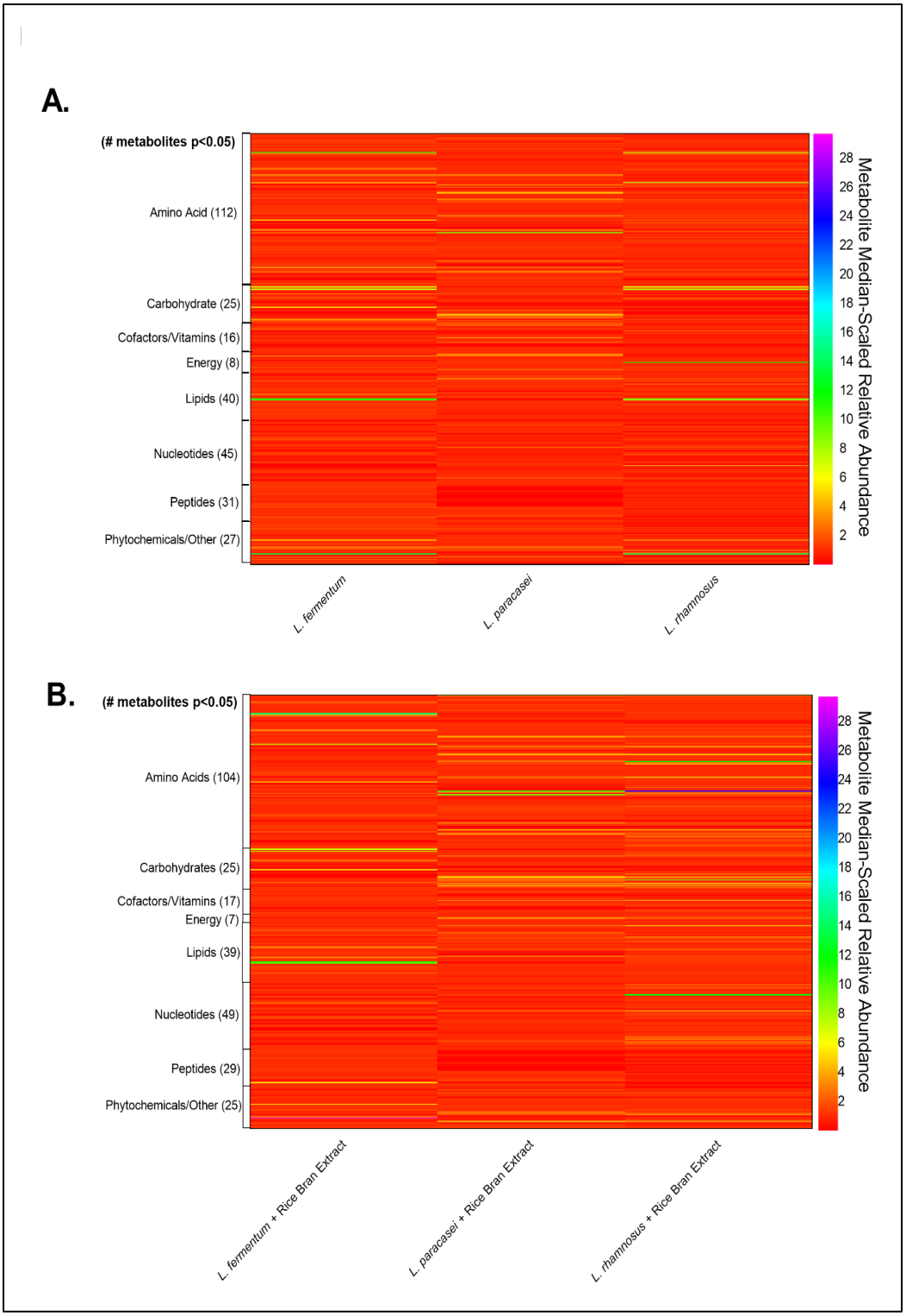

Figure 3.4. *Lactobacillus* spp. produce distinct metabolite profiles that are modulated during rice bran fermentation.

*Non-targeted metabolome heat map comparing Lactobacillus spp. supernatant in the absence of rice bran extract (**3.4A**), examining synbiotic versus Lactobacillus spp. (**3.4B**), and*

*comparing Lactobacillus spp. + rice bran extract supernatants (**3.4C**). Metabolites are organized by chemical class. Numbers next to class names refer to (# metabolites statistically-different between two or three treatments, % of metabolites in each class that were statistically-different). Heat map scale bars show metabolite median-scaled relative abundances from three independent mass-spectrometry runs.*

3.4.4 Rice bran extract drives differences in Lactobacillus spp. metabolic pathway and metabolite regulation.

Both the *L. fermentum* + rice bran extract and *L. paracasei* + rice bran extract cell-free supernatant exhibited significantly enhanced growth suppression of both *Salmonella* isolates at 16h compared to each *Lactobacillus* spp. supernatant alone. To determine whether *L. fermentum* + rice bran extract cell-free supernatant and *L. paracasei* + rice bran extract supernatant enhanced *Salmonella* growth suppression via different metabolic processes, pathway enrichment scores were calculated to identify the major metabolic pathways contributing to *Lactobacillus* spp. + rice bran extract supernatant differences (**Figure 3.5**). Metabolic pathways with a score of greater than or equal to 1.50 were considered major contributors to treatment differences, and these included 14 pathways that distinguished *L. paracasei* + rice bran extract from *L. fermentum* + rice bran extract. Lipid, amino acid and nucleotide pathways contributed to ~64% of differentially-regulated metabolic pathways between these two synbiotic supernatants. The two amino acid metabolic pathways differentially-regulated were aminosugars (1.51 score in the *L. paracasei* + rice bran extract supernatant versus the *L. fermentum* + rice bran extract supernatant) and creatine (1.50). Five lipid pathways contributed to *L. paracasei* + rice bran extract supernatant and *L. fermentum* + rice bran extract supernatant differences and included acyl carnitines (1.50), polyunsaturated fatty acids (1.51), long chain fatty acids (1.51), glycerolipids (1.51), fatty acid synthesis (1.51). Two nucleotide metabolic pathways distinguished the *L. paracasei* + rice bran extract and *L. fermentum* + rice bran extract

supernatants: orotate (1.50) and thymine (1.50) (**Figure 3.5**).

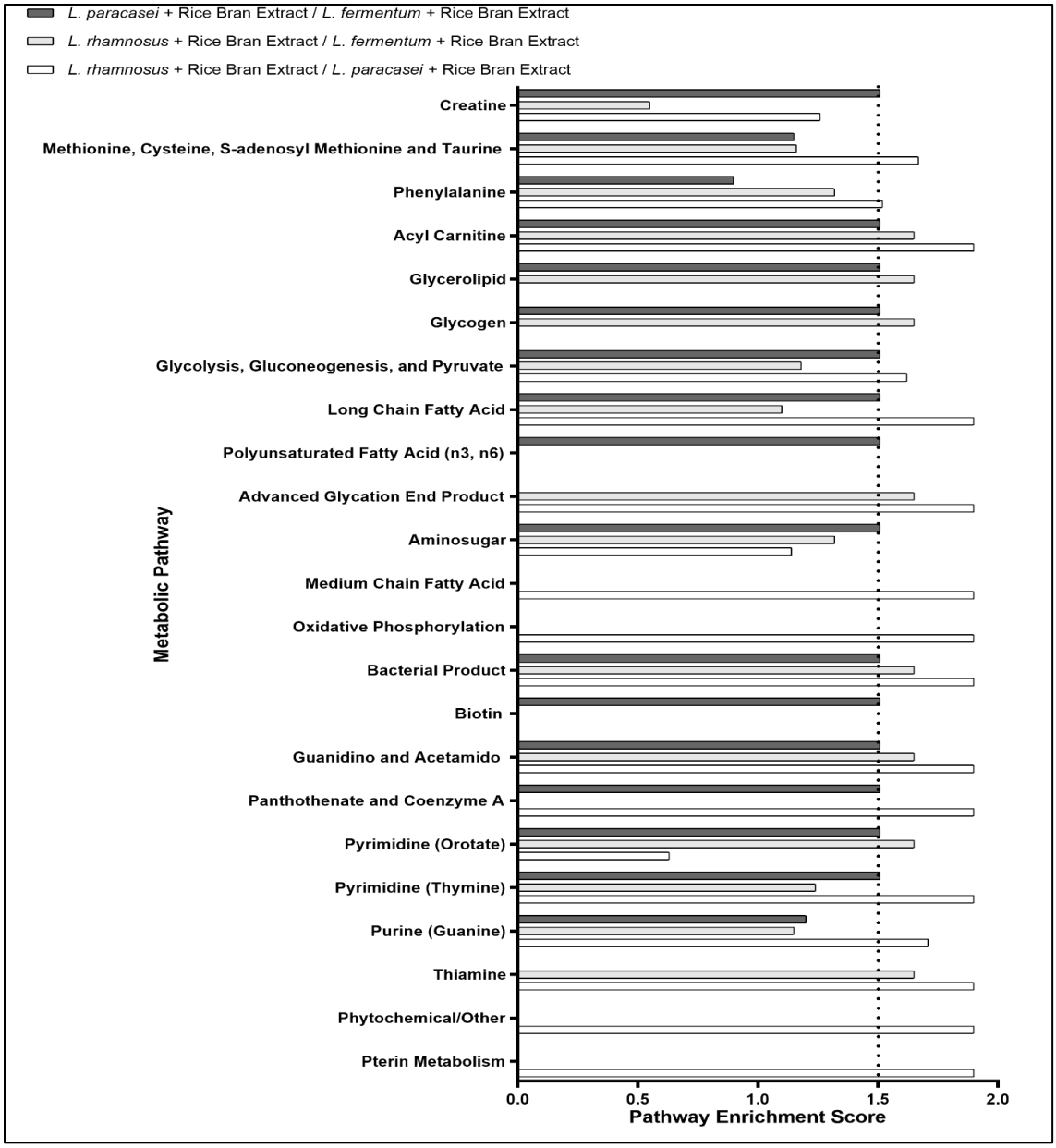

Figure 3.5. *Lactobacillus* spp. synbiotic supernatants have differentially-regulated metabolic pathways.

Pathway enrichment scores comparing metabolic pathway differences across Lactobacillus + rice bran extract supernatants. For each panel, dark grey bars compare L. paracasei + rice bran extract and L. fermentum + rice bran extract, light grey bars compare L. rhamnosus + rice bran extract and L. fermentum + rice bran extract, and white bars compare L. rhamnosus + rice bran extract and L. paracasei + rice bran extract. Numbers in parentheses indicate metabolites with statistically-different ($p<0.05$) abundance between treatment pairs, and absence of a bar for any pair of treatments indicates that there were no metabolites that statistically-differed across treatments. Bars extending to the left of the dotted line (score ≥ 1.5) were defined as major contributors to treatment differences.

3.4.5. Lactobacillus spp. + rice bran extract supernatants contained differentially-abundant antimicrobial metabolites.

Eighty-seven total metabolites contributed to the metabolic pathway differences observed between the *Lactobacillus* spp. + rice bran extract supernatants. Given the enhanced *Salmonella* growth suppression observed for the *L. fermentum* + rice bran extract *and L. paracasei* + rice bran extract cell-free supernatants compared to their *Lactobacillus*-only supernatant treatments, the metabolites that were statistically-different between the *L. paracasei* + rice bran extract and *L. fermentum* + rice bran extract supernatants were further screened for reported antimicrobial functions and roles in *Salmonella* growth regulation. **Table 3.2** reports 48 metabolites that met these criteria including 7 amino acids, 8 carbohydrates, 5 energy metabolites, 9 lipids, 15 nucleotides, 2 vitamins and cofactors, and 2 phytochemicals/ other. Among these metabolites were the amino acid metabolite 1-methylguanidine (5.01-fold increase in the *L. paracasei* + rice bran extract supernatant versus the *L. fermentum* + rice bran extract supernatant), the polyunsaturated fatty acid linoleate (0.58 fold-decrease), and the glycerolipid glycerol (0.28-fold decrease). Antimicrobial nucleotide metabolites exhibited the largest abundance fold-differences between the *L. fermentum* + rice bran extract and *L. paracasei* + rice bran extract supernatants. These nucleotide metabolites included orotate (327.85-fold increase in *L. paracasei* + rice bran extract versus *L. fermentum* + rice bran extract), guanosine (97.59 fold-increase), and guanine (0.42 fold-decrease).

Table 3.2. Antimicrobial and growth-modulatory functions of select metabolites distinguishing *Lactobacillus* spp. + Rice Bran Extract cell-free supernatants[1]

Metabolite	Fold-Difference			Antimicrobial and Growth-Modulatory Functions	References
	LP + RBE / LF + RBE	**LR + RBE / LF + RBE**	**LR+ RBE / LP + RBE**		
N-acetyl-glucosamine /galactosamine	**↓0.21**	**↓0.22**	**↑1.11**	N-acetylglucosamine is a precursor for major cell-wall synthesis components. Under starvation conditions, *S.* Typhimurium catabolized N-acetylglucosamine for energy metabolism.	(Jiang *et al.*, 2018; Yoo *et al.*, 2016)
N-acetyl-glucosamine 1-phosphate	**↓0.72**	**↓0.80**	1.11	As a downstream product of N-acetylglucosamine metabolism, N-acetylglucosamine-1-phosphate is an intermediate in cell wall synthesis. Downregulation of N-acetylglucosamine 1-phosphate catabolism *Mycobacterium smegmatis* increased rifampin susceptibility *in vitro*.	(Xu *et al.*, 2016; Yoo *et al.*, 2016)
N-acetyl-neuraminate	**↓0.27**	**↑0.36**	1.36	None Reported.	-
N-acetyl-glucosamine 6-phosphate	**↑1.49**	-	**↓0.67**	None Reported.	-
creatine	**↑1.43**	**↑1.11**	**↓0.77**	None Reported.	-
4-guanidino butanoate	**↑3.02**	**↑1.78**	**↓0.59**	None Reported.	-
1-methylguanidine	**↑5.01**	**↓3.26**	**↓0.65**	Increased abundance in *L. paracasei* + rice bran extract supernatant compared to *L. paracasei* supernatant and was associated with decreased growth of *S.* Typhimurium 14028s.	(Nealon *et al.*, 2017a)

Table 3.2. Antimicrobial and growth-modulatory functions of select metabolites distinguishing *Lactobacillus* spp. + Rice Bran Extract cell-free supernatants[1]

Metabolite	Fold-Difference			Antimicrobial and Growth-Modulatory Functions	References
	LP + RBE / LF + RBE	**LR + RBE / LF + RBE**	**LR+ RBE / LP + RBE**		
isomaltose	**↑11.82**	**↑10.82**	0.91	When fed prophylactically at 1% w/v to conventional broiler chicks, isomaltose reduced *Salmonella* cecal colonization levels compared to chicks receiving a control diet; isomaltose has been previously shown to stimulate the growth of *Lactobacillus* spp. but not *Salmonella*.	(Chung and Day, 2004; Thitaram *et al.*, 2005)
3-phosphoglycerate	**↑1.32**	0.86	**↓0.66**	None Reported.	-
erythronate	**↑4.86**	**↑43.92**	**↓0.80**	None Reported.	-
glucose 6-phosphate	**↑73.44**	**↑39.56**	**↓0.54**	Increased levels promote *S.* Typhimurium growth *in vitro*, but do not enhance its intracellular replication in Caco-2 cells.	(Gotz and Goebel, 2010)
glucose	**↑311.52**	**↑955.60**	**↑3.07**	Decreased environmental glucose promoted increased release of various antimicrobial metabolites by *Lactobacillus* spp. including various fatty acids, cyclic dipeptides, ketones, alkanes, and alcohols and was associated with damage to S. Typhimurium outer and cytoplasmic membranes and bacterial cell leakage under an *in vitro* mimicked proximal colon environment.	(Kanjan and Hongpattarakere, 2016)
glycerate	**↑15.09**	**↑9.97**	**↓0.66**	None Reported.	-
lactate	**↑1.36**	0.90	**↓0.67**	Suppressed *S.* Typhimurium growth *in vitro* and *ex vivo* in one day old chick digestive organs, and its minimum inhibitory concentrations varied based on the *Salmonella* isolate examined.	(El Baaboua *et al.*, 2018)
3-phosphoglycerate	**↑1.31**	0.86	**↓0.66**	None Reported.	-

Table 3.2. Antimicrobial and growth-modulatory functions of select metabolites distinguishing *Lactobacillus* spp. + Rice Bran Extract cell-free supernatants[1]

Metabolite	Fold-Difference			Antimicrobial and Growth-Modulatory Functions	References
	LP + RBE / LF + RBE	**LR + RBE / LF + RBE**	**LR+ RBE / LP + RBE**		
arabonate/xylonate	**↑3.84**	**↑4.65**	**↑1.21**	Increased abundance in *L. paracasei* + rice bran extract compared to *L. paracasei* and was associated with decreased growth of *S.* Typhimurium	(Nealon *et al.*, 2017a)
malonate	**↓0.51**	**↓0.43**	**↓0.85**	In mice, increased blood levels of malonate were associated with increased *S.* Typhimurium bacteremia.	(Berry and Mitchell, 1954)
pyruvate	**↑3.78**	**↑8.84**	**↑2.34**	Supplementation to culture broth increased *S.* Typhimurium viability when subjected to oxidative stress by triggering the synthesis of DNA and proteins; Antimicrobial resistance to triclosan by *S.* Typhimurium is associated with alterations in pyruvate metabolism/usage.	(Morishige *et al.*, 2013; Webber *et al.*, 2008)
tricarballylate	**↑5.06**	**↑8.27**	**↑1.63**	Intracellular levels that accumulate have been shown to be toxic and growth-suppressive to *S.* Typhimurium *in vitro*.	(Boyd *et al.*, 2012)
acetylcarnitine	**↓0.60**	**↓0.79**	**↑1.33**	None Reported.	-
glycerol	**↓0.28**	**↓0.29**	1.01	Supplementing culture broth with glycerol induced time-dependent stress responses on *S.* Typhimurium over 24 hours, including glycolysis and tricarboxylic acid cycle impairment, reduced carbohydrate synthesis, and increased oxidative stress.	(Finn *et al.*, 2015)
glycerol-3-phosphate	**↓0.64**	**↓0.63**	0.98	None Reported.	-
digalactosyl-glycerol*[2]	**↑1.32**	**↑1.28**	0.97	None Reported.	-
glycerophosphoryl glycerol	**↑4.41**	**↑3.88**	0.87	None Reported.	-

Table 3.2. Antimicrobial and growth-modulatory functions of select metabolites distinguishing *Lactobacillus* spp. + Rice Bran Extract cell-free supernatants[1]

Metabolite	Fold-Difference			Antimicrobial and Growth-Modulatory Functions	References
	LP + RBE / LF + RBE	**LR + RBE / LF + RBE**	**LR+ RBE / LP + RBE**		
oleate/vaccenate	**↓0.26**	**↓0.48**	**↑1.85**	Bacteriostatic against *S.* Typhimurium after 1h of incubation at 0.1% w/v suspension in culture media. Co-cultures of *Lactobacillus* spp. and *S.* Typhimurium exhibited differential *Salmonella* growth reduction, which was attributed in-part to differences in oleic acid production.	(Kanjan and Hongpattarakere, 2016; Zhang *et al.*, 2016)
eicosenoate	**↑1.88**	1.13	**↓0.61**	None Reported.	-
palmitate	**↓0.74**	**↓0.93**	**↑1.25**	As part of an oil extract from *Jacaranda cuspidifolia* Mart, palmitate suppressed the growth of *E. coli*, *S. aureus*, and *Candida albicans*, as measured by Kirby-Bauer disk diffusion.	(Yuan *et al.*, 2018)
linoleate	**↓0.58**	0.70	1.22	Shown to inhibit efflux pumps in *S.* Typhimurium to enhance microbial susceptibility to ciprofloxacin.	(Garvey *et al.*, 2011)
guanine	**↓0.42**	**↑1.20**	**↑2.84**	Limiting exogenous guanine concentrations was shown to decrease *S.* Typhimurium growth in isolates with an inosine 5'-monophosphate dehydrogenase knock out due to decreased guanosine-triphosphate and cytidine-triphosphate production.	(Jensen, 1979)
7-methylguanine	**↓0.82**	0.97	**↑1.19**	None Reported.	-
2'-O-methylguanosine	**↑5.20**	**↑7.32**	**↑1.41**	None Reported.	-
guanosine 3'-monophosphate	**↓0.41**	**↓0.52**	**↑1.29**	None Reported.	-
N2,N2-dimethylguanosine	**↑3.62**	**↑2.27**	**↓0.63**	None Reported.	-
guanosine 2'-monophosphate*	**↓0.89**	1.00	**↑1.12**	None Reported.	-

Table 3.2. Antimicrobial and growth-modulatory functions of select metabolites distinguishing *Lactobacillus* spp. + Rice Bran Extract cell-free supernatants[1]

Metabolite	Fold-Difference			Antimicrobial and Growth-Modulatory Functions	References
	LP + RBE / LF + RBE	**LR + RBE / LF + RBE**	**LR+ RBE / LP + RBE**		
guanosine	**↑97.59**	**↑140.50**	**↑1.44**	Exogenous guanosine concentrations modulated *S.* Typhimurium transcription of replication and metabolism genes during late stationary phase growth; Increased exogenous guanosine concentrations activated aminoglycoside resistance genes in *S.* Typhimurium *in vitro*.	(Koskiniemi *et al.*, 2011; Ramachandran *et al.*, 2014)
guanosine-2',3'-cyclic monophosphate	**↓0.51**	**↓0.87**	**↑1.72**	None Reported.	-
orotate	**↑330.73**	**↑522.84**	**↑1.58**	Low orotate:succinate ratios in growth media reduced *S.* Typhimurium growth rate by slowing down the rate of pyrimidine biosynthesis.	(Baker *et al.*, 1996)
dihydroorotate	**↑7.18**	**↑6.96**	0.97	None Reported.	-
orotidine	**↓0.50**	**↓0.50**	-	None Reported.	-
thymidine-3'-monophosphate	**↓0.57**	**↓0.73**	**↑1.28**	None Reported.	-
thymine	**↓0.53**	**↓0.71**	**↑1.35**	In *S.* Typhimurium isolated from broiler chicken feces, trimethoprim resistance was associated with thymine auxotrophism; limiting thymine in growth agar suppressed growth and virulence of these auxotrophic *S.* Typhimurium isolates.	(Smith and Tucker, 1975; 1976)
thymidine	**↑1.21**	**↑1.68**	**↑1.39**	High environmental thymidine concentrations increased sulfamethoxazole-trimethoprim resistance in *S. typhi* and *E. coli*.	(Smith and Tucker, 1976)
thymidine 5'-monophosphate	**↓0.85**	1.02	**↑1.21**	None Reported.	-
tartronate (hydroxymalonate)	**↑8.59**	**↑4.71**	**↓0.54**	None Reported.	-
pyrraline	**↓0.61**	**↓0.77**	**↑1.25**	None Reported	-
biotin	**↓0.17**	0.39	2.41	None Reported.	-
pantothenate	**↓0.85**	1.08	**↑1.27**	None Reported.	-

Table 3.2. Antimicrobial and growth-modulatory functions of select metabolites distinguishing *Lactobacillus* spp. + Rice Bran Extract cell-free supernatants[1]

Metabolite	Fold-Difference			Antimicrobial and Growth-Modulatory Functions	References
	LP + RBE / LF + RBE	**LR + RBE / LF + RBE**	**LR+ RBE / LP + RBE**		

1. Fold difference of the median-scaled abundances of each metabolite for *L. fermentum* + Rice Bran Extract (**LF + RBE**), *L. paracasei* + Rice Bran Extract (**LP + RBE**), and *L. rhamnosus* + RBE (**LR + RBE**). Bold indicates metabolites had statistically-significant abundance differences ($p<0.05$) for the given comparison, where ↑ indicates the metabolite was increased in the numerator treatment compared to the denominator, and ↓ indicates the metabolite was decreased in the numerator treatment compared to the denominator.
2. * indicates metabolite identification was based on identity match to a chemical structure database versus with a commercial chemical standard.

3.5. Discussion and Conclusions:

The study described herein examined three cell-free supernatants collected from synbiotics of *Lactobacillus* spp. + rice bran extract and screened them for growth suppression against phenotypically antimicrobial-resistant and non-resistant *Salmonella* Typhimurium isolates (**Figure 3.1.**). Rice bran extract was predicted to enhance *Salmonella* growth suppression by *Lactobacillus* spp. cell-free supernatant, and it was hypothesized that growth suppression levels would be influenced by *Lactobacillus* spp. differences in secreted metabolites. The results of these experiments support that rice bran differentially modulates the *Salmonella* suppression capacity of supernatant collected from three *Lactobacillus* spp. and that lower concentrations of synbiotic supernatants may function differently to suppress the growth of antimicrobial-resistant versus non-resistant *Salmonella* Typhimurium isolates. Our metabolomics analysis of synbiotic supernatants further identifies supernatant metabolite variations that may contribute to these observed growth suppression differences.

In the presence of rice bran extract, *L. fermentum* and *L paracasei* cell-free supernatants enhanced *Salmonella* growth suppression for both the non-resistant and antimicrobial-resistant *Salmonella* isolates at 16h when compared to supernatant collected from these *Lactobacillus* spp.

alone (**Figure 3.2**). Cell-free supernatant prepared from *L. paracasei* + rice bran extract was previously shown to suppress *S.* Typhimurium 14028s 16h growth by 13.1% compared to *L. paracasei* alone (Nealon *et al.*, 2017a), which was similar to the 11.30% growth enhancement for *L. paracasei* + rice bran extract versus *L. paracasei* supernatant reported herein for the ST-14028s isolate. While *L. fermentum* fed to mice was shown to reduce *S.* Typhimurium infectivity while beneficially-modulating anti-*Salmonella* immune responses (Harris *et al.*, 2018), and has been reported to produce antimicrobial bacteriocin proteins effective against a broad array of microbial pathogens (Heredia-Castro *et al.*, 2015), the bioactivity of *L. fermentum* + rice bran extract-derived synbiotics has not been previously-characterized, and warrants further examination given the broadly-reported efficacy of *L. fermentum* strains in suppressing pathogen growth.

Salmonella growth suppression assays with the *Lactobacillus*-only and *Lactobacillus* + rice bran extract cell-free supernatants further revealed that a lower cell-free supernatant concentration was needed to achieve maximal growth suppression of the phenotypically-resistant ST-AMR-11 (18% v/v treatments) versus the phenotypically non-resistant isolate ST-14028s (22% v/v treatments) (**Figure 3.2**, **Table 3.1**). An explanation for this could be found when comparing the growth rates of the *Salmonella* isolates, where ST-AMR-11 grew more rapidly during the exponential growth phase than ST-14028s (**Figure 3.1C**). Microbes with antimicrobial resistance often have increased energy demands needed to support the transcription and translation of these extra genes (Baquero and Martínez, 2017; Rojo and Martínez, 2011). In the presence of a nutrient-rich environment such as culture broth, the increased growth rate of the multi-drug resistant ST-AMR-11 compared to the ST-14028s isolate may suggest it has greater metabolic demands needed to fuel this more rapid growth rate. However, antimicrobial drugs

preferentially target rapidly-dividing, metabolically-active bacteria to antagonize a variety of microbial processes including cell wall synthesis, replication of genetic material, protein production, and the function of efflux pumps that remove toxic compounds from cells (Kohanski *et al.*, 2010). Consequently, when the cell-free supernatant treatments were added to *Salmonella* culture broth, increased environmental nutrient utilization by ST-AMR-11 compared to ST-14028s may have driven more rapid accumulation of bacteriostatic and bactericidal cell-free supernatant components into ST-AMR-11 so that a lower total treatment concentration was needed to achieve growth suppression by 16h in this isolate compared to ST-14028s.

Given the enhanced capacity of the *L. paracasei* + rice bran extract and *L. fermentum* + rice bran extract cell-free supernatants to suppress both non-resistant and phenotypically antimicrobial resistant *Salmonella* growth compared to their probiotic-only supernatants, the global, non-targeted metabolite profiles of these two treatments were compared to examine if shared versus different metabolic mechanisms were contributing to their effects on *Salmonella* growth suppression. Amino acid, lipid, carbohydrate, energy and nucleotide metabolic pathways were differentially-regulated between the *L. fermentum* + rice bran extract *L. paracasei* + rice bran extract (**Figure 3.4**, **Figure 3.5**), supporting that inherent metabolic differences between these *Lactobacillus* spp. may be driving *Salmonella* growth suppression by these cell-free supernatants via secretion of different metabolites. To confirm this, metabolites within these differentially-regulated metabolic pathways were compared, and 84 metabolites were found to have differential abundances in the cell-free supernatant of *L. paracasei* + rice bran extract versus *L. fermentum* + rice bran extract.

A comprehensive literature search screened these metabolites for previously-reported antimicrobial activity and roles in *Salmonella* growth (**Table 3.2**). Among these compounds

were the amino acid N-acetylglucosamine, which was 0.21-fold lower in *L. fermentum* + rice bran extract versus *L. paracasei* + rice bran extract (**Table 3.2**). N-acetylglucosamine has previously-reported roles in *S.* Typhimurium replication as a key intermediate in cell-wall synthesis of peptidoglycans and lipopolysaccharide (Yoo *et al.*, 2016). Lower concentrations of N-acetylglucosamine in the *L. paracasei* synbiotic compared to the *L. fermentum* synbiotic may indicate that the *L. paracasei* synbiotic preferentially reduces *Salmonella* growth via limiting the rate of cell-wall synthesis compared to the *L. fermentum* synbiotic.

A distinct mechanism by which the *L. fermentum* + rice bran extract supernatant drives enhanced *Salmonella* growth suppression compared to that of *L. paracasei* + rice bran extract may be via decreased glucose production. The *L. fermentum* + rice bran extract supernatant contained 311.52-fold less glucose than the *L. paracasei* + rice bran extract supernatant (**Table 3.2**). A previous study examining glucose metabolism by *Lactobacillus* spp. established that decreased environmental glucose was associated with increased *Lactobacillus* production of various fatty acid compounds that functioned bactericidally via damaging *Salmonella* outer cell wall and cytoplasmic membrane structures (Kanjan and Hongpattarakere, 2016), suggesting that *L. fermentum* + rice bran extract may be producing higher levels of these antimicrobial metabolites than *L. paracasei* + rice bran extract. *L. fermentum* + rice bran extract levels of the long-chain fatty acids palmitate, oleate/vaccenate, and linoleate (0.74-fold, 0.26-fold and 0.58-fold less abundant in the *L. paracasei* versus *L. fermentum* synbiotic supernatants respectively) provide support for this mechanism, where all three have previously-reported bactericidal and bacteriostatic effects when applied to *Salmonella* (Yuan, 2018; Zhang, 2016; Kanjan, 2016; Garvey, 2011). Differential metabolism of carbohydrates, which is captured by the obligate heterofermentative versus facultative heterofermentative phenotypes of *L. fermentum* versus *L.*

paracasei (**Table 3.1**) thus may be important metabolic features to consider when supplementing probiotics with different prebiotic carbohydrate sources such as rice bran extract and screening the resultant secreted synbiotic metabolites for pathogen growth suppression.

In comparison to amino acid, carbohydrate, and lipid metabolism, nucleotide metabolism represents an unexplored area contributing to synbiotic activity against pathogens. Of the 15 nucleotides that were differentially-abundant between the *L. paracasei* + rice bran extract and *L. fermentum* + rice bran extract supernatants, five had previously-reported antimicrobial functions. Among these metabolites was orotate (330.73-fold increase in the *L. paracasei* + rice bran extract supernatant versus the *L. fermentum* + rice bran extract supernatant), where low ororate:succinate ratios in growth media were shown to reduce *Salmonella* growth via slowing the nucleotide synthesis (Baker *et al.*, 1996). When comparing relative levels of orotate and succinate between these two treatments (0.65-fold less abundant in *L. paracasei* + rice bran extract versus in the *L. fermentum* + rice bran extract), the *L. fermentum* + rice bran extract supernatant had a lower orotate:succinate abundance ratio compared to the *L. paracasei* + rice bran extract supernatant (**Table 3.2**), suggesting that depletion of nucleotide biosynthesis substrates may be an additional molecular mechanism distinguishing *L. fermentum* + rice bran extract supernatant suppression of *Salmonella* growth from the *L. paracasei* + rice brane extract supernatant. Differential production of guanine by *L. paracasei* + rice bran extract and *L. fermentum* + rice bran extract (0.42-fold decrease in *L. paracasei* + rice bran extract versus in *L. fermentum* + rice bran extract) represents a second nucleotide mechanism distinguishing synbiotic mechanisms of action. Decreased environmental guanosine concentrations were previously shown to decrease *Salmonella* growth, which was hypothesized to occur via reducing synthesis of the energy intermediate guanosine triphosphate that facilitates multiple metabolic

reactions inside the microbial cell (Jensen, 1979). The lower exogenous guanosine concentrations produced in the *L. paracasei* + rice bran extract supernatant versus the *L. fermentum* + rice bran extract supernatant may consequently reflect an additional mechanism by which synbiotic secreted products from different *Lactobacillus* spp. may suppress *Salmonella* growth via distinct, probiotic species-dependent mechanisms.

This study supports that rice bran extract can differentially enhance the natural growth suppressive capacities of *Lactobacillus* cell-free supernatants against antimicrobial-resistant *Salmonella* Typhimurium via mechanisms independent of increasing total *Lactobacillus* growth. The metabolite profile differences between *L. paracasei* + rice bran extract and *L. fermentum* + rice bran extract supernatants warrant further investigation into probiotic species-dependent metabolism of prebiotics that may influence their health effects and secreted compounds when these probiotics are prepared as synbiotics.

Notably, *L. fermentum* + rice bran extract and *L. paracasei* + rice bran extract differential production of lipids, amino acids and metabolites warrants further investigation into how these chemical classes, derived from a whole-food prebiotic, contribute to probiotic function and act as antimicrobials against enteric pathogens. Finally, the ability of *Lactobacillus* + rice bran extract cell-free supernatants to differentially suppress growth of an antimicrobial-resistant *Salmonella* isolate versus an isolate that only harbored antimicrobial resistance genes warrants further investigation into the unique metabolic mechanisms by which drug-resistant pathogens respond to synbiotic compounds when compared to phenotypically non-resistant pathogens. Ultimately, the capacity of synbiotic secreted products to enhance *Salmonella* growth suppression supports further examination of their effects on other pathogens, including drug-resistant pathogens, where these compounds can be applied as sustainable alternatives to conventional antimicrobial

agents or used in conjunction with them to reduce human and animal dependency these antimicrobials.

3.6. Availability of data and material:

The whole genome sequencing datasets generated and/or analyzed during the current study are available in the National Center for Biotechnology Information (**NCBI**) Genome repository: https://www.ncbi.nlm.nih.gov/sra/PRJNA530250

REFERENCE

Aminov R. History of antimicrobial drug discovery: Major classes and health impact. Biochemical Pharmacology. 2017;133:4-19.

Atlanta, Georgia. USA: Centers for Disease Control and Prevention; 2018.Baker KE, Ditullio KP, Neuhard J, Kelln RA. Utilization of orotate as a pyrimidine source by Salmonella typhimurium and Escherichia coli requires the dicarboxylate transport protein encoded by dctA. Journal of bacteriology. 1996;178(24):7099-105.

Baquero F, Martínez J-L. Interventions on Metabolism: Making Antibiotic-Susceptible Bacteria. mBio. 2017;8(6):e01950-17.

CDC, (DHQP). Atlanta, Georgia, USA.: Centers for Disease Control and Prevention; 2018.

Distrutti E, Monaldi L, Ricci P, Fiorucci S. Gut microbiota role in irritable bowel syndrome: New therapeutic strategies. World journal of gastroenterology. 2016;22(7):2219-41.

Fernandez J, Guerra B, Rodicio MR. Resistance to Carbapenems in Non-Typhoidal Salmonella enterica Serovars from Humans, Animals and Food. Veterinary sciences. 2018;5(2).

Garvey MI, Rahman MM, Gibbons S, Piddock LJ. Medicinal plant extracts with efflux inhibitory activity against Gram-negative bacteria. International journal of antimicrobial agents. 2011;37(2):145-51.

Han F., et al. Effects of Whole-Grain Rice and Wheat on Composition of Gut Microbiota and Short-Chain Fatty Acids in Rats. Journal of agricultural and food chemistry. 2018;66(25):6326-35.

Harris HMB, et al., Draft Genome Sequence of Lactobacillus fermentum Lf2, an Exopolysaccharide-Producing Strain Isolated from Argentine Cheese. Microbiology resource announcements. 2018;7(18).

Henderson AJ, et al., Consumption of rice bran increases mucosal immunoglobulin A concentrations and numbers of intestinal Lactobacillus spp. Journal of medicinal food. 2012;15(5):469-75.

Heredia-Castro PY, et al., Antimicrobial activity and partial characterization of bacteriocin-like inhibitory substances produced by Lactobacillus spp. isolated from artisanal Mexican cheese. Journal of dairy science. 2015;98(12):8285-93.

Jensen KF. Apparent involvement of purines in the control of expression of Salmonella typhimurium pyr genes: analysis of a leaky guaB mutant resistant to pyrimidine analogs. Journal of bacteriology. 1979;138(3):731-8.

Kanjan P., Hongpattarakere T., Antibacterial metabolites secreted under glucose-limited environment of the mimicked proximal colon model by lactobacilli abundant in infant feces. Applied microbiology and biotechnology. 2016;100(17):7651-64.

Kohanski MA, Dwyer DJ, Collins JJ. How antibiotics kill bacteria: from targets to networks. Nature reviews Microbiology. 2010;8(6):423-35.

Kumar A., et al. Dietary rice bran promotes resistance to Salmonella enterica serovar Typhimurium colonization in mice. BMC microbiology. 2012;12:71.

Lakin SM, et al. MEGARes: an antimicrobial resistance database for high throughput sequencing. Nucleic acids research. 2017;45(D1):D574-D80.

Lamas A., et al., A comprehensive review of non-enterica subspecies of Salmonella enterica. Microbiological research. 2018;206:60-73.

Luoma A, et al., Effect of synbiotic supplementation on layer production and cecal Salmonella load during a Salmonella challenge. Poultry science. 2017;96(12):4208-16.

Marianelli C., Cifani N, Pasquali P. Evaluation of antimicrobial activity of probiotic bacteria against Salmonella enterica subsp. enterica serovar typhimurium 1344 in a common medium under different environmental conditions. Research in microbiology. 2010;161(8):673-80.

Markowiak P, Slizewska K. Effects of Probiotics, Prebiotics, and Synbiotics on Human Health. Nutrients. 2017;9(9).

NARMS. Antibiotics Tested by NARMS. In: National Center for Emerging and Zoonotic Infectious Diseases (NCEZID): Division of Foodborne W, and Environmental Diseases (DFWED).

Nealon NJ, Worcester CR, Ryan EP. Lactobacillus paracasei metabolism of rice bran reveals metabolome associated with Salmonella Typhimurium growth reduction. Journal of applied microbiology. 2017;122(6):1639-56.

Piatek J., et al., Persistent infection by Salmonella enterica servovar Typhimurium: are synbiotics a therapeutic option? - a case report. Beneficial microbes. 2019;10(2):211-7.

Rojo F., Martínez JL., Metabolic regulation of antibiotic resistance. FEMS Microbiology Reviews. 2011;35(5):768-89.

Rubinelli P.M., et al., Differential effects of rice bran cultivars to limit Salmonella Typhimurium in chicken cecal in vitro incubations and impact on the cecal microbiome and metabolome. PLOS ONE. 2017;12(9):e0185002.

Nealon N.J., et al., Rice Bran and Probiotics Alter the Porcine Large Intestine and Serum Metabolomes for Protection against Human Rotavirus Diarrhea. Frontiers in microbiology. 2017;8:653.

Ryan E.P., et al., Rice bran fermented with saccharomyces boulardii generates novel metabolite profiles with bioactivity. Journal of agricultural and food chemistry. 2011;59(5):1862-70.

Sheflin A.M., et al. Dietary supplementation with rice bran or navy bean alters gut bacterial metabolism in colorectal cancer survivors. Molecular nutrition & food research. 2017;61(1).

Smirnov K.S., et al., Challenges of metabolomics in human gut microbiota research. International journal of medical microbiology : IJMM. 2016;306(5):266-79.

Thomas M., et al., Whole genome sequencing-based detection of antimicrobial resistance and virulence in non-typhoidal Salmonella enterica isolated from wildlife. Gut pathogens. 2017;9:66.

Vitaglione P., et al., Whole-grain wheat consumption reduces inflammation in a randomized controlled trial on overweight and obese subjects with unhealthy dietary and lifestyle behaviors: role of polyphenols bound to cereal dietary fiber. The American journal of clinical nutrition. 2015;101(2):251-61.

Yoo W., et al., Fine-tuning of amino sugar homeostasis by EIIA(Ntr) in Salmonella Typhimurium. Scientific reports. 2016;6:33055-.

Yuan J., et al. Composition and antimicrobial activity of the essential oil from the branches of Jacaranda cuspidifolia Mart. growing in Sichuan, China. Natural product research. 2018;32(12):1451-4.

Zarei I., et al., Rice Bran Metabolome Contains Amino Acids, Vitamins & Cofactors, and Phytochemicals with Medicinal and Nutritional Properties. Rice (New York, NY). 2017;10(1):24.

Zarei I., et al., Comparative Rice Bran Metabolomics across Diverse Cultivars and Functional Rice Gene(-)Bran Metabolite Relationships. Metabolites. 2018;8(4).

Zhang X., et al., Inactivation of Salmonella spp. and Listeria spp. by Palmitic, Stearic, and Oleic Acid Sophorolipids and Thiamine Dilauryl Sulfate. Frontiers in microbiology. 2016;7:2076

CHAPTER FOUR

BIOACTIVITY-GUIDED FRACTIONATION OF CELL FREE SUPERNATANT METABOLOMES FROM *LACTOBACILLUS* SPP. AND RICE BRAN SYNBIOTICS FOR THE IDENTIFICATION OF NOVEL COMPOUNDS THAT SUPPRESS ANTIMICROBIAL RESISTANT *SALMONELLA* TYPHIMURIUM GROWTH

4.1. Summary:

Antimicrobial-resistant *Salmonella* Typhimurium is an emerging global threat to human and animal health. Synbiotic combinations of *Lactobacillus* spp. and rice bran have been demonstrated to enhance *Salmonella* growth suppression, and their cell-free supernatants contains diverse, *Lactobacillus* species-specific suites of metabolites associated with this growth suppression. To further elucidate the small molecule mechanisms through which *Lactobacillus* + rice bran synbiotics drive antimicrobial-resistant *Salmonella* growth suppression, the cell-free supernatants of *L. fermentum* and *L. paracasei* synbiotics produced during rice bran fermentation were subjected to bioactivity-guided separation, and the resultant fractions were screened for *Salmonella* growth suppression. Both *L. fermentum* and *L. paracasei* synbiotic supernatant fractions enhanced *Salmonella* growth suppression between 8-20% compared to the negative control treatment. When the non-targeted metabolome of representative bioactive (*Salmonella*-suppressive) and ineffective fractions was established, the bioactive fractions of both synbiotics contained a larger proportion of lipid metabolites compared to the ineffective fraction. The bioactive *L. fermentum* and *L. paracasei* fractions both contained 21 significantly-increased lipids compared to the ineffective fraction including oleoyl-linoleoyl glycerol, that was differentially-abundant across synbiotics (123.29-fold and 42.38-fold increase in *L. fermentum*

and *L. paracasei* synbiotics respectively). However, *L. fermentum* bioactive fractions were uniquely-enriched in the energy metabolite fumarate (2.25-fold increase), and *L. paracasei* bioactive fractions exclusively contained the amino acid metabolites imidazole lactate and ornithine (1.34-fold and 3.60-fold increase respectively), suggesting that *Lactobacillus* + rice bran synbiotics additionally drive growth suppression via multiple species-specific small molecule mechanisms. Integrated gene and protein analysis of these synbiotic-specific metabolites identified multiple microbial alleles and associated biosynthetic enzymes that were potential contributors to these metabolite profile differences that could be screened for in probiotic species when selecting them for antimicrobial metabolite production. The results of this study can be used to optimize *Lactobacillus* + rice bran synbiotic supernatants as preventives and treatments against antimicrobial-resistant *Salmonella* Typhimurium infections in people, animals, and the environment.

4.2. Introduction:

The Centers for Disease Control lists antimicrobial resistant bacterial infections as one of the top ten global disease threats to human health (CDC, 2018). The distinct cell wall composition of Gram-negative bacteria confers innate resistance to many antimicrobial agents such as first-generation beta lactams (Adler *et al.*, 2016), and over time, widespread antimicrobial use places selective pressures on these microbes allowing them to acquire additional drug resistance, including against fluoroquinolones and the last-resort antimicrobials carbapenems and colistin (Mukerji *et al.*, 2017). Among the Gram-negative bacteria driving human and animal disease outbreaks is the zoonotic pathogen *Salmonella* enterica serovar Typhimurium that infects over 1.2 million people each year in the United States alone (CDC,

2018a; 2019). Over 100,000 of these infections are estimated to occur with multidrug resistant *Salmonella* Typhimurium isolates that are resistant to three or more antimicrobial drug classes (CDC, 2018a). Collectively, these drug-resistant outbreaks have added an estimated additional $365 million dollars to healthcare costs (CDC, 2018a). Efforts to prevent and contain multidrug resistant *Salmonella* outbreaks are further complicated given the costly and time-consuming development of safe and effective new antimicrobial agents (Aminov, 2017). In consideration of these factors, sustainable alternative approaches designed to suppress the growth of multidrug resistant *Salmonella* are necessary and merit further investigation.

The synbiotic combination of health-containing probiotic bacteria and prebiotic carbon sources that support probiotic growth and metabolism are gaining increased attention for their efficacy against enteric pathogens, including *Salmonella* Typhimurium (Abdel-Wareth *et al.*, 2019; Kanjan and Hongpattarakere, 2017; Lepine and de Vos, 2018; Markazi *et al.*, 2018; Piatek *et al.*, 2019). Notably, synbiotics containing *Lactobacillus* spp. and rice bran, the outer coating of brown rice, have demonstrated efficacy in suppressing *Salmonella* Typhimurium growth in mice (Henderson *et al.*, 2012a; Kumar *et al.*, 2012), and enhance provide enhanced *Salmonella* growth suppression compared to either *Lactobacillus* spp. or rice bran alone (Nealon *et al.*, 2017a). Global, non-targeted metabolomics studies, which can systematically separate, detect, and identify the small molecules within these synbiotics, have identified hundreds of bioactive metabolites in *Lactobacillus* + rice bran cell-free supernatants that suppressed the growth of antimicrobial-resistant *Salmonella* Typhimurium including multiple lipids, amino acids and phytochemicals that are differentially-produced by *Lactobacillus* spp. during rice bran metabolism (Nealon *et al.*, 2017a), and which have not been extensively studied for their antimicrobial potentials. Given the reported *Lactobacillus* species differences in antimicrobial

metabolite production, and the potential these synbiotics hold as *Salmonella* growth suppressors, additional research is needed to identify the synbiotic components that drive antimicrobial-resistant *Salmonella* Typhimurium growth suppression.

The current study used bioactivity-guided fractionation to separate the metabolites within cell-free supernatant of two *Lactobacillus* + rice bran synbiotics that previously suppressed the growth of antimicrobial-resistant *Salmonella* Typhimurium (**Chapter 3**), and screened these fractions for their individual capacities to suppress *Salmonella* growth. The overarching hypothesis was that fractionated cell-free supernatant collected from two different *Lactobacillus* spp. + rice bran synbiotics would reveal distinct, probiotic-species dependent metabolite suites that suppressed *Salmonella* growth in magnitude and time-dependent manners. It was predicted that differential metabolism of lipids, amino acids and phytochemicals by *Lactobacillus* spp., which are major constituents of *Lactobacillus* + rice bran synbiotics, would contribute to *Salmonella* growth suppression and distinguish the *Salmonella*-suppressive fractions of these two synbiotics from each other.

4.3. Materials and Methods:

4.3.1. Bacterial culture preparation:

Two *Lactobacillus* spp. with previously-demonstrated capacities to suppress antimicrobial-resistant *Salmonella* Typhimurium growth, were examined in this study: *L. fermentum* (ATCC-23271) and *L. paracasei* (ATCC-27092). Each *Lactobacillus* spp. was cultured in deMann Rogasa Sharpe Broth (**MRS**) (Becton, Dickinson and Company, Difco Laboratories, Franklin Lakes, NJ) at 37°C under aerobic conditions for the experiments described herein. An antimicrobial-resistant *Salmonella* Typhimurium isolate was generously provided by Dr.

Sangeeta Rao from Colorado State University. *Salmonella* cultures were maintained in Luria Bertani broth (**LB**) (MOBIO Laboratories Inc., Carlsbad, CA) incubated at 37°C under aerobic conditions for all experiments reported herein. **Table 4.1** provides the antimicrobial-resistance profile of the examined *Salmonella* Typhimurium isolate was determined by the Colorado State University-Veterinary Teaching Hospital Diagnostic Medicine Center. This resistance profile and designations of "susceptible" and "resistant" were obtained using broth microdilution against a standard panel of antimicrobial agents as recommended by the National Antimicrobial Resistance Monitoring Systems guidelines for testing of Enterobacteriaceae and following Clinical and Laboratory Standards Institute Guidelines (CLSI, 2010).

Table 4.1. *Salmonella* Typhimurium antimicrobial resistance profile

Antimicrobial Agent	Susceptibility	Minimum Inhibitory Concentration (µg/mL)
Amoxicillin-Clavulanate	Resistant	>32
Ampicillin	Resistant	>32
Azithromycin	Susceptible	2
Ceftiofur	Resistant	>8
Chloramphenicol	Resistant	>32
Ciprofloxacin	Susceptible	0.5
Sulfisoxazole	Resistant	>256
Tetracycline	Resistant	>32
Trimethoprim-sulfamethoxazole	Resistant	>4

Minimum inhibitory concentrations for each agent reflect the lowest drug concentration at which ≥99.9% of microbial growth is prevented.

4.3.2. Rice bran extraction:

Rice bran extracts were created to improve its solubility within bacterial growth media. Heat-stabilized Calrose rice bran (USDA-ARS Rice Research Unit, Stuttgart, AK) was extracted using the methods previously described (Nealon *et al.*, 2017a). Briefly, rice bran was mixed in a 1:4 v/v ratio with an -80°C ice-cold 80% methanol aqueous solution. Following overnight incubation at -80°C, the methanol and rice bran slurries were centrifuged at 4000xg for 10 minutes (Beckman Coulter Allegra X-14R, Indianapolis, IN). Extracts were collected and dried

under a sterile fume hood at 37C. Dried rice bran extract was weighed and stored at -20°C until further use.

4.3.3. Lactobacillus and rice bran extract cell-free supernatant preparation:

To prepare synbiotic cell-free supernatant, $1x10^8$ colony forming units/mL (**CFU/mL**) of *Lactobacillus* spp. were cultured for 24h in 15 mL of sterile MRS with 100 µg/mL of supplemented rice bran extract. These *Lactobacillus* spp. CFU/mL and rice bran extract concentrations were selected due to the previously-demonstrated capacities of their cell-free supernatants to suppress *S.* Typhimurium growth as probiotics-alone when combined as a synbiotic (Nealon *et al.*, 2017a). Flasks containing 15mL of sterile MRS and sterile MRS+ rice bran extract media were incubated as negative controls to confirm media sterility prior to inoculation with *Lactobacillus* spp. and subsequent supernatant collection. After 24h, cultures were centrifuged at 4000xg for 10 minutes, and the spent media was separated from its pellet. To adjust for small pH differences produced by *Lactobacillus* spp., all supernatant was titrated to pH of 4.5 using a pH meter (Corning Pinnacle 530, Cole-Parmer, Vernon Hills, IL). Prior to storage, all supernatant was filtered through a 0.22 µm filter (Pall Corporation LifeSciences Acrodisc syringe filters, Port Washington, NY) and was frozen at -80°C until further use. Supernatant sterility was confirmed by reading its optical density at 600 nm (**OD600**) for 24h on a Biotek Cytation3 (BioTek Instruments Inc., Winooski, VT).

4.3.4. Salmonella growth suppression assay with synbiotic cell-free supernatant fractions:

Five mL samples of *L. fermentum* + rice bran extract and *L. paracasei* + rice bran extract supernatants were separated into 24 fractions using reverse-phase flash chromatography on a

Combiflash® RF+ Flash Chromatography Purification System (Teledyne ISCO, Thousand Oak, California). The 5 mL starting volume was determined following a range-finding analysis that optimized sample injection volume for metabolite recovery during non-targeted metabolomics analysis. The stationary phase column was a C18-aq, 15.5g-Gold Redisep column (Teledyne ISCO, Thousand Oaks, California), and the mobile phase gradient consisted of a water:methanol solution that increased in hydrophobicity over the course of the separation. To account for machine fractionation variability and batch-to-batch supernatant variability in antimicrobial activity, each supernatant was fractionated three times using a minimum of three batches collected on different days. A chromatogram absorbing at 214 and 254 nm wavelengths was collected and compared across each run to confirm that there was minimal chromatographic drift between subsequently-run samples, and *L. fermentum* and *L. paracasei* samples were run interchangeably on the same column. Following separation, fractions were dried at 55°C under a sterile fume hood and then re-constituted to the original supernatant concentration in LB broth titrated to a pH of 4.5. All re-constituted fractions were stored at -80°C until use.

4.3.5. Examination of cell-free supernatant fractions for Salmonella growth suppression:

Following chromatographic separation, fractions were dried at 55°C under a sterile fume hood and then re-constituted in 5 mL of pH 4.5 LB broth. All re-constituted fractions were stored at -80°C until use. $1X10^6$ CFU of each *S.* Typhimurium were added to LB broth on a 96 well plate and treated with each re-constituted fraction to create a 22% v/v concentration in LB, which was a supernatant dose that previously exhibited growth suppression for this *Salmonella* isolates (**Chapter 3**). In each assay, *Salmonella* inoculated in 4.5 pH-adjusted LB was used as the negative control. To adjust for starting differences in fraction optical densities and to confirm

media sterility over the course of the assay, blank LB and blank fraction + LB were included as controls. *S.* Typhimurium growth over time was measured every 20 minutes for 16h using repeated OD600 reads. At each time point, the OD600 of each fraction was compared to that of the negative control using a repeated measures 2-way analysis of variance with a Tukey post-test to adjust for multiple comparisons, and significance was defined as $p<0.05$. All statistical analysis for the growth curve analysis was performed in GraphPad Prism, Version 8.0.0 (La Jolla, CA).

To assess the *S.* Typhimurium growth suppression of each fraction compared to the negative control, percent growth suppression was calculated using the following equation:

$$\left|\frac{(OD600\ Treatment\ 1 - OD600\ Treatment\ 2)}{(OD600\ Treatment\ 2)}\right| * 100\%$$

Each assay contained a minimum of two technical replicates for each treatment and was repeated three times for each *S.* Typhimurium isolate incubated with either *L. fermentum* or *L. paracasei* synbiotic supernatant treatments.

4.3.6. Global, non-targeted metabolomics sample processing:

For *L. fermentum* and *L. paracasei* treatments, fractions representative of the entire chromatogram mobile phase gradient that both exhibited differential magnitudes of *Salmonella* growth suppression (fractions 18, 21, 22) or did not exhibit *Salmonella* growth suppression (fraction 4) were profiled using global, non-targeted metabolomics at Metabolon Inc © (Durham, NC). Briefly, dried fractions from *L. fermentum* and *L. paracasei* were shipped on dry ice to Metabolon and frozen at -80°C until sample processing with ultra-high-performance liquid chromatography tandem mass spectrometry (**UPLC-MS/MS**). Fractions were re-solubilized in methanol, centrifuged at room temperature, and separated into five aliquots for downstream

analysis: two aliquots for reverse-phase chromatography coupled with positive ion mode electrospray ionization (**ESI**), one aliquot for reverse phase chromatography coupled with negative ion mode ESI, a fourth aliquot for hydrophilic-interaction UPLC-MS/MS coupled with negative ion mode ESI, and the fifth aliquot saved as a back-up sample. Quality control samples were prepared by pooling similar aliquots across all fraction samples to account for chromatographic drift across subsequent UPLC-MS/MS runs.

Prior to injection, each aliquot was dried using an automated evaporation system (TurboVap ®, LV Automated Evaporation System, Thermo Scientific, Pittsburgh, PA). Each dried sample was re-constituted, mixed with internal standard compounds of known concentration, and processed for the following UPLC-MS/MS workflows: Acidic positive ion mode conditions optimized for hydrophilic metabolite extraction with a C18 column (Waters UPLC BEH C18-2.1x100 mm, 1.7 µm) stationary phase and a mobile phase solution of water and methanol with 0.05% v/v perfluoropentanoic acid and 0.1% v/v formic acid; Acidic positive ion mode conditions optimized for hydrophobic metabolite extraction with the same C18 column stationary phase as the previous condition and a mobile phase solution of methanol, acetonitrile and water with 0.05% perfluoropentanoic acid and 0.01% formic acid; Basic negative ion mode conditions with a C18 column (Waters UPLC BEH C18-2x100 mm, 1.7 µm) stationary phase and a mobile phase solution of methanol and water adjusted to a pH of 8 with ammonium bicarbonate; Negative ESI coupled with a hydrophilic interaction stationary phase column (Waters UPLC BEH Amide 2.1x150 mm, 1.7 µm) and a mobile phase solution of water and acetonitrile adjusted to a pH of 10.8 with ammonium formate. All workflows used Waters AQUITY ultra-performance liquid chromatography columns coupled to a Thermo Scientific Q-Exactive high resolution mass spectrometers equipped with a heated ESI source and an Orbitrap

mass analyzer set to a 35,000 mass:charge (**m/z**) resolution, with a tandem mass spectrometry setup that fluxed between dynamic exclusion MS and data-dependent MS^n scans covering 70-1000 m/z.

4.3.7. Metabolomics data analysis:

Raw mass spectral data was extracted using software developed by Metabolon where data was peak-extracted and normalized using area under the curve abundances with reference to quality control samples and internal standard recoveries. To account for signal intensity variation across sample runs, the raw abundance of each peak-extracted mass spectral feature was median-scaled by dividing its raw abundance by the median raw abundance for that metabolite across the entire dataset.

Mass spectral features were identified to known compounds using their retention indices, accurate masses (+/- 10 parts per million), and their MS/MS forward and reverse scores compared to Metabolon's internal compound library containing over 3,300 purified chemical standards. Metabolite identities were cross-validated and linked to their profiles on curated online public mass spectral databases (Human Metabolome Database, "**HMDB**"; Kyoto Encyclopedia of Genes and Genomes, "**KEGG**", and PubChem) (Consortium, 2018; Kanehisa *et al.*, 2017; Kanehisa and Goto, 2000; Kanehisa *et al.*, 2019; Wishart *et al.*, 2018; Wishart *et al.*, 2013; Wishart *et al.*, 2009; Wishart *et al.*, 2007). For compounds that did not have a matching internal standard with the Metabolon library, identifies were directly made using these public databases, and mass spectral features that were not identifiable by either Metabolon or these databases were defined as "unknown" and annotated with their m/z and retention indices.

Median-scaled abundances of each metabolite from each *L. fermentum* or *L. paracasei* fraction that suppressed *Salmonella* growth (fractions 18, 21, 22) were compared to their median-scaled abundance in *L. fermentum* or *L. paracasei* fraction 4 (fraction that did not exhibit *Salmonella* growth suppression) to identify fractions that were significantly-increased ($p<0.05$) only in bioactive fractions. Furthermore, the median-scaled abundances of metabolites between *L. fermentum* versus *L. paracasei* fractions were compared between analogous fractions (e.g. *L. paracasei* fraction 18 versus *L. fermentum* 18) to evaluate synbiotic fractions for differential abundance of antimicrobial metabolites across *Lactobacillus* species. All median-scaled abundance analyses were examined using a two-way analysis of variance where multiple comparisons were evaluated using Welch's two-sample t-tests. Statistical significance was defined as $p<0.05$ following false-discovery rate adjustment of p-values. Metabolites with a false discovery rate of $q>0.10$ were excluded from downstream analysis. All statistical analysis was performed by Metabolon using ArrayStudio (Omicsoft Corporation, Cary, NC) and R version 3.5.2. Metabolite median-scaled abundance differences between treatments were depicted as fold differences, where the average median-scaled abundance of one treatment was divided by the average median-scaled abundance of the second treatment.

4.3.8. Identification of gene and protein precursors for select metabolites:

Metabolites that distinguished the *Salmonella*-suppressive *L. fermentum* and *L. paracasei* fractions were further screened for reported upstream biosynthetic enzymes and genes using the following publicly-available gene and protein databases: Kyoto Encyclopedia of Genes and Genomes (**KEGG**), the National Center for Biotechnology Information (**NCBI**), and the UniProt Knowledge Base (**UniProtKB**). Across each of these databases, metabolite cross-references to

genes and proteins were made using database annotations supporting their presence in a prokaryotic (bacterial) microorganism from over 5,117 archived reference species.

4.4. Results:

4.4.1. Bioactivity-guided fractionation identified synbiotic supernatant fractions that suppressed Salmonella Typhimurium growth:

Twenty-four fractions were collected from the cell free supernatants of *L. fermentum* and *L. paracasei* synbiotics, and all 24 fractions were screened for *Salmonella* Typhimurium growth suppression. Of the 24 *L. fermentum* fractions, four fractions (fraction 18, fraction 20, fraction 21, fraction 22) significantly suppressed *Salmonella* growth suppression compared to the negative control ($p<0.05$) and three fractions (fraction 2, fraction 3, fraction 4) significantly increased *Salmonella* growth compared to the negative control ($p<0.05$). For the 24 *L. paracasei* fractions, seven fractions (fraction 18, fraction 19, fraction 20, fraction 21, fraction 22, fraction 23, fraction 24) significantly suppressed *Salmonella* growth compared to the negative control ($p<0.05$), and one fraction (fraction 2) exhibited increased growth compared to the negative control. **Figure 4.1** visualizes fractions with statistically-significant growth differences for *L. fermentum* + rice bran extract (panel **4.1A**) and *L. paracasei* + rice bran extract (panel **4.1B**) synbiotics. **Table 4.2** shows the percent difference in *Salmonella* growth suppression compared to the negative control treatment. All fractions with *Salmonella* growth suppressive bioactivity eluted within the hydrophobic region of the mobile phase gradient. Fractions (18, 19, 20- 24) exhibited bioactivity for 8-22% enhancement of *Salmonella* growth suppression between 10-16h (mid-late exponential phase of *Salmonella* growth). Four fractions exhibited *Salmonella* growth suppression for both *L. fermentum* and *L. paracasei* synbiotics (fraction 18, fraction 21, fraction

22, fraction 23). *L. paracasei* fractions showed higher magnitudes of growth suppression compared to the *L. fermentum* synbiotic.

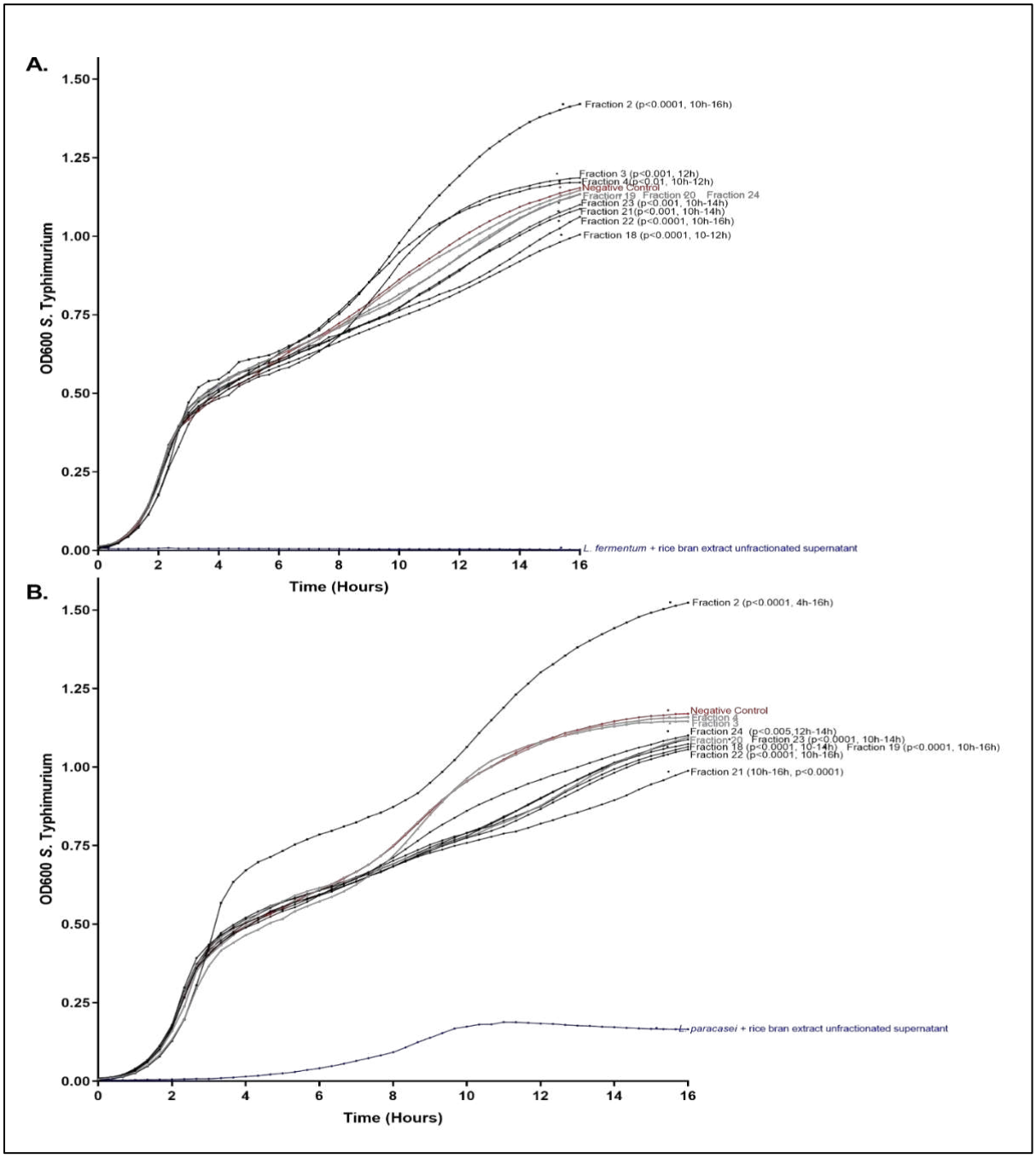

Figure 4.1. *L. fermentum* (A) and *L. paracasei* (B) synbiotics produce fractions that modulate *Salmonella* Typhimurium growth.

Black lines represent fractions that exhibited significantly-different growth ($p<0.05$) compared to the negative control (red line) over the time interval (hours) reported in parentheses. Gray lines represent fractions that did not exhibit growth differences compared to

the negative control. Blue line shows unfractionated synbiotic supernatant. Each point represents the mean of three independent experiments.

Table 4.2. Growth suppression of *Salmonella* by synbiotic supernatant fractions compared to the negative control

Fraction	Mobile Phase Solvent		*S.* Typhimurium Percent Growth Suppression	
	% Water	% Methanol	*L. fermentum* + rice bran extract	*L. paracasei* + rice bran extract
2	95%	5%	**↑21.68%** ***(14h)***	**↑28.73** ***(4h)***
3	95%	5%	**↑8.67%** **(12h)**	↓24.65% *(2h)*
4	95%	5%	**↑10.38%** ***(12h)***	↓5.83% *(2h)*
18	12.5%	87.5%	**↓11.39%** ***(12h)***	**↓15.95%** ***(12h)***
19	0%	100%	↓ 9.11% *(4h)*	**↓16.74%** ***(12h)***
20	0%	100%	↓8.70% *(2h)*	**↓17.70%** ***(12h)***
21	0%	100%	**↓7.83%** ***(12h)***	**↓22.30%** ***(12h)***
22	0%	100%	**↓12.79%** ***(12h)***	**↓19.90%** ***(12h)***
23	100%	0%	**↓8.01%** ***(10h)***	**↓17.05%** ***(10h)***
24	100%	0%	↓23.28% *(12h)*	**↓10.96%** ***(12h)***

↑indicates fraction had significantly higher *Salmonella* growth compared to the negative control, and ↓ indicates fraction had significantly lower *Salmonella* growth compared to the negative control, and treatments are **bolded** when growth was significantly-different ($p<0.05$). Times in parentheses reflect the hour at which the fraction achieved maximal growth difference compared to the negative control. Results reflect three independent experiments for each *Salmonella* isolate with each treatment.

4.4.2. Bioactive fractions from L. fermentum and L. paracasei are enriched in lipid metabolites.

Non-targeted metabolite profiling was completed on three fractions that exhibit *Salmonella* growth suppression (fraction 18, fraction 21, fraction 22), as well as for one fraction that did not suppress *Salmonella* growth (fraction 4). **Figure 4.2** displays the number of metabolites from each fraction across major chemical classes for both *L. fermentum* (panel **4.2A**) and *L. paracasei* (panel **4.2B**). The metabolite profiles from the 4 selected bioactive fractions was yielded 665 total metabolites with known and unknown identity. The total number of metabolites per fraction decreased over the course of the elution series: fraction 4 (323 metabolites in *L. fermentum*, 296

metabolites in *L. paracasei*), fraction 18 (182 metabolites *L. fermentum*, 167 metabolites *L. paracasei*), fraction 21 (138 metabolites *L. fermentum,* 158 metabolites *L. paracasei*) and fraction 22 (88 metabolites *L. fermentum,* 115 metabolites *L. paracasei*). In both strains of *Lactobacillus* spp., the proportion of lipid metabolites relative to the total number of metabolites in the fraction was increased in bioactive fractions (18, 21, 22) compared to the ineffective fraction 4. In *L. fermentum*, fraction 4 contained ~16% lipids, fraction 18 had ~24% lipids, fraction 21 contained 31% lipids, and fraction 22 had ~45% lipids. In *L. paracasei*, fraction 4 contained ~13.5% lipids, fraction 18 had ~25% lipids, fraction 21 contained ~33% lipids, and fraction 22 had ~30% lipids.

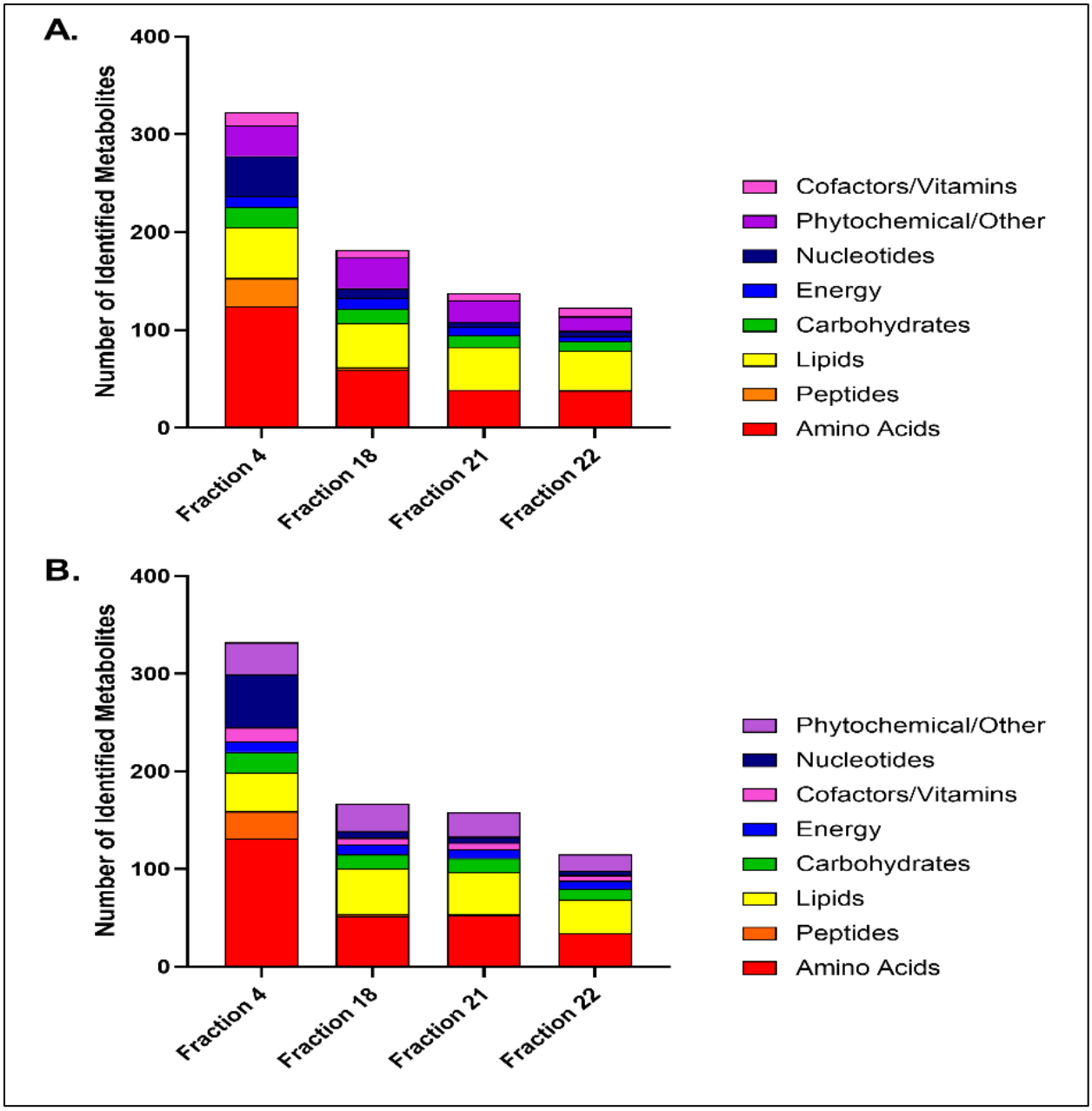

Figure 4.2. Metabolite profiles of fractions reveal different metabolite compositions across fractions and between synbiotic treatments.

L. fermentum ***(A)*** *and L. paracasei* ***(B)*** *synbiotic fractions visualized by the number of metabolites identified within each chemical class.*

4.4.3. Bioactive fractions from L. fermentum and L. paracasei contain distinct amino acid and energy metabolite profiles.

Figure 4.3 shows the bioactive fraction metabolites that overlap and are distinct between *L. fermentum* and *L. paracasei* synbiotics, and **Table 4.3** shows the fold difference in abundance of these metabolites within bioactive *L. fermentum* and *L. paracasei* fractions relative to their abundance in the ineffective fraction. All metabolites depicted had statistically significant increases in the bioactive fractions relative to the ineffective fractions ($p<0.05$). Bioactivity guided fractionation led to 65 metabolites that were associated with *Salmonella* growth suppression. *L. fermentum* bioactive fractions contained 33 metabolites enriched in *Salmonella*-suppressive fractions compared to the ineffective fraction. A majority (~84%) of these compounds were lipids including the long-chain fatty acid oleate (26.21-fold increase and 3.17-fold increase in fraction 18 and fraction 21 versus fraction 4 respectively) and the cyclic propane fatty acid lactobacillic acid (5.44-fold increase in fraction 18 versus fraction 4).

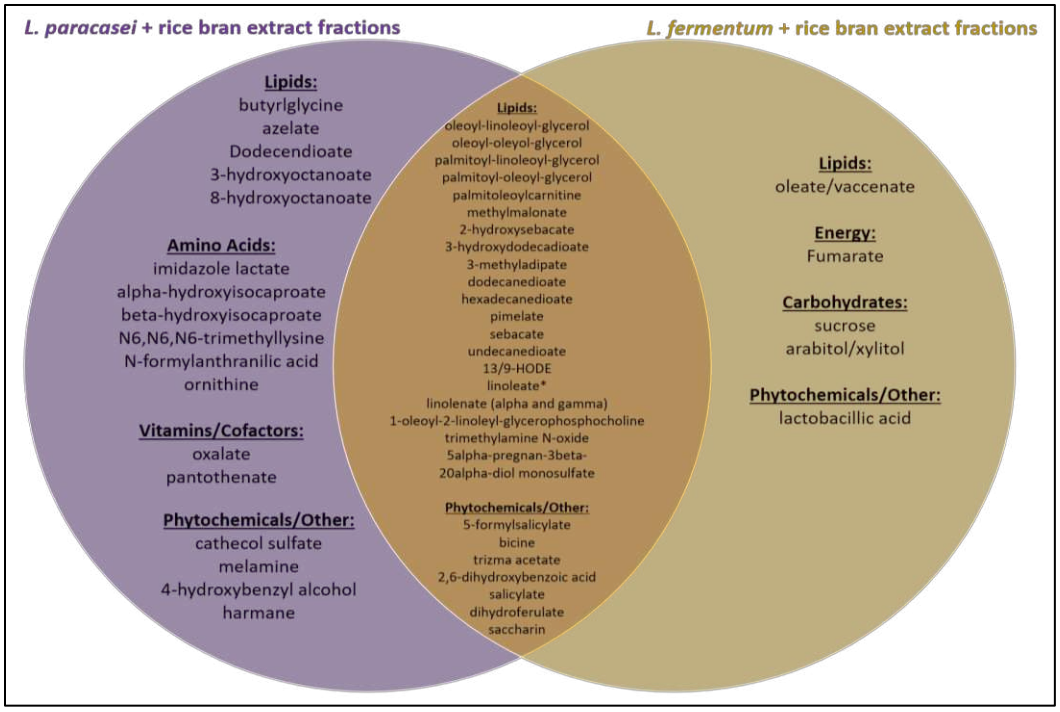

Figure 4.3. *L. fermentum* and *L. paracasei* produce *Salmonella* growth-suppressive fractions with distinct metabolite profiles.

Metabolites represented were significantly-different ($p<0.05$) when comparing Salmonella-suppressive fractions to the ineffective fraction that were only increased in in the L. fermentum or the L. paracasei fractions.

In *L. paracasei* bioactive fractions, 45 metabolites were significantly increased compared to the ineffective fraction. When organized by chemical class, a majority (~57%) were lipids followed by phytochemicals (~24%). Amino acids were solely detected in *L. paracasei* bioactive fractions. These accounted for ~13% of the total significant metabolites. Among *L. paracasei* fraction lipid metabolites were the dicarboxylic acid azelate (53.11-fold, 6.88-fold, and 13.24-fold increase in fraction 18, fraction 21, and fraction 22 versus fraction 4 respectively) and the monohydroxy fatty acid 8-hydroxyoctanoate (14.59-fold increase in fraction 18 versus fraction 4). *L. paracasei* phytochemicals in these bioactive fractions included the aromatic nitrogen-containing compounds harmane (2.39-fold increase in fraction 18 versus fraction 4) and

melamine (134.35-fold and 31.64-fold increase in fraction 18 and fraction 22 versus fraction 4 respectively). Among amino acid metabolites, the bioactive *L. paracasei* fractions contained the arginine metabolite ornithine (2.09-fold, 3.60-fold, and 3.01-fold increase in fraction 18, fraction 21 and fraction 22 versus fraction 4 respectively), and the branched chain amino acid alpha-hydroxyisocaproate (1.38-fold increase in fraction 18 versus fraction 4).

Table 4.3. Metabolites with an increased relative abundance in *L. fermentum* and *L. paracasei* fractions that suppressed *Salmonella* Typhimurium growth

Metabolites		***L. fermentum* + rice bran extract**			***L. paracasei* + rice bran extract**		
Metabolic Pathway	**Biochemical Name**	**F18/ F4**	**F21/ F4**	**F22/ F4**	**F18/ F4**	**F21/ F4**	**F22/ F4**
Amino Acids							
Histidine	imidazole lactate	-	-	-	-	**1.34**	-
Leucine, Isoleucine and Valine	alpha-hydroxy-isocaproate	-	-	-	**1.38**	**-**	**-**
	beta-hydroxy-isovalerate	0.12	0.020	0.030	**6.63**	**2.46**	**6.39**
Lysine	N6,N6,N6-trimethyl-lysine	-	-	-	-	**2.32**	-
Tryptophan	N-formyl-anthranilic acid	6.72	1.36	1.73	**4.32**	1.29	**2.32**
Arginine and Proline	ornithine	1.58	2.13	2.77	**2.09**	**3.60**	**3.01**
Carbohydrates							
Disaccharides and Oligosaccharides	sucrose	2.61	1.23	1.07	**4.38**	**3.57**	**13.14**
Pentose	arabitol/ xylitol	1.13	**-**	**-**	-	**4.07**	-
Energy Metabolites							
Tricarboxylic Acid Cycle	fumarate	**2.25**	1.11	1.03	0.98	0.52	0.72
Lipids							
Diacylglycerol	oleoyl-linoleoyl-glycerol [1]	-	**68.85**	**123.29**	0.86	**67.43**	**42.38**

Table 4.3. Metabolites with an increased relative abundance in *L. fermentum* and *L. paracasei* fractions that suppressed *Salmonella* Typhimurium growth

Metabolites		*L. fermentum* + rice bran extract			*L. paracasei* + rice bran extract		
Metabolic Pathway	**Biochemical Name**	**F18/ F4**	**F21/ F4**	**F22/ F4**	**F18/ F4**	**F21/ F4**	**F22/ F4**
	oleoyl-linoleoyl-glycerol [2]	1.17	**48.62**	**109.13**	0.95	**45.37**	**38.52**
	oleoyl-oleoyl-glycerol [1]*	-	5.86	**68.96**	0.64	2.08	**33.24**
	oleoyl-oleoyl-glycerol [2]*	0.63	2.36	**27.19**	1.23	3.45	**36.25**
	palmitoyl-linoleoyl-glycerol [1]*	1.46	**57.82**	**40.10**	1.06	**28.65**	**8.41**
	palmitoyl-linoleoyl-glycerol [2]*	-	**52.37**	**48.66**	-	**27.42**	**11.22**
	palmitoyl-oleoyl-glycerol [1]*	-	1.08	**4.57**	**-**	**-**	1.78
	palmitoyl-oleoyl-glycerol [2]*	-	2.35	**17.98**	-	1.18	**6.63**
Fatty Acid (Acyl Carnitine, Mono-unsaturated)	palmitoleoyl-carnitine*	**7.40**	1.98	1.64	**6.87**	**2.46**	1.76
Fatty Acid/ Branched Chain Amino Acid	butyryl-glycine	**-**	1.66	1.03	-	**1.68**	-
	methyl-malonate	**1.35**	0.53	0.53	**2.82**	1.40	1.85
Fatty Acid, Dicarboxylate	2-hydroxy-sebacate	**10.28**	1.12	1.07	**4.22**	1.29	**3.00**
	3-hydroxy-dodecane-dioate*	**50.89**	2.20	2.35	**34.28**	-	1.74
	3-methyl-adipate	**7.91**	**2.85**	**2.90**	**2.31**	0.74	1.81
	azelate	79.34	5.88	4.81	**53.11**	**6.88**	**13.24**
	dodecane-dioate	**5.91**	**2.18**	**1.64**	**3.43**	1.11	1.35
	dodecane-dioate*	**78.58**	-	-	**73.12**	1.04	1.13
	hexadecane-dioate	**3.47**	**1.90**	1.27	**3.50**	1.44	1.16
	pimelate	**11.54**	**4.45**	**4.57**	**4.22**	1.48	**2.84**
	sebacate	**78.62**	**4.31**	**4.17**	**18.39**	**2.48**	**3.92**
	undecane-dioate	**126.76**	**4.77**	**4.16**	**13.75**	**3.91**	**5.92**

Table 4.3. Metabolites with an increased relative abundance in *L. fermentum* and *L. paracasei* fractions that suppressed *Salmonella* Typhimurium growth

Metabolites		*L. fermentum* + rice bran extract			*L. paracasei* + rice bran extract		
Metabolic Pathway	**Biochemical Name**	**F18/ F4**	**F21/ F4**	**F22/ F4**	**F18/ F4**	**F21/ F4**	**F22/ F4**
Fatty Acid, Monohydroxy	8-hydroxy-octanoate	30.03	1.87	1.53	**14.59**	1.52	2.79
	13/9-hydroxy-octadece-dienoic acid	**40.96**	-	1.08	**16.30**	1.42	-
Long Chain Mono-unsaturated Fatty Acid	oleate/ vaccenate	**26.21**	**3.17**	1.37	2.15	2.13	1.25
Long Chain Polyunsaturated Fatty Acid (n3 and n6)	linoleate	**117.91**	2.61	1.31	**62.00**	2.24	1.32
	linolenate (alpha or gamma; 18:3n3 or 6)	**72.62**	**2.91**	1.52	**86.93**	1.78	0.98
Phosphatidyl-choline	1-oleoyl-2-linoleoyl-glycero-phosphoryl-choline*	-	**34.49**	1.52	-	**32.12**	1.70
Phospholipid	trimethyl-amine N-oxide	**9.71**	**3.61**	2.54	**4.60**	2.88	**6.84**
Progestin Steroids	5alpha-pregnan-3beta, 20alpha-diol monosulfate	**3.26**	2.57	2.03	**4.15**	**2.36**	2.47
Carbocyclic Fatty Acid	lactobacillic acid	**5.44**	1.55	1.03	1.08	1.12	-
Cofactors/Vitamins							
Ascorbate and Aldarate	oxalate (ethane-dioate)	2.97	1.20	1.57	**2.27**	0.56	1.19
Pantothenate and Co-enzyme A	pantothenate	1.51	1.36	-	-	**4.63**	1.07
Phytochemicals/Others							
Benzoate	catechol sulfate	**-**	-	-	-	**9.58**	-
Phytochemical	2,6-dihydroxy-benzoic acid	**2.54**	1.13	0.71	**2.19**	1.40	**1.77**
	4-hydroxy-benzyl alcohol	1.60	1.19	-	**1.81**	-	1.22
	salicylate	**8.98**	**3.77**	**3.26**	**6.73**	**3.24**	**5.23**

Table 4.3. Metabolites with an increased relative abundance in *L. fermentum* and *L. paracasei* fractions that suppressed *Salmonella* Typhimurium growth

Metabolites		*L. fermentum* + rice bran extract			*L. paracasei* + rice bran extract		
Metabolic Pathway	**Biochemical Name**	**F18/ F4**	**F21/ F4**	**F22/ F4**	**F18/ F4**	**F21/ F4**	**F22/ F4**
	dihydro-ferulate	**41.36**	**14.46**	**11.88**	**30.05**	**9.43**	**15.39**
	ferulate	**4.40**	1.71	**2.45**	**4.44**	1.41	**2.71**
	harmane	1.34	1.63	-	**2.39**	1.88	1.44
	saccharin	**76.51**	**29.20**	**28.70**	**75.60**	**24.89**	**36.17**
	5-formyl-salicylate	**7.77**	**2.51**	**2.58**	**7.98**	**2.09**	**3.76**
	bicine	**7.83**	2.76	**3.06**	**4.49**	1.07	2.66
	melamine	15.41	4.13	5.17	**134.35**	3.46	**31.64**
Unknowns							
Unknown	X - 13007	**19.37**	-	-	**8.26**	1.22	1.13
	X - 14904	**16.44**	-	-	**7.68**	1.23	1.05
	X - 23240	7.74	3.42	3.45	**6.84**	**2.75**	**4.47**
	X - 24188	**7.18**	-	-	**2.56**	-	-
	X - 24931	1.05	-	-	**2.14**	-	-
	X - 25343	**3.84**	2.33	1.36	2.15	1.01	**2.36**
	X - 25611	**37.68**	**17.99**	**19.60**	**36.98**	**17.60**	**21.75**
	X - 25656	17.38	14.82	5.92	**24.57**	**9.96**	**7.40**
	X - 25948	**2.28**	0.42	0.42	**0.45**	**0.10**	**0.10**
	X - 25966	**25.57**	**17.58**	**14.25**	**29.86**	**12.84**	**50.43**
	X - 25968	61.66	28.85	32.30	**65.50**	**27.08**	**39.03**
	X - 25971	**12.40**	**3.91**	**3.60**	**11.81**	**3.47**	**6.02**
	X - 25976	**95.18**	**33.95**	**37.18**	**97.80**	**30.35**	**53.57**

Bold metabolites had a significantly-increased ($p<0.05$) abundance only in fractions exhibiting *S.* Typhimurium growth suppression and had a false discovery rate of $q<0.10$.
* indicates metabolite identity was made against a database external to Metabolon Inc ©
- indicates metabolite not detected in the given comparison.
↑ designates metabolites that had statistically significant relative abundance increases in the numerator treatment compared to the denominator; ↓ designates metabolites significantly decreased in the numerator treatment compared to the denominator treatment.

4.4.4. Genes and biosynthetic enzymes for metabolites enriched in bioactive L. fermentum versus L. paracasei fractions.

To evaluate *Lactobacillus* spp. metabolic differences contributing to differences in their bioactive fraction metabolite profiles, metabolites that were significantly-increased in and unique to either *L. fermentum* (**Table 4.4.**) or *L. paracasei* (**Table 4.5.**) bioactive fractions were further examined for known biosynthetic genes and their associated enzymes. For *L. fermentum* fractions, this analysis included 6 metabolites spanning energy, carbohydrate, and lipid chemical

classes. Notably, the energy metabolite fumarate, which was only increased in *L. fermentum* bioactive fractions, was associated with ten biosynthetic enzymes encoded by a total of 102 genes with reported involvement in the tricarboxylic acid cycle, arginine metabolism, aspartate metabolism, and fatty acid metabolism. *L. fermentum* bioactive fractions were additionally enriched in the lipid lactobacillic acid, which is produced during fatty acid cyclopropanation with the enzyme cyclopropane fatty acid synthase that is encoded in ~ 33 genes spanning *cfa*, *cma*, *mmaA*, *ufa*, and *uma* alleles.

Table 4.4. Genes and their biosynthetic enzymes for metabolites enriched in *L. fermentum* that suppressed *Salmonella* growth.

Metabolites	Associated Gene(s)	Biosynthetic Enzyme(s)	Database Identities and Reference(s)
Energy Metabolites			
fumarate	*fum, fumA, fumA1, fumA2, fumB, fumB2, fumC, ttdA, ttdB*	Fumarate hydratase, class I	KEGG: K01676
	frdA, frdA2, fccA, ifcA, ifcA2, yqiG, sdhA, sdhA1, sdhA2, urdA, tctC, ifcA2, frdC, nadB	Fumarate reductase flavoprotein subunit/ NADH-dependent fumarate reductase subunit A	KEGG: K00244, K18556
	sdhA	Succinate dehydrogenase (ubiquinone) flavoprotein subunit	KEGG: K00234 UniProtKB: P0AC41
	fah, fahA, hmgB, mhpD	Fumaryl-acetoacetase	KEGG: K01555
	argH, argH_2, argH1, argH2, argH-1, argH-2, argH3, purB	Argininosuccinate lyase	KEGG: K01755
	ansB, ansB2, aspA, aspA1, aspA2, aspA3	Aspartate ammonia lyase	KEGG: K01744
	purB, purB1, purB2, pcaB	Adenylosuccinate lyase	KEGG: K01756
	mhpC, bphD, bphD2	2-hydroxy-6-oxonona-2,4-dienedioate hydrolase	KEGG: K05714
	eutA, igiC, maiA, nicE	Maleate isomerase	KEGG: K01799
Carbohydrates			
sucrose	*scrB*	Sucrose 6-phosphate hydrolase	KEGG: K07024 UniProtKB: P27217
	susA, spsA	Sucrose synthase	KEGG: gvip490; K00695 UniProtKB: Q8DK23

Table 4.4. Genes and their biosynthetic enzymes for metabolites enriched in *L. fermentum* that suppressed *Salmonella* growth.

Metabolites	Associated Gene(s)	Biosynthetic Enzyme(s)	Database Identities and Reference(s)
	yjcM, scrP, amy, treY, spl, amyA	Sucrose phosphorylase	KEGG: K00690
arabitol/xylitol	*yafB*	Aldose reductase	KEGG: K00011 UniProtKB: Q32JQ6
	dalD, mtlK, por, por1, por2	D-arabinitol 4-dehydrogenase	KEGG: 00007
	ard	D-arabitol dehydrogenase 1	KEGG: K17818 UniProtKB: A0A212KEA2
	dhs, nodG	L-xylulose reductase	KEGG: K03331 UniProtKB: A0A0D6I9Q6; A0A2Z4LR95; W6K2I1; A0A2Z4YIP3
	dkgA	D-xylose reductase	KEGG: K17743
	aldo	Alditol oxidase	KEGG: K00594 NCBI: 1101588
	ydjJ, xyl2, sorD, sord, xdh, xylD, tdh3	D-xyulose reductase	KEGG: K05351
	gutB4, gutB5, tdh, gatD, gutB, gutB2, gutB3, gatD2, ydjL, gatD1, gatD2, ydjJ1, ydjJ3, xpdH1, xpdH2, gutB1, tdh2, adh, adhP	L-iditol 2-dehydrogenase	KEGG: K00008
Lipids			
palmitoyl-oleoyl-glycerol	*dgkA, dagK*	Diacyl-gylcerolkinase	NCBI: 948543; 1028846
	pldA	Phospholipase D	NCBI: 880040
	lip, lipL, hlyC, lipA, llpA, lipC, lipA2, lipA3, lipA1, hlyC, lipx, tgl2, estA, estB, lipB, lip1, lip2, lip3, geh, geh1, geh2, geh'', fold5, lipY, estB2	Triacylglycerol lipase	KEGG: K01046
	pgpB	Phosphatidate phosphatase	KEGG: K01080 UniProtKB: P0A924
	pgpB, pgpB5, pgpB3, pgpB1, pgpB2	Diacylglycerol diphosphate phosphatase	KEGG: K18693
	plcA	Phosphatidyl-inositol Phospholipase C	KEGG: K01116 NCBI: 987032
	plcH1, plcN, plcN2, phlN1, phlN2, plcC, plcH2, plcD, acpA, plcN3, plcN4, plcN1, phlC1, phlC2, plcA, plcB, cerA, plc, hlb, sph, phlc, plcB1, plcB2, plcB4, plcB5, plcB6	Phospholipase C	KEGG: K01114
oleate/vaccenate	*mycA1, mycA, lai, l1n, sph, mycA2, ohyA*	Oleate hydratase	KEGG: K10254

Table 4.4. Genes and their biosynthetic enzymes for metabolites enriched in *L. fermentum* that suppressed *Salmonella* growth.

Metabolites	Associated Gene(s)	Biosynthetic Enzyme(s)	Database Identities and Reference(s)
	tesA, apeA, pdlC, pfaD, pteH, aveG, fat, srfAD, las1, bacT, salGII, fatA, lgrE, mycT, hdeA, ylfFG, cpp2, snap, xcnI, pyr26, olmC, rifR, irp4, abyT, pchC, fas-IB, fas-IA, tueT, aveG	Oleoyl-acyl carrier protein thioesterase	KEGG: K10782 UniProtKB: P0ADA1; A0A0F6EZH4; A0A378Y0J5; A0A378XZD0; B1MVT0; A0A2X1GRV6; B5M9K2; E1PKV9; H1ZZU3; M1WJV0; A0A3S4H0W4; A0A073CGX1; A0A1W6VRK6; J0YTE5; D9UBT7; A0A0A8NZH8; K4R0M8; G8SKU8; A0A0H3CVZ3; E5B8A3; F4F6Q2; G7ZCF8; C3PK08; C3PIL8; A0A0M7BIQ7; A0A378ZNB4
lactobacillic acid	*cfa, cfs3-1, cfs3-2, cfs3-3, cfs3-4, cfa1, cfa2, cfa3, cdfA, cfa4, cfa5, cfaA, cfaS, cfa_[H], cfa_[C], ufaA1, cmaS, mmaA1, mmaA2, mmaA2-1, mmaA3, mma4, mmaA5, mmaA5-1, ufaM, umaA, pcaA, cmaA1, cmaA2*	Cyclopropane fatty acid synthase	(Jones *et al.*, 2011) KEGG: K00574

Metabolites depicted were significantly increased ($p<0.05$) in the bioactive fractions (18, 21, 22) of *L. fermentum* when compared to fraction 4 (ineffective fractions). Gene and enzyme annotations are from prokaryotic organisms indexed in KEGG, UniProtKB, and NCBI databases, , and from other peer-reviewed literature as cited.

L. paracasei effective fractions contained 15 unique metabolites spanning amino acid, lipid, cofactor/vitamin, and phytochemical/other chemical classes. Amino acids represented ~40% of these metabolites including the histidine metabolite imidazole lactate produced by histidine transaminase (linked to *hisA* and *hisB* genes), and ornithine which is produced during arginine and glutamine metabolism via glutamate N-acetyltransferase (encoded by *oat1* and *argJ*), aminocyclase (encoded by the *acy*l gene), and acetylornithine deacetylase (encoded by *argE*). Additional *L. paracasei* metabolites included the lipid azelate, produced by omega amylase (encoded by 9 genes) and the heterocyclic nitrogen-containing compound harmane that

is synthesized by monoamine oxidase and which is encoded by 21 reported prokaryotic genes including alleles of *aof*, *gox*, *iaa*, *lao*, *mao*, *puo*, *reb*, and *yox*. Melamine was a second heterocyclic nitrogen compound only increased in *L. paracasei* effective fractions, but no biosynthetic enzymes and associated genes of prokaryotic origin were linked to microbial production of this metabolite.

Table 4.5. Genes and their biosynthetic enzymes for metabolites enriched in *L. paracasei* that suppressed *Salmonella* growth.

Metabolites	Associated Gene(s)	Biosynthetic Enzyme(s)	Database Identities and Reference(s)
Amino Acids			
imidazole lactate	*hisB, hisC*	Histidine transaminase	KEGG: EC 2.6.1.38 UniProtKB: Q8R5Q4
alpha-hydroxyisocaproate	*hadA*, *fldA*	(R)-2-hydroxy-4-methylpentanoate CoA-transferase	KEGG: K20882
beta-hydroxyisovalerate	*paaF*, *fadJ, fadB*	Enoyl-CoA hydratase; enoyl hydrase	KEGG: EC 4.2.1.17
N6, N6, N6-trimethyllysine	*mll2, fliJ*	Histone-lysine N-methyltransferase	KEGG: EC 2.1.1.43 UniProtKB: A0A2S2E5X4; A0A061D308
	coIII	Cytochrome-c-lysine N-methyltransferase	KEGG: K18804 UniProtKB: G8PXA6
N-formylanthranilic acid	*kynU*	Formylkynurenine hydrolase	KEGG: R03936
Ornithine	*oat2*, *argJ*	Glutamate N-acetyltransferase	UniProtKB: P0DJQ5; Q9HW04
	acy1	Aminoacylase	KEGG: K14677
	argE	Acetylornithine deacetylase	UniProtKB: P23908
Lipids			
butyrylglycine	*nodA*	Glycine-N-acyltransferase	KEGG: K00628 UniprotKB: A0A0S1TF61
azelate	*yafV*, *ramA1, ramA3, cpa, ramA, mntU, ramA2, ykrU, amiE, niT2, cnhA*	Omega amidase	KEGG: K13566
8-hydroxyoctanoate	*cypC*	Fatty acid peroxygenase	UniProtKB: O31440

Table 4.5. Genes and their biosynthetic enzymes for metabolites enriched in *L. paracasei* that suppressed *Salmonella* growth.

Metabolites	Associated Gene(s)	Biosynthetic Enzyme(s)	Database Identities and Reference(s)
Cofactors/Vitamins			
oxalate (ethanedioate)	*ggt, ywrD, ggt1, ggt2, ggt3, ggt4, ggt7*	Oxamate amidohydrolase	KEGG: K22602
	dhlC, dl-dex, ddh	DL-2-haloacid dehalogenase	KEGG: R09157 UniProtKB: Q59168; A6BM74; B1Q2C1
	glo	Glycolate oxidase	KEGG: EC 1.2.3.5 UniProtKB: A0A2H1XBM4
	frc, uctC, yfdE, caiB, caiB3, frc2, frc1, caiB1, yfdW, frc3, frc8, frc6, frc9, frc10, frc11, frc19, frc5	Oxalate coenzyme A-transferase	KEGG: EC 2.8.3.2 UniProtKB: P69902; A9X6P9; A0A335E7J9; P76518; A6T0J2; A4G242; A4G241; A6SUZ4; W8ZV13; A0A0B5FHP1; T1XFN4; F8GQ91; A0A378YX13; A0A378Z2N1; A0A378YWG5; A0A0U5MHC6 A0A239SM15; A0A239SM16; A0A378Z0N9
pantothenate	*panC, panC1, panC2, panC3*	Pantothenate synthetase	KEGG: K01918
	-	Pantothenase	UniProtKB: Q87BJ2
Phytochemicals/Others			
catechol sulfate	*assT*	Aryl sulfotransferase	KEGG: K01014 UniProtKB: Q8FDI4
4-hydroxybenzyl alcohol	*pchF, pchF1, pchF2, pchF3, pchF4, pcmI, vaoA*	4-methylphenol dehydrogenase	KEGG: EC 1.17.9.1
harmane	*pao, maoAB, lao, lao1, aofA, aofH, aofH1, aofH2, rebO, puo, puo1, puo2, maoB, iaaM, rebO, rebO1, yobN, yobN1, yobN2, gox*	Monoamine oxidase	(Aassila *et al.*, 2003) KEGG: K00274
melamine	-	-	-

Metabolites depicted were significantly increased ($p<0.05$) in the bioactive fractions (18, 21, 22) of *L. paracasei* when compared to fraction 4 (ineffective fractions). Gene and enzyme annotations are from prokaryotic organisms indexed in KEGG, UniProtKB, and NCBI databases, and from other peer-reviewed literature as cited.

4.5. Discussion and Conclusions:

The objective of this study was to examine fractionated *Lactobacillus* + rice bran synbiotic supernatants for metabolites driving antimicrobial-resistant *Salmonella* Typhimurium growth suppression. The two *Lactobacillus* synbiotic supernatants tested herein were previously shown to suppress antimicrobial-resistant *Salmonella* Typhimurium growth and had distinct small molecule profiles associated with growth suppression (**Chapter 3**). Bioactivity guided fractionation identified multiple lipids and amino acids that have previously been reported as exhibiting antimicrobial functions. The hypothesis was that fractionation of the cell free supernatants from *Lactobacillus* spp. cultured with rice bran would yield distinct suites of metabolites that inhibit *Salmonella* growth. These results further show that the magnitude of pathogen growth suppression differed across bioactive fractions based on their metabolite composition.

Bioactivity-guided fractionation identified multiple cell-free supernatant fractions from *L. fermentum* and *L. paracasei* treatments that suppressed *Salmonella* Typhimurium growth (**Figure 4.1.**). Given that the flash chromatography procedure removed proteins during fraction collection, the capacity of these fractions to suppress *Salmonella* growth supports that their small molecules were directly responsible for their growth suppression effects. Despite the capacity of both *L. fermentum* and *L. paracasei* fractions to suppress *Salmonella* growth, neither treatment was able to produce fractions that achieved growth suppression levels similar to those observed in unfractionated supernatant (**Figure 4.1.**). This pattern indicates that optimal growth suppression by *Lactobacillus* spp. synbiotic supernatant fractions likely occurs due to the production of multiple small molecules acting in synergy, and that synbiotic supernatant fractionation results in a loss of molecular synergy. Despite this loss of total growth suppression

capacity, the ability of *L. fermentum* and *L. paracasei* fractions to produce *Salmonella* growth suppression provides a valuable model to identify components driving their antimicrobial effects, and allows for different fractions and fraction concentrations to be combined together to examine whether growth suppression levels of the unfractionated supernatant could be re-created using a minimum metabolite profile.

Salmonella-inhibitory fractions collected from *L. fermentum* and *L. paracasei* were all extracted under relatively hydrophobic conditions (**Table 4.2**) further indicating that synbiotic supernatant molecules driving growth suppression had non-polar chemical properties. Non-polar metabolite mediated reductions in *S*. Typhimurium invasion and intracellular replication in murine and porcine intestinal epithelial cells has been previously reported for rice bran extracts, where dicarboxylate fatty acids, phospholipids and dipeptides (amino acid dimers) were identified in rice bran extracts with antimicrobial activity against *Salmonella* (Ghazi *et al.*, 2016). When these bioactive *L. fermentum* and *L. paracasei* fractions were compared to each other (e.g. *L. fermentum* fraction 18 versus *L. paracasei* fraction 18), *L. paracasei* fractions consistently exhibited higher *Salmonella* growth suppression levels than the corresponding *L. fermentum* fractions. One potential explanation for this observation could be that *L. paracasei* fractions produce higher abundances of antimicrobial metabolites or distinct suites of antimicrobial metabolites when compared to *L. fermentum* fractions.

The global, non-targeted metabolite profiles of representative *L. fermentum* and *L. paracasei* fractions that both suppressed or did not suppress *Salmonella* growth were established to examine small molecule profiles associated with *Salmonella* growth suppression. Over the course of the separation, synbiotic supernatant fractions contained fewer metabolites per fraction that dually had higher proportions of lipids relative to the total number of metabolites in the

fraction, such that the *Salmonell*a-suppressive fractions for *L. fermentum* and *L. paracasei* treatments (fraction 18, fraction 21, fraction 22) contained ~20% more lipids compared to the ineffective fraction that was profiled (fraction 4) (**Figure 4.2**). While the higher lipid abundances in these later fractions is influenced in-part by the reverse-phase chromatography procedure, which optimizes the extraction and separation of non-polar metabolites (Hedrick, 1964), the capacity of these high-lipid abundance fractions to dually suppress *Salmonella* growth supported that these lipid metabolites were important contributors to overall *Salmonella* growth suppression by synbiotic supernatants.

To further identify shared versus distinct metabolites contributing to *Salmonella* growth suppression by *L. fermentum* versus *L. paracasei* supernatant fractions, the *Salmonella*-suppressive fractions (fractions 18, 21, 22) were compared to the ineffective fraction (fraction 4) for both treatments to identify metabolites that were significantly increased ($p<0.05$) in only the effective fractions compared to the ineffective fraction (**Table 4.3**, **Figure 4.3**). This metabolite enrichment analysis revealed that *L. fermentum* and *L. paracasei* effective fractions contained many shared lipid metabolites that contributed to their *Salmonella* growth suppression, including diacylglycerols like oleoyl-linoleoyl-glycerol (increased 42.38 to 123.29-fold in *L. fermentum* and *L. paracasei* effective fractions (compared to the ineffective fraction) and dicarboxylic fatty acids such as dodecenedioate (increased 73.12 to 78.58-fold in *L. fermentum* and *L. paracasei* bioactive fractions compared to the ineffective fraction). These shared lipid metabolites are consistent with the known production of these metabolites by different *Lactobacillus* spp. (Nealon *et al.*, 2017a; Nealon *et al.*, 2017b), and they may also reflect a common origin from rice bran extract, where they have been previously identified in rice bran (Ghazi *et al.*, 2016; Zarei *et al.*, 2017; Zarei *et al.*, 2018). *L. fermentum* and *L. paracasei* may have metabolized rice bran

extract to release these lipids into the cell-free supernatant, and it is plausible that the abundance of these lipid metabolites contributed to the differential magnitudes of *Salmonella* growth suppression observed between analogous *L. fermentum* and *L. paracasei* fractions.

Metabolite profile analysis further identified multiple chemical classes that were unique to the *L. fermentum* versus *L. paracasei* fractions, and these metabolites were subsequently searched for associated genes and biosynthetic enzymes that could be screened for presence or absence in these *Lactobacillus* spp. to evaluate species-specific metabolic capacities. In *L. fermentum* bioactive fractions, a notable chemical class included the energy metabolism compound fumarate. Fumarate is an intermediate in the tricarboxylic acid cycle and product of glucogenic amino acid metabolism (Berg, 2002) that has been reported to have bactericidal activity against *Escherichia coli* O157:H7, *Salmonella* Typhimurium, *Listeria monocytogenes*, and *Staphylococcus aureus* attached to lettuce and beef (Kondo *et al.*, 2006; Tango *et al.*, 2014). While previous studies highlight the beneficial roles of *Lactobacillus*-produced fumarate in host health, food palatability, and reduced *E. coli*-associated diarrhea and virulence factor production (Lan and Kim, 2018; Ming *et al.*, 2018), there are currently no studies examining enhanced fumarate production by *Lactobacillus*-containing synbiotics. Given that many different genes and enzyme isoforms can produce fumarate (**Table 4.4**), identifying the *L. fermentum* gene and enzyme alleles that maximize synbiotic production of fumarate represent one potential application for *L. fermentum* + rice bran extract synbiotics.

L. paracasei bioactive fractions were uniquely-enriched in multiple amino acid metabolites including those involved in histidine metabolism (imidazole lactate) as well as arginine metabolites (ornithine) (**Table 4.5**). Imidazole-containing antibiotics including econazole, ketoconazole, clotrimazole and miconazole have been demonstrated to reduce the

growth of multiple Gram-negative bacterial and fungal pathogens (Helmick *et al.*, 2005), but no studies have examined synbiotic-produced imidazole lactate for antimicrobial activity. The capacity of imidazole lactate to suppress antimicrobial-resistant *Salmonella* as evidenced herein supports the utility for and further examination of histidine metabolites produced by *L. paracasei* + rice bran synbiotics and may be especially beneficial as a treatment in cases where the pathogen is resistant to existing imidazole drugs, or in instances where use of conventional imidazole-based drugs may be contraindicated. Further evaluations of synbiotic-produced imidazole lactate can additionally include examinations of histidine transaminase gene and protein expression by *L. paracasei* isolates that can readily produce this antimicrobial, and how rice bran can influence probiotic expression of this enzyme when compared to other prebiotic sources.

Ornithine produced by *L. paracasei* + rice bran extract represents a novel function of ornithine in acting as an antimicrobial metabolite. While previous studies have demonstrated that ornithine-containing antimicrobials effectively suppressed *Salmonella* growth (Lohan *et al.*, 2014; Staiano *et al.*, 1980), no studies have examined the roles of the parent compound, ornithine, for its potential antimicrobial activity. Rationale for examining the antimicrobial potential of ornithine can be justified given that ornithine can be metabolized into metabolites with known antimicrobial activity including N-alpha-acetylornithine and N-delta-acetylornithine that interfere with protein synthesis via inhibiting ornithine synthesis (Adio *et al.*, 2011; Hlavacek *et al.*, 2010; Lemarie *et al.*, 2015; Oka *et al.*, 1984). Consequently, potential synbiotics designed for *Salmonella* growth suppression could be screened for probiotic presence of *argE*, *acyl*, *oat2*, and *argJ* genes and their capacity to produce enzymes that drive ornithine synthesis, which can be evaluated as measures of predicted synbiotic efficacy against *Salmonella*.

This study identified *L. fermentum* and *L. paracasei* synbiotic supernatant fractions that can suppress antimicrobial resistant *Salmonella* Typhimurium growth. Our results for synbiotic fractions validated previous research and led to the discovery of novel sets of small molecules with bioactivity. This works begins to fill knowledge gaps for integrating prebiotics driving probiotic metabolic capacity at the gene, enzyme and small molecule interface across *Lactobacillus* spp. Developing predictive models for assessing antimicrobial capacity of synbiotics with a focus on supernatants produced by combinations of probiotics and rice bran merit immediate attention. Optimizing production systems for antimicrobials that span a diversity of unexplored chemical combinations warrant optimization against emerging antimicrobial-resistance and the urgent need for prevention of infectious outbreaks in people, animals, foods and environments.

REFERENCES

Abdel-Wareth, A.A.A., et al., Synbiotic as eco-friendly feed additive in diets of chickens under hot climatic conditions. Poult Sci, 2019.

Adio, A.M., et al., Biosynthesis and defensive function of Ndelta-acetylornithine, a jasmonate-induced Arabidopsis metabolite. Plant Cell, 2011. 23(9): p. 3303-18.

Adler, A., N.D. Friedman, and D. Marchaim, Multidrug-Resistant Gram-Negative Bacilli: Infection Control Implications. Infect Dis Clin North Am, 2016. 30(4): p. 967-997.

Ali, S.M., R. Siddiqui, and N.A. Khan, Antimicrobial discovery from natural and unusual sources. J Pharm Pharmacol, 2018. 70(10): p. 1287-1300.

Antibiotics Tested by NARMS, W. National Center for Emerging and Zoonotic Infectious Diseases (NCEZID): Division of Foodborne, and Environmental Diseases (DFWED), Editor. 2018, Centers for Disease Control and Prevention: Atlanta, Georgia. USA.

Aassalia, H. et al., Identification of Harman as the Antibiotic Compound Produced by a Tunicate-Associated Bacterium. Mar Biotechnol, 2003. 5(2): p.163-6.

CDC, Antibiotic/Antimicrobial Resistance (AR/AMR): Biggest Threats and Data, D.o.H.Q.P. (DHQP), 2018: Atlanta, Georgia.

CDC, Tracking antibiotic resistance in dangerous bacteria that affect people and cattle, D.o.F. National Center for Emerging and Zoonotic Infectious Diseases (NCEZID), Waterborne, and Environmental Diseases (DFWED), 2019, Centers for Disease Control: Atlanta, Georgia.

Consortium, T.U., 2018. UniProt: a worldwide hub of protein knowledge. Nucleic Acids Res 47: D506-D515. 10.1093/nar/gky1049

Ghazi, I.A., et al., Rice Bran Extracts Inhibit Invasion and Intracellular Replication of Salmonella typhimurium in Mouse and Porcine Intestinal Epithelial Cells. Medicinal and Aromatic Plants, 2016. 5(5): p. 10.

Hedrick, C.E., Separations by reversed-phase chromatography, in Chemistry. 1964, Iowa State University: Ames, Iowa.

Helmick, R.A., et al., Imidazole antibiotics inhibit the nitric oxide dioxygenase function of microbial flavohemoglobin. Antimicrob Agents Chemother, 2005. 49(5): p. 1837-43.

Henderson, A.J., et al., Consumption of rice bran increases mucosal immunoglobulin A concentrations and numbers of intestinal Lactobacillus spp. J Med Food, 2012. 15(5): p. 469-75.

Hlavacek, J., et al., Inhibitors of N(alpha)-acetyl-L-ornithine deacetylase: synthesis, characterization and analysis of their inhibitory potency. Amino Acids, 2010. 38(4): p. 1155-64.

J.M. Berg, J.L.T., and L. Stryer, Carbon Atoms of Degraded Amino Acids Emerge as Major Metabolic Intermediates. 5 ed. Biochemistry. 2002, New York: W. H. Freeman and Company.

Jones, S.E., et al., Cyclopropane fatty acid synthase mutants of probiotic human-derived Lactobacillus reuteri are defective in TNF inhibition. Gut Microbes, 2011. 2(2): p.69-79.

Kanehisa, M., et al., KEGG: new perspectives on genomes, pathways, diseases and drugs. Nucleic Acids Res 45: D353-d361. 10.1093/nar/gkw1092

Kanehisa, M. and Goto, S., 2000., KEGG: kyoto encyclopedia of genes and genomes. Nucleic Acids Res 28: 27-30. 10.1093/nar/28.1.27

Kanehisa, M., et al., 2019. New approach for understanding genome variations in KEGG. Nucleic Acids Res 47: D590-d595. 10.1093/nar/gky962

Kanjan, P. and T. Hongpattarakere, Prebiotic efficacy and mechanism of inulin combined with inulin-degrading Lactobacillus paracasei I321 in competition with Salmonella. Carbohydr Polym, 2017. 169: p. 236-244.

Kondo, N., M. Murata, and K. Isshiki, Efficiency of sodium hypochlorite, fumaric acid, and mild heat in killing native microflora and Escherichia coli O157:H7, Salmonella typhimurium DT104, and Staphylococcus aureus attached to fresh-cut lettuce. J Food Prot, 2006. 69(2): p. 323-9.

Kumar, A., et al., Dietary rice bran promotes resistance to Salmonella enterica serovar Typhimurium colonization in mice. BMC Microbiol, 2012. 12: p. 71.

Lan, R. and I. Kim, Effects of organic acid and medium chain fatty acid blends on the performance of sows and their piglets. Anim Sci J, 2018. 89(12): p. 1673-1679.

Lemarie, S., et al., Both the Jasmonic Acid and the Salicylic Acid Pathways Contribute to Resistance to the Biotrophic Clubroot Agent Plasmodiophora brassicae in Arabidopsis. Plant Cell Physiol, 2015. 56(11): p. 2158-68.

Lepine, A. and P. de Vos, Synbiotic Effects of the Dietary Fiber Long-Chain Inulin and Probiotic Lactobacillus acidophilus W37 Can be Caused by Direct, Synergistic Stimulation of Immune Toll-Like Receptors and Dendritic Cells. Mol Nutr Food Res, 2018: p. e1800251.

Lohan, S., et al., In vitro and in vivo antibacterial evaluation and mechanistic study of ornithine based small cationic lipopeptides against antibiotic resistant clinical isolates. Eur J Med Chem, 2014. 88: p. 19-27.

Markazi, A., et al., Effects of drinking water synbiotic supplementation in laying hens challenged with Salmonella. Poult Sci, 2018. 97(10): p. 3510-3518.

Ming, T., et al., A metabolomics and proteomics study of the Lactobacillus plantarum in the grass carp fermentation. BMC Microbiol, 2018. 18(1): p. 216.

Mukerji, S., et al., Development and transmission of antimicrobial resistance among Gram-negative bacteria in animals and their public health impact. Essays Biochem, 2017. 61(1): p. 23-35.

Nealon, N.J., C.R. Worcester, and E.P. Ryan, Lactobacillus paracasei metabolism of rice bran reveals metabolome associated with Salmonella Typhimurium growth reduction. J Appl Microbiol, 2017. 122: p. 1639-1656.

Nealon, N.J., et al., Rice Bran and Probiotics Alter the Porcine Large Intestine and Serum Metabolomes for Protection against Human Rotavirus Diarrhea. Front Microbiol, 2017. 8: p. 653.

Oka, Y., T. Ogawa, and K. Sasaoka, First evidence for the occurrence of N delta-acetyl-L-ornithine and quantification of the free amino acids in the cultivated mushroom, Pleurotus ostreatus. J Nutr Sci Vitaminol (Tokyo), 1984. 30(1): p. 27-35.

Piatek, J., et al., Persistent infection by Salmonella enterica servovar Typhimurium: are synbiotics a therapeutic option? - a case report. Benef Microbes, 2019. 10(2): p. 211-217.

Staiano, N., et al., Mutagenicity of D- and L-azaserine, 6-diazo-5-oxo-L-norleucine and N-(N-methyl-N-nitroso-carbamyl)-L-ornithine in the Salmonella test system. Mutat Res, 1980. 79(4): p. 387-90.

Tango, C.N., et al., Synergetic effect of combined fumaric acid and slightly acidic electrolysed water on the inactivation of food-borne pathogens and extending the shelf life of fresh beef. J Appl Microbiol, 2014. 117: p. 1709-20.

Wishart, D.S., et al., 2018. HMDB 4.0: the human metabolome database for 2018. Nucleic Acids Res 46: D608-d617. 10.1093/nar/gkx1089

Wishart, D.S., et al., 2013. HMDB 3.0--The Human Metabolome Database in 2013. Nucleic Acids Res 41: D801-807. 10.1093/nar/gks1065

Wishart, D.S., et al., 2009. HMDB: a knowledgebase for the human metabolome. Nucleic Acids Res 37: D603-610. 10.1093/nar/gkn810

Wishart, D.S., et al., HMDB: the Human Metabolome Database. Nucleic Acids Res 35: D521-526. 10.1093/nar/gkl923

Zarei, I., et al., Comparative Rice Bran Metabolomics across Diverse Cultivars and Functional Rice Gene(-)Bran Metabolite Relationships. Metabolites, 2018. 8(4).

Zarei, I., et al., Rice Bran Metabolome Contains Amino Acids, Vitamins & Cofactors, and Phytochemicals with Medicinal and Nutritional Properties. Rice (N Y), 2017. 10(1): p. 24.

CHAPTER FIVE

HOST AND GUT MICROBIAL METABOLISM OF *BIFIDOBACTERIUM LONGUM*-FERMENTED RICE BRAN AND RICE BRAN IN HEALTHY MICE

5.1. Summary:

Food fermentation by native gut probiotics has historical foundations for gut health promotion metabolic comparisons of fermented foods alongside the non-fermented forms have been largely unexplored using non-targeted metabolomics and thus merit evaluation before and after exposure to the gastrointestinal tract. This study investigated host and microbial derived metabolites in the study diets as well as in the colon and systemic circulation of healthy mice following dietary intake of fermented versus non-fermented rice bran. Adult male BALB/c mice were fed a control diet or one of two experimental diets containing 10% w/w rice bran fermented with *Bifidobacterium longum* or 10% w/w non-fermented rice bran for 15 weeks. The global, non-targeted metabolome of each study diet (food), the murine colon and whole blood were examined. A total of 530 small molecules including 39% amino acids and 21% lipids were revealed through differential abundance testing across food, colon, and blood matrices. The amino acid metabolite, N-delta-acetylornithine, was notably increased by *B. longum* rice bran fermentation when compared to non-fermented rice bran and control groups across food, colon, and blood metabolomes. These findings support that dietary intake of rice bran fermented with *B. longum* modulates multiple metabolic pathways associated with antimicrobial actions and cancer prevention in the host via gut microbial metabolism.

5.2. Introduction:

Rice bran, the outer coating of brown rice, contributes the prebiotic, phytochemical and nutritional health benefits of whole grain brown rice. Numerous studies performed in humans and animals have shown colonic health and disease protective functions of a diet rich in rice bran (Henderson *et al.*, 2012a; Henderson *et al.*, 2012b; Lei *et al.*, 2016; Sheflin *et al.*, 2015; Sheflin *et al.*, 2017; Yang, 2015). Metabolite profiling of heat-stabilized rice bran has revealed a large suite of bioactive compounds including various amino acids, small peptides, lipids, nucleotides, vitamins and cofactors, and plant phytochemicals available in digestible and non-digestible forms to the host (Zarei *et al.*, 2017). Many rice bran components have previously-reported roles in slowing tumor and pathogen growth via altering cell proliferation, combating oxidative stress, reducing inflammation and modulating the gut microbiome and metabolism (Fabian and Ju, 2011; So *et al.*, 2016; Sohail *et al.*, 2017). Gut commensal microbes have shown the capacity for fermenting rice bran carbohydrates, phytochemicals, lipids and amino acids in animals and people (Sheflin *et al.*, 2017; Tuncil *et al.*, 2018). Emerging evidence supports that rice bran components modulate host and gut microbial metabolism to benefit enterocytes and the mucosal immune system (Brown *et al.*, 2017; Si *et al.*, 2018; Yang *et al.*, 2015; Zarei *et al.*, 2017). Genome sequencing of the fecal microbial communities and identification of small molecule profiles using metabolomics are promising tools to evaluate the effects of dietary interventions broadly (Bazanella *et al.*, 2017; Derkach *et al.*, 2017; Hernandez-Alonso *et al.*, 2017; Lee *et al.*, 2017; McIntosh *et al.*, 2017; Tovar *et al.*, 2017; Vandeputte *et al.*, 2017), and were previously utilized for rice bran (Brown *et al.*, 2017; Henderson *et al.*, 2012a; Sheflin *et al.*, 2015; Sheflin *et al.*, 2017; Si *et al.*, 2018). However, these studies have not yet advanced our understanding of

how rice bran fermentation impacts the colon tissue microbiome and the availability of the fermented food microbial-metabolic components to the colon and systemic circulation.

Few studies have evaluated the effects of fermented foods on healthy gut microbiomes (Cowan *et al.*, 2014; Zheng *et al.*, 2015), and to the best of the authors' knowledge, no studies currently provide a direct comparison to the non-fermented form of the same food type. Globally, lactic acid bacteria are the widest order of microbes involved in food fermentation (Pessione, 2012; Pessione and Cirrincione, 2016), and a variety of these organisms, existing as part of the native gut microbiome, confer benefits to their host. *Bifidobacterium* represents another important genus of native gut probiotics that were shown to increase in relative percentages after 28 days of rice bran consumption (30g/day) by healthy adults alongside modulations to rice bran-derived carbohydrates, phytochemicals, amino acids and lipids (Sheflin *et al.*, 2015), supporting the Bifidogenic properties of rice bran components. In a related study with daily rice bran intake by adult colorectal cancer survivors, favorable modulations were captured in the stool metabolome, including shifts in fatty acid, branched chain amino acid, and B-vitamin metabolism (Brown *et al.*, 2017; Sheflin *et al.*, 2017). Multiple strains of *Bifidobacterium* have been tested in food fermentation and exhibited health effects related to increased production of short chain and branched chain fatty acids that are critical for normal colonocyte function (Bunesova *et al.*, 2016; Celiberto *et al.*, 2017; Gagnon *et al.*, 2015; Kim *et al.*, 2018; Phoem *et al.*, 2015), yet other metabolites contributing to *Bifidobacteria* health promotion need further characterization.

This study aimed to distinguish host and microbe metabolic impacts of consuming dietary rice bran fermented with *Bifidobacterium longum* from the effects of consuming rice bran or a nutrient-matched control diet. Daily intake of *B. longum*-fermented rice bran for 15-weeks in

healthy mice was hypothesized to elicit changes to host and intestinal microbiome metabolism and result in differences between bioactive metabolites in colon tissue and blood. This study used next-generation sequencing approaches to characterize murine caecum, colon, and faecal microbiomes and non-targeted metabolomics to determine metabolite profiles of study diets (food), colon tissue, and whole blood metabolomes of mice consuming each study diet. Multivariate statistical approaches were utilized to assess differential abundance of bacterial sequence variants and differential production of bioactive compounds with previously reported cancer-protective and antimicrobial functions. Exploiting both microbial sequencing and metabolomic platforms provided a thorough and sensitive analysis for revealing *B. longum*-fermented rice bran influences on gut microbiome metabolism and bioavailability of disease protective compounds.

5.3. Materials and methods:

5.3.1. Rice bran and food fermentation:

Ri300 heat-stabilized rice bran was purchased from Rice Bran Technologies (Sacramento, CA, USA). Ten kilograms of rice bran was thoroughly mixed with 10 liters of $1.5x10^8$ cells/mL of *Bifidobacterium longum (B. longum)* ATCC-55813 (American Type Culture Collection, Manassas, VA, USA) suspended in milliQ water (Millipore Corporation, Burlington, MA, USA). The mixture was placed in an airtight stainless-steel pot that was incubated at 37ºC under ambient oxygen conditions. After 48hrs, the resultant slurry was harvested at room temperature, and frozen at -20ºC until lyophilization.

5.3.2. Mouse diet preparation and composition:

B. longum-fermented rice bran was thawed and lyophilised overnight using a Labconco Freezone 4.5 Liter Freeze Dry System attached to an Edwards RV5 vacuum pump (Marshall Scientific, Hampton, NH, USA). Mouse diets were prepared as previously described using AIN-93 purified components as the control diet (Kumar *et al.*, 2012). The heat-stabilized rice bran and the *B. longum*-fermented rice bran was incorporated at 10% w/w into the diets at Envigo (Madison, WI, USA). Diets were matched for macronutrient and micronutrient contents with compositions listed in **Table 5.1**. Briefly, the control diet (TD.160791) was composed of four percent w/v corn oil, casein, L-cystine, corn starch, maltodextrin, sucrose, cellulose, mineral and vitamin mix, choline bitartrate, and tertiary butyl-hydroquinone (**TBHQ**) antioxidant. The 10% w/w heat-stabilized rice bran diet and 10% w/w *B. longum*-fermented rice bran diet were adjusted across ingredients to account for nutrients supplied by the rice bran. Prior to animal feeding, diets were gamma-irradiated and determined to be free of pathogens and microbial toxins using standardized tests for anaerobic plate counts, coliform counts, *Escherichia coli* counts, mold counts, yeast counts, mesophilic aerobic spore counts, mesophilic anaerobic spore counts, and *Salmonella* counts.

Table 5.1. Composition of mouse diets for each study group.			
Constituents (g/kg)	Control	10% Rice bran	10% *B. longum*-fermented rice bran
Casein	140.0	125.0	125.0
L-Cystine	1.8	1.8	1.8
Corn Starch	465.692	422.692	422.692
Maltodextrin	155.0	155.0	155.0
Sucrose	95.0	102.312	102.312
Corn Oil	40.0	19.0	19.0
Cellulose	50.0	29.0	29.0
Mineral Mix (with calcium and phosphate)	35.0	0	0
Mineral Mix (without calcium and phosphate)	0	13.388	13.388
Calcium Phosphate, Dibasic	0	7.5	7.5
Calcium Carbonate	0	6.8	6.8
Vitamin Mix	15.0	15.0	15.0
Choline Bitartrate	2.5	2.5	2.5
TBHQ (Tertiary-butyl-hydroquinone), Antioxidant	0.008	0.008	0.008
Rice bran	0	100.0	0
B. longum-fermented rice bran	0	0	100.00

5.3.3 Ethics statement:

Animal experiments were done under institutional guidelines using approved Institutional Animal Care and Use Committee (**IACUC**) protocol and an Inter-Institutional Agreement with Colorado State University.

5.3.4 Animal study design and sample collection:

Animals were maintained in a specific-pathogen free (**SPF**) animal housing facility in UC Denver-Anschutz Medical Campus and monitored under an active Sentinel Monitoring Program. Mice were kept under standard conditions in SPF-ventilated isolators with built in systems for free access to water. Pellet diet was added in cage feeders and mice had free access to it. Six-week old male BALB/c mice (Charles River Laboratories) were fed a control AIN-93 pellet diet for a one-week acclimatization period and then switched to rice bran (n=4), *B. longum*-fermented rice bran (n=4) or maintained on a control diet (n=5) for 15 weeks. During the 15-week feeding phase, faecal samples for each diet group were collected as a function of time for the following

time points: 48 hours after diet intervention (considered week one), and thereafter on two, six, ten and fourteen weeks after diet intervention. Throughout the study, weekly body weight, diet consumption, and general health of mice was recorded. To avoid cross contamination of microbiota between different groups, only cages of one particular sub-group were opened under aseptic conditions in an animal transfer station at a given time. At the end of 15-week feeding phase (time of sacrifice), animals were subjected to CO2 asphyxiation and then euthanized by exsanguination. Whole blood was collected in BD vacutainer K2 EDTA coated tubes and stored at -80°C. Caecum and its contents were collected, snap frozen, and stored at -80°C until later use. The entire colon was excised from the caecum onwards to the distal end and cut open longitudinally along its main axis. Next, colons were gently flushed with ice cold saline solution and cleaned with a fine brush to remove remnants of colonic contents. Approximately 2-3mm slivers of clean colon tissue from proximal and distal ends were cut, snap frozen, and stored at -80°C until later use for metabolomics analysis. An overview of the study design and experimental timeline is depicted in **Figure 5.1.**

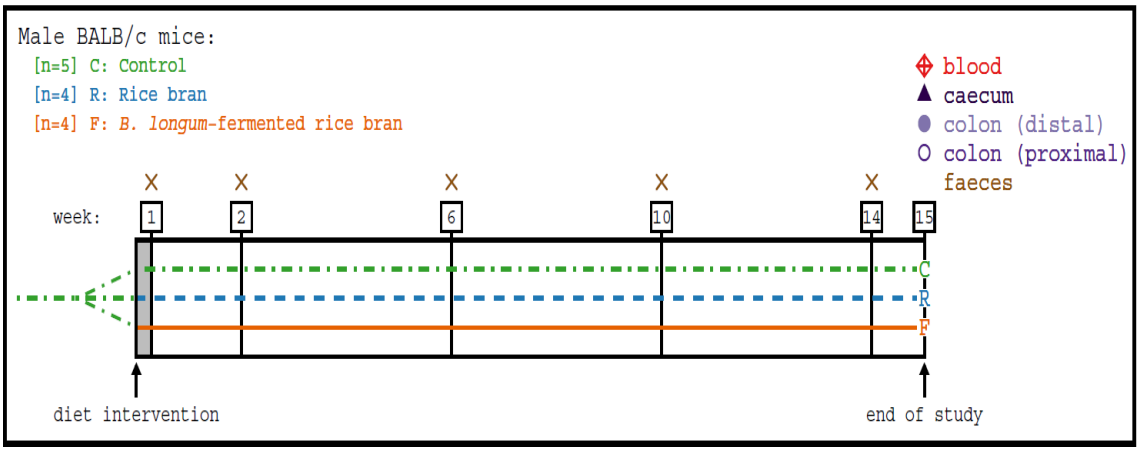

Figure 5.1. Study design and experimental timeline:

Male BALB/c mice were fed control, rice bran, or B. longum-fermented rice bran diets for 15 weeks. Feces, caecum, and colon were collected for both microbiota (data not shown) and metabolite analysis; blood was collected for metabolite analysis only.

5.3.5. Non-targeted metabolomics sample processing:

The mouse diets, proximal and distal colon tissues, and whole blood samples were sent to Metabolon Inc © (Durham, NC, USA) for metabolite extraction and metabolite identifications. Mouse diets (200mg), colon tissue (50 milligrams) and whole blood (one mL) were provided on dry ice and were stored at -80ºC until use. Each matrix was extracted with 80% methanol and divided into five equal parts for chromatographic extraction including two rounds of reverse-phase ultra-high performance liquid chromatography tandem mass-spectrometry (**UPLC-MS/MS)** with positive ion mode electrospray ionization (**ESI**), one round of reverse-phase UPLC-MS/MS with negative ion mode ESI, one round of hydrophilic-interaction (**HILIC**)/UPLC-MS/MS with negative ion mode ESI and one back-up sample. Aliquots collected under acidic conditions for positive ion mode analysis of hydrophilic compounds were separated on a C18 column (Waters UPLC BEH C18-2.1x100 mm, 1.7 µm) and gradient-eluted using a water and methanol mobile phase with 0.1% v/v formic acid. Aliquots collected under acidic conditions for positive ion mode analysis of hydrophobic compounds were separated on

the same column but were gradient-eluted with a mobile phase containing water, methanol, 0.05% v/v penta-fluoropropionic anhydride and 0.01% formic acid. Aliquots collected under basic conditions for negative ion ESI were separated using a separate C18 column (Waters UPLC BEH C18-2.1x100 mm, 1.7 µm) and gradient-eluted using a water and acetonitrile mobile phase with 6.5 millimolar ammonium bicarbonate at pH of eight. The HILIC aliquot was separated using a HILIC column (Waters UPLC BEH Amide 2.1x150 mm, 1.7µm) and gradient-eluted using a water and acetonitrile mobile phase with 10 millimolar ammonium formate at pH 10.8. Each chromatographically-extracted sample was stored overnight under nitrogen gas before mass-spectral analysis, which was performed on a Thermo Scientific Q-Exactive mass spectrometer operated with a heated-ESI source and at a 35,000-mass resolution. Tandem mass spectrometry scans alternated between MS and MSn scans using dynamic exclusion and covered a range of 70 mass to charge ratio (**m/z**) to 1,000 m/z. Mass spectral profiles were peak identified and quality-control processed at Metabolon Inc ©. Quality control during sample processing was measured by injecting a cocktail of known chemical standards into each sample prior to chromatography and mass spectrometry, via spectral analysis of a pooled matrix sample containing an equal volume of each sample and using extracted water samples as negative controls. Compound identities were made based on an internal library containing over 3,300 commercially available chemical standards and were annotated based on matches to retention time/index, having an m/z within 10 parts per million to a database standard, and by assessing the overall mass spectral profile matches to database standards. Spectral profiles that were structurally resolved but were otherwise not archived in internal chemical database were reported as ‘unknown’.

5.3.6. Metabolomics statistical analysis:

Metabolite raw abundances were normalized by dividing the median raw abundance of that metabolite across the entire dataset for each matrix, and to produce median-scaled abundances. For samples lacking a metabolite, the minimum median scaled abundance of that metabolite across the dataset was input as a minimum value before downstream statistical analysis. Metabolite fold differences were calculated for each metabolite by dividing the average median-scaled abundance of the metabolite in one treatment group by that of a second treatment group for all pairs of treatments within a matrix. For the colon tissue, metabolite median-scaled abundances and fold differences were calculated by pooling together proximal and distal colon into a single sample type. For the study diets (food), colon tissue, and blood, median-scaled abundances for each metabolite were compared using two-way analysis of variance (Ly and Casanova) with a Welch's post-hoc test, where significance was defined as $P<0.05$. To account for false discovery rate errors, a *q*-value was calculated for each metabolite and metabolites with a *q*-value less than 0.1 were excluded from downstream analysis.

5.3.7. Metabolic network visualization:

Metabolic network visualization with Cytoscape Network Analysis version 2.8.3 was performed to compare the abundances of metabolites that were statistically-different ($P<0.05$) between *B. longum*-fermented rice bran and rice bran samples in the food, colon tissue, and blood metabolomes. Metabolites were organized into nodal clusters by chemical class (e.g. lipid, amino acid) and were further separated by metabolic pathway (e.g. sphingolipid, polyamine). Node diameters measured the magnitude of each metabolite's fold difference between *B. longum*-fermented rice bran and rice bran samples where larger node diameters reflected larger

fold difference magnitudes between *B. longum*-fermented rice bran versus rice bran. Red nodes indicated metabolites that increased in *B. longum*-fermented rice bran versus rice bran and blue nodes indicated metabolites that were significantly decreased. Numbers in nodes are pathway enrichment scores (**PES**) that indicate a metabolic pathway's relative contribution of statistically-significant metabolites to treatment differences. Pathway enrichment scores were calculated using the following equation:

$$\text{PES} = \frac{(m - k)}{(N - n)}$$

The score is determined by subtracting a pathway's number of statistically-different metabolites (k) from the total number of metabolites in the pathway (m) and then dividing this by the difference in the total number of statistically different metabolites in the entire dataset (n) and the total number of metabolites in the dataset (N). Metabolic pathways with a PES >1.0 containing at least five metabolites, indicated that this pathway had a higher proportion of statistically-different metabolites compared to all other pathways and were used to designate pathways contributing to treatment differences.

5.4. Results:

5.4.1. Metabolome differences between control, rice bran and B. longum fermented rice bran dietary treatments.

Metabolomics of the food identified 663 distinct metabolites that were organized by chemical class and metabolic pathway. A total of 327 metabolites were statistically-different in abundances between two or more study diets tall three study diets including 82 amino acids four peptides, 18 carbohydrates, eight energy pathway metabolites, 87 lipids, 29 nucleotides, 13 cofactors and vitamins, 33 phytochemicals/other, and 53 unknown metabolites. Lipids and amino

acids contributed to ~51% of the metabolite differences between the three diets with nucleotides (~8% of differences), phytochemicals (~10% of differences), and unknown/unnamed metabolites (~16% of differences). Multiple metabolic pathways distinguished the three diets and are reported in **Figure 5.2**. These metabolic pathways included 14 amino acid pathways, 11 lipid pathways, two carbohydrate pathways, one energy pathway, five nucleotide pathways, two cofactor/vitamin pathways, and two phytochemical/other pathways. Lactate, a metabolic end-product of fermentation, was significantly increased ($P<0.05$) in the fermented rice bran diet compared to the control diet (33.27-fold increase) and to the rice bran diet (95.94-fold increase). Amino acids driving the metabolic pathway differences included the arginine metabolite N-delta-acetylornithine (224.67-fold increase in fermented rice bran versus control, 170.87-fold-increase in fermented rice bran versus rice bran) and the polyamine 5-methylthioadenosine (2.11-fold increase and 0.070-fold decrease for both fermented rice bran versus control and fermented rice bran versus rice bran respectively). Other compounds contributing to these metabolic pathway differences between dietary treatments included the tricarboxylic acid metabolite tricarballylate (2.42-fold increase rice bran versus control, 3.00-fold increase in fermented rice bran versus control, 1.24-fold increase fermented rice bran versus rice bran), and the phytochemical salicylate (5.74-fold increase rice bran versus control, 7.77-fold increase in fermented rice bran versus control, 1.35-fold increase fermented rice bran versus rice bran) (**Figure 5.2**).

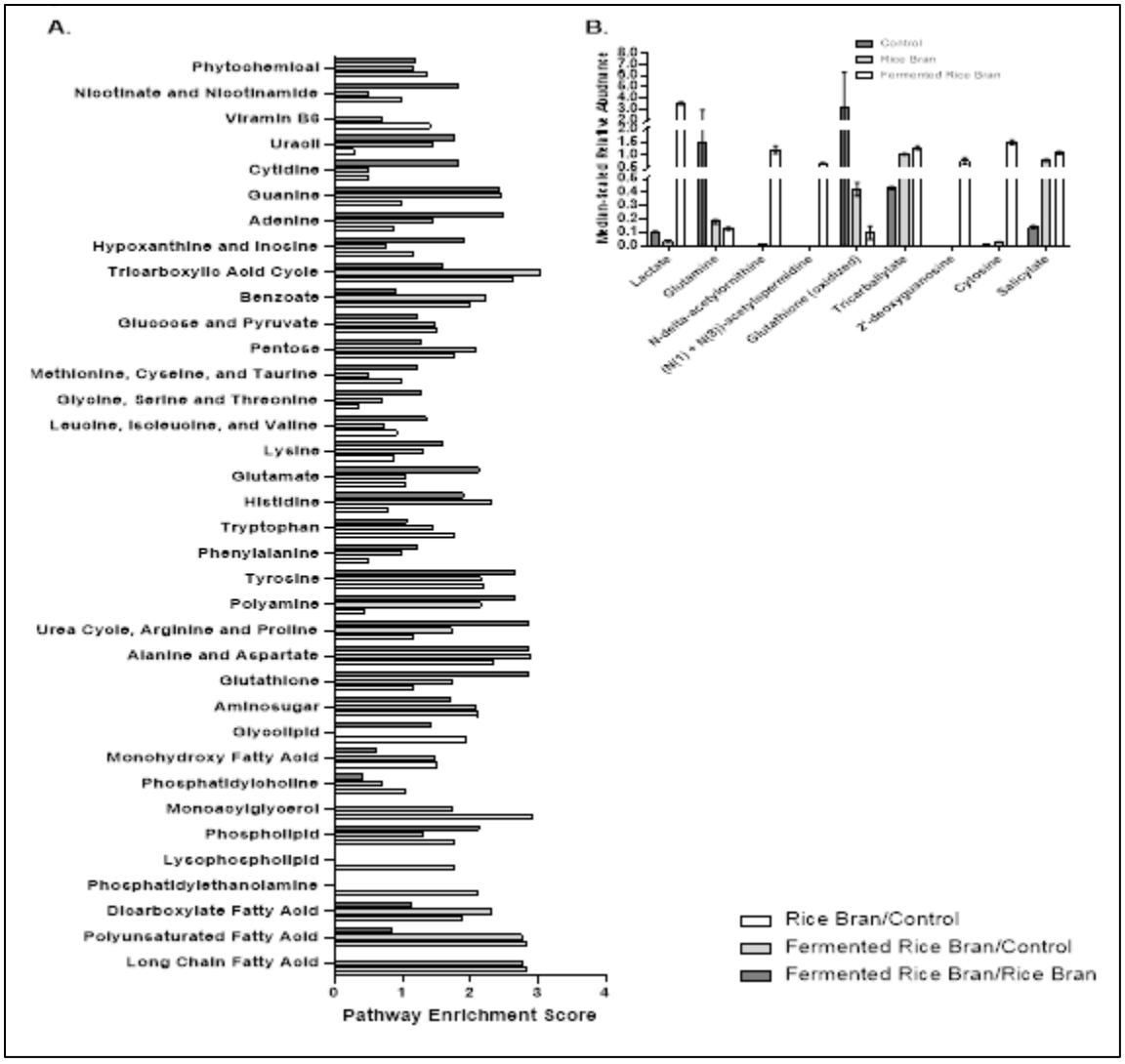

Figure 5.2. The food metabolome differs across control, rice bran and *B. longum* fermented rice bran diets.

[A] Pathway enrichment scores distinguishing control, rice bran and B. longum fermented rice bran diets. ***[B]*** *Median-scaled relative abundances for selected metabolites distinguishing the three food metabolomes. Depicted metabolites have a $p<0.05$ when comparing their abundance between two or more treatments.*

5.4.2. Control, rice bran and B. longum-fermented rice bran diets modulate bioavailability of compounds in the colon metabolome of healthy mice.

A total of 664 metabolites were identified in the colon metabolome. In the colon tissue, there were 125 amino acids, 25 peptides, 33 carbohydrates, 12 energy metabolites, 301 lipids, 43

nucleotides, 34 cofactors/vitamins, 25 phytochemicals/others, and 66 unknown metabolites. **Figure 5.3** shows the metabolic pathways differentiating the colon tissue metabolomes across control, rice bran and *B. longum*-fermented rice bran-fed mice. Metabolic pathways driving these colon metabolite differences across the three dietary groups. These metabolic pathways included five amino acid pathways, one peptide pathway, thirteen lipid pathways, one nucleotide pathway, two cofactor/vitamin pathways, and one phytochemical/other pathway. Across the three dietary groups, 159 metabolites significantly-differed in abundance ($P<0.05$) in the colon tissue including 13 amino acids, one peptide, one carbohydrate, one energy metabolite, 121 lipids, two nucleotides, four cofactors/vitamins, five phytochemicals/other, and twelve unknown metabolites.

Lipids, which contributed to ~76% of the differentially-abundant colon metabolites between study groups, included sphingadienine (0.32-fold decrease in fermented rice bran versus control, 0.45 fold-decrease in fermented rice bran versus rice bran), and sphingosine (0.48-fold decrease in fermented rice bran versus control, 0.57-fold decrease in fermented rice bran versus rice bran Amino acid metabolite contributors included arginine metabolite N-delta-acetylornithine (11.18-fold increase in fermented rice bran versus control, 11.77-fold increase in fermented rice bran versus rice bran), and the tricarboxylic acid metabolite tricarballylate (23.34-fold increase in fermented rice bran versus rice bran). Additional metabolites contributing to colon metabolome differences included the vitamin E metabolite alpha-tocopherol (0.33-fold decrease in fermented rice bran versus control, 0.38-fold decrease in fermented rice bran versus rice bran), and the phytochemical salicylate (16.65-fold increase in fermented rice bran versus control, 18.78-fold increase in fermented rice bran versus rice bran).

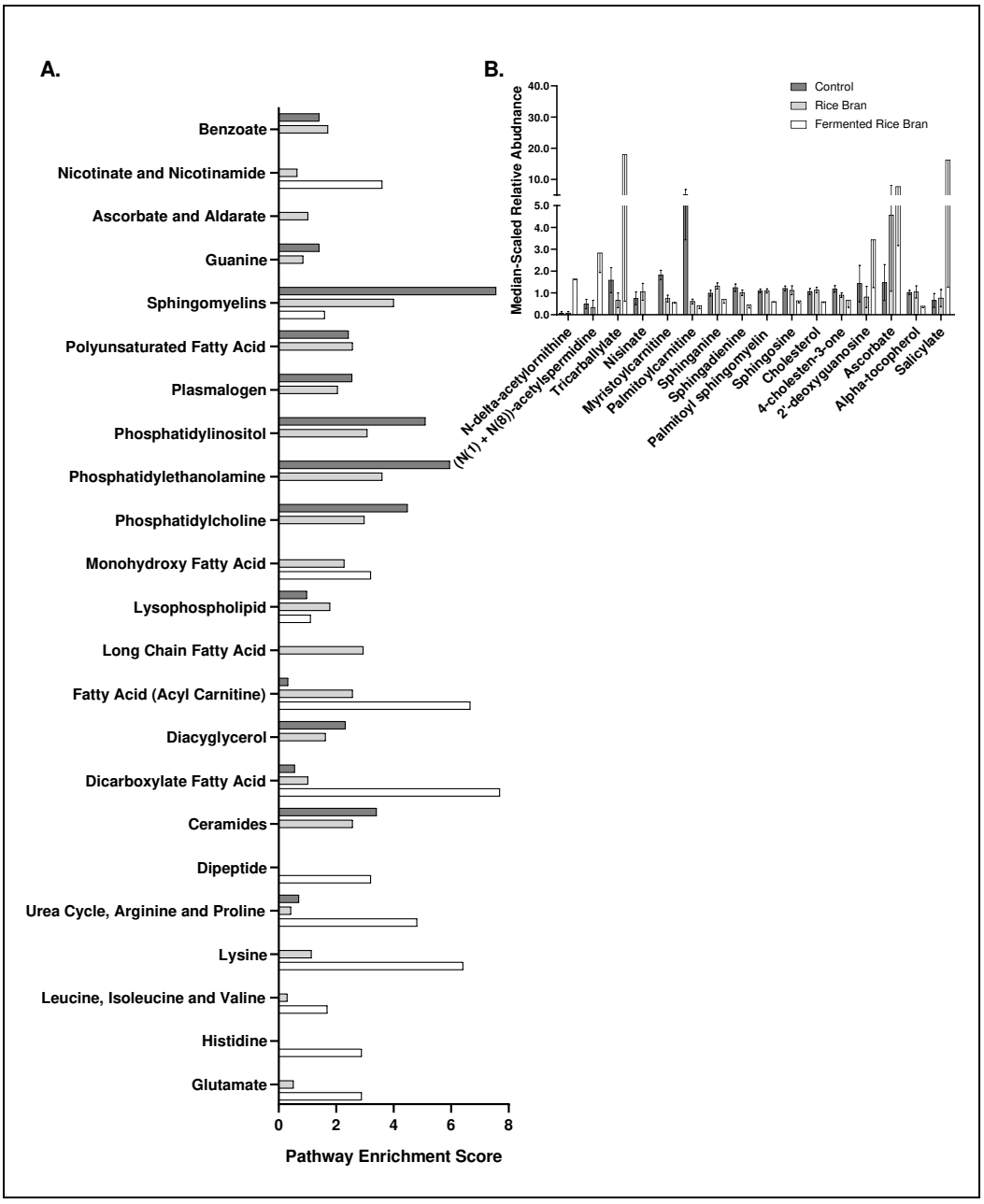

Figure 5.3. Consumption of *B. longum*-fermented rice bran versus rice bran and control diets differentially modulate the colon tissue metabolome of healthy mice.

[A] Pathway enrichment scores distinguishing the colon tissue of mice consuming the control, rice bran and B. longum fermented rice bran diets. ***[B]*** *Median-scaled relative abundances for selected metabolites distinguishing the three colon metabolomes. Depicted metabolites have a $p<0.05$ when comparing their abundance between two or more treatments.*

5.4.3. Dietary treatments differentially modulate the blood metabolome of healthy mice.

A total of 802 metabolites were identified in the blood metabolome including 172 amino acids, 36 peptides, 31 carbohydrates, 11 energy metabolites, 354 lipids, 43 nucleotides, 20 cofactors/vitamins, 44 phytochemicals/others, and 91 unknown metabolites (Sheet S1). One hundred fifty-four blood metabolites had significantly-different (P<0.05) abundances two or more treatments including 32 amino acids, three peptides, seven carbohydrates, one energy metabolite, 53 lipids, 59 nucleotides, six cofactors/vitamins, 21 phytochemicals/ others, and 16 unknown metabolites. Lipid (~34%), nucleotide (~38%) and amino acid (~21%) metabolites accounted for the majority of blood metabolites with statistically-different (P<0.05) abundances between the control group, rice bran, and *B. longum*-fermented rice bran-fed mice.

Metabolic pathways and metabolites that distinguished the blood metabolome of diet groups are shown in **Table 5.2** and those with selected bioactivities are described in **Table 5.3**. These included ten amino acid pathways, 14 lipid pathways, three nucleotide pathways, three peptide pathways, two carbohydrate pathways, one energy pathway, one cofactor/vitamin pathway, and one phytochemical pathway. included Metabolites contributing to blood metabolome differences included the arginine metabolite N-delta-acetyl-ornithine (2.16-fold increase in rice bran versus control, 9.59-fold fermented rice bran versus rice bran, 4.44-fold-increased in fermented rice bran versus rice bran), and the polyamine 5-methylthioadenosine (1.51-fold increase in fermented rice bran versus control, 1.54-fold increase in fermented rice bran versus rice bran. Additional metabolite contributors included the secondary bile acid deoxycholate (0.78-fold decrease fermented rice bran versus control, 1.49-fold-increase fermented rice bran versus rice bran) and the nucleotide cytosine (6.48-fold increase in fermented rice bran versus control, 5.67-fold increase in fermented rice bran versus rice bran).

Table 5.2. Differentially abundant blood metabolites in mice consuming control, rice bran and *B. longum*-fermented rice bran diets.

Metabolic Pathway[2]	Metabolites	Fold Difference[1]		
		RB / CON	FRB / CON	FRB / RB
Alanine and Aspartate	N-acetylasparagine	↑**1.35**	↑**1.81**	↑**1.33**
Glutamate	glutamine	0.96	1.26	↑**1.31**
	pyroglutamine	1.33	↑**2.07**	1.56
Histidine	1-methyl-4-imidazole acetate	↓**0.80**	1.01	↑**1.26**
	3-methylhistidine	1.12	↑**1.35**	1.21
	anserine	↓**0.63**	0.76	1.21
Tryptophan	N-formylanthranilic acid	1.00	↑**1.24**	↑**1.25**
	picolinate	↑**3.15**	1.62	0.51
	indoleacetylglycine	↑**2.56**	↑**2.52**	0.98
Lysine	2-oxoadipate	↑**1.56**	1.07	↓**0.69**
	tyrosine	0.84	1.10	↑**1.32**
	1-carboxyethyltyrosine	1.37	↑**2.05**	↑**1.49**
	N-acetyltyrosine	↓**0.65**	↓**0.64**	0.97
	phenol sulfate	↑**3.44**	↑**6.02**	1.75
	phenol glucuronide	2.91	↑**5.02**	1.72
	4-methoxyphenol sulfate	↑**32.41**	↑**13.31**	0.41
Methionine, Cysteine, Taurine	N-formylmethionine	1.03	↑**1.27**	↑**1.24**
	taurine	↓**0.82**	0.90	1.10
Urea Cycle, Arginine and Proline	N-delta-acetylornithine	↑2.16	↑9.59	↑**4.44**
	N2, N5-diacetylornithine	-	↑**2.09**	↑**2.09**
Polyamine	5-methylthioadenosine	0.98	↑**1.51**	↑**1.54**
	(N (1) + N (8)-acetylspermidine	0.63	↓**0.41**	0.65
Glutathione	glutathione, oxidised	0.87	1.34	↑**1.53**
	ophthalmate	0.96	1.33	↑**1.39**
Dipeptide	valylglycine	↓**0.29**	0.84	↑**2.87**
Gamma-glutamyl amino acid	gamma-glutamylglycine	↑**2.06**	1.71	0.83
	gamma-glutamyl-epsilon-lysine	↑**2.70**	1.87	0.69
Pentose	arabitol/xylitol	0.91	↑**1.34**	↑**1.48**
	arabonate/xylonate	↓**0.88**	0.98	↑**1.12**
Aminosugar	N-acetylneuraminate	0.79	↓**0.53**	0.67
	N6-carboxymethllysine	↓**0.60**	0.72	1.19
Tricarboxylic Acid Cycle	alpha-ketoglutarate	2.74	↑**3.49**	1.27
Carnitine	propionylcarnitine	1.26	↑1.93	↑**1.53**
	cis-4-decenoylcarnitine	↓**0.56**	0.89	↑**1.59**
	methylmalonate	↑**1.38**	↑**1.57**	1.14
	acetylcarnitine	↓**0.83**	↓**0.79**	0.95
	3-hydroxyhexanoylcarnitine	↑**1.10**	1.07	0.97
	decanoylcarnitine	↓**0.63**	0.81	1.29
	myristoylcarnitine	↓**0.62**	↓**0.58**	0.93
Long Chain Fatty Acid	margarate	↑**1.27**	↑**1.28**	1.01
	stearate	↑**1.07**	↑**1.07**	1.01
	eicosanoate	↑**1.62**	1.40	0.86
Polyunsaturated Fatty Acid	arachidonate	1.18	↓**1.51**	↑**1.28**
	eicosapentaenoate	↑**1.89**	↑**1.78**	0.94
	docosahexaenoate	↑**1.34**	↑**1.47**	1.10
	docosatrienoate	↑**1.64**	1.27	0.77
	arachidonate	1.18	↑**1.51**	↑**1.28**
Branched Fatty Acid	15-methylpalmitate	↑**1.29**	↑**1.25**	0.97

Table 5.2. Differentially abundant blood metabolites in mice consuming control, rice bran and *B. longum*-fermented rice bran diets.

Metabolic Pathway[2]	Metabolites	Fold Difference[1]		
		RB / CON	FRB / CON	FRB / RB
Dicarboxylate Fatty Acid	octadecenedioate*	↑**2.82**	↑**3.82**	↑**1.36**
	pimelate	↓**0.31**	↓**0.28**	0.91
	suberate	↓**0.44**	↓**0.45**	1.02
	azelate	↓**0.19**	↓**0.14**	0.77
	sebacate	0.79	↓**0.61**	0.76
	dodecadienoate	↓**0.34**	0.66	1.95
	octadecadeinedioate	↓**0.46**	0.71	1.55
Phopspholipid	choline	↓**0.82**	1.08	↑**1.30**
Plasmalogen	1-(1-enyl-palmitoyl)-2-linoleoyl-glycerophosphocholine	0.87	↓**0.68**	↓**0.78**
Monoacylglycerol	1-linoleoylglycerol	↑**1.93**	↑**2.11**	1.09
Diacylglycerol	oleoyl-oleoyl-glycerol [1]*	0.76	↓**0.27**	↓**0.36**
	linoleoyl-linolenoyl-glycerol	↑**3.72**	2.29	0.62
	stearoyl-arachidonoyl-glycerol	↓**0.49**	↓**0.35**	0.70
	hexadecasphingosine	↓**0.54**	↓**0.58**	1.07
	heptadecasphingosine	↓**0.68**	↓**0.68**	0.99
Ceramide	ceramide (d18:1/17:0, d17:1/18:0)*	0.45	↓**0.33**	0.74
Endocannabinoid	oleoyl ethanolamide	1.21	↑**1.51**	1.25
Sterol	7-alpha-hydroxy-3-oxo-4-cholestenoate	1.01	↑**1.16**	↑**1.15**
	campesterol	↓**0.75**	↓**0.73**	0.97
Primary Bile Acid	chenodeoxycholate	0.66	1.18	↑**1.79**
Secondary Bile Acid	deoxycholate	↓**0.78**	1.17	↑**1.49**
Uracil	N-acetyl-beta-alanine	↓**0.69**	↓**0.14**	↓**0.20**
	Uridine-5'monophosphate	0.67	↓**0.46**	0.69
Xanthine and Inosine	Inosine 5'-monophosphate	↓**0.54**	0.72	1.35
Cytidine	cytosine	1.14	↑**6.48**	↑**5.67**
	5-methylcytidine	↓**0.52**	↓**0.45**	0.88
Nicotinate and Nicotinamide	trigonelline	↑**51.32**	↑**70.30**	1.37
	N1-Methyl-2-pyridone-5-carboxamide	↓**0.40**	0.65	1.60
Phytochemical	2-hydroxyhippurate (salicylurate)	↑**9.89**	↑**22.46**	↑**2.27**
	thioproline	1.33	1.02	↓**0.77**
	hippurate	↑**3.79**	↑**4.17**	1.10
	4-hydroxyhippurate	↑**4.07**	↑**3.24**	0.80
	catechol sulfate	↑**3.11**	↑**3.52**	1.13
	4-methylcathecol sulfate	↑**4.66**	3.74	0.80
	4-vinylphenol sulfate	↑**6.57**	↑**5.25**	0.80
	3-phenylproprionate	1.85	↑**4.19**	2.27
	2,3-dihydroxyisovalerate	1.29	↑**1.46**	1.14
	caffeic acid sulfate	↑**3.61**	↑**5.13**	1.42
	2-oxindole-3-acetate	1.42	↑**3.99**	2.81
	Ferulic acid 4-sulfate	↑**80.32**	↑**73.77**	0.92
	N-glycolylneuraminate	0.79	↓**0.57**	0.73
	stachydrine	↑**4.44**	↑**2.55**	0.57
	tartarate	↑**3.87**	3.06	0.79
	N-acetylpyrraline	↑**1.85**	↑**2.60**	1.41
Other	ergothionine	0.93	↑1.65	↑**1.77**
	erythritol	↑**1.35**	↑**1.77**	↑**1.32**
	salicylate	↑**5.88**	↑**6.57**	1.12

Table 5.2. Differentially abundant blood metabolites in mice consuming control, rice bran and *B. longum*-fermented rice bran diets.

Metabolic Pathway[2]	Metabolites	Fold Difference[1]		
		RB / CON	FRB / CON	FRB / RB
	ethyl-glucuronide	2.21	↑**8.68**	3.92
	1,2,3-benzenetriol sulfate (2)	↑**5.66**	2.31	0.41

Table 5.3. Metabolites with previously-reported antimicrobial functions that were differentially-abundant between fermented rice bran and rice bran treatments.

Metabolite	Fold Difference FRB/RB[1,2,3]			Antimicrobial Functions	References
	Food	Colon Tissue	Blood		
glutamine	↓**0.72**	0.91	↑**1.31**	As an antimicrobial, glutamine supplements reduced enterotoxigenic *E. coli* infection into the murine small intestine in part via up-regulation of mucosal immunity.	(Hu *et al.*, 2018; Liu *et al.*, 2017)
N-delta-acetylornithine	↑**170.87**	↑**11.77**	↑**4.44**	Involved in plant protection against pathogens via salicylic acid-mediated responses.	(Adio *et al.*, 2011; Oka *et al.*, 1984)
5-methyl-thioadenosine	1.00	1.06	↑**1.54**	Accumulation within microbes has a bactericidal effect.	(North *et al.*, 2017)
tricarballylate	↑**1.24**	↑**23.34**	-	As part of a probiotic and rice bran cell-free supernatant treatment, tricarballylate was associated with *Salmonella* Typhimurium growth suppression in *vitro*.	(Nealon *et al.*, 2017a; Watson *et al.*, 1969)
palmitoylcarnitine	1.00	↓**0.71**	0.78	Increased the uptake of cefotoxin antimicrobial in the rat and dog colon compared to animals not supplemented with palmitoylcarnitine. In Sprague-Dawley rats and beagle dogs, palmitoylcarnitine increased colonic uptake of cefotoxin and gentamicin.	(Fix *et al.*, 1986)
myo-inositol	0.82	0.68	↓**0.67**	When supplemented to carp, increased intestinal levels were associated with decreased production of pro-inflammatory cytokines, increased production of antimicrobial proteins, and increased intestinal immunity to *Aeromonas hydrophila* infection	(Li *et al.*, 2018)
sphinganine	-	↓**0.53**	0.90	Bactericidal to gram positive bacteria and reduced the adhesion of *Staphylococcus aureus* and *Streptococcus mitis* to host epithelial cells *in vitro*.	(Bibel *et al.*, 1992)
sphingosine	-	↓**0.57**	0.88	Disrupted the cell wall and cell membrane of *Staphylococcus aureus* and created intracellular inclusion bodies associated with cell death in *S. aureus* and *E. coli in vitro*.	(Fischer *et al.*, 2013)

Table 5.3. Metabolites with previously-reported antimicrobial functions that were differentially-abundant between fermented rice bran and rice bran treatments.

Metabolite	Fold Difference FRB/RB[1,2,3]			Antimicrobial Functions	References
	Food	Colon Tissue	Blood		
chenodeoxycholate	-	1.08	↑**1.79**	Attenuated *Salmonella* Typhimurium and *Citrobacter rodentium* infections in mice to promote lower systemic infection rates and improved pathogen clearance. Shown to be associated with increased production of bactericidal alpha defensins by intestinal Paneth cells.	(Tremblay *et al.*, 2017)
ascorbate (Vitamin C)	0.59	↓**0.83**	-	In brine shrimp larvae, ascorbate exhibited antimicrobial activity against *Vibrio harveyi*.	(Li *et al.*, 2018)
alpha-tocopherol	-	↑**1.69**	0.22	As part of a wild apple extract, alpha tocopherol exhibited bactericidal effects against *Staphylococcus aureus*, *Escherichia coli*, *Pseudomonas aeruginosa*, *Enterococcus faecalis*, and *Streptococcus pyogenes*. Increases elastase production in neutrophils to enhance digestion of *Streptococcus pneumoniae*.	(Bou Ghanem *et al.*, 2017; Radenkovs *et al.*, 2018)
salicylate	↑**1.35**	↑**18.78**	1.12	As part of an *Anthemis stiparum* plant extract, salicylate exhibited bactericidal and anti-biofilm effects on *Staphylococcus aureus* and *Bacillus subtillis*, and reduced adhesion of *Candida albicans* to growth agar.	(Chemsa *et al.*, 2018)

1. Table includes metabolites with a statistically-different ($p<0.05$) relative abundance between fermented rice bran and rice bran treatments, where **bold** indicates statistically difference in the corresponding metabolite profile and un-bolded metabolites were not statistically-different in abundance.
2. FRB: Fermented rice bran; RB: Rice bran.
3. ↑indicates metabolite abundance was significantly-higher in fermented rice bran compared to rice bran and ↓ indicates metabolite abundance was lower in fermented rice bran compared to rice bran. "-" indicates metabolite not detected in the given sample matrix.

5.5. Discussion and Conclusions:

We examined daily dietary intake of *B. longum*-fermented rice bran for metabolic distinctions to non-fermented rice bran or a control diet intake for 15 weeks in healthy mice. Dietary interventions were assessed for effects of uptake of metabolites in the colon tissue and blood. When comparing the metabolite profiles of all three diets, considerable differences existed

in the food metabolomes of *B. longum*-fermented rice bran versus non-fermented rice bran and consequently this comparison was explored further. Using a healthy murine model in a long-term (15-week diet study) was a key aspect of these investigations as the differences in the colon tissue and blood metabolomes detected between mice fed *B. longum*-fermented rice bran versus the non-fermented form have strong implications for mechanisms involved in infectious enteric disease prevention.

The *B. longum*-fermented rice bran and rice bran diets exhibited large differences in host uptake and metabolism of bioactive molecules in the colon and blood. These compounds had reported antioxidant, immune-modulatory, gut barrier protective, antitoxicant, and health promoting functions. Given the many roles of rice bran and fermented rice bran in colorectal cancer protection and for its antimicrobial capacities, bioactive compounds were analyzed in the context of preventing these gastrointestinal conditions. The lipid and amino acid metabolic pathways represented the majority of metabolite abundance changes in the food, colon tissue, and blood metabolomes when with *B. longum*-fermented rice bran fed mice were compared to rice bran fed mice. Increased bioavailability of N-delta-acetylornithine in colon (11.77-fold increase) and blood (4.44-fold increase) when comparing mice consuming fermented rice bran versus rice bran was supported by substantially increased abundance in the food (170.87-fold increase). N-delta-acetylornithine is a secondary metabolite of plants that has roles in protecting plant tissues from herbivore damage and bacterial infections. Given its high levels in fermented rice bran versus rice bran in colon and blood, N-delta-acetylornithine merits mechanistic examination for its effects on host colonocyte metabolism and as a potential biomarker of *B. longum*-fermented rice bran consumption.

Increased uptake of tricarballylate (23.34 fold-increase) was another notable metabolite distinguishing fermented rice bran versus rice bran consuming mice Tricarballylate has been previously reported to function as an aconitase inhibitor where it decreased the conversion of citrate into isocitrate to reduce metabolite flux through the tricarboxylic acid cycle and diminished *Salmonella* proliferation (Nealon *et al.*, 2017a; Watson *et al.*, 1969). When tricarballylate was administered to rats, decreased succinate was produced in colonocytes, which is a downstream product of citrate metabolism in the tricarboxylic acid cycle, suggesting that its biochemical mechanisms also function in mammalian systems (Wolffram *et al.*, 1994). Also noteworthy was that a decreased pH in the lumen enhanced tricarballylate uptake into colonocytes (Zhou *et al.*, 2012). Rice bran fermentation in the colon lumen, with *B. longum*-may increase the availability of fermentable substrates to the murine colon microbiota and create an acidifying environment favoring enhanced tricarballylate uptake in the colon. Future investigations can measure the pH of colon contents following consumption of rice bran and *B. longum* fermented rice bran to examine for potential pH influences on colon tissue tricarballylate levels that can be modulated by fermented foods.

B. longum-fermented rice bran produced a suite of unique food and microbial metabolites in the host colon and bloodstream. Most of these changes were amino acids and lipids produced by both the host and the gut microbiome that have important implications for detailed assessments of fermented diets and for enhancing bioavailability and promoting colon health and for providing infectious disease prophylaxis and have not been explored previously in fermented rice bran. This study design can be used for screening of probiotic strains that will optimize rice bran's capacity for safety, prophylaxis and therapeutic potential aimed toward gastrointestinal disorders. Additional investigations for *B. longum*-fermented rice bran protection against gut

pathogen challenge can be explored to provide further confirmation of the bioactivity conferred by the fermented rice bran metabolites discussed herein. Furthermore, the many gut-microbial mediated metabolomic changes between fermented rice bran and rice bran-fed animals can be explored using transcriptomic platforms for elucidation of the mechanisms by which rice bran modulates but microbial metabolism. The integrated assessment of both food and host metabolomes provided an important and powerful approach to further our understanding of how fermentation modulates bioactivity of rice bran in a healthy host system.

REFERENCES

Adio, A.M., et al., 2011. Biosynthesis and defensive function of Ndelta-acetylornithine, a jasmonate-induced Arabidopsis metabolite. Plant Cell 23: 3303-3318. 10.1105/tpc.111.088989

Bazanella, M., et al., D., 2017. Randomized controlled trial on the impact of early-life intervention with bifidobacteria on the healthy infant fecal microbiota and metabolome. Am J Clin Nutr 106: 1274-1286. 10.3945/ajcn.117.157529

Bibel, D.J., Aly, R. and Shinefield, H.R., 1992. Inhibition of microbial adherence by sphinganine. Can J Microbiol 38: 983-985.

Bou Ghanem, E.N., et al., 2017. The Alpha-Tocopherol Form of Vitamin E Boosts Elastase Activity of Human PMNs and Their Ability to Kill Streptococcus pneumoniae. Front Cell Infect Microbiol 7: 161. 10.3389/fcimb.2017.00161

Brown, D.G., et al., 2017. Heat-stabilised rice bran consumption by colorectal cancer survivors modulates stool metabolite profiles and metabolic networks: a randomised controlled trial. Br J Nutr 117: 1244-1256. 10.1017/s0007114517001106

Bunesova, V., Lacroix, C. and Schwab, C., 2016. Fucosyllactose and L-fucose utilization of infant Bifidobacterium longum and Bifidobacterium kashiwanohense. BMC Microbiol 16: 248-248. 10.1186/s12866-016-0867-4

Celiberto, L.S., et al., 2017. Effect of a probiotic beverage consumption (Enterococcus faecium CRL 183 and Bifidobacterium longum ATCC 15707) in rats with chemically induced colitis. PLoS One 12: e0175935. 10.1371/journal.pone.0175935

Chemsa, A.E., et al., 2018. Chemical composition, antioxidant, anticholinesterase, antimicrobial and antibiofilm activities of essential oil and methanolic extract of Anthemis stiparum subsp. sabulicola (Pomel) Oberpr. Microb Pathog 119: 233-240. 10.1016/j.micpath.2018.04.033

Cowan, T.E., et al., 2014. Chronic coffee consumption in the diet-induced obese rat: impact on gut microbiota and serum metabolomics. J Nutr Biochem 25: 489-495. 10.1016/j.jnutbio.2013.12.009

Derkach, A., et al., 2017. Effects of dietary sodium on metabolites: the Dietary Approaches to Stop Hypertension (DASH)-Sodium Feeding Study. Am J Clin Nutr 106: 1131-1141. 10.3945/ajcn.116.150136

Fabian, C. and Ju, Y.H., 2011. A review on rice bran protein: its properties and extraction methods. Crit Rev Food Sci Nutr 51: 816-827. 10.1080/10408398.2010.482678

Fischer, C.L., et al., 2013. Sphingoid Bases Are Taken Up by Escherichia coli and Staphylococcus aureus and Induce Ultrastructural Damage. Skin Pharmacology and Physiology 26: 36-44. 10.1159/000343175

Fix, J.A., et al., 1986. Acylcarnitines: drug absorption-enhancing agents in the gastrointestinal tract. Am J Physiol 251: G332-340. 10.1152/ajpgi.1986.251.3.G332

Gagnon, M., et al., 2015. Bioaccessible antioxidants in milk fermented by Bifidobacterium longum subsp. longum strains. BioMed research international 2015: 169381-169381. 10.1155/2015/169381

Han, B., et al., 2019. High doses of sodium ascorbate act as a prooxidant and protect gnotobiotic brine shrimp larvae (Artemia franciscana) against Vibrio harveyi infection coinciding with heat shock protein 70 activation. Dev Comp Immunol 92: 69-76. 10.1016/j.dci.2018.11.007

Henderson, A.J., et al., 2012a. Consumption of rice bran increases mucosal immunoglobulin A concentrations and numbers of intestinal Lactobacillus spp. J Med Food 15: 469-475. 10.1089/jmf.2011.0213

Henderson, A.J., et al., 2012b. Chemopreventive properties of dietary rice bran: current status and future prospects. Adv Nutr 3: 643-653. 10.3945/an.112.002303

Hernandez-Alonso, P., et al., 2017. Effect of pistachio consumption on the modulation of urinary gut microbiota-related metabolites in prediabetic subjects. J Nutr Biochem 45: 48-53. 10.1016/j.jnutbio.2017.04.002

Kim, J.M., et al., 2018. Safety Evaluations of Bifidobacterium bifidum BGN4 and Bifidobacterium longum BORI. Int J Mol Sci 19. 10.3390/ijms19051422

Kumar, A., et al., 2012. Dietary rice bran promotes resistance to Salmonella enterica serovar Typhimurium colonization in mice. BMC Microbiol 12: 71. 10.1186/1471-2180-12-71

Lee, T., et al., 2017. Oral versus intravenous iron replacement therapy distinctly alters the gut microbiota and metabolome in patients with IBD. Gut 66: 863-871. 10.1136/gutjnl-2015-309940

Lei, S., et al., 2016. High Protective Efficacy of Probiotics and Rice Bran against Human Norovirus Infection and Diarrhea in Gnotobiotic Pigs. Front Microbiol 7: 1699. 10.3389/fmicb.2016.01699

Li, S.A., et al., 2018. Dietary myo-inositol deficiency decreased intestinal immune function related to NF-kappaB and TOR signaling in the intestine of young grass carp (Ctenopharyngodon idella). Fish Shellfish Immunol 76: 333-346. 10.1016/j.fsi.2018.03.017

Liu, G., et al., 2017. L-Glutamine and L-arginine protect against enterotoxigenic Escherichia coli infection via intestinal innate immunity in mice. Amino Acids 49: 1945-1954. 10.1007/s00726-017-2410-9

McIntosh, K., et al., 2017. FODMAPs alter symptoms and the metabolome of patients with IBS: a randomised controlled trial. Gut 66: 1241-1251. 10.1136/gutjnl-2015-311339

Nealon, N.J., Worcester, C.R. and Ryan, E.P., 2017. Lactobacillus paracasei metabolism of rice bran reveals metabolome associated with Salmonella Typhimurium growth reduction. J Appl Microbiol 122: 1639-1656. 10.1111/jam.13459

North, J.A., et al., 2017. Microbial pathway for anaerobic 5'-methylthioadenosine metabolism coupled to ethylene formation. Proc Natl Acad Sci U S A 114: E10455-e10464. 10.1073/pnas.1711625114

Oka, Y., T. Ogawa, and K. Sasaoka, First evidence for the occurrence of N delta-acetyl-L-ornithine and quantification of the free amino acids in the cultivated mushroom, Pleurotus ostreatus. J Nutr Sci Vitaminol (Tokyo), 1984. 30(1): p. 27-35.

Pessione, E. (2012), Lactic acid bacteria contribution to gut microbiota complexity: lights and shadows. Front Cell Infect Microbiol 2, 86.

Pessione, E. and Cirrincione, S., 2016, Bioactive Molecules Released in Food by Lactic Acid Bacteria: Encrypted Peptides and Biogenic Amines. 7. 10.3389/fmicb.2016.00876

Phoem, A.N., Chanthachum, S. and Voravuthikunchai, S.P., 2015. Applications of microencapsulated Bifidobacterium longum with Eleutherine americana in fresh milk tofu and pineapple juice. Nutrients 7: 2469-2484. 10.3390/nu7042469

Radenkovs, V., et al., 2018. Valorization of Wild Apple (Malus spp.) By-Products as a Source of Essential Fatty Acids, Tocopherols and Phytosterols with Antimicrobial Activity. Plants (Basel) 7. 10.3390/plants7040090

Sheflin, A.M., et al., 2017. Dietary supplementation with rice bran or navy bean alters gut bacterial metabolism in colorectal cancer survivors. Mol Nutr Food Res 61. 10.1002/mnfr.201500905

Sheflin, A.M., et al., 2015. Pilot dietary intervention with heat-stabilized rice bran modulates stool microbiota and metabolites in healthy adults. Nutrients 7: 1282-1300. 10.3390/nu7021282

Si, X., et al., 2018. Gamma-aminobutyric Acid Enriched Rice Bran Diet Attenuates Insulin Resistance and Balances Energy Expenditure via Modification of Gut Microbiota and Short-Chain Fatty Acids. J Agric Food Chem 66: 881-890. 10.1021/acs.jafc.7b04994

So, W.K.W., et al., 2016. Current Hypothesis for the Relationship between Dietary Rice Bran Intake, the Intestinal Microbiota and Colorectal Cancer Prevention. Nutrients 8: 569. 10.3390/nu8090569

Sohail, M., et al., 2017. Rice bran nutraceutics: A comprehensive review. Crit Rev Food Sci Nutr 57: 3771-3780. 10.1080/10408398.2016.1164120

Tovar, J., et al., 2017. Reduction in cardiometabolic risk factors by a multifunctional diet is mediated via several branches of metabolism as evidenced by nontargeted metabolite profiling approach. Mol Nutr Food Res 61. 10.1002/mnfr.201600552

Tremblay, S., et al., 2017. Bile Acid Administration Elicits an Intestinal Antimicrobial Program and Reduces the Bacterial Burden in Two Mouse Models of Enteric Infection. Infect Immun 85. 10.1128/iai.00942-16

Tuncil, Y.E., et al., 2018. Fecal Microbiota Responses to Bran Particles Are Specific to Cereal Type and In Vitro Digestion Methods That Mimic Upper Gastrointestinal Tract Passage. J Agric Food Chem 66: 12580-12593. 10.1021/acs.jafc.8b03469

Vandeputte, D., et al., 2017. Prebiotic inulin-type fructans induce specific changes in the human gut microbiota. Gut 66: 1968-1974. 10.1136/gutjnl-2016-313271

Watson, J.A., Fang, M. and Lowenstein, J.M., 1969. Tricarballylate and hydroxycitrate: Substrate and inhibitor of ATP: Citrate oxaloacetate lyase. Archives of Biochemistry and Biophysics 135: 209-217. https://doi.org/10.1016/0003-9861(69)90532-3

Wolffram, S., Badertscher, M. and Scharrer, E., 1994. Carrier-mediated transport is involved in mucosal succinate uptake by rat large intestine. Exp Physiol 79: 215-226.

Yang, X., 2015. Study of Infection, Immunity, Vaccine and Therapeutics Using Gnotobiotic Pig Models for Human Enteric Viruses, Virginia Polytechnic Institute and State University, Blacksburg, Virginia, 231 pp.

Yang, X., et al., 2015. High protective efficacy of rice bran against human rotavirus diarrhea via enhancing probiotic growth, gut barrier function, and innate immunity. Sci Rep 5: 15004. 10.1038/srep15004

Zarei, I., et al., 2017. Rice Bran Metabolome Contains Amino Acids, Vitamins & Cofactors, and Phytochemicals with Medicinal and Nutritional Properties. Rice (N Y) 10: 24. 10.1186/s12284-017-0157-2

Zheng, H., et al., 2015. Metabolomics investigation to shed light on cheese as a possible piece in the French paradox puzzle. J Agric Food Chem 63: 2830-2839. 10.1021/jf505878a

Zhou, Y., et al., 2012. Intracellular ATP Levels Are a Pivotal Determinant of Chemoresistance in Colon Cancer Cells. Cancer Research 72: 304. 10.1158/0008-5472.CAN-11-1674

CHAPTER SIX

RICE BRAN AND PROBIOTICS ALTER THE PORCINE LARGE INTESTINE AND SERUM METABOLOMES FOR PROTECTION AGAINST HUMAN ROTAVIRUS DIARRHEA[3]

6.1. Summary:

Human rotavirus **(HRV)** is a leading cause of severe childhood diarrhea, and there is limited vaccine efficacy in the developing world. Neonatal gnotobiotic pigs consuming a prophylactic synbiotic combination of probiotics and rice bran **(Pro+RB)** did not exhibit HRV diarrhea after challenge. Multiple immune, gut barrier protective and anti-diarrheal mechanisms contributed to the prophylactic efficacy of Pro+RB when compared to probiotics **(Pro)** alone. In order to understand the molecular signature associated with diarrheal protection by Pro+RB, a global non-targeted metabolomics approach was applied to investigate the large intestinal contents **(LIC)** and serum of neonatal gnotobiotic pigs. The ultra-high-performance liquid chromatography-tandem mass spectrometry platform revealed significantly-different metabolites (293 in LIC and 84 in serum) in the pigs fed Pro+RB compared to Pro, and many of these metabolites were lipids and amino acid/peptides. Lipid metabolites included 2-oleoylglycerol, (increased 293.40-fold in LIC of Pro+RB, p = 3.04E-10), which can modulate gastric emptying, and hyodeoxycholate (decreased 0.054-fold in the LIC of Pro+RB, p = 0.0040) that can increase colonic mucus production to improve intestinal barrier function. Amino acid metabolites

---

[3] **Nealon, N.J.**, Yuan, L., Yang, X., and Ryan, E.P. *Rice Bran and Probiotics Alter the Porcine Large Intestine and Serum Metabolomes for Protection against Human Rotavirus Diarrhea*. Frontiers in Microbiology. 8(653):eCollection. April 2017.

included cysteine, (decreased 0.40-fold in LIC, p = 0.033, and 0.62-fold in serum, p = 0.014 of Pro+RB), which has been found to reduce inflammation, lower oxidative stress and modulate mucosal immunity, and histamine (decreased 0.18-fold in LIC, p = 0.00030, of Pro+RB and 1.57-fold in serum, p = 0.043), which modulates local and systemic inflammatory responses as well as influences the enteric nervous system. Alterations to entire LIC and serum metabolic pathways further contributed to the anti-diarrheal and antiviral activities of Pro+RB such as sphingolipid, mono/diacylglycerol, fatty acid, secondary bile acid, and polyamine metabolism. Sphingolipid and long chain fatty acid profiles influenced the ability of HRV to both infect and replicate within cells, suggesting that Pro+RB created a protective lipid profile that interferes with HRV activity. Polyamines act on enterocyte calcium sensing receptors to modulate intracellular calcium levels and may directly interfere with rotavirus replication. These results support that multiple host and probiotic metabolic networks, notably those involving lipid and amino acid/peptide metabolism, are important mechanisms through which Pro+RB protected against HRV diarrhea in neonatal gnotobiotic pigs.

6.2. Introduction:

Globally, human rotavirus **(HRV)** is the most common cause of severe diarrhea in children under 5, and annually it is responsible for approximately 450,000 deaths worldwide (Clarke and Desselberger, 2015). Live attenuated vaccines, including RV5 and Rotarix, have greatly reduced overall mortality and gastroenteritis in many international vaccine programs, yet they have a markedly lower efficacy in developing countries where most HRV outbreaks still occur (Yen *et al.*, 2014). Underlying pathological processes in the host intestinal tract may contribute to this reduced HRV vaccine efficacy and include environmental enteric dysfunction, where abnormal

intestinal barrier and mucosal immune functions result primarily or secondarily from dysbiosis of the microbiome (Keusch *et al.*, 2016). The combination of limited vaccine efficacy and compromised gut function warrants the need for more effective preventive strategies against HRV, especially in developing countries.

Probiotic bacteria, including *Lactobacillus rhamnosus* GG **(LGG)** and *Escherichia coli Nissle* 1917 **(EcN)**, represent a safe, alternative therapeutic that can reduce the severity of HRV diarrhea. In humans and animals, probiotics modulate mucosal immunity, reduced HRV binding and infection, and produced antimicrobial peptides with antiviral activity against HRV (Chenoll *et al.*, 2016; Olaya Galan *et al.*, 2016; Vlasova *et al.*, 2016; Wang *et al.*, 2016). In gnotobiotic pigs, LGG demonstrated a strong adjuvant effect when supplemented with an oral attenuated HRV vaccine and increased mucosal populations of HRV-specific IFN-gamma producing T lymphocytes (Wen *et al.*, 2015). Collectively, these results support that probiotics can function as an effective component of a prophylactic HRV treatment.

The ability of probiotics to combat HRV can be enhanced when they are combined into a synbiotic with appropriate prebiotics, which are exclusive nutrient sources for probiotic bacteria that cannot be digested by the host. Rice bran **(RB)**, the outer covering of the rice grain, represents an affordable, sustainable, and globally-produced source of prebiotics. Prior research demonstrated that gnotobiotic neonatal pigs fed a prophylactic synbiotic combination of LGG/EcN and RB **(Pro+RB)** did not experience diarrhea after oral challenge with a high dose of live, virulent HRV, whereas pigs consuming LGG/EcN alone **(Pro)** or RB showed only reductions in diarrhea (Yang *et al.*, 2015). In piglets consuming Pro+RB, diarrhea elimination was associated with normal tissue histology and healthy levels of serum gut permeability markers throughout the HRV challenge (Yang *et al.*, 2015). Additional studies with this pig

model have demonstrated the ability of Pro+RB to substantially reduce human norovirus-associated diarrhea, while stimulating more potent adaptive immune responses against viral antigens and preserving colonic tissue architecture during infection (Lei *et al.*, 2016). These findings suggested that the synbiotic combination of a probiotic and a prebiotic functioned through multiple immune, gut barrier protective and anti-diarrheal mechanisms to enhance protection against HRV diarrhea. The increased efficacy may arise in part through RB modulations of probiotic metabolism (Henderson *et al.*, 2012a).

Metabolomics, the systematic study of metabolites, metabolic pathways and their interconnected networks, can be utilized to evaluate how RB alters probiotic function to prevent diarrhea. The objective of this study was to compare the large intestinal content and serum metabolome of pigs consuming a prophylactic combination of Pro+RB to those consuming probiotics alone. This metabolic fingerprint shows how alterations to metabolic networks and pathways function to protect the host against HRV diarrhea. The hypothesis is that the large intestinal content **(LIC)** and serum metabolome of neonatal gnotobiotic pigs consuming Pro+RB contains pathways and networks of metabolites associated with enhanced anti-diarrheal and gut mucosal immune-modulatory activities.

6.3. Materials and methods:

6.3.1. Experimental design and sample collection:

Neonatal piglets (Large White crossbred) were reared in gnotobiotic isolators and maintained on experimental treatments as described previously by Yang *et al*. 2015. Briefly, piglets were started on a diet of ultra-pasteurized bovine milk, and from postnatal day **(PND)** 3 through 40, the animals were separated into dietary treatments. Piglets in Pro group were

inoculated with a sub-therapeutic dosage of 1 X 10^4 LGG/EcN on PND 3, 5 and 7 to ensure adequate colonization of the intestinal tract. Animals in the Pro+ RB treatment group were also fed heat-stabilized Calrose RB daily at 10% of their caloric intake. On PND 40, piglets were euthanized and LIC and serum samples were collected from each animal. The experimental design, including a time course for sample collection, is included as **Figure 6.1**. All animal care and use procedures were approved by the Institutional Animal Care and Use Committee at Virginia Polytechnic Institute and State University and all ample collection and experimental procedures were conducted with accordance to the approved guidelines.

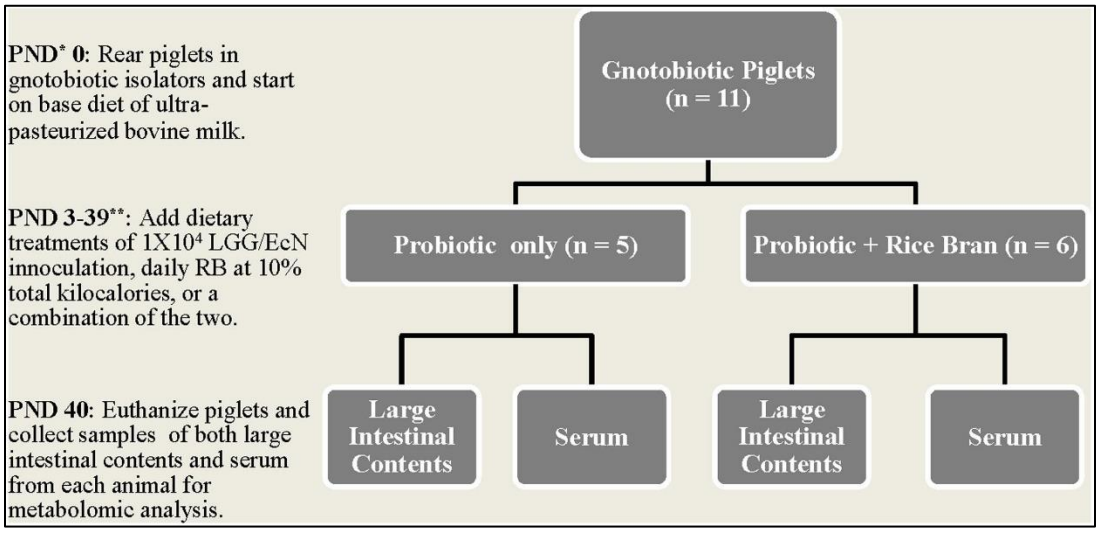

Figure 6.1. Experimental design and sample collection:
** **PND** indicates postnatal day; ** **LGG/EcN** refers to a 1:1 cocktail of Lactobacillus rhamnosus GG/ Escherichia coli Nissle, which was provided to the appropriate treatment groups on post-natal days 3, 5, and 7. **RB** refers to Calrose rice bran.*

6.3.2. Metabolome sample preparation:

To evaluate differences between Pro+RB and Pro treatments, a metabolomic analysis was performed by Metabolon Inc © (Durham, NC). Briefly, 0.5 mL of LIC or serum were collected in triplicate from each animal, stored at -80° C in microcentrifuge tubes, and were shipped to Metabolon on dry ice. Samples were stored at -80°C until processing. Prior to metabolite

detection, a methanol solution was added to each sample to extract proteins and improve the recovery of small molecules. Samples were vigorously shaken for two minutes and then centrifuged. The resulting extracts were split into five parts for analysis via ultra-high performance liquid chromatography-tandem mass spectrometry **(UPLC-MS/MS)**: two replicates for reverse phase UPLC-MS/MS using positive ion mode electrospray ionization, a third replicate for reverse phase UPLC-MS/MS with negative ion mode electrospray ionization, a fourth replicate for high performance liquid chromatography- tandem mass spectrometry **(HPLC-MS/MS)**MS/MS negative ion mode electrospray ionization, and a fifth replicate saved as a back-up. To remove any remaining organic solvent from the fractionation, extracts were placed on a TurboVap © (Zymark) and were then stored in liquid nitrogen prior to analysis.

6.3.3. UPLC-MS/MS analysis:

Metabolite detection was accomplished using a Waters ACQUITY UPLC, a Thermo Scientific Q-exactive heated electrospray ionization source, and an Orbitrap mass analyzer operated at a 35,000-mass resolution. Each extract was dried and reconstituted in solvents appropriate for each detection method. Internal standards were added for quality control purposes. Acidic positive ion mode replicates were optimized for detection of either hydrophobic or hydrophilic compounds by gradient eluting in a mobile phase of water, methanol and 0.05% perfluoropentanoic acid and 0.1% formic acid (hydrophilic compounds), or methanol, acetonitrile, water, 0.05% perfluoropentanoic acid and 0.01% formic acid. All acidic positive ion mode replicates were ran on a C18 column (Waters UPLC BEH C100 18-2.1x mm, 1.7 µm). One basic ion extract was eluted using an identical, separate C18 column with methanol, water, and 6.5 mM of Ammonium Bicarbonate at pH 8. The fourth extract was eluted using a high-

performance liquid chromatography column (Waters UPLC BEH Amide 2.1x150 mm, 1.7 µm) with water, acetonitrile and 10 mM ammonium formate at pH 10.8. Mass spectrometry was performed using MS and data-dependent MSn scans using dynamic exclusion, and the total scan range covered 70-10,000 m/z.

6.3.4. Data extraction and compound identification:

Raw data was extracted, peak-identified and quality-controlled as described previously (Brown *et al.*, 2016). Briefly, compound identifications were compared to an internal library of over 3300 purified standards or recurrent unknown entities and were matched to library entities based on a narrow retention time/index, a mass to charge ratio within 10 parts per million of the standard, and chromatographic data including MS/MS forward and reverse scores between the experimental data and authentic standards. The raw counts of each sample were quantified using area under the curve and converted into relative abundances which were median-scaled to one. For each metabolite, fold difference was calculated by dividing the scaled relative abundance of Pro+RB by Pro.

6.3.5. Metabolic pathway analysis:

Identified metabolites were organized into metabolic pathways based on their biochemical and physiological properties. Pathway enrichment scores were calculated by dividing the number of significant metabolites in a pathway **(k)** by the total number of detected metabolites in the pathway **(m)**. This value was then divided by the total number of significant metabolites in the data set **(n)** over the total number of detected metabolites in the complete dataset **(N)**:

$$\frac{k/m}{n/N}$$

Metabolic pathways with enrichment scores greater than one indicated that the pathway contained more metabolites with statistically-significant fold differences compared to all other pathways within the matrix. In this investigation, there were 20 LIC and 16 serum pathways with a score greater than one. An additional layer to score interpretation was applied such that pathways containing only metabolites with established functions related to antidiarrheal activity were selected for significance in results interpretations and further network analysis.

For both LIC and serum lipid metabolites, pathway enrichment scores were calculated for the following pathways: steroid, lysolipid and lysoplasmalogen, acyl choline, glycine and carnitine, phospholipid, dicarboxylate fatty acid, mevalonate, endocannabinoid, primary bile acid, medium chain fatty acid, amide and branched fatty acid, mono/dihydroxy fatty acid, sterols, polyunsaturated (n3 and n6) fatty acid, long chain fatty acid, secondary bile acid, mono/diacylglycerol, sphingolipid, ketone and glycerolipid. For LIC and serum amino acids/peptides, pathway enrichment scores were calculated for the following pathways: leucine isoleucine and valine, tryptophan, dipeptide and dipeptide derivative, phenylalanine and tyrosine, glycine, serine and threonine, urea, arginine and proline, lysine, glutamate, methionine, cysteine, taurine and S-adenosyl methionine, glutathione, polyamine, histidine, creatine, alanine and aspartate, gamma-glutamyl amino acid, and guanidino and acetamido. Pathway enrichment scores were visualized using GraphPad Prism 6.07 (San Diego, CA).

6.3.6. Metabolic network analysis:

Pathways containing metabolites with established functions related to antidiarrheal activity were selected for visualization using Cytoscape 2.8.3 © software as previously described (Brown *et al.*, 2016). Visualization of Pro+RB versus Pro included all metabolites from selected lipid and

amino acid/peptide pathways in either the LIC or serum matrix. Node diameter was determined by the magnitude of the fold difference between Pro+RB and Pro, and node color was determined by the direction of fold difference when comparing Pro+RB and Pro. Pathway enrichment scores are presented as a number on each pathway node. The LIC lipid pathways visualized in Cytoscape were: phospholipid, sphingolipid, mono/diacylglycerol, polyunsaturated (n3 and n6) fatty acid, endocannabinoid, sterol, long chain fatty acid, mevalonate, medium chain fatty acid, dihydroxy fatty acid, primary bile acid, and secondary bile acid. A visual of the serum lipid pathways included: mono/dihydroxy fatty acid, monoacylglyercol, endocannabinoid, phospholipid, and dicarboxylate fatty acid. A visual of the LIC amino acid/peptide pathways included: glutamate, histidine, urea, arginine and proline, tryptophan, polyamine, alanine and aspartate, methionine, cysteine, S-adenosyl methionine and taurine, carnitine, dipeptide/derivatives, and gamma glutamyl amino acid. A visual of the serum amino acid/peptide pathways included: guanidino and acetamido, creatine, histidine, glutamate, urea, arginine and proline, and methionine, cysteine, taurine and S-adenosyl methionine.

6.3.7. Statistical analysis:

Statistical analysis was performed by Metabolon Inc © using ArrayStudio (Omnicsoft, Cary, NC). Briefly, the raw abundance of each metabolite from each sample of Pro or Pro+RB was median-scaled into a relative abundance. In both the LIC and serum, the contrast of Pro+RB versus Pro was selected for analysis from a larger, multi-treatment data set where at two-way analysis of variance (Ly and Casanova) was applied across all treatments (data not shown). Specifically, scaled metabolite abundance values were compared between Pro+RB and Pro using a Welch's two-sample t test. Statistical significance was determined at the level of $p<0.05$. Due

to the multiple comparisons inherent to the 2-way ANOVA analysis, a false discovery rate (q) was calculated for each metabolite.

6.4. Results:

6.4.1. Non-targeted, global metabolomics revealed differences between Pro+RB and Pro treatments.

Across Pro+RB and Pro treatments, 625 total metabolites were detected in the LIC and 532 metabolites were detected in the serum **(Table 6.1)**. Seven hundred forty-six unique metabolites were detected across both matrices, where 415 were shared between LIC and serum, 214 were exclusive to the LIC, and 117 were exclusive to the serum. Of the 625 LIC metabolites, 170 were classified as amino acids, 31 peptides, 30 carbohydrates, 10 tricarboxylic acid cycle, 238 lipids, 39 Nucleotides, 32 cofactors and vitamins, 54 phytochemicals/other. Of the 532 serum metabolites, 153 were classified as amino acids, 22 peptides, 21 carbohydrates, 9 tricarboxylic acid cycle, 229 lipids, 39 nucleotides, 25 cofactors and vitamins, and 32 phytochemicals.

Table 6.1. Metabolite profiles of large intestinal contents and serum metabolomes for pigs consuming probiotics in the presence and absence of rice bran

Metabolite Classification	Number of Identified Metabolites across Pro + RB and Pro (**p<0.05**)	
	Large Intestinal Contents	**Serum**
Amino Acids	170* **(↑7, ↓78)****	153 **(↑14, ↓15)**
Peptides	31 **(↑2, ↓14)**	23 **(↑0, ↓1)**
Carbohydrates	32 **(↑2, ↓11)**	21 **(↑0, ↓1)**
Energy Metabolism	10 **(↑0, ↓3)**	9 **(0)**
Lipids	257 **(↑47, ↓ 58)**	229 **(↑15, ↓17)**
Nucleotides	39 **(↑1, ↓14)**	39 **(↑6, ↓1)**
Cofactors and Vitamins	32 **(↑4, ↓16)**	25 **(↑8, ↓0)**
Phytochemical/Other	54 **(↑15, ↓21)**	32 **(↑3, ↓3)**
Total Number of Identified Metabolites	625 **(293)**	531 **(84)**

* Indicates the total number of metabolites detected in a given metabolite class.
** Values in parentheses indicate the number of significantly-different (p<0.05) metabolites that increased (↑) or decreased (↓) when comparing the fold difference of its scaled relative abundance in Pro+RB by Pro.

There were 293 LIC metabolites and 84 serum metabolites with statistically-significant (p<0.05) fold differences when comparing Pro+RB to Pro **(Table 6.1)**. In the LIC, 78 metabolites had a significantly higher scaled relative abundance in Pro+RB compared to Pro and included: 7 amino acids, 2 peptides, 2 carbohydrates, 47 lipids, 1 nucleotide, 4 cofactors/ vitamins, and 15 phytochemical/other. 215 LIC metabolites had a significantly lower scaled relative abundance in Pro+RB compared to Pro and included: 78 amino acids, 14 peptides, 11 carbohydrates, 3 tricarboxylic acid cycle, 58 lipids, 14 nucleotides, 16 cofactors/vitamins, and 21 phytochemical/other.

In the serum, 45 metabolites had a significantly higher scaled relative abundance in Pro+RB compared to Pro and included: 14 amino acids, 15 lipids, 6 nucleotides, 8 cofactors/vitamins, and 3 phytochemical/other. 38 metabolites had a significantly lower scaled

relative abundance in Pro+RB compared to Pro and included: 15 amino acids, 1 peptide, 1 carbohydrate, 17 lipids 1 Nucleotide, and 1 cofactor/vitamin.

6.4.2. Lipid metabolite profiles were differentially-expressed between Pro+RB and Pro treatment groups and were associated with anti-diarrheal activity.

Across both the LIC and serum, lipids represented ~41% and ~43% of the identified metabolites respectively, and thus were examined more closely for their prospective antidiarrheal-related properties. **Table 6.2** lists the significant ($p<0.05$) lipids with the fold difference and p-values provided across both LIC and serum matrices, and **Table 6.3** presents a comprehensive literature search into the antidiarrheal functions the lipids with statistically-significant fold differences between Pro+RB and Pro. Analysis revealed 26 metabolites that possessed immunomodulatory, gut barrier protective and antiviral functions related to anti-diarrheal activity. In the LIC, these lipids included long chain fatty acid (12 significant metabolites), polyunsaturated fatty acid (8 significant metabolites), phospholipid (5 significant metabolites) mono/diacylglycerol (14 significant metabolites), endocannabinoid (3 significant metabolites), sterol (4 significant metabolites), mevalonate (1 significant metabolite), primary bile acid (5 significant metabolites), secondary bile acid (7 significant metabolites), dihydroxy fatty acid (2 significant metabolites), medium chain fatty acid (3 significant metabolites) and sphingolipids (16 significant metabolites). In the serum, these lipids included mono/dihydroxy fatty acid (5 significant metabolites), endocannabinoid (1 significant metabolite), phospholipid (8 significant metabolites), and dicarboxylate fatty acid (5 significant metabolites).

Table 6.2. Large intestinal content and serum lipids in pigs consuming probiotics in the presence and absence of rice bran.

Metabolite*	HMDB**	Large Intestinal Contents		Serum	
		Fold Difference***	p-value	Fold Difference	p-value
1-linoleoylglycerol (18:2)	-	320.72 ↑	1.04E-08	-	
2-oleoylglycerol (18:1)	-	293.40 ↑	3.04E-10	-	
2-linoleoylglycerol (18:2)	11538	187.09 ↑	9.27E-10	-	
1-oleoyl-3-linoleoyl-glycerol (18:1/18:2)	-	177.20 ↑	2.26E-08	-	
9,10-dihydroxyoctadecenoic acid (DiHOME)	04704	111.38 ↑	1.90E-07	9.63 ↑	0.00016
1-oleoylglycerol (18:1)	11567	93.63 ↑	3.37E-07	-	
glycocholenate sulfate	-	71.16 ↑	0.011	-	
1-linolenoylglycerol (18:3)	11569	45.81 ↑	9.59E-07	-	
taurochenodeoxycholate	00951	16.34 ↑	0.012	-	
beta-sitosterol	00852	15.59 ↑	4.72E-11	-	
glycolithocholate sulfate	02639	12.09 ↑	0.0088	-	
1-palmitoyl-3-linoleoyl-glycerol (16:0/18:2)	-	10.51 ↑	0.00013	-	
1-oleoyl-2-linoleoyl-glycerol (18:1/18:2)	-	9.37 ↑	0.00021	1.79 ↑	0.033
1-palmitoylglycerol (16:0)	31074	9.33 ↑	0.00014	-	
glycohyodeoxycholate	-	9.27 ↑	0.046	-	
sphingomyelin (d18:1/21:0, d17:1/22:0, d16:1/23:0)	-	8.89 ↑	0.0010	-	
behenoyl sphingomyelin (d18:1/22:0)	-	7.98 ↑	0.0012	-	
1-palmitoyl glycerophosphatidic acid (16:0)	00327	7.27 ↑	0.011	-	
2-palmitoylglycerol (16:0)	11533	7.08 ↑	6.33E-05	-	
1-palmitoleoylglycerol (16:1)	-	6.70 ↑	0.00015	-	
palmitoyl dihydrosphingomyelin (d18:0/16:0)	-	6.48 ↑	0.0028	-	
sphingomyelin (d18:1/14:0, d16:1/16:0)	-	6.33 ↑	0.0010	-	
1,2-dioleoyl-glycerophosphocholine (18:1/18:1)	-	5.88 ↑	0.0035	0.65 ↓	0.014
sphingomyelin (d18:1/15:0, d16:1/17:0)	-	5.75 ↑	0.0021	-	
1-palmitoyl-2-linoleoyl-glycerol (16:0/18:2)	05207, 07103	5.71 ↑	0.0031	-	
stearoyl sphingomyelin (d18:1/18:0)	01348	5.61 ↑	0.0074	-	
palmitoyl sphingomyelin (d18:1/16:0)	-	5.42 ↑	0.017	-	
12,13-dihydroxyoctadecenoic acid (DiHOME)	04705	5.26 ↑	0.0012	15.03 ↑	0.00031
heptanedioate (pimelate)	00857	5.17 ↑	0.00033	1.58 ↑	0.010
malonate	00691	4.81 ↑	1.26E-06	-	
linoleoyl ethanolamide	12252	4.42 ↑	0.0014	-	
glycerol	00131	4.32 ↑	0.00088	-	
nonanedioate (azelate)	00784	4.23 ↑	0.0015	1.73 ↑	0.023
stearoylcarnitine	00848	4.13 ↑	0.044	-	
13 + 9 Hydroxyoctadecadienoic acid (13+9 HODE)	-	3.93 ↑	0.010	-	
sphingomyelin (d18:1/17:0, d17:1/18:0, d19:1/16:0)	-	3.88 ↑	0.0059	-	
1-palmitoyl-2-linoleoyl-glycerophosphocholine (16:0/18:2)	-	3.66 ↑	0.039	-	
16-hydroxypalmitate	06294	3.45 ↑	0.00037	-	
choline phosphate	01565	3.43 ↑	0.0027	1.61 ↑	0.046
campesterol	02869	3.17 ↑	0.00047	10.69 ↑	1.58E-06
2-palmitoleoylglycerol (16:1)	-	3.00 ↑	0.015	-	
1-palmitoyl-2-oleoyl-glycerophosphoglycerol (16:0/18:1)	-	2.47 ↑	0.0023	-	

Table 6.2. Large intestinal content and serum lipids in pigs consuming probiotics in the presence and absence of rice bran.

Metabolite*	HMDB**	Large Intestinal Contents		Serum	
		Fold Difference***	p-value	Fold Difference	p-value
mevalonate	00227	2.44 ↑	0.013	-	
1-pentadecanoylglycerol (15:0)	-	2.34 ↑	0.0074	-	
1-oleoyl-2-linoleoyl-glycerophosphocholine (18:1/18:2)	-	1.84 ↑	0.033	-	
sphingomyelin (d18:1/24:1, d18:2/24:0)	-	1.77 ↑	0.0079	-	
sphingomyelin (d18:1/20:0, d16:1/22:0)	-	1.65 ↑	0.032	-	
stearate (18:0)	00827	0.65 ↓	0.015	-	
phytosphingosine	04610	0.63 ↓	0.034	-	
palmitate (16:0)	00220	0.59 ↓	0.0087	-	
N-palmitoyl-sphingosine (d18:1/16:0)	04949	0.59 ↓	0.025	-	
3-hydroxylaurate	00387	0.58 ↓	0.014	0.60 ↓	0.046
oleate (vaccenate) (18:1)	-	0.56 ↓	0.030	-	
sphingosine	00252	0.53 ↓	0.029	-	
nonadecanoate (19:0)	00772	0.52 ↓	0.022	-	
sphinganine	00269	0.52 ↓	0.034	-	
N-palmitoyl-sphinganine (d18:0/16:0)	11760	0.50 ↓	0.0070	-	
palmitoleoylcarnitine	-	0.50 ↓	0.042	-	
eicosenoate (20:1)	02231	0.47 ↓	0.024	-	
2-hydroxystearate	-	0.44 ↓	0.00034	-	
margarate (17:0)	02259	0.41 ↓	0.0062	-	
17-methylstearate	-	0.40 ↓	0.0038	-	
cholesterol	00067	0.36 ↓	0.00052	-	
docosapentaenoate (22:5n6)	01976	0.34 ↓	0.032	-	
lactosyl-N-palmitoyl-sphingosine	-	0.33 ↓	0.041	-	
2-methylmalonyl carnitine	13133	0.29 ↓	0.0012	1.52 ↑	0.034
malonylcarnitine	02095	0.28 ↓	$1.23E^{-06}$	-	
2-hydroxypalmitate	31057	0.27 ↓	$3.07E^{-05}$	-	
pentadecanoate (15:0)	00826	0.26 ↓	0.00066	-	
docosapentaenoate (22:5n3)	01976	0.26 ↓	0.0048	-	
5-dodecenoate (12:1n7)	00529	0.26 ↓	0.00045	-	
eicosapentaenoate (20:5n3)	01999	0.26 ↓	0.041	0.63 ↓	0.010
myristoleate (14:1n5)	02000	0.25 ↓	0.0018	-	
15-methylpalmitate	-	0.24 ↓	0.00014	-	
tetradecanoic acid (myristate, 14:0)	00806	0.24 ↓	0.00082	-	
caprate (10:0)	00511	0.24 ↓	0.0012	-	
N-palmitoylglycine	-	0.23 ↓	0.00017	-	
suberylglycine	00953	0.23 ↓	0.0013	-	
3-hydroxybutyrate	00357	0.23 ↓	0.026	-	
palmitoleate (16:1n7)	03229	0.22 ↓	0.00026	-	
dihomo-linoleate (20:2n6)	05060	0.22 ↓	0.00028	-	
dihomo-linolenate (20:3n3 or n6)	02925	0.22 ↓	0.00047	-	
N-palmitoyltaurine	-	0.21 ↓	0.0020	-	
propionylcarnitine	00824	0.20 ↓	0.00015	-	
pristanate	00795	0.20 ↓	0.0027	-	
7-hydroxycholesterol (alpha or beta)	-	0.20 ↓	0.00010	-	
3b-hydroxy-5-cholenoic acid	00308	0.19 ↓	$3.69E^{-05}$	-	
laurate (12:0)	00638	0.18 ↓	$8.17E^{-05}$	-	
docosadienoate (22:2n6)	61714	0.16 ↓	$6.88E^{-06}$	-	
3-hydroxymyristate	-	0.16 ↓	$7.73E^{-06}$	-	

Table 6.2. Large intestinal content and serum lipids in pigs consuming probiotics in the presence and absence of rice bran.

Metabolite*	HMDB**	Large Intestinal Contents		Serum	
		Fold Difference***	p-value	Fold Difference	p-value
7-ketolithocholate	00467	0.16 ↓	0.0083	-	
erucate (22:1n9)	02068	0.16 ↓	$4.83E^{-05}$	0.66 ↓	0.037
hyocholate	00760	0.15 ↓	0.030	-	
adrenate (22:4n6)	02226	0.15 ↓	$1.60E^{-05}$	-	
5,8,11-eicosatrienoic acid (mead acid; 20:3n9)	10378	0.15 ↓	0.00017	0.57 ↓	0.031
beta-muricholate	00415	0.13 ↓	0.049	-	
nervonate (24:1n9)	02368	0.12 ↓	$4.76E^{-06}$	-	
cholate sulfate	-	0.12 ↓	$5.26E^{-05}$	-	
13-methylmyristate	-	0.11 ↓	0.00010	-	
5alpha-androstan-3alpha,17beta-diol disulfate	-	0.11 ↓	0.014	-	
N-oleoyltaurine	-	0.084 ↓	0.022	-	
cholate	00619	0.061 ↓	0.028	-	
chenodeoxycholate	00518	0.054 ↓	0.0078	-	
hyodeoxycholate	00733	0.054 ↓	0.0040	-	
caprylate (8:0)	00482	-		1.33 ↑	0.029
suberate (octanedioate)	00893	-		1.72 ↑	0.018
2-hydroxyglutarate	00606	-		0.64 ↓	0.0087
3-methyladipate	00555	-		0.44 ↓	0.00086
2-aminoheptanoate	-	-		2.81 ↑	0.013
2-aminooctanoate	00991	-		0.45 ↓	0.016
butyrylcarnitine	02013	-		0.73 ↓	0.041
3-hydroxybutyrylcarnitine (2)	-	-		0.66 ↓	0.036
alpha-hydroxycaproate	01624	-		0.73 ↓	0.039
2-hydroxyoctanoate	02264	-		0.61 ↓	0.039
palmitoyl ethanolamide	02100	-		0.60 ↓	0.035
1-palmitoyl-2-linoleoyl-glycerophosphoinositol (16:0/18:2)	-	-		1.54 ↑	0.012
1-stearoyl-2-linoleoyl-glycerophosphoinositol (18:0/18:2)	-	-		1.33 ↑	0.019
1-palmitoyl-2-stearoyl-glycerophosphocholine (16:0/18:0)	-	-		1.33 ↑	0.017
1-stearoyl-2-oleoyl-glycerophosphocholine (18:0/18:1)	-	-		0.73 ↓	0.045
1-palmitoyl-2-palmitoleoyl-glycerophosphocholine (16:0/16:1)	-	-		0.71 ↓	0.028
1-palmitoyl-2-linolenoyl-glycerophosphocholine (16:0/18:3)	-	-		0.59 ↓	0.015
1-(1-enyl-stearoyl)-2-linoleoyl-glycerophosphoethanolamine (P-18:0/18:2)	-	-		1.55 ↑	0.021
glycochenodeoxycholate	00637	-		0.48 ↓	0.021

* Table displays lipid metabolites with a statistically-significant fold difference between Pro+RB and Pro in both LIC and serum matrices.

** HMDB refers to the Human Metabolome Database, and access numbers are provided for each metabolite identified in the database.

*** For each metabolite, fold difference was calculated by dividing the scaled relative abundance of Pro+RB by Pro, where ↑ indicates that the metabolite had a higher scaled relative abundance in Pro+RB compared to Pro, and ↓ indicates the metabolite had a lower scaled relative abundance in Pro+RB compared to Pro.

Table 6.3. Large intestinal content and serum lipids with immunomodulatory, gut barrier protective and antiviral functions related to anti-diarrheal activity.

Metabolite*	Large Intestinal Contents		Serum		Functions	References
	Fold Difference**	p-value	Fold Difference	p-value		
1-linoleoylglycerol (18:2)	320.72 ↑	$1.04E^{-08}$	-	-	Has been demonstrated to systemically reduce inflammation in porcine models.	(Han *et al.*, 2015)
2-oleoylglycerol	293.40 ↑	$3.04E^{-10}$	-	-	Influences gastric emptying via modulation of cholecystokinin release.	(Mandoe *et al.*, 2015)
2-linoleoyl glycerol (18:2)	187.09 ↑	$9.27E^{-10}$	-	-	Serves as an important precursor of 2-arachidonyl glycerol that goes on to modulate inflammation through direct binding to endocannabinoid receptors, or via its catabolism into ligands of cyclooxygenases, cytochrome P450 enzymes, and lipoxygenase enzymes.	(Mechoulam *et al.*, 1995; Turcotte *et al.*, 2015)
beta-sitosterol	15.59 ↑	$4.72E^{-11}$	-	-	As part of an herbal extract, it acted on gut muscarinic and histamatergic receptors to reduce gut motility associated with diarrhea.	(Mehmood *et al.*, 2014)
2-palmitoyl-glycerol	7.08 ↑	$6.33E^{-05}$	-	-	Produced by mammalian and bacterial cells and influences cannabinoid-1 receptor expression in peripheral organs, including the gut, and thereby influences intestinal motility.	(Aviello *et al.*, 2008; Murataeva *et al.*, 2016; Yuan *et al.*, 2016)
palmitoyl sphingomyelin (d18:1/16:0)	5.42 ↑	0.017	-	-	Influences the composition of the intestinal microbiome and colon mucosal cell shedding.	(Sinha *et al.*, 2016)
12,13-dihydroxyoctadecenoic acid (DiHOME)	5.26 ↑	0.0012	-	-	Influences the composition of the neonatal intestinal microbiome and modulates T-regulatory cell development.	(Fujimura *et al.*, 2016)

Table 6.3. Large intestinal content and serum lipids with immunomodulatory, gut barrier protective and antiviral functions related to anti-diarrheal activity.

Metabolite*	Large Intestinal Contents		Serum		Functions	References
	Fold Difference**	p-value	Fold Difference	p-value		
heptanedioate (pimelate)	5.17 ↑	0.00033	1.58 ↑	0.010	Acts to increase butyrate and biotin metabolism in the gut lumen, and thus indirectly influences colonic T-regulatory cell populations.	(Sugahara *et al.*, 2015)
malonate	4.81 ↑	$1.26E^{-06}$	-	-	As part of a fruit extract, exhibited anti-diarrheal properties in humans.	(Pandey *et al.*, 2016)
linoleoyl ethanolamide	4.42 ↑	0.0014	-	-	Present in plants and has demonstrated anti-inflammatory effects in vitro and in vivo by suppressing interleukin 1B, 6, tumor necrosis factor alpha, cyclooxygenase enzyme-2, and toll-like receptor 4, and nuclear factor kB expression in macrophages.	(Ishida *et al.*, 2013)
nonanedioate (azelate)	4.23 ↑	0.0015	1.73 ↑	0.023	Associated with decreased pro-inflammatory interleukin-6 expression in the serum of human adults.	(Lustgarten and Fielding, 2016)
13 + 9 hydroxy-octadecadienoic acid (13 + 9 HODE)	3.93 ↑	0.010	-	-	In humans, 13 and 9-HODE are released by peripheral blood populations of neutrophils, eosinophils, basophils, monocytes and lymphocytes to modulate inflammatory and immune processes. 9-HODE has demonstrated anti-inflammatory properties by scavenging free radicals.	(Collino *et al.*, 2013; Engels *et al.*, 1996)

Table 6.3. Large intestinal content and serum lipids with immunomodulatory, gut barrier protective and antiviral functions related to anti-diarrheal activity.

Metabolite*	Large Intestinal Contents		Serum		Functions	References
	Fold Difference**	p-value	Fold Difference	p-value		
choline phosphate	3.43 ↑	0.0027	1.61 ↑	0.046	Provides structural integrity to cell membranes, including the mucosal lining of the intestinal tract.	(Liu *et al.*, 2014)
mevalonate	2.44 ↑	0.013	-	-	Modulates innate immune responses by influencing interleukin 1-B production	(Akula *et al.*, 2016)
stearate (18:0)	0.65 ↓	0.015	-	-	As part of a plant oil supplement, it reduced castor-oil induced murine diarrhea.	(Zavala-Mendoza *et al.*, 2013)
palmitate (16:0)	0.59 ↓	0.0087	-	-	As part of a plant oil supplement, it reduced castor-oil induced murine diarrhea.	(Zavala-Mendoza *et al.*, 2013)
oleate (vaccenate) (18:1)	0.56 ↓	0.030	-	-	As part of plant oil supplements, it reduced diarrhea and inflammation in an experimentally-induced rat colitis model and also in a castor-oil induced murine diarrhea model. In humans, it slowed gastrointestinal time and reduced diarrhea by activating nutrient-triggered inhibitory feedback mechanisms in the small intestine responsible for gut motility.	(Lin *et al.*, 2001; Naouar *et al.*, 2016; Zavala-Mendoza *et al.*, 2013)

Table 6.3. Large intestinal content and serum lipids with immunomodulatory, gut barrier protective and antiviral functions related to anti-diarrheal activity.

Metabolite*	Large Intestinal Contents		Serum		Functions	References
	Fold Difference**	p-value	Fold Difference	p-value		
sphingosine	0.53 ↓	0.029	-	-	Converted in the gut into the bioactive intermediate sphingosine-1-phosphate that modulates mucosal lymphocyte trafficking, influences mucosal cell proliferation, promotes gut integrity, and increases populations of IgA-producing intraepithelial lymphocytes. Also converted within intestinal epithelial cells to palmitate, which may reduce diarrhea arising from inflammatory processes.	(Nilsson, 2016; Zavala-Mendoza *et al.*, 2013)
cholesterol	0.36 ↓	0.00052	-	-	In a rat induced-colitis model of diarrhea being treated with *Lactobacillus plantarum*, protection against diarrhea was associated with lower colonic lumen levels of cholesterol, and its presence in the intestinal lumen was inversely related to diarrhea in children with rotavirus-induced diarrhea.	(Alp Avci, 2016; Trabelsi *et al.*, 2016)
docosa-pentanaenoate (n3 DPA; 22:5n3)	0.26 ↓	0.0048	-	-	Lower intestinal luminal levels have been correlated with decreased inflammation of the gut mucosa, and this metabolite has been demonstrated to modulate ileal contractility.	(Patten *et al.*, 2002; Pearl *et al.*, 2014)
eicosapentaenoate (EPA; 20:5n3)	0.26 ↓	0.041	-	-	When fed as an oral supplement to mice, eicosapentaenoate enhanced helper T-cell function.	(Wee *et al.*, 1988)

Table 6.3. Large intestinal content and serum lipids with immunomodulatory, gut barrier protective and antiviral functions related to anti-diarrheal activity.

Metabolite*	Large Intestinal Contents		Serum		Functions	References
	Fold Difference**	p-value	Fold Difference	p-value		
caprate (10:0)	0.24 ↓	0.00082	-	-	Concentration in human intestinal lumen is inversely associated with tight junction integrity.	(Soderholm *et al.*, 2002)
palmitoleate (16:1n7)	0.22 ↓	0.00026	-	-	In humans, oral intake was associated with decreased gastric emptying times, and evidence supports microbial generation of this metabolite. In mice given dietary supplementation, it reduced the expression of pro-inflammatory cytokines tumor necrosis factor alpha, interleukin-1B, 6, and 8.	(Frigolet and Gutiérrez-Aguilar, 2017; Schirmer *et al.*, 2016)
chenodeoxycholate	0.054 ↓	0.0078	-	-	Lower levels in the colonic lumen may be associated with decreased motility and longer digests transit time.	(Goyal *et al.*, 2015; Peleman *et al.*, 2016)
hyodeoxycholate	0.054 ↓	0.0040	-	-	Rodent studies suggest that it may act directly on colonic mucosal goblet cells to increase mucus production, thereby modulating barrier function.	(Barcelo *et al.*, 2001)
palmitoyl ethanolamide	-	-	0.60 ↓	0.035	In the gastrointestinal tract, reduces inflammation by inhibiting mast cell degranulation, and modulates the enteric nervous system via inhibiting the degradation of the endocannabinoid anandamide to influence gut motility.	(Cordaro *et al.*, 2016)

Table 6.3. Large intestinal content and serum lipids with immunomodulatory, gut barrier protective and antiviral functions related to anti-diarrheal activity.

Metabolite*	Large Intestinal Contents		Serum		Functions	References
	Fold Difference**	p-value	Fold Difference	p-value		

* Table displays lipid metabolites with a statistically-significant fold difference between Pro+RB and Pro in both LIC and Serum matrices that were determined to have anti-diarrheal properties after a comprehensive peer-reviewed literature search.
** For each metabolite, fold difference was calculated by dividing the scaled relative abundance of Pro+RB by Pro, where ↑ indicates that the metabolite had a higher scaled relative abundance in Pro+RB compared to Pro, and ↓ indicates the metabolite had a lower scaled relative abundance in Pro+RB compared to Pro.

6.4.3. Amino acid and peptide metabolite profiles differ between Pro+RB and Pro treatment groups and are associated with anti-diarrheal activity.

The LIC and serum amino acid/peptide metabolites represented ~27% and ~28% of the total number of identified metabolites respectively, and like lipids, were examined more closely for compounds with potential antidiarrheal activity. **Table 6.4** lists the amino acid/peptide metabolites with statistically-significant ($p<0.05$) fold differences and p-values between Pro+RB and Pro across both LIC and serum matrices. **Table 6.5** presents a comprehensive literature search of the anti-diarrheal functions of amino acids/peptides with statistically-significant fold differences between Pro+RB and Pro. Analysis revealed 22 metabolites that possessed immunomodulatory, gut barrier protective and antiviral functions related to anti-diarrheal activity **(Table 6.5)**. In the LIC these amino acids/peptides included glutamate (6 significantly different metabolites), histidine (10 significantly-different metabolites), urea cycle arginine and proline (10 significantly-different metabolites), tryptophan (5 significantly-different metabolites), polyamine (6 significantly-different metabolites), alanine and aspartate (6 significantly-different metabolites), methionine, cysteine, S-adenosyl methionine, and taurine (11 significantly-different metabolites), dipeptide/derivatives (6 significantly-different metabolites), gamma-glutamyl amino acid (10 significantly-different metabolites), and carnitine (2

significantly-different metabolites). In the serum, these amino acid/peptide metabolites included urea cycle, arginine and proline (5 significantly-different metabolites), phenylalanine and tyrosine (2 significantly-different metabolites), methionine, cysteine, S-adenosyl methionine and taurine (4 significantly-different metabolites), histidine (6 significantly-different metabolites), and glutamate (3 significantly-different metabolites).

Table 6.4. Large intestinal content and serum amino acids/peptides in pigs consuming probiotics in the presence and absence of rice bran.

Metabolite*	HMDB*	Large Intestinal Contents		Serum	
		Fold Difference***	p-value	Fold Difference	p-value
4-hydroxycinnamate	02035	14.75 ↑	$1.75E^{-05}$	-	
urea	00294	12.83 ↑	0.0011	-	
indoleacetate	00197	8.89 ↑	0.00028	-	
vanillylmandelate	00291	5.26 ↑	$2.21E^{-09}$	-	
glycylisoleucine	28844	4.08 ↑	0.012	-	
5-methylthioadenosine	01173	3.38 ↑	0.0022	-	
gentisate	00152	2.99 ↑	0.0025	-	
4-guanidinobutanoate	03464	2.73 ↑	0.0013	1.64 ↑	0.017
threonylphenylalanine	-	2.17 ↑	0.0039	-	
carnitine	00062	0.68 ↓	0.034	-	
imidazole lactate	02320	0.63 ↓	0.025	-	
saccharopine	00279	0.58 ↓	$3.23E^{-05}$	-	
S-1-pyrroline-5-carboxylate	01301	0.57 ↓	0.026	-	
N-acetylserine	02931	0.57 ↓	0.026	-	
guanidinoacetate	00128	0.56 ↓	0.011	0.64 ↓	0.009
pipecolate	00070	0.54 ↓	0.016	-	
N6,N6,N6-trimethyllysine	01325	0.49 ↓	0.0045	-	
3-sulfo-L-alanine	02757	0.48 ↓	0.011	-	
histidine	00177	0.48 ↓	0.012	-	
valine	00883	0.48 ↓	0.036	-	
creatine	00064	0.47 ↓	0.0078	-	
gamma-aminobutyrate	00112	0.46 ↓	0.023	-	
cysteine sulfinic acid	00996	0.45 ↓	0.015	-	
dimethylarginine (Symmetrical and Asymmetrical)	01539	0.44 ↓	0.0012	-	
homoarginine	00670	0.43 ↓	0.049	-	
methionine sulfoxide	02005	0.42 ↓	0.0085	-	
argininosuccinate	00052	0.42 ↓	0.0017	-	
4-hydroxyglutamate	01344	0.42 ↓	0.049	-	
cystathionine	00099	0.41 ↓	0.0019	-	
homocitrulline	00679	0.41 ↓	0.016	-	
homocysteine	00742	0.41 ↓	0.029	-	
kynurenate	00715	0.40 ↓	0.0015	-	
cysteine	00574	0.40 ↓	0.033	0.62 ↓	0.014
alanine	00161	0.40 ↓	0.026	-	
1-methylhistamine	00898	0.40 ↓	0.044	1.40 ↑	0.010
aspartate	00191	0.38 ↓	0.0029	-	
trans-urocanate	00301	0.38 ↓	0.0022	-	

Table 6.4. Large intestinal content and serum amino acids/peptides in pigs consuming probiotics in the presence and absence of rice bran.

Metabolite*	HMDB*	Large Intestinal Contents		Serum	
		Fold Difference***	p-value	Fold Difference	p-value
2-aminobutyrate	00650	0.38 ↓	0.031	-	
N-acetylcarnosine	12881	0.37 ↓	$3.92E^{-06}$	-	
ornithine	03374	0.37 ↓	0.040	0.71 ↓	0.047
glutamate	00148	0.36 ↓	$2.38E^{-05}$	-	
N-acetylputrescine	02064	0.36 ↓	0.00028	-	
anserine	00194	0.36 ↓	$2.04E^{-06}$	-	
N-acetylhistidine	32055	0.36 ↓	0.046	1.64 ↑	0.0025
N-acetylthreonine	-	0.35 ↓	0.017	-	
citrulline	00904	0.35 ↓	0.047	0.83 ↓	0.048
5-oxoproline	00267	0.34 ↓	0.0018	-	
N-acetylhistamine	13253	0.34 ↓	0.014	1.66 ↑	0.024
N6-carboxyethyllysine	-	0.33 ↓	0.0010	-	
ophthalmate	05765	0.33 ↓	0.0026	-	
proline	00162	0.31 ↓	0.0069	-	
gamma-glutamylleucine	11171	0.31 ↓	0.025	-	
5-hydroxylysine	00450	0.30 ↓	0.0017	0.76 ↓	0.011
putrescine	01414	0.30 ↓	$9.20E^{-08}$	-	
N-acetylalanine	00766	0.30 ↓	0.023	-	
cadaverine	02322	0.29 ↓	$8.58E^{-06}$	-	
N-acetylasparagine	06028	0.28 ↓	0.0040	-	
3-hydroxyanthranilate	01476	0.28 ↓	0.016	-	
3-methylhistidine	00479	0.26 ↓	$2.70E^{-05}$	-	
carnosine	00033	0.26 ↓	0.00043	-	
N-acetyltaurine	-	0.26 ↓	0.00051	-	
guanidinosuccinate	03157	0.25 ↓	0.00027	-	
N-acetyl-cadaverine	-	0.24 ↓	$9.36E^{-05}$	-	
N1,N12-diacetylspermine	02172	0.24 ↓	0.00012	-	
1-methylguanidine	01522	0.24 ↓	0.00084	0.53 ↓	0.034
lysine	00182	0.23 ↓	0.00071	-	
taurine	00251	0.21 ↓	0.00034	-	
gamma-glutamylhistidine	-	0.21 ↓	0.0023	-	
glycine	00123	0.20 ↓	0.0021	-	
N-acetylglutamate	01138	0.20 ↓	0.0030	-	
N-methylhydantoin	03646	0.20 ↓	0.0039	-	
C-glycosyltryptophan	-	0.19 ↓	$3.52E^{-06}$	-	
histamine	00870	0.18 ↓	0.00030	1.57 ↑	0.043
N-acetylmethionine sulfoxide	-	0.18 ↓	0.038	-	
proline-hydroxy-proline	06695	0.18 ↓	0.032	1.38 ↑	0.00014
N-formylmethionine	01015	0.17 ↓	0.010	-	
formiminoglutamate	-	0.16 ↓	0.00061	-	
N-acetylcitrulline	00856	0.16 ↓	0.0027	-	
N-acetylmethionine	11745	0.16 ↓	0.027	-	
N6-acetyllysine	00206	0.15 ↓	0.00014	-	
gamma-glutamylvaline	11172	0.15 ↓	0.0011	-	
N-acetylleucine	11756	0.15 ↓	0.036	-	
gamma-glutamylisoleucine	11170	0.14 ↓	0.00086	-	
N-acetylkynurenine	-	0.14 ↓	$2.57E^{-05}$	2.01 ↑	0.021
homogentisate	00130	0.14 ↓	0.0011	-	
N-formylphenylalanine	-	0.14 ↓	0.016	-	
N-acetylvaline	11757	0.13 ↓	0.0010	-	

Table 6.4. Large intestinal content and serum amino acids/peptides in pigs consuming probiotics in the presence and absence of rice bran.

Metabolite*	HMDB*	Large Intestinal Contents		Serum	
		Fold Difference***	p-value	Fold Difference	p-value
gamma-glutamyltyrosine	11741	0.13 ↓	0.0028	-	
N-acetylaspartate	00812	0.11 ↓	$7.12E^{-05}$	0.76 ↓	0.025
N-acetylphenylalanine	00512	0.075 ↓	0.0031	-	
pyroglutamine	-	0.074 ↓	0.0077	0.43 ↓	0.021
N2-acetyllysine	00446	0.07 ↓	0.0068	-	
gamma-glutamylglutamate	11737	0.063 ↓	$1.62E^{-05}$	-	
gamma-glutamylalanine	29142	0.063 ↓	$8.15E^{-05}$	-	
gamma-glutamyl-epsilon-lysine	03869	0.061 ↓	$2.18E^{-05}$	-	
gamma-glutamylglycine	11667	0.058 ↓	$3.85E^{-05}$	-	
imidazole propionate	02271	0.058 ↓	0.038	-	
prolylglycine	-	0.057 ↓	0.0015	0.44 ↓	0.014
gamma-glutamylmethionine	29155	0.045 ↓	0.00019	-	
spermidine	01257	0.038 ↓	$1.64E^{-10}$	-	
N(1)-acetylspermine	01186	0.038 ↓	1.03E-09	-	
N-acetyltyrosine	00866	0.034 ↓	0.00028	-	
phenyllactate	00779	-		2.08 ↑	0.0031
1-methylimidazoleacetate	02820	-		1.57 ↑	0.0020
S-methylcysteine	02108	-		1.48 ↑	0.013
4-acetamidobutanoate	03681	-		1.34 ↑	0.018
dimethylglycine	00092	-		1.34 ↑	0.038
cystine	00192	-		1.30 ↑	0.044
trans-4-hydroxyproline	00725	-		1.14 ↑	0.046
creatinine	00562	-		0.89 ↓	0.035
thyroxine	01918	-		0.73 ↓	0.023
glutamine	00641	-		0.70 ↓	0.017
N-acetylglutamine	06029	-		0.71 ↓	0.031
hypotaurine	00965	-		0.65 ↓	0.028
N-delta-acetylornithine	-	-		0.52 ↓	0.014

* Table displays amino acid metabolites with a statistically-significant fold difference between Pro+RB and Pro in both LIC and serum matrices.

** HMDB refers to the Human Metabolome Database, and access numbers are provided for each metabolite identified in the database.

*** For each metabolite, fold difference was calculated by dividing the scaled relative abundance of Pro+RB by Pro, where ↑ indicates that the metabolite had a higher scaled relative abundance in Pro+RB compared to Pro, and ↓ indicates the metabolite had a lower scaled relative abundance in Pro+RB compared to Pro.

Table 6.5. Large intestinal content and serum amino acids/peptides with immunomodulatory, gut barrier protective and antiviral functions related to anti-diarrheal activity.

Amino Acid/ Peptide*	Large Intestinal Contents		Serum		Functions	References
	Fold Difference**	p-value	Fold Difference	p-value		
histidine	0.49 ↓	0.012	-	-	As part of a rice-based oral rehydration solution, functioned as an anti-secretory agent to reduce Cholera-associated diarrhea in adult males.	Rabanni *et al.*, 2005
gamma-amino-butyrate	0.46 ↓	0.024	-	-	In the mammalian enteric nervous system, GABA-ergic signaling is important in modulating intestinal fluid balance, gut motility and inflammation.	Li *et al.*, 2012; Auteri *et al.*, 2015
cysteine	0.41 ↓	0.033	0.63 ↓	0.014	Reduced oxidative stress, decreased inflammation, lowered permeability and modulated the mucosal immune system in the intestinal tract of neonatal pigs.	Bauchart-Thevret *et al.*, 2009; Ruth and Field, 2013
homocysteine	0.41 ↓	0.029	-	-	Potentiated the activity of S-adenosyl hydrolase antiviral drugs against vaccinia and vesicular stomatitis viruses.	Hasobe *et al.*, 1989
alanine	0.40 ↓	0.026	-	-	When supplemented into an oral rehydration salt in adult males, reduced diarrhea associated with Cholera and ETEC *E. coli*.	Patra *et al.*, 1989
glutamate	0.37 ↓	2.39 E^{-05}	-	-	Supplementation prevented diarrhea in rats challenged with a diarrhea-inducing intra-gastric tube diet, and reduced diarrhea in neonatal pigs at 1-week post-weaning.	(Rezaei *et al.*, 2013; Somekawa *et al.*, 2012)
ornithine	0.37 ↓	0.041	0.71 ↓	0.047	In calves supplemented with lysine, increased fecal shedding of ornithine was associated with increased diarrhea, and modulations to ornithine metabolism are	(Abe *et al.*, 2001; Mounce *et al.*, 2016)

Table 6.5. Large intestinal content and serum amino acids/peptides with immunomodulatory, gut barrier protective and antiviral functions related to anti-diarrheal activity.

Amino Acid/ Peptide*	Large Intestinal Contents		Serum		Functions	References
	Fold Difference**	p-value	Fold Difference	p-value		
					associated with decreased in-vitro and in-vivo replication of multiple RNA viruses.	
citrulline	0.36 ↓	0.047	0.84 ↓	0.048	Serum levels are an indicator of functional enterocytes mass and citrulline has been used as a biomarker for assessing mucosal barrier dysfunction.	(Kong *et al.*, 2015; Wang *et al.*, 2015a)
proline	0.31 ↓	0.0069	-	-	Prophylactic dietary supplementation in mice infected with porcine circovirus-2 was associated with enhanced innate and adaptive immune responses, reduced microscopic lesion scores, and lower viral loads.	(Ren *et al.*, 2013)
3-methyl-histidine	0.27 ↓	$2.70E^{-05}$	-	-	Used as a marker of tissue protein breakdown, where lower levels were indirectly indicative of improved tissue integrity.	(Nielsch *et al.*, 1991)
carnosine	0.27 ↓	0.0004	-	-	In humans, decreased diarrhea due to irritable bowel syndrome.	(Baraniuk *et al.*, 2013)
taurine	0.21 ↓	0.0003	-	-	In mice experimentally induced with colitis, supplementation attenuated the severity of the diarrhea, improved histopathology scores, and inhibited TNF-α and IL-8 production.	(Shimizu *et al.*, 2009, Zhao et al. 2009)
histamine	0.19 ↓	0.0003	-	-	A key modulator of intestinal mucosal immune homeostasis in states of health and inflammation.	(Smolinska *et al.*, 2014)

Table 6.5. Large intestinal content and serum amino acids/peptides with immunomodulatory, gut barrier protective and antiviral functions related to anti-diarrheal activity.

Amino Acid/ Peptide*	Large Intestinal Contents		Serum		Functions	References
	Fold Difference**	p-value	Fold Difference	p-value		
gamma-glutamyl-valine	0.16 ↓	0.0011	-	-	Functions as a ligand for the intestinal extracellular calcium sensing receptor, where binding leads to reductions in TNF- α. IL-8, IL-6, IL-17 and IL-1B and increases in IL-10 in the colon.	(Zhang *et al.*, 2015)
gamma-glutamyl-epsilon-lysine	0.06 ↓	$2.19E^{-05}$	-	-	Presence is associated with the repair of the colonic mucosa during inflammatory ulcerative processes.	(D'Argenio *et al.*, 2005)
spermidine	0.04 ↓	$1.03E^{-09}$	-	-	Influences the development of the intestinal tract postnatally, influences enterocyte protein and nuclei acid metabolism, and may modulate mucosal immunity.	(Plaza-Zamora *et al.*, 2013; Timmons *et al.*, 2012)
cystine	-	-	1.30 ↑	0.044	In humans and rodents, serves as an excitatory neurotransmitter in the brainstem where it functions downstream to delay gastric emptying and suppresses food intake and also functions as a gut extracellular antioxidant that can improve the viability of probiotic species.	(Khan *et al.*, 2014; McGavigan *et al.*, 2015)
trans-4-hydroxy-proline	-	-	1.15 ↑	0.046	In neonatal pigs, may be a multi-systemic indicator of tissue collagen remodeling and growth.	(Brundige *et al.*, 2010)
thyroxine	-	-	0.74 ↓	0.023	Influences gastric acid secretion and modulate nutrient absorption across the small intestine, including decreasing glucose uptake into enterocytes. Modulates the	(Jourdan *et al.*, 1998; Matty and Seshadri, 1965; Yeh

Table 6.5. Large intestinal content and serum amino acids/peptides with immunomodulatory, gut barrier protective and antiviral functions related to anti-diarrheal activity.

Amino Acid/ Peptide*	Large Intestinal Contents		Serum		Functions	References
	Fold Difference**	p-value	Fold Difference	p-value		
					sucrose-isomaltase brush border activity in the small intestine, which may interfere with rotavirus pathogenicity.	*et al.*, 1989)
butyryl-carnitine	-	-	0.73 ↓	0.041	*In vitro* studies support that it may reduce inflammation by promoting normal fatty acid oxidation, deregulation of which is associated with colonic inflammation.	(Srinivas *et al.*, 2007)
glutamine	-	-	0.71 ↓	0.017	When provided as a dietary supplement to rats, reduced secretory diarrhea due to cholera toxin, and in humans and animals, supplementation reduces intestinal damage and improves mucosal immunity.	(Gutiérrez *et al.*, 2007; Swami *et al.*, 2013)
hypotaurine	-	-	0.66 ↓	0.028	Functions as an osmoprotectant to reduce hyperosmotic stress and the associated inflammation.	(Brocker *et al.*, 2012)

* Table displays lipid metabolites with a statistically-significant fold difference between Pro+RB and Pro in both LIC and Serum matrices that were determined to have anti-diarrheal properties after a comprehensive peer-reviewed literature search.
** For each metabolite, fold difference was calculated by dividing the scaled relative abundance of Pro+RB by Pro, where ↑ indicates that the metabolite had a higher scaled relative abundance in Pro+RB compared to Pro, and ↓ indicates the metabolite had a lower scaled relative abundance in Pro+RB compared to Pro.

6.4.4. Metabolic pathways in the large intestinal contents and serum containing anti-diarrheal metabolites were associated with high pathway enrichment scores.

To examine how individual metabolic pathways contributed to Pro+RB versus Pro differences in protection from HRV diarrhea in pigs, pathway enrichment scores were calculated

for each individual lipid **(Figure 6.2A)** and amino acid/peptide **(Figure 6.2B)** pathway in the LIC and serum as described in the methods. In general, many of these pathways exhibited a high pathway enrichment score (>1.00), supporting that these pathways are major contributors to treatment differences between Pro+RB and Pro. Lipid pathways in the LIC that contained antidiarrheal metabolites included: phospholipid (score 0.41), sphingolipid (score 1.90), mono/diacylglycerol (score 1.20), polyunsaturated fatty acid (score 1.43), endocannabinoid (score 0.92), sterol (score 1.51), long chain fatty acid (score 1.84), mevalonate (score 0.75), medium chain fatty acid (score 1.07), mono/dihydroxy fatty acid (score 1.20), primary bile acid (score 0.97), and secondary bile acid (score 1.84). In the serum, lipid metabolic pathways containing antidiarrheal metabolites included mono/dihydroxy fatty acid (score 2.11), endocannabinoid (score 3.16), phospholipid (score 1.49), dicarboxylate fatty acid (score 2.43). For lipids, metabolic pathways that contained antidiarrheal metabolites in both the LIC and serum matrices included dicarboxylate fatty acid, endocannabinoid, phospholipid, and mono/dihydroxy fatty acid.

Amino acid/peptide metabolic pathways in the LIC containing anti-diarrheal metabolites included: glutamate (score 1.28), histidine (score 1.43), urea cycle, arginine and proline (score 1.26), tryptophan (score 0.59), polyamine (score 1.43), alanine and aspartate (score 1.61), methionine, cysteine, S-adenosyl methionine and taurine (score 1.31), dipeptide/derivatives (score 0.64), gamma-glutamyl amino acids (score 1.95), and carnitine (score 1.07). In the serum, amino acid/peptide metabolic pathways containing anti-diarrheal metabolites included: urea cycle arginine and proline (score 1.86), phenylalanine and tyrosine (score 0.79), methionine, cysteine, S-adenosyl methionine and taurine (score 1.40), histidine (score 3.80), and glutamate

(score 2,11). For amino acids, metabolic pathways that contained antidiarrheal metabolites included histidine, glutamate, urea, arginine and proline, and methionine **(Figure 6.2B)**.

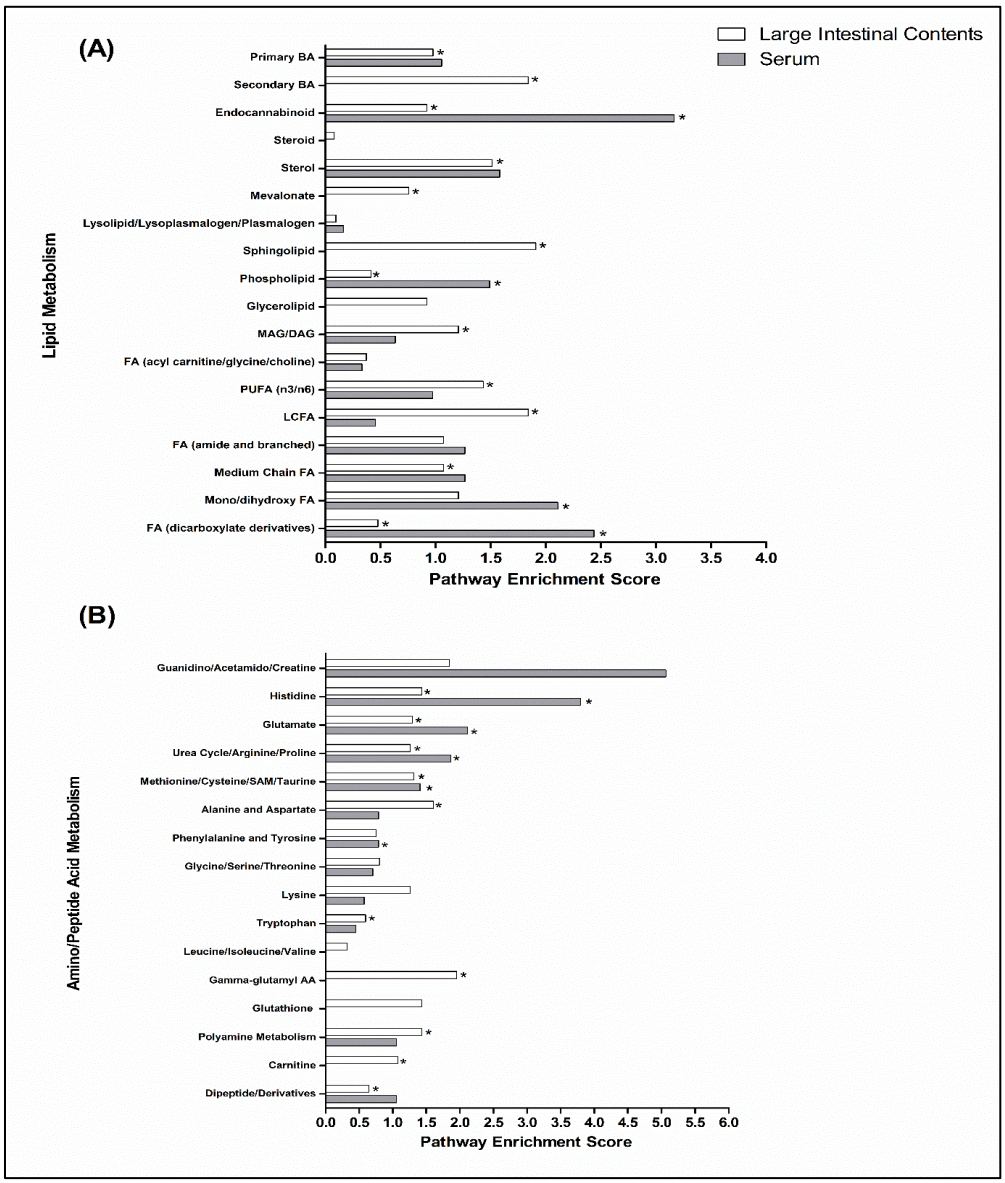

Figure 6.2. Lipid and amino acid/peptide pathway enrichment scores in the large intestinal contents and serum when comparing Probiotic + Rice Bran versus Probiotic.

Pathway enrichment scores of ***(A)*** *lipid pathways and* ***(B)*** *amino acid/peptide pathways are plotted for both large intestinal (white bars) and serum matrices (black bars). * Indicates a pathway containing metabolites identified as having anti-diarrheal activity. In* ***(A)****,* ***FA*** *indicates fatty acid,* ***BA*** *indicates bile acid,* ***MAG/DAG*** *indicates monoacyl/diacylglycerol,* ***PUFA*** *indicates polyunsaturated fatty acid, and* ***LCFA*** *indicates long chain fatty acid. In* ***(B)****,* ***SAM*** *indicates S-adenosyl methionine, and* ***AA*** *indicates amino acid.*

6.4.5. Cytoscape analysis reveals network-wide alterations in lipid and amino acid metabolite profiles associated with antidiarrheal activity.

The Cytoscape visualization tool classified individual metabolites into metabolic networks of their corresponding pathways. Lipid metabolites and pathways containing metabolites with antidiarrheal activity were visualized in the LIC **(Figure 6.3)** and the serum **(Figure 6.4)**. In the LIC, the lipid metabolic network displayed large increases in multiple lipid metabolites from Pro+RB when compared to Pro. Many of these increases corresponded to metabolites from mono/diacylglycerol, and sphingolipid pathways and included the anti-diarrheal associated metabolites 2-palmitoylglycerol (Increased 7.08-fold in Pro+RB, p = 6.33E-05), 1-linoleoyl glycerol (Increased 320.72-fold in Pro+RB, p = 1.04E-08), 2-linoleoylglycerol (Increased 187.08-fold in Pro+RB, p = 9.27E-10), palmitoyl sphingomyelin (d18:1/16:0) (Increased 5.42-fold in Pro+RB, p = 0.017) and sphingosine (Decreased 0.29-fold in Pro+RB, p = 0.029). **(Figure 6.3)**.

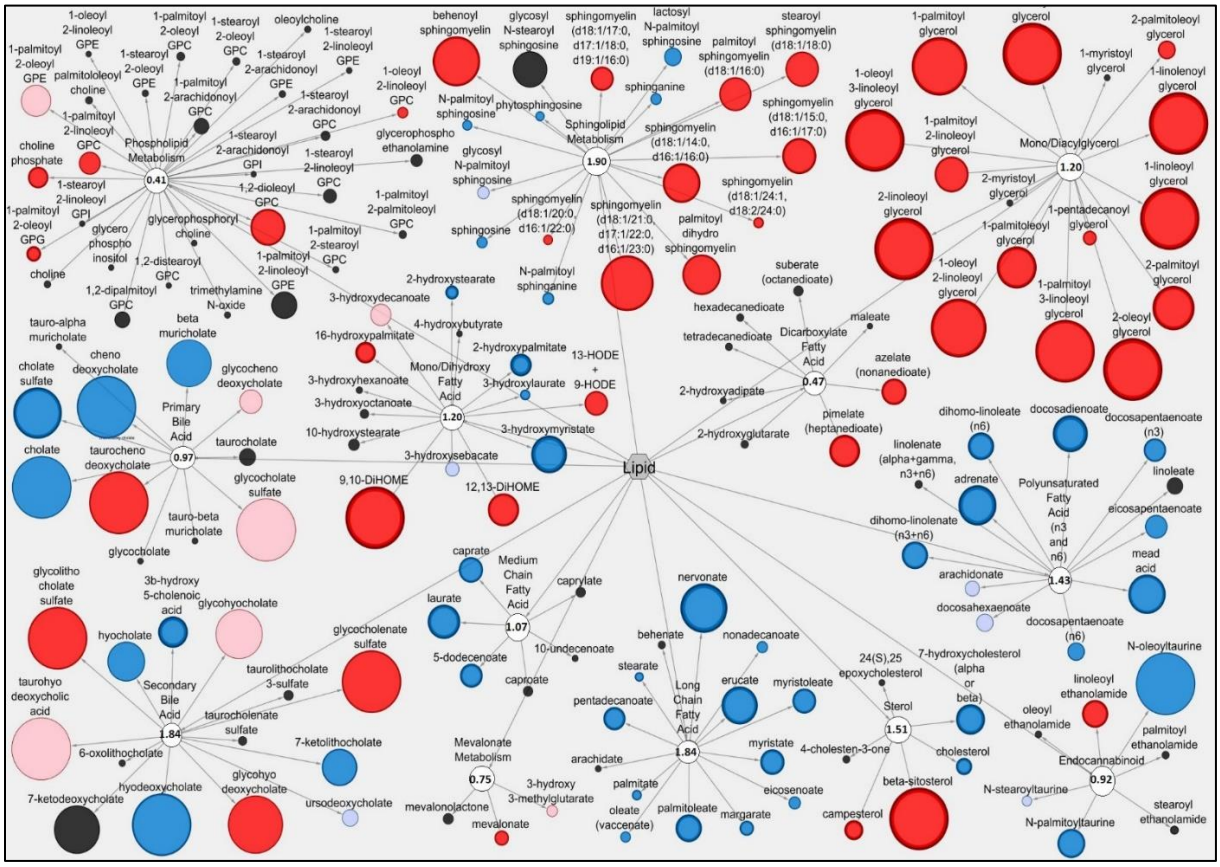

Figure 6.3. Cytoscape network analysis of select lipid pathways in the large intestinal contents when comparing Probiotic + Rice Bran and Probiotic.

Cytoscape visualization of lipid metabolites in LIC metabolic pathways associated with anti-diarrheal activity across Pro+RB and Pro. For each metabolite, node diameter is proportional to the magnitude of the fold difference in Pro+RB compared to Pro. Node color indicates the direction of a metabolite's fold difference: red indicates metabolites with a higher scaled abundance in Pro+RB ($p<0.05$), blue indicates lower abundance in Pro+RB ($p<0.05$), pink indicates trending higher in Pro+RB ($0.05<p<0.10$), and light blue indicates trending lower in Pro+RB ($0.05<p<0.10$). Black nodes indicate metabolites with fold differences that were not significantly altered between treatments. The pathway enrichment score is the number in the circle for each pathway.

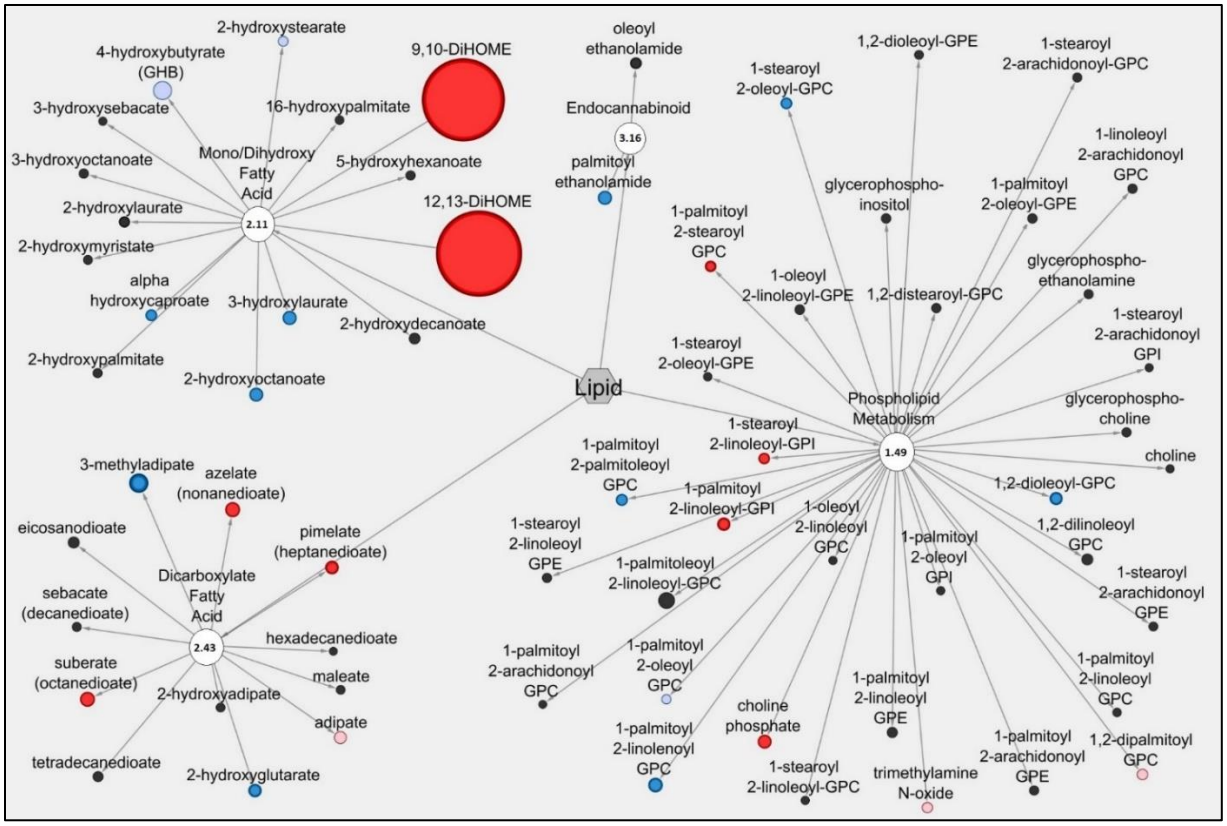

Figure 6.4. Cytoscape network analysis of select lipid pathways in the serum when comparing Probiotic + Rice Bran and Probiotic.

Cytoscape visualization of lipid metabolites in serum metabolic pathways associated with anti-diarrheal activity across Pro+RB and Pro. For each metabolite, node diameter is proportional to the magnitude of the fold difference in Pro+RB compared to Pro. Node color indicates the direction of a metabolite's fold difference: red indicates metabolites with a higher scaled abundance in Pro+RB ($p<0.05$), blue indicates lower abundance in Pro+RB ($p<0.05$), pink indicates trending higher in Pro+RB ($0.05<p<0.10$), and light blue indicates trending lower in Pro+RB ($0.05<p<0.10$). Black nodes indicate metabolites with fold differences that were not significantly altered between treatments. The pathway enrichment score is the number in the circle for each pathway.

There were LIC lipid pathways with large decreases in multiple lipid metabolites from Pro+RB when compared to Pro involving medium chain, long chain, and polyunsaturated fatty acids. Associated anti-diarrheal metabolites included stearate (Decreased 0.65-fold in Pro+RB, $p = 0.015$), palmitate (Decreased 0.59-fold in Pro+RB, $p = 0.0087$), oleate/vaccenate (Decreased 0.56-fold in Pro+RB $p = 0.030$), caprate (Decreased 0.24-fold in Pro+RB, $p = 0.0012$),

docaspentaenoate (22:5n3) (Decreased 0.26-fold in Pro+RB, p = 0.032), eicosapentaenoate (20:5n3) (Decreased 0.26-fold in Pro+RB, p= 0.041), and palmitoleate (16:1n7) (Decreased 0.22-fold in Pro+RB, p = 0.00026) **(Figure 6.3)**. In the serum, the lipid metabolic network displayed both large increases and decreases in lipid metabolites when Pro+RB was compared to Pro. Specifically, mono/dihydroxy and dicarboxylate fatty acid pathways exhibited large increases in the anti-diarrheal metabolites 12,13-dihydroxyoctadecenoic acid (Increased 15.03-fold in Pro+RB, p = 0.00031), pimelate (Increased 1.58-fold in Pro+RB, p = 0.010) and azelate (Increased 1.73-fold in Pro+RB, p = 0.023) in Pro+RB compared to Pro. Phospholipid metabolism resulted in large decreases in 1-palmitoyl-2-palmitoleyol-glycerophosphocholine (Decreased 0.71-fold in Pro+RB, p = 0.028), 1-palmitoyl-2-linoleyol glycerophosphocholine (Decreased 0.59-fold in Pro+RB, p = 0.015), 1-stearoyl-2-oleoyl glycerophosphocholine (Decreased 0.73-fold in Pro+RB, p = 0.045), and 1,2-dioleoyl glycerophosphocholine (Decreased 0.65-fold in Pro+RB, p = 0.014) when comparing Pro+RB and Pro (**Figure 6.4**).

Figures 6.5 and 6.6 display amino acid/peptide LIC and serum metabolic pathways respectively, containing antidiarrheal-associated metabolites. In the LIC, Pro+RB displayed large decreases in multiple metabolites, across numerous pathways, when compared to Pro. These decreases corresponded to metabolites from gamma-glutamyl amino acid, polyamine, alanine and aspartate, histidine, glutamate, and methionine, cysteine, SAM and taurine metabolism and included the anti-diarrheal associated metabolites gamma-glutamyl valine (Decreased 0.15-fold in Pro+RB, p = 0.0011), gamma-glutamyl-epsilon-lysine (Decreased 0.061-fold in Pro+RB, p = 2.18E-05), spermidine (Decreased 0.038-fold in Pro+RB, p = 1.64E-10), alanine (Decreased 0.40-fold in Pro+RB, p = 0.026), histidine (Decreased 0.48-fold in Pro+RB, p = 0.012), histamine (Decreased 0.18-fold in Pro+RB, p = 0.00030), 3-methylhistidine (Decreased 0.26-

fold in Pro+RB, p = 2.70E-05), gamma-aminobutyrate (GABA) (Decreased 0.46-fold in Pro+RB, p = 0.023), glutamate (Decreased 0.36-fold in Pro+RB, p = 2.38E-05), cysteine (Decreased 0.40-fold, p = 0.033), homocysteine (Decreased 0.41-fold in Pro+RB, p = 0.029), and taurine (Decreased 0.21-fold in Pro+RB, p = 0.00034) (**Figure 6.5**). In the serum, amino acid/peptide metabolic network displayed both multiple increases in histidine metabolites of Pro+RB compared to Pro, including the anti-diarrheal associated metabolite histamine (Increased 1.57-fold in Pro+RB, p = 0.043) (**Figure 6.6**).

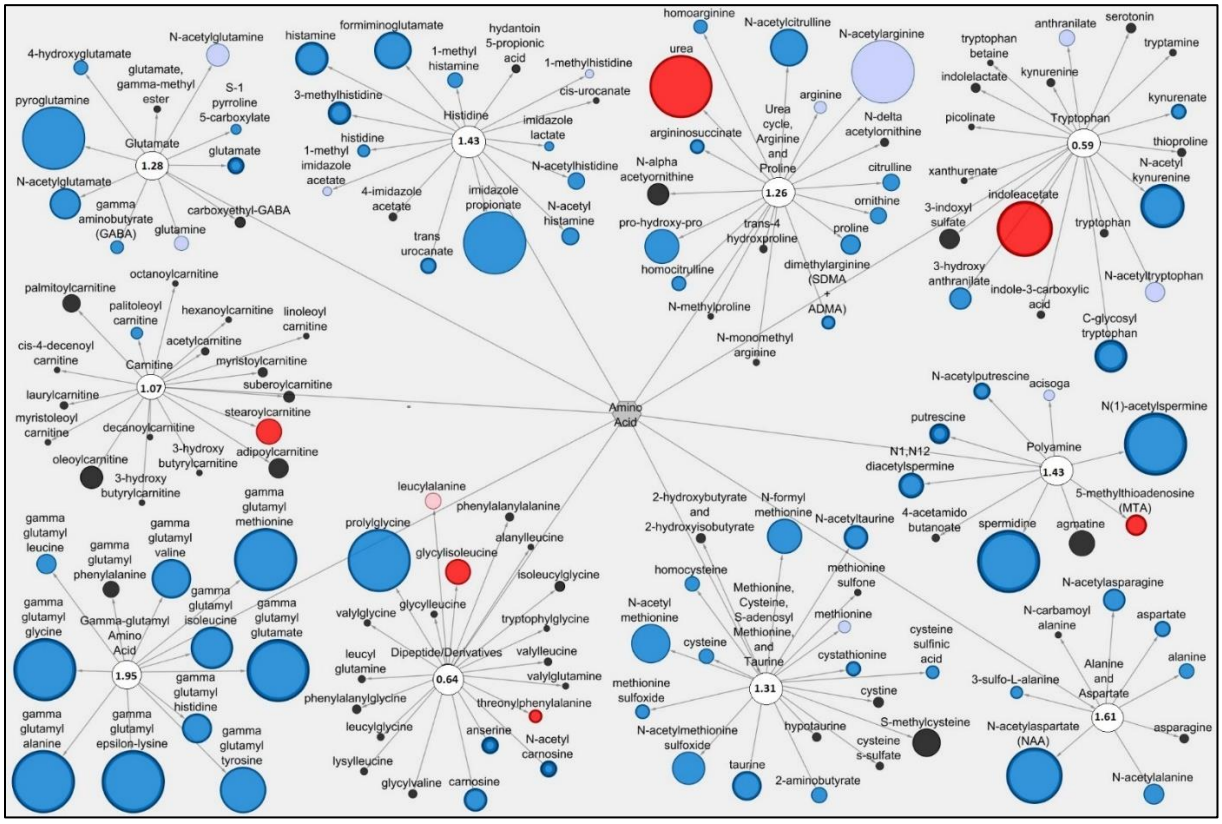

Figure 6.5. Cytoscape network analysis of select amino acid/peptide pathways in the large intestinal contents when comparing Probiotic + Rice Bran and Probiotic.

Cytoscape visualization of amino acid/peptide metabolites in large intestinal contents metabolic pathways associated with anti-diarrheal activity across Pro+RB and Pro. For each metabolite, node diameter is proportional to the magnitude of the fold difference in Pro+RB compared to Pro. Node color indicates the direction of a metabolite's fold difference: red indicates metabolites with a higher scaled abundance in Pro+RB ($p<0.05$), blue indicates lower abundance in Pro+RB ($p<0.05$), pink indicates trending higher in Pro+RB ($0.05<p<0.10$), and light blue indicates trending lower in Pro+RB ($0.05<p<0.10$). Black nodes indicate metabolites

with fold differences that were not significantly altered between treatments. The pathway enrichment score is the number in the circle for each pathway.

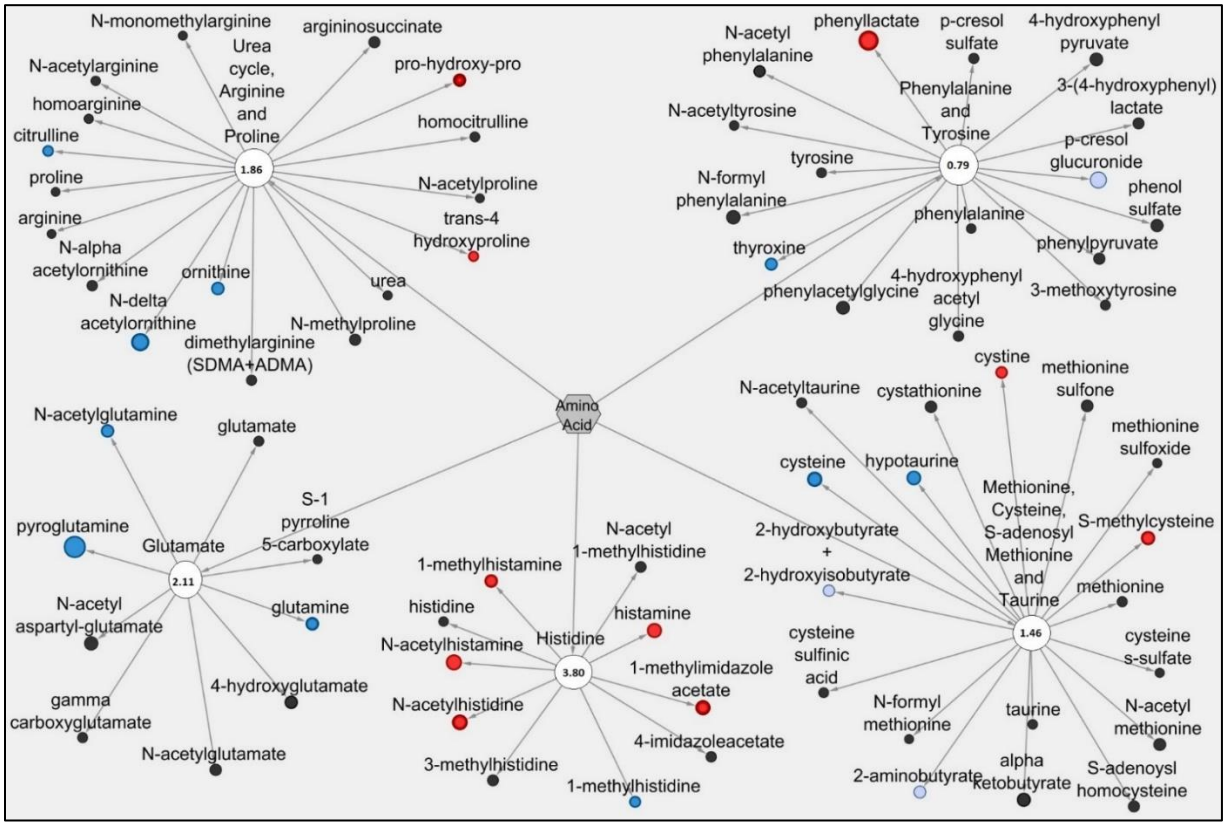

Figure 6.6. Cytoscape network analysis of select amino acid/peptide pathways in the serum when comparing Probiotic + Rice Bran and Probiotic.

Cytoscape visualization of amino acid/peptide metabolites in serum metabolic pathways associated with anti-diarrheal activity across Pro+RB and Pro. For each metabolite, node diameter is proportional to the magnitude of the fold difference in Pro+RB compared to Pro. Node color indicates the direction of a metabolite's fold difference: red indicates metabolites with a higher scaled abundance in Pro+RB ($p<0.05$), blue indicates lower abundance in Pro+RB ($p<0.05$), pink indicates trending higher in Pro+RB ($0.05<p<0.10$), and light blue indicates trending lower in Pro+RB ($0.05<p<0.10$). Black nodes indicate metabolites with fold differences that were not significantly altered between treatments. The pathway enrichment score is the number in the circle for each pathway.

6.5. Discussion and Conclusions:

Non-targeted global metabolomics revealed substantial alterations to both lipid and amino acid/peptide metabolism in the LIC and serum **(Table 6.1)**, and multiple metabolite and

metabolic pathway contributions to prophylactic diarrhea protection **(Figure 6.2, Table 6.3, Table 6.5)**. This manuscript further highlights those compounds associated with protection against HRV diarrhea related to increased production of gut-protective, immunomodulatory and antiviral compounds.

RB-mediated alterations to probiotic lipid metabolism represent one route through which a combination of probiotics and prebiotics create a gut-protective environment against HRV infection. RB provides probiotic bacteria with a source of complex lipids that can be catabolized to release additional lipids into the large intestinal lumen or converted into bacterial lipid products (Buccioni *et al.*, 2012). Alterations to LIC mono/diacylglycerol metabolism (pathway enrichment score 1.20) represent one area of lipid metabolism associated with anti-diarrheal activity (**Figure 2**). Elevations of multiple mono/diacylglycerols in the LIC of Pro+RB included 1-linoleoyl glycerol (increased 320.72-fold in Pro+RB, p = 1.04E-08), 2-linoleoyl glycerol (increased 187.09-fold in Pro+RB, p = 9.27E-10) and 2-palmitoyl glycerol (increased 7.08-fold in Pro+RB, p = 6.33E-05) (supplementary data not shown)**.** 1-linoleoyl glycerol has been demonstrated to systemically reduce inflammation in porcine models (Han *et al.*, 2015). 2-linoleoyl glycerol serves as an important precursor in the formation of 2-arachidonyl glycerol that can broadly modulate inflammation through direct binding to endocannabinoid receptors, or via its catabolism into ligands of cyclooxygenases, cytochrome P450 enzymes, and lipoxygenase enzymes (Mechoulam *et al.*, 1995; Turcotte *et al.*, 2015). Similarly, 2-palmitoylglycerol is produced by mammalian and bacterial cells and influences cannabinoid receptor expression in the gastrointestinal tract (Aviello *et al.*, 2008; Murataeva *et al.*, 2016; Yuan *et al.*, 2016). Collectively, probiotic catabolism of complex RB triacylglycerides may release mono/diacylglycerols into the intestinal lumen and increase their bioavailability in the intestinal

lumen, where they can be utilized in host enterocyte metabolism to exert their anti-diarrhea effects. Reducing inflammation along the gastrointestinal tract may provide the host with improved barrier function (Lei *et al.*, 2016), and modulating cannabinoid receptor function can alter intestinal motility (Taschler *et al.*, 2017) that can help prevent them against HRV-induced diarrhea. Ultimately, these released mono/diacylglycerols could be utilized in host enterocyte metabolism and promote anti-inflammatory and anti-viral activities that protect the host from HRV diarrhea.

In a healthy gut, primary bile acids play key roles in facilitating the digestion and absorption of fats, nutrients and vitamins (Martinot *et al.*, 2017). A major function of probiotic bacteria is the bioconversion of host-derived primary bile acids into bacterially-modified secondary bile acids which function as antimicrobials, regulate host lipid and glucose metabolism, and influence the growth and activity of gut flora (Nie *et al.*, 2015). Analysis of LIC primary and secondary bile acid metabolites in Pro+RB versus Pro revealed antidiarrheal activities of the primary bile acid chenodeoxycholate (decreased 0.054-fold in Pro+RB , $p = 0.0078$), and the secondary bile acid hyodeoxycholate (decreased 0.054-fold in Pro+RB, $p = 0.0040$) (**Tables 6.2, 6.4**). Investigations have suggested that lower luminal levels of chenodeoxycholate are associated with decreased gastric emptying times and reduced expression of the pro-inflammatory cytokines TNF-a, IL-1B, IL-6 and IL-8 (Goyal *et al.*, 2015; Peleman *et al.*, 2016). The decrease in chenodeoxycholate may be associated with metabolism of hyodeoxycholate, a secondary bile acid resulting from bacterial metabolism of chenodeoxycholate (Theriot *et al.*, 2016). In the colonic lumen, rodent studies suggest that hyodeoxycholate acts directly on goblet cells to increase mucus production, thereby modulating barrier function (Barcelo *et al.*, 2001). RB supplementation may have increased probiotic

conversion of chenodeoxycholate into hyodeoxycholate, which provided, that ultimately was taken-up by enterocytes, out of the lumen, and used to mediate anti-inflammatory processes in the cell, and thus improve barrier function that provided protection during challenge with HRV.

Probiotic production of fatty acids, along with bioconversion or release of RB fatty acids, may influence immune and metabolic processes that contribute to diarrheal protection. The dicarboxylic fatty acid pimelate was elevated in 5.17-fold the LIC ($p = 0.00033$) and 1.58-fold the serum ($p = 0.01$) of Pro+RB versus Pro **(Tables 6.2, 6.4)** and is produced by a variety of bacterial species. Past investigations have demonstrated that pimelate produced by the probiotic *Bifidobacterium* spp. in mice can alter gut luminal metabolism by increasing the bioavailability of biotin to enterocytes, modulating the development of T-regulatory cells, and influencing the composition of the gut microbiome (Sugahara *et al.*, 2015). In healthy human and animal enterocytes, biotin is an essential cofactor produced by gut flora and it has multiple roles in lipid and amino acid metabolism, including as a modulator of mucosal immune responses and gut microbial populations (Ghosal *et al.*, 2015). Although not established in this gnotobiotic model of disease, HRV infections are thought to contribute to disruption of normal intestinal microflora (Zhang *et al.*, 2014), suggesting HRV pathogenesis may indirectly alter host biotin metabolism. Pimelate may have enhanced biotin uptake into enterocytes to promote gut metabolic, microbial and immune homeostasis, thereby improving barrier function and reducing inflammation, and may have thus allowed the host to better resist diarrhea.

RB modification to probiotic amino acid/peptide metabolism also provided prophylactic diarrhea protection. Probiotic bacteria can catabolize complex RB and host proteins to release smaller bioactive peptides and amino acids, or bioconvert plant and host amino acids into bacterial-derived amino acids (Neis *et al.*, 2015; Pessione and Cirrincione, 2016) to create a

novel profile of amino acids/peptides that participate in anti-diarrheal and antiviral responses against HRV. Probiotic and host histidine metabolism was differentially modulated between Pro+RB and Pro groups. Histidine, which was decreased 0.12-fold in the LIC of Pro+RB when compared to Pro ($p = 0.012$) **(Tables 6.3, 6.5)**, functioned as an anti-secretory agent to reduce Cholera-associated diarrhea when supplemented into a rice-based oral rehydration salt (Rabbani *et al.*, 2005), suggesting that it could function similarly to reduce the onset of HRV diarrhea.

Histamine, a downstream metabolite of histidine that can be produced by both animals and probiotics (Gao *et al.*, 2015), decreased 0.19-fold in the LIC ($p = 0.00030$) and increased 1.57-fold in the serum ($p = 0.043$) of Pro+RB compared to Pro **(Tables 6.3, 6.5)**. Histamine is a well-characterized mediator of inflammation, mucosal immunity and the enteric nervous system (Smolinska *et al.*, 2014), yet it can suppress these processes when bound to specific receptors in the colon (Gao *et al.*, 2015). Previous investigations with *Lactobacillus reuteri* demonstrated that probiotics can use a bacterial-derived histidine deacetylase to convert dietary histidine into histamine in the colonic lumen, which acts on H2 receptors to suppress colonic inflammation and reduce damage to the colonic epithelium (Gao *et al.*, 2015). Probiotics may have converted RB histidine into histamine that left the LIC to bind H2 receptors, caused local modulation of colonic inflammatory responses, and increased barrier function, all of which ultimately interfered with HRV pathogenesis and provided diarrhea protection.

Other contributors to osmotic balance and thus likely anti-diarrheal mediators include cysteine and cystine metabolites. Cysteine, 0.40-fold-decreased in the LIC ($p = 0.033$) and 0.62-fold-decreased in the serum ($p = 0.014$) of Pro+RB compared to Pro **(Tables 6.3, 6.5)**, reduces oxidative stress, decreases inflammation, lowers permeability and modulates the mucosal immune system in the intestinal tract of neonatal pigs (Bauchart-Thevret *et al.*, 2009; Ruth and

Field, 2013). Cystine, increased 1.30-fold ($p = 0.044$) in the serum of Pro+RB compared to Pro **(Tables 6.3, 6.5),** serves as an excitatory neurotransmitter in the brainstem of humans and other animals, where it functions peripherally to delay gastric emptying and suppress food intake (Khan *et al.*, 2014; McGavigan *et al.*, 2015). During HRV infections, inflammation can cause enterocyte damage and increase gut permeability which both exacerbate HRV diarrhea (Yang *et al.*, 2015). Prophylactic modulations to cysteine and cysteine induced by Pro+RB may favorably shape the mucosal immune response and enteric nervous system to protect enterocytes and gut flora against oxidative damage and maintain normal gut motility during HRV infections to diarrhea.

Pro+RB alterations to entire pathways, containing multiple metabolites working in synergy, have been theorized to have anti-diarrheal effects on HRV. This was most evident in the LIC lipid pathways including long chain fatty acid (pathway enrichment score 1.84), sphingolipid (score 1.90, LIC) and secondary bile acid (score 1.84, LIC) pathways **(Figure 6.2A, Figure 6.3A),** all of which contained multiple antidiarrheal-associated metabolites and had pathway enrichment scores higher than one. This suggests that these pathways were contributors to treatment differences contributing to the antidiarrheal enhancement of Pro+RB versus Pro. Systems of long chain fatty acids have been reported to influence HRV infectivity and replication in the intestinal tract (Kim *et al.*, 2012b), whereas pathway-wide shifts in sphingolipid metabolism can influence the composition of host membrane lipid rafts (Barenholz, 2004), where HRV must successfully bind to infect enterocytes. Similarly, entire profiles of secondary bile acids have been associated with reductions in HRV diarrhea in Kenyan children, and likely function to disrupt HRV function by altering the pH of the intestinal lumen (Tazume *et al.*, 1990).

Entire amino acid/peptide pathways associated with anti-diarrheal function included gamma-glutamyl amino acid (pathway enrichment score 1.95, LIC) and polyamine metabolism (score 1.43, LIC). HRV diarrhea results in part due to impaired transport of gamma-glutamyl amino acids from the intestinal lumen and into enterocytes (Katyal *et al.*, 1999). Large differences in the LIC gamma-glutamyl amino acid profile between Pro+RB and Pro **(Figure 6.2B, Figure 6.5)** suggest that prophylactic alterations to luminal amino acid transport are associated with anti-diarrheal effects. In addition, HRV de-regulates host calcium metabolism and induces massive intracellular calcium increases to support HRV replication (Hyser *et al.*, 2013). Pathway-wide modulation of LIC polyamine metabolites **(Figure 6.2B, Figure 6.5)** in Pro+RB can work to reduce diarrhea and interfere with HRV replication. Past investigations support that polyamines in the intestinal lumen act on the enterocyte calcium-sensing receptor to inhibit the intracellular release of calcium and reduce chloride secretion into the intestinal lumen (Rogers *et al.*, 2015), simultaneously interfering with rotavirus replication and altering luminal osmolarity to reduce the onset of diarrhea. Collectively, analysis of entire lipid and amino acid/peptide pathways supports that a more comprehensive understanding of antidiarrheal activity can be achieved when clusters of closely-related metabolites are considered as part of an entire, functioning metabolic system.

While many pathways appeared to be differentially-regulated exclusively in the LIC or serum, multiple lipid and amino acid/peptide pathways contained antidiarrheal-associated metabolites in both LIC and serum matrices. These pathways included dicarboxylate fatty acid, endocannabinoid, phospholipid, and mono/dihydroxy fatty acid, histidine, glutamate, urea, arginine and proline, and methionine. When coupled with their high pathway enrichment scores, this suggests that these pathways may be important both locally and systemically for promoting

enhanced diarrheal protection in Pro+RB compared to Pro. For example, the glutamate metabolism (pathway enrichment score 1.28, LIC and 2.11 serum) **(Figure 6.2B),** works through the central and enteric nervous systems to modulate gut motility, intestinal fluid balance, and inflammation (Auteri *et al.*, 2015; Kondoh *et al.*, 2009; Li *et al.*, 2012). In addition, endocannabinoid metabolism, (score 0.92 LIC and 3.16 serum) works locally in the intestinal lumen to improve barrier function, modulate motility, and improve mucosal integrity and systemically to influence immune-mediated inflammatory responses and central nervous system functioning that could ultimately influence the course of diarrheal diseases in the gastrointestinal tract (Lee *et al.*, 2016, Gertsch, 2017).

Currently, variable vaccine efficacy and environmental enteric dysfunction exacerbate HRV outbreaks in the developing countries and warrant the development of stronger preventive strategies. The combination of probiotics and RB has the potential to serve as a safe, natural, prophylactic treatment aimed at reducing HRV diarrhea, and accomplishes this in part via multiple modulations to bacterial and host lipid and amino acid/peptide metabolism. Probiotic metabolism of RB can exert direct antiviral activity against HRV by interfering with HRV infection, replication and pathogenesis, but also interfere with HRV pathogenicity by improving gut barrier function, and modulating mucosal immune responses, especially inflammatory processes that influence the course of HRV diarrhea. Direct modulations to host metabolism and immunity also indicate that while Pro+RB is effective against HRV, it is likely that this combination can provide broad protection against a wide range of pathogenic diarrheal diseases. Although the current investigation focused primarily on modulations to lipid and amino acid/peptide metabolism, there are likely other classes of metabolites that contribute to the antiviral and antidiarrheal enhancement associated with combinations of probiotics and RB. An

evaluation of these other metabolic pathways can serve as future investigations into the molecular mechanisms of diarrhea protection by this combination. Probiotic and RB prophylactic therapies address a global need for more accessible, natural, antimicrobial agents, and have the potential to protect people and animals against a wide variety of enteric diseases.

REFERENCES

Abe, M., et al., (2001). Adverse effects of excess lysine in calves. *J Anim Sci,* 79, 1337-45.

Akula, M. K., et al., (2016). Control of the innate immune response by the mevalonate pathway. *Nat Immunol,* 17, 922-929.

Alp Avci, G. (2016). Selection of superior bifidobacteria in the presence of rotavirus. *Braz J Med Biol Res,* 49, e5562.

Aviello, G., Romano, B., and Izzo, A. A. 2008. Cannabinoids and gastrointestinal motility: animal and human studies. *Eur Rev Med Pharmacol Sci,* 12 Suppl 1, 81-93.

Auteri, M., Zizzo, M. G. and Serio, R. (2015). GABA and GABA receptors in the gastrointestinal tract: from motility to inflammation. *Pharmacol Res*. 93, 11-21.

Barcelo, A., et al., (2001). Effect of bile salts on colonic mucus secretion in isolated vascularly perfused rat colon. *Dig Dis Sci,* 46, 1223-31.

Barenholz, Y. (2004). Sphingomyelin and cholesterol: from membrane biophysics and rafts to potential medical applications. *Subcell Biochem.* 37, 167-215.

Baraniuk, J.N., et al., Carnosine treatment for gulf war illness: a randomized, controlled trial. (2013). *Glob J Health Sci*. 5:3, 69-81.

Bauchart-Thevret, C., et al., (2009). Sulfur amino acid deficiency upregulates intestinal methionine cycle activity and suppresses epithelial growth in neonatal pigs. *Am J Physiol Endocrinol Metab.* 296, E1239-50.

Brown, D. G., et al., (2016). Metabolomics and metabolic pathway networks from human colorectal cancers, adjacent mucosa, and stool. *Cancer Metab*. 4:11.

Brocker, C., Thompson, D. C., and Vasiliou, V. (2012). The role of hyperosmotic stress in inflammation and disease. *Biomolecular concepts,* 3, 345-364.

Brundige, D. R., et al., (2010). Consumption of pasteurized human lysozyme transgenic goats' milk alters serum metabolite profile in young pigs. *Transgenic Research,* 19, 563-574.

Buccioni, A., et al., (2012). Lipid metabolism in the rumen: New insights on lipolysis and biohydrogenation with an emphasis on the role of endogenous plant factors. *Anim Feed Sci and Technol*. 174, 1-25.

Chenoll, E., et al., (2016). Identification of a Peptide Produced by Bifidobacterium longum CECT 7210 with Antirotaviral Activity. *Front Microbiol*. 7:655.

Clarke, E. and Desselberger, U. (2015). Correlates of protection against human rotavirus disease and the factors influencing protection in low-income settings. *Mucosal Immunol.* 8, 1-17.

Collino, S., et al., (2013). Metabolic signatures of extreme longevity in northern Italian centenarians reveal a complex remodeling of lipids, amino acids, and gut microbiota metabolism. *PLoS One,* 8, e56564.

Cordaro, M., et al., (2016). Adelmidrol, a Palmitoylethanolamide Analogue, as a New Pharmacological Treatment for the Management of Inflammatory Bowel Disease. *Molec Pharmacol,* 90, 549-561.

D'Argenio, G., et al., (2005). Differential expression of multiple transglutaminases in human colon: impaired keratinocyte transglutaminase expression in ulcerative colitis. *Gut,* 54, 496-502.

De Jong, P. R., González-Navajas, J. M., and Jansen, N. J. G. (2016). The digestive tract as the origin of systemic inflammation. *Crit Care,* 20, 279.

Engels, F., et al., (1996). Preferential formation of 13-hydroxylinoleic acid by human peripheral blood eosinophils. *Prostaglandins,* 52, 117-24.

Frigolet, M. E. and Gutiérrez-Aguilar, R. (2017). The Role of the Novel Lipokine Palmitoleic Acid in Health and Disease. *Adv in Nutr: An Internat Rev J,* 8, 173S-181S.

Fujimura, K. E., et al., (2016). Neonatal gut microbiota associates with childhood multisensitized atopy and T cell differentiation. *Nat Med,* 22, 1187-1191.

Gao, C., Major et al., (2015). Histamine H2 Receptor-Mediated Suppression of Intestinal Inflammation by Probiotic Lactobacillus reuteri. *MBio*. 6:6.

Gertsch, J. (2017). Cannabimimetic phytochemicals in the diet – an evolutionary link to food selection and metabolic stress adaptation?. *British J Pharmacol*.

Ghosal, A., Jellbauer, S., Kapadia, R., Raffatellu, M. and Said, H. M. (2015). Salmonella infection inhibits intestinal biotin transport: cellular and molecular mechanisms. *Am J Physiol - Gastrointest Liver Physiol*. 309:2.

Goodgame, R. W. (1999). Viral infections of the gastrointestinal tract. *Curr Gastroenterol Rep,* 1, 292-300.

Goyal, N., et al., (2015). Effect of chenodeoxycholic acid and sodium hydrogen sulfide in dinitro benzene sulfonic acid (DNBS)-Induced ulcerative colitis in rats. *Pharmacol Rep,* 67, 616-23.

Guttíerez, C., et al., (2007). Does an L-glutamine-containing, Glucose-free, Oral Rehydration Solution Reduce Stool Output and Time to Rehydrate in Children with Acute Diarrhoea? A Double-blind Randomized Clinical Trial. *J Health, Popul, and Nutr,* 25, 278-284.

Han, X., et al. (2015). Apolipoprotein CIII regulates lipoprotein-associated phospholipase A2 expression via the MAPK and NFκB pathways. Biol. Open 4, 661–665. doi: 10.1242/bio.201410900

Hasobe, M., et al., (1989). Elucidation of the mechanism by which homocysteine potentiates the anti-vaccinia virus effects of the S-adenosylhomocysteine hydrolase inhibitor 9-(trans-2',trans-3'-dihydroxycyclopent4'-enyl)-adenine. *Mol Pharmacol*. 36:3, 490-96.

Henderson, A. J., et al., (2012). Consumption of rice bran increases mucosal immunoglobulin A concentrations and numbers of intestinal Lactobacillus spp. *J Med Food*. 15, 469-75.

Hyser, J. M., et al., (2013). Activation of the Endoplasmic Reticulum Calcium Sensor STIM1 and Store-Operated Calcium Entry by Rotavirus Requires NSP4 Viroporin Activity. *J Virol.* 87, 13579-13588.

Ishida, T., et al., (2013). Linoleoyl ethanolamide reduces lipopolysaccharide-induced inflammation in macrophages and ameliorates 2,4-dinitrofluorobenzene-induced contact dermatitis in mice. *Eur J Pharmacol,* 699, 6-13.

Jourdan, N., et al., (1998). Rotavirus Infection Reduces Sucrase-Isomaltase Expression in Human Intestinal Epithelial Cells by Perturbing Protein Targeting and Organization of Microvillar Cytoskeleton. *J Virol,* 72, 7228-7236.

Katyal, R., et al., (1999). Effect of rotavirus infection on small gut pathophysiology in a mouse model. *J Gastroenterol Hepatol.* 14, 779-84.

Keush, G.T., et al. (2016). "Diarrheal Diseases," in *Reproductive, Maternal, Newborn and Child Health: Disease Control Priorities*, ed. Laxminarayan R., *et al*. (Washington DC: The World Bank).

Khan, M. T., Van Dijl, J. M. and Harmsen, H. J. M. (2014). Antioxidants Keep the Potentially Probiotic but Highly Oxygen-Sensitive Human Gut Bacterium Faecalibacterium prausnitzii Alive at Ambient Air. *PLoS ONE*. 9:5.

Kim, Y., et al., (2012). Novel triacsin C analogs as potential antivirals against rotavirus infections. *Eur J Med Chem*. 50, 311-8.

Kondoh, T., Mallick, H. N. and Torii, K. (2009). Activation of the gut-brain axis by dietary glutamate and physiologic significance in energy homeostasis. *Am J Clin Nutr*. 90, 832S-837S.

Kong, W., et al., (2015). Biomarkers for assessing mucosal barrier dysfunction induced by chemotherapy: Identifying a rapid and simple biomarker. *Clin Lab,* 61, 371-8.

Lee, Y., et al., (2016). Endocannabinoids in the gastrointestinal tract. *Am J Physiol Gastrointest Liver Physiol,* 311, G655-G666.

Lei, S., et al., (2016). High Protective Efficacy of Probiotics and Rice Bran against Human Norovirus Infection and Diarrhea in Gnotobiotic Pigs. *Front Microbiol*. 7:1699.

Li, Y., et al., (2012). A novel role of intestine epithelial GABAergic signaling in regulating intestinal fluid secretion. *Am J Physiol Gastrointest Liver Physiol*. 303, G453-60.

Lin, H. C., et al., (2001). Slowing of gastrointestinal transit by oleic acid: a preliminary report of a novel, nutrient-based treatment in humans. *Dig Dis Sci,* 46, 223-9.

Liu, G., et al., (2014). Metabolomic Strategy for the Detection of Metabolic Effects of Spermine Supplementation in Weaned Rats. *J Agr Food Chem,* 62, 9035-9042.

Lustgarten, M. S., and Fielding, R. A. (2016). Metabolites Associated With Circulating Interleukin-6 in Older Adults. *J Gerontol A Biol Sci Med Sci*.

Khan, M. T., Van Dijil, J. M., and Harmsen, H. J. M. (2014). Antioxidants Keep the Potentially Probiotic but Highly Oxygen-Sensitive Human Gut Bacterium Faecalibacterium prausnitzii Alive at Ambient Air. *PLoS ONE,* 9, e96097.

MandØe, J. M., et al., (2015). The 2-monoacylglycerol moiety of dietary fat appears to be responsible for the fat-induced release of GLP-1 in humans. Am J Clin Nutr, 102:3, 548-55.

Matty, A. J., and Seshardi, B. (1965). Effect of thyroxine on the isolated rat intestine. *Gut,* 6, 200-202.

Mcgavigan, A. K., et al., (2015). l-cysteine suppresses ghrelin and reduces appetite in rodents and humans. *Internat J Obesity.* 39, 447-455.

Martinot, E., et al., (2017). Bile acids and their receptors. *Mol Aspects Med*. doi: 10.1016/j.mam.2017.01.006

Mechoulam, R., et al., (1995). Identification of an endogenous 2-monoglyceride, present in canine gut, that binds to cannabinoid receptors. *Biochem Pharmacol*. 50, 83-90.

Mehmood, M. H., et al., (2014). Pharmacological basis for the medicinal use of Carissa carandas in constipation and diarrhea. *J Ethnopharmacol,* 153, 359-67.

Mounce, B. C., et al., (2016). Inhibition of Polyamine Biosynthesis Is a Broad-Spectrum Strategy against RNA Viruses. *J Virol,* 90, 9683-9692.

Murataeva, N. D. et al., (2016). Where's my entourage? The curious case of 2-oleoylglycerol, 2-linolenoylglycerol, and 2-palmitoylglycerol. *Pharmacol Res,* 110, 173-80.

Naouar, M. S., et al., (2016). Preventive and curative effect of Pistacia lentiscus oil in experimental colitis. *Biomed Pharmacother,* 83, 577-583.

Neis, E. P., Dejong, C. H. and Rensen, S. S. (2015). The role of microbial amino acid metabolism in host metabolism. *Nutrients*. 7, 2930-46.

Nie Y. F., Hu, J., and Yan, X. H. (2015). Cross-talk between bile acids and intestinal microbiota in host metabolism and health. *J Zhejiang Univ Sci B,* 16, 436-46.

Nielsch, A.S., et al., (1991). Influence of dietary protein and gut microflora on endogenous synthesis of nitrate induced by bacterial endotoxin in the rat. *Food Chem Toxicol*. 29:6, 387-90.

Nilsson, Å. (2016). Role of Sphingolipids in Infant Gut Health and Immunity. *J Pediatr,* 173, Supplement, S53-S59.

Olaya Galan, N. N., et al., (2016). In vitro antiviral activity of Lactobacillus casei and Bifidobacterium adolescentis against rotavirus infection monitored by NSP4 protein production. *J Appl Microbiol*. 120, 1041-51.

Pandey, G., et al., (2016). Grilling enhances antidiarrheal activity of Terminalia bellerica Roxb. fruits. *J Ethnopharmacol*.

Patra, F.C., et al., (1989), Oral rehydration formula containing alanine and glucose for the treatment of diarrhoea: a controlled trial. *Brit med J*. 298:6684, 1353-6.

Patten, G., et al., (2002), Dietary fish oil increases acetylcholine- and eicosanoid-induced contractility of isolated rat ileum. *J Nutr,* 132, 2506-13.

Pearl, D. S., et al., (2014), Altered colonic mucosal availability of n-3 and n-6 polyunsaturated fatty acids in ulcerative colitis and the relationship to disease activity. *J Crohns Colitis,* 8, 70-9.

Peleman, C., et al., (2016), Colonic Transit and Bile Acid Synthesis or Excretion in Patients With Irritable Bowel Syndrome-Diarrhea Without Bile Acid Malabsorption. *Clin Gastroenterol Hepatol*.

Pessione, E. and Cirrincione, S. (2016). Bioactive Molecules Released in Food by Lactic Acid Bacteria: Encrypted Peptides and Biogenic Amines. *Front Microbiol.* 7:876.

Plaza-Zamora, J., et al., (2013). Polyamines in human breast milk for preterm and term infants. *Brit J Nutr,* 110, 524-528.

Rabbani, G. H., et al., (2005). Antidiarrheal effects of L-histidine-supplemented rice-based oral rehydration solution in the treatment of male adults with severe cholera in Bangladesh: a double-blind, randomized trial. *J Infect Dis*. 191, 1507-14.

Ren, W., et al., (2013). Dietary supplementation with proline confers a positive effect in both porcine circovirus-infected pregnant and non-pregnant mice. *Br J Nutr,* 110, 1492-9.

Rezaei, R., et al., (2013). Dietary supplementation with monosodium glutamate is safe and improves growth performance in postweaning pigs. *Amino Acids,* 44, 911-23.

Rogers, A. C., et al., (2015). The effects of polyamines on human colonic mucosal function. *Eur J Pharmacol*. 764, 157-63.

Ruth, M. R. and Field, C. J. (2013). The immune modifying effects of amino acids on gut-associated lymphoid tissue. *J Anim Sci Biotechnol*. 4:27.

Sabbatini, P., et al., (2013). Synthesis and Quantitative Structure-Property Relationships of Side Chain-Modified Hyodeoxycholic Acid Derivatives. *Molecules,* 18, 10497.

Schirmer, M., et al., (2016). Linking the Human Gut Microbiome to Inflammatory Cytokine Production Capacity. *Cell,* 167, 1125-1136.e8.

Shimizu, M., et al., (2009). Dietary taurine attenuates dextran sulfate sodium (DSS)-induced experimental colitis in mice. *Adv Exp Med Biol,* 643, 265-71.

Sinha, R., et al., (2016). Fecal Microbiota, Fecal Metabolome, and Colorectal Cancer Interrelations. *PLoS One,* 11, e0152126.

Smolinska, S., et al., (2014). Histamine and gut mucosal immune regulation. *Allergy*. 69, 273-81.

Soderholm, J. D., Olaison, G., Peterson, K. H., Franzen, L. E., Lindmark, T., Wiren, M., Tagesson, C., and Sjodhal, R. (2002). Augmented increase in tight junction permeability by luminal stimuli in the non-inflamed ileum of Crohn's disease. *Gut,* 50, 307-13.

Somekawa, S., et al., (2012). Dietary free glutamate prevents diarrhoea during intra-gastric tube feeding in a rat model. *Br J Nutr,* 107, 20-3.

Srnivias, S. R., et al., (2007). Transport of butyryl- carnitine, a potential prodrug, via the carnitine transporter OCTN2 and the amino acid transporter ATB. *Am J Physiol - Gastrointest Liver Physiol,* 293, G1046-G1053.

Sugahara, H., et al., (2015). Probiotic Bifidobacterium longum alters gut luminal metabolism through modification of the gut microbial community. *Sci Rep*. 5:13548

Swami, U., Goel, S., and Mani, S. (2013). Therapeutic Targeting of CPT-11 Induced Diarrhea: A Case for Prophylaxis. *Curr drug targets,* 14, 777-797.

Tazume, S., et al.,(1990). Ecological studies on intestinal microbial flora of Kenyan children with diarrhoea. *J Trop Med Hyg*. 93, 215-21.

Taschler, U., et al., (2017). Cannabinoid Receptors in Regulating the GI Tract: Experimental Evidence and Therapeutic Relevance. Handb Exp Pharmacol. doi: 10.1007/164_2016_105

Theriot, C. M., Bowman, A. A., and Young, V. B. Antibiotic-Induced Alterations of the Gut Microbiota Alter Secondary Bile Acid Production and Allow for Clostridium difficile Spore Germination and Outgrowth in the Large Intestine. (2016). mSphere. doi: 10.1128/mSphere.00045-15

Timmons, J., et al., (2012). Polyamines and Gut Mucosal Homeostasis. *J gastrointest & digest syst,* 2, 001.

Trabelsi, I., et al., (2016). Effect of a probiotic Lactobacillus plantarum TN8 strain on trinitrobenzene sulphonic acid-induced colitis in rats. *J Anim Physiol Anim Nutr (Arumugam et al.).*

Turcotte, C., et al., (2015). Regulation of inflammation by cannabinoids, the endocannabinoids 2-arachidonoyl-glycerol and arachidonoyl-ethanolamide, and their metabolites. *J Leukoc Biol*. 97, 1049-70.

Vlasova, A. N., et al., (2016). Comparison of probiotic lactobacilli and bifidobacteria effects, immune responses and rotavirus vaccines and infection in different host species. *Vet Immunol Immunopathol*. 172, 72-84.

Wen, K., et al., (2015). Lactobacillus rhamnosus GG dosage affects the adjuvanticity and protection against rotavirus diarrhea in gnotobiotic pigs. *J Pediatr Gastroenterol Nutr*. 60, 834-843.

Wang, H., et al., (2016). Lactobacillus rhamnosus GG modulates innate signaling pathway and cytokine responses to rotavirus vaccine in intestinal mononuclear cells of gnotobiotic pigs transplanted with human gut microbiota. *BMC Microbiol,* 16, 109.

Wang, A., et al., (2015). Gut microbial dysbiosis may predict diarrhea and fatigue in patients undergoing pelvic cancer radiotherapy: a pilot study. *PLoS One,* 10, e0126312.

Wee, L. H., et al., (1988). Ethyl eicosapentaenoate restored the immunosuppression in mice fed fat-free diet. *Res Commun Chem Pathol Pharmacol,* 62, 49-66.

Yang, X., et al., (2015). High protective efficacy of rice bran against human rotavirus diarrhea via enhancing probiotic growth, gut barrier function, and innate immunity. *Sci Rep*. 5:15004.

Yeh, K. Y., Yeh, M., and Holt, P. R. (1989). Differential effects of thyroxine and cortisone on jejunal sucrase expression in suckling rats. *Am J Physiol,* 256, G604-12.

Yuan, D., Wu, Z., and Wang, Y. (2016). Evolution of the diacylglycerol lipases. *Progress in Lipid Research,* 64, 85-97.

Yen, C., et al., (2014). Rotavirus vaccines: Current status and future considerations. *Human vaccines & immunotherapeutics*. 10, 1436-1448.

Zavala-Mendoza, et al., (2013). Composition and Antidiarrheal Activity of Bidens odorata Cav. *Evid Based Complement Alternat Med,* 2013, 170290.

Zhang, H., et al., (2014). Probiotics and virulent human rotavirus modulate the transplanted human gut microbiota in gnotobiotic pigs. *Gut Pathog*. 6:39

CHAPTER SEVEN

CONCLUSIONS AND FUTURE DIRECTIONS

7.1. Conclusions:

Probiotics are currently and too often lumped collectively as broad-acting health-promoting microorganisms, and despite established genetic and functional differences (Bottacini *et al.*, 2017; Engevik and Versalovic, 2017; Goldstein *et al.*, 2015; Hidalgo-Cantabrana *et al.*, 2017; Hiippala *et al.*, 2018; Yousefi *et al.*, 2019), their metabolism and production of bioactive compounds is minimally-characterized. Consequently, when probiotics are combined with prebiotics to elevate their innate health benefits, the resultant synbiotics show variable efficacy when applied to different infectious enteric diseases. This thesis examined multiple probiotic species-dependent mechanisms by which rice bran-containing synbiotics confer host protection against gut pathogens using novel high-throughput metabolomics technologies. The major conclusions of this thesis demonstrated that in the presence of rice bran, probiotic species produced distinct metabolomes associated with differential *Salmonella* Typhimurium growth suppression (**Chapters 2**, **3** and **4**), that probiotic-fermented rice bran beneficially-modulated gastrointestinal and systemic metabolism in healthy mice, and in neonatal pigs, rice bran synbiotics produced a metabolome associated with enhanced protection against human rotavirus diarrhea (**Chapters 5** and **6**).

7.1.1. Rice bran-based synbiotics produced small molecules contributing to Salmonella Typhimurium growth suppression.

Chapter 2 demonstrated that the synbiotic cell-free supernatant prepared with the human gut-native *L. paracasei* and rice bran enhanced *Salmonella* growth suppression when compared to either *L. paracasei* supernatant or rice bran alone. This study provided proof of concept that probiotic metabolism of rice bran modulates the release of small molecules into the environment that had antimicrobial activity. Further validation of this concept was evident in the synbiotic supernatant metabolite profile, where 22 metabolites that differentially abundant in the cell-free supernatant of the synbiotic versus *L. paracase*i-only that had reported antimicrobial activity. Many of these metabolites were lipids and identified as fatty acids, where probiotic production of antimicrobial fatty acids, especially among lactic acid bacteria like *L. paracasei*, is well-established (Hemalatha *et al.*, 2017; Plaza-Diaz *et al.*, 2014). Fatty acids produced by probiotics and present in rice bran have been shown to interfere with pathogen cell wall synthesis, promote pathogen lysis, and are widely reported to exhibit a myriad of other bacteriostatic and bactericidal functions (**Table 2.4**).

The non-targeted metabolomics analysis further revealed that multiple amino acids (e.g. methionine sulfone) and tricarboxylic acid metabolites (e.g. tricarballylate) additionally contributed to synbiotic antimicrobial activity (**Table 2.4**). Although these compounds have been previously-explored for their roles in antagonizing *Salmonella* protein synthesis and interfering with reduced carrier formation in the tricarboxylic acid cycle (**Table 2.4**), they have never been studied as health-promoting synbiotic components. Further examination of amino acid and energy metabolites may reveal additional mechanisms through which probiotics interact with dietary components to exert health benefits and suggests that multiple chemical classes within

synbiotic supernatant suppress *Salmonella* growth via multiple, simultaneous, interconnected mechanisms.

7.1.2. Differential metabolism by Lactobacillus spp. and rice bran synbiotics for achieving Salmonella Typhimurium growth suppression.

Given the efficacy of the *Lactobacillus paracasei* + rice bran synbiotic against *Salmonella* Typhimurium, **Chapter 3** compared three different *Lactobacillus* spp. + rice bran synbiotics and established that synbiotics prepared with different *Lactobacillu*s spp. differentially suppressed *Salmonella* growth. Both *L. fermentum* and *L. paracasei* synbiotic supernatants enhanced *Salmonella* growth suppression compared to their respective probiotic-only supernatants (**Figure 3.2**) and produced synbiotic supernatant profiles with 44 differentially-abundant metabolites. **Figure 7.1** organizes these *L. fermentum* and *L. paracasei* metabolites by their reported antimicrobial functions and identified 22 metabolites with previously-reported bactericidal, bacteriostatic, and *Salmonella* growth-modulatory functions (**Table 3.2**) that supported our hypothesis of *Lactobacillus* spp. differential metabolism of rice bran driving the *Salmonella* growth suppression differences. Furthermore, the other 22 metabolites differentially-abundant between *L. fermentum* and *L. paracasei* that did not have previously-reported antimicrobial functions highlights additional metabolic pathways that could be explored for their contributions to *Salmonella* growth suppression and other antimicrobial capacities.

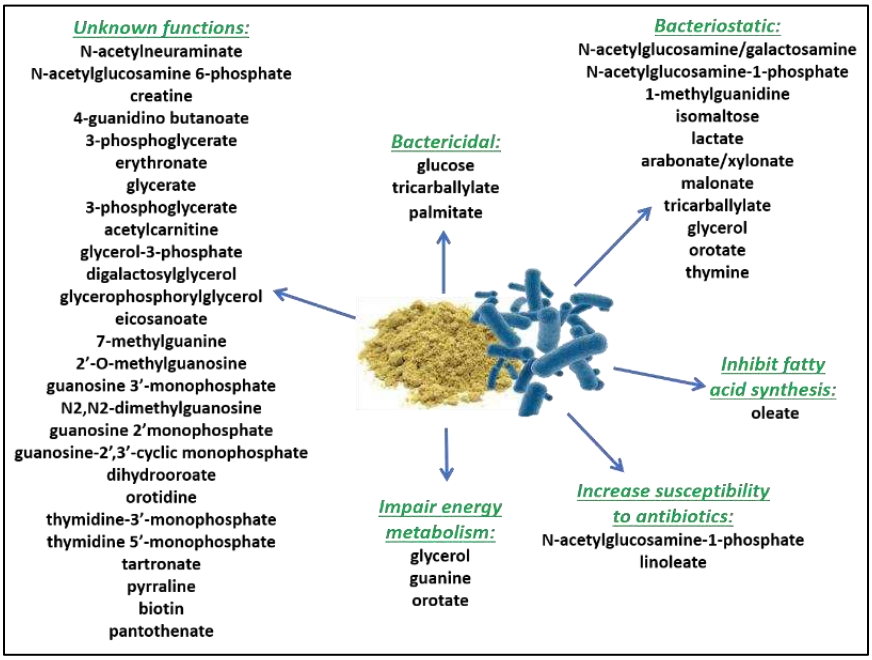

Figure 7.1. Potential mechanisms by which *Lactobacillus* + rice bran synbiotics differentially suppress *Salmonella* Typhimurium growth.

*The 44 metabolites reported in **Chapter 3** that were differentially-abundant in L. fermentum and L. paracasei synbiotic supernatants are organized by known functions. "Unknown functions" refers to metabolites that do not have any reported roles in growth suppression of Salmonella or other pathogens, or any known antimicrobial functions.*

As anticipated from the synbiotic metabolome established in **Chapter 2**, lipid and amino acid metabolites were major chemical classes contributing to metabolite profile differences across the three synbiotics. However, this comparative synbiotic study additionally revealed that nucleotide metabolism, especially guanine and thymine metabolic pathways further distinguished the two synbiotics that exhibited enhanced *Salmonella* growth suppression compared to their respective probiotic-only treatments. *L. fermentum* and *L. paracasei* synbiotics which contained metabolites shown to modulate *Salmonella* replication and metabolism in concentration-dependent manners (**Table 3.2**). There is a lack of research examining nucleotide metabolism by synbiotics, and this analysis provides a role for nucleotides in revealing the distinct mechanisms

by which different probiotic species interact with rice bran to achieve *Salmonella* growth suppression. Further examination of synbiotic nucleotides may reveal additional metabolites that can be applied as novel antimicrobial agents, and supports the screening of other synbiotic preparations using global, non-targeted metabolomics platforms for drug-discovery outside of conventionally-studied compound classes in fermented foods.

This study further revealed that a lower concentration synbiotic treatments (18% v/v versus 22% v/v) was needed to achieve 16h growth suppression for a *Salmonella* isolate expressing antimicrobial resistant genes versus for a phenotypically non-resistant *Salmonella* isolate (**Figure 3.2**). One explanation for this can be supported by the concept that most antimicrobial agents target rapidly growing pathogens (Greulich *et al.*, 2015). The antimicrobial-resistant *Salmonella* isolate grew at a faster rate than the phenotypically non-resistant *Salmonella* isolate (**Figure 3.1**), suggesting that it might be more metabolically-active and dependent on nutrients in its environment to sustain its rapid metabolic rate. This dose-dependent activity of synbiotics on resistant versus non-resistant pathogens suggests that antimicrobial-resistant pathogen strains within a species may need specialized treatment doses that cannot be predicted from screening of non-resistant isolates. Further characterization of how different patterns of genotypic and phenotypic multidrug resistance influence pathogen growth and metabolism may provide useful in predicting the efficacy of treatments targeting drug-resistant pathogens.

7.1.3: Identification of synbiotic metabolites from cell free supernatants that drove rice bran-based synbiotic growth suppression:

Chapter 4 examined fractionated *L. fermentum* and *L. paracasei* synbiotic fractions and established that fractions that exhibited time, magnitude, and synbiotic treatment-dependent

Salmonella growth suppression. Most of these fractions achieved maximal growth suppression between 10 and 16 hours, which corresponded to the exponential phase of *Salmonella* growth. This trend is consistent with our experiments examining growth suppression by unfractionated synbiotic supernatant (**Figure 3.1**) and is supported by the concept that antimicrobial compounds work most effectively on cells that are rapidly-dividing (Greulich *et al.*, 2015). These kinetics may suggest that these synbiotic-secreted metabolites need to diffuse into *Salmonella* or become actively-transported inside of the cell to exert their growth suppressive mechanisms of action.

The metabolite profiles of selected fractions that suppressed *Salmonella* growth revealed that these fractions were enriched in lipid and amino acid metabolites and that these were differentially-abundant between *L. fermentum* and *L. paracasei* and further-validated the observations concluded in **Chapter 3.** These metabolites are depicted in **Figure 7.2**, which additionally highlights metabolites that were identified in **Chapters 2** and **3** as contributing to the enhanced *Salmonella* growth suppression of rice bran synbiotics in the synbiotic cell-free supernatants. Most noticeably, *L. paracasei* synbiotic effective fractions were enriched in amino acids that were absent in their corresponding *L. fermentum* effective fractions, indicating that differential metabolism of amino acids by probiotics from rice bran may be a primary chemical class distinguishing synbiotic mechanisms of *Salmonella* growth suppression.

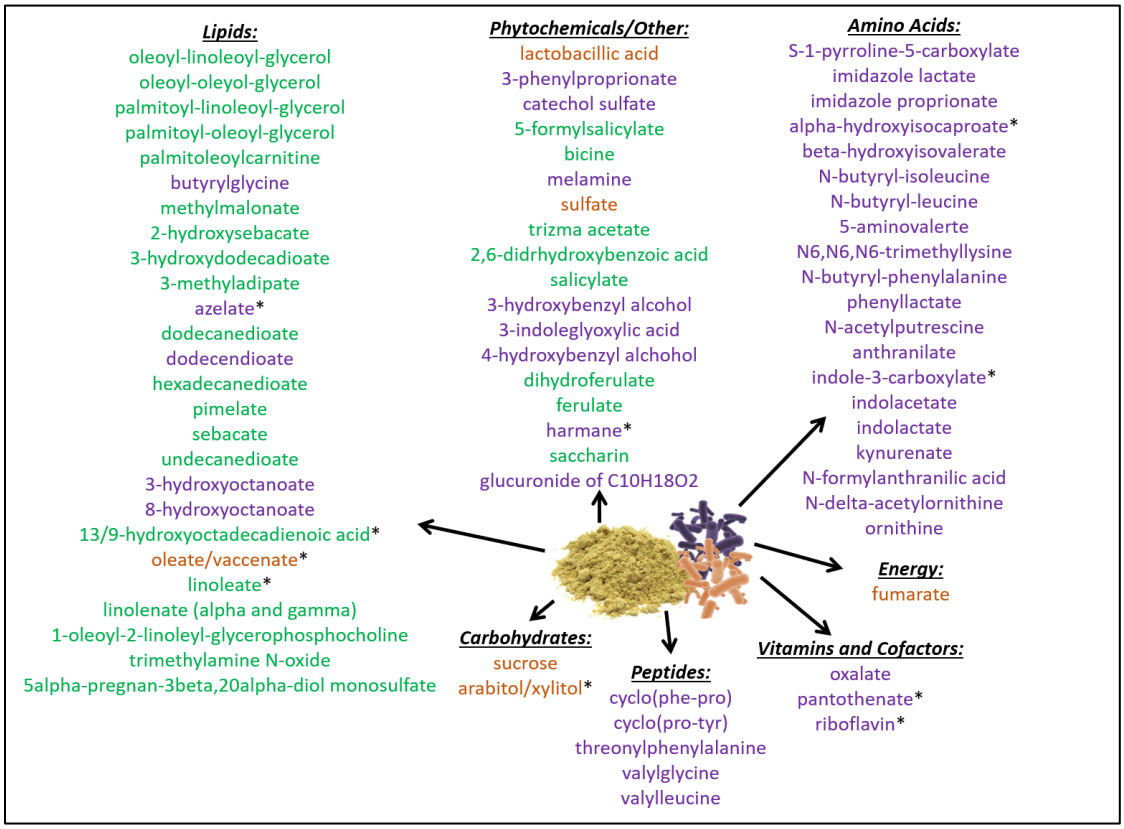

Figure 7.2. Metabolites driving enhanced *Salmonella* Typhimurium growth suppression by *Lactobacillus* + rice bran synbiotics.

*Orange metabolites were identified in effective L. fermentum + rice bran extract fractions; purple metabolites were identified in effective L. paracasei + rice bran extract fractions. Green metabolites were identified in both L. fermentum + rice bran extract and L. paracasei + rice bran extract treatments. * Indicates metabolite identified with antimicrobial function in L. fermentum + rice bran extract or L. paracasei + rice bran extract in **Chapters 2** and **3**.*

7.1.4. Healthy mice fed Bifidobacterium longum-fermented rice bran versus rice bran exhibited enhanced metabolism of bioactive compounds in the colon and blood.

Chapter 5 fed *B. longum*-fermented rice bran versus rice bran to healthy mice and observed extensive differences in the lipid and amino acid metabolite profiles between the fermented rice bran and rice bran diets. Over 100 of these metabolites were subsequently modulated in the colon and blood of these mice, where they have been reported to improve gut

barrier function, modulate immune responses, facilitate healthy colonocyte metabolism, and exert antimicrobial effects on enteric pathogens (**Table 5.3**), supporting that consumption of a synbiotic (versus consumption of prebiotics that promote gut native probiotic metabolism) represents a second route via which synbiotics can deliver bioactive compounds to the host. Development of biologically-effective pre-fermented synbiotics may be important for populations of people and animals that do not contain adequate populations of gut flora that can interact with prebiotics, or if their intestinal tract resists colonization of live probiotic supplements (Klemashevich *et al.*, 2014). This synbiotic preparation method could be explored and compared to consumption of live probiotics and rice bran in clinically-healthy populations versus populations experiencing gut dysbiosis, inflammation, or other conditions that compromise gastrointestinal function. The efficacy of each delivery method for exerting antimicrobial effects on gastrointestinal pathogens could be assessed and used to optimize synbiotic delivery for protection against different pathogens, in varying age groups, and in different animal species.

Cross-matrix analysis of the food, colon and blood metabolomes of mice consuming *B. longum*-fermented rice bran versus rice bran identified one metabolite, a product of arginine metabolism called N-delta-acetylornithine, that was increased in the fermented rice bran group. Although N-delta-acetylornithine was been identified in plants and fungi (Adio *et al.*, 2011; Kite and Ireland, 2002; Lemarie *et al.*, 2015; Oka *et al.*, 1984), probiotic production of or release of this metabolite from food has not been previously characterized. Consequently, N-delta-acetylornithine merits further investigation as a microbially-derived biomarker of *B. longum*-fermented rice bran intake and can be explored for production in fermented rice bran produced with other probiotic species.

7.1.5. Synbiotics of L. rhamnosus GG, E. coli Nissle and rice bran produced a metabolome associated with human rotavirus diarrhea protection in gnotobiotic, neonatal pigs.

Chapter 6 established that synbiotic metabolomes in the colon and blood of healthy animals were dually present in gnotobiotic, neonatal pigs that exhibited enhanced protection from human rotavirus diarrhea when compared to pigs consuming either *L. rhamnosus* GG/*E. coli* Nissle or rice bran alone. As in the healthy mice, the majority of metabolic pathways and bioactive metabolites differentially regulated in the synbiotic-fed pigs versus pigs gavaged with probiotics alone involved lipid and amino acid pathways containing immune-modulatory, antimicrobial, antiviral, gut barrier protective, and antidiarrheal compounds. Large intestinal metabolic pathways in both healthy mice and pigs that were differentially-regulated by synbiotic-consuming animals included monoacylglycerols/ diacylglycerols, sphingolipids, fatty acids, polyamines, sulfur-containing amino acids, arginine, glutamine, and histidine metabolism. In the blood, these metabolic pathways included dicarboxylic acids, primary bile acids, secondary bile acids, sulfur-containing amino acids, arginine, polyamine and dipeptide metabolism. The metabolomic parallels across animal studies support that synbiotic modulations to lipid and amino acid metabolism are core mechanisms driving their enhanced gastrointestinal health benefits when compared to probiotics alone, and that these changes occur both during the consumption of pre-fermented rice bran, as well as when consuming live probiotics and unfermented rice bran. A summary of these conserved synbiotic mechanisms is visualized in **Figure 7.3**. Optimization of rice bran synbiotics can come from understanding probiotic species differences in regulating these pathways and understanding how different probiotic species utilize these pathways to achieve pathogen growth suppression via distinct mechanisms that all contribute to the phenotype of enhanced synbiotic protection against enteric pathogens.

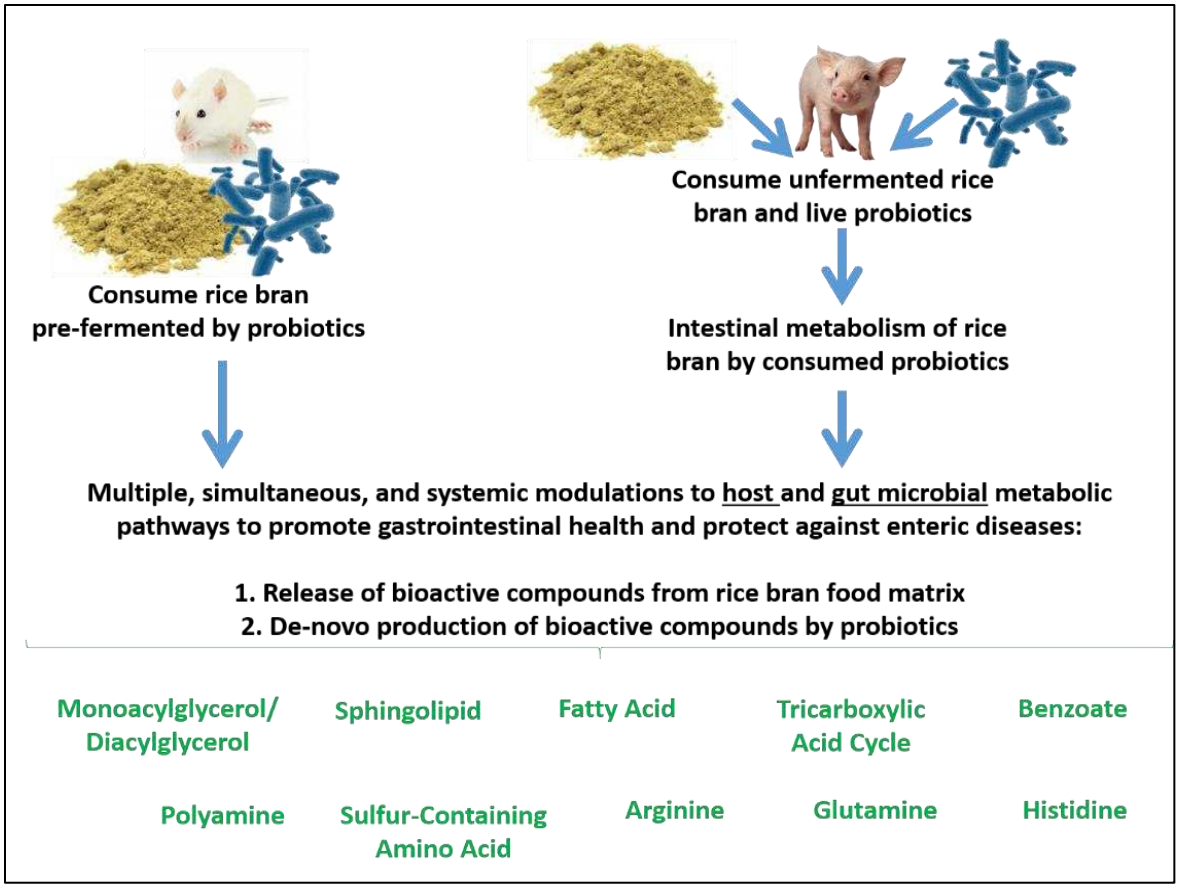

Figure 7.3. Metabolic pathways contributing to synbiotic protection against infectious enteric diseases in animal models.

7.2. Future Directions:

The experiments discussed in this thesis support the further examination and development of rice bran-based synbiotics as alternative or adjunctive treatments for health promotion and protection against infectious gastrointestinal diseases across the lifespan. Moving forward, there are many opportunities through which synbiotics can be optimized for efficacy, with the ultimate goal of developing targeted combinations of probiotics and rice bran for different infectious enteric diseases across human and animal populations and age groups. Factors that can be easily-modulated and examined under controlled laboratory conditions include development of rice bran-based growth media, an assessment of bioactive proteins within synbiotic cell-free

supernatant, and the application of synbiotics to human and animal *ex vivo* intestinal systems. Ultimately, these future studies can inform on and prioritize variables on which to optimize synbiotics for use as infectious disease preventives and treatments, and these experiments will help to elucidate new synbiotic mechanisms of action, and validate synbiotic bioactivity that is suggested by genomic, proteomic, and metabolomic data.

7.2.1. Synbiotic growth conditions optimization for Salmonella growth suppression:

The metabolite profiles reported in **Chapters 2**, **3**, and **4** contained small molecules present in bacterial culture media and were consequently evaluated alongside the metabolite profiles of sterile media samples to assess synbiotic antimicrobial production. The culture media used for growing probiotic bacteria depends heavily on the species being investigated and varies across probiotic and synbiotic studies (Marianelli *et al.*, 2010; Wang *et al.*, 2015b). One-way media bias can be addressed when examining rice bran synbiotics is to develop a non-selective rice bran-based media capable of culturing wide spectrum of probiotics. Culturing probiotics in this media could eliminate media-effect bias that could come from producing rice bran synbiotics with different starting reagents and would add an additional layer of control in synbiotic analyses. Furthermore, different components of the media could be adjusted and comparative transcriptomic, metabolomic, and proteomic studies could be done to assess how the presence or absence and amount of different rice bran components influence synbiotic function.

Along with media selection, the pH of and oxygen concentration at which synbiotics are grown can be modulated to optimize their functions. The gastrointestinal environment or food matrices in which most probiotics exert their health functions are acidic and have an oxygen content that is microaerophilic to anaerobic (Marianelli *et al.*, 2010; Talwalkar and Kailasapathy,

2004). Both pH and oxygen concentrations could be adjusted and accounted for when preparing rice bran synbiotic supernatant, and their impacts on *Salmonella* growth suppression could be compared to maximize the function of different rice bran synbiotics. While decreasing the pH and oxygen concentrations might enhance the production of some metabolites by *Lactobacillus* synbiotics (such as lactic acid), synbiotic production of other antimicrobial metabolites, such amino acids, nucleotides and energy compounds has not been described and may not be optimally-produced under these conditions. Additional research examining how growth media selection, oxygen concentrations, and cell-free supernatant pH influences the metabolite profiles and *Salmonella* growth suppression of *Lactobacillus* + rice bran synbiotics will help optimize their production for use in many different biological systems.

7.2.2. Synbiotic immune and gut microbiome modulation in human and animal ex vivo colon tissue systems for Salmonella Typhimurium and enteric virus protection:

The synbiotic cell-free supernatants examined in this thesis could be applied dose-dependently to tissue slice systems to measure epithelial cell uptake and metabolism of synbiotic compounds, screened for effects on immune responses, gut microbiota composition and function, muscle contractility, and enteric nerve function. These synbiotic effects can be compared across sexes and evaluated in aerobic versus anaerobic condition when the microbiota is either present or absent. Alternatively, rice bran synbiotics can be screened in human and murine tissue slices maintained in a microfluidic device, which could produce an oxygen gradient across the apical and basal tissue surfaces that more accurately replicates the i*n vivo* oxygen conditions in which *Salmonella* and these synbiotics would be exposed to *in vivo* (McLean *et al.*, 2018). Intestinal tissue slices maintained in microfluidic devices have been examined for colonization by

probiotic *L. rhamnosus* GG and their mucosal immune responses were assessed (Shah *et al.*, 2016), supporting that these microfluidic systems can be readily utilized to examine synbiotic functions *ex vivo*.

Ex vivo intestinal systems can be dually applied to validate the synbiotic growth suppression of *Salmonella* in the presence of host factors, which are important factors to consider when optimizing synbiotics for use in people and animals. The *ex vivo* model of *Salmonella* infections additionally allows for examination of how synbiotics may modulate *Salmonella* invasion into and replication within the intestinal epithelium, which are the primary mechanisms by which it causes disease in the host (Ghazi *et al.*, 2016; LaRock *et al.*, 2015). Studies could examine *Salmonella* rates of invasion into the epithelium as well as intracellular replication suppression by synbiotic versus a probiotic-only or rice bran-only treatment. Innate and adaptive mucosal immune responses to *Salmonella*, intestinal epithelial barrier functions (e.g. mucus production, defensin secretion, tight junction protein up-regulation) contribute to host defenses of *Salmonella* and are modulated by probiotics (Klemashevich *et al.*, 2014; Mao *et al.*, 2016; Martin *et al.*, 2019; Sherman *et al.*, 2009; van Baarlen *et al.*, 2013; Wan *et al.*, 2016) that can additionally be measured. To examine whether the same synbiotic metabolites contributing to *in-vitro Salmonella* growth suppression function within the colon environment, synbiotic fractions can be applied to the tissue slice systems and their *Salmonella* growth suppression efficacies compared to unfractionated supernatant. Given the many roles of lipid and amino acid metabolites in immune-modulation , supporting colonocyte metabolism, and enhancing gut barrier function (Chung *et al.*, 2018; Liang *et al.*, 2018; Pessione and Cirrincione, 2016), it is anticipated that examination of synbiotic fractions enriched in these metabolites within an *ex vivo* model will reveal additional mechanisms by which they contribute to *Salmonella* growth

suppression outside of their direct antimicrobial bactericidal and bacteriostatic activities. The long-term goal of these synbiotic fraction examinations may reveal compounds or small suites of compounds that can be used by people and animals to protect against *Salmonella* or treat salmonellosis post-infection.

7.2.3. Examining cell-free supernatant proteome contributions to synbiotic bioactivity:

The capacities of synbiotic cell-free supernatant small molecules to directly mediate *Salmonella* growth suppression was demonstrated during bioactivity-guided fractionation, during which all protein content from the supernatants was removed during chromatographic separation of the supernatant prior to applying the fractions to *Salmonella* to screen them for growth suppression. Consequently, another study could examine protein removal from synbiotics modulates their capacities to suppress *Salmonella* growth. Probiotics produce a diversity of antimicrobial proteins and peptides including bacteriocins and microcins (Dicks *et al.*, 2018; Palmer *et al.*, 2018), and an evaluation of protein-free rice bran-based synbiotics on *Salmonella* growth could be performed to see if loss of protein modulates the growth-suppressive effects of these synbiotics against *Salmonella*.

Preliminary analysis has revealed that protein-extracted synbiotic cell-free supernatant collected from *L. fermentum*, *L. paracasei*, and *L. rhamnosus* cultured with rice bran extract exhibited a 4 to 10-fold loss of total growth suppressive function at 16h against the antimicrobial-resistant *Salmonella* isolates analyzed in **Chapters 2**, **3** and **4** when compared to their protein-intact synbiotic supernatant treatments (**Figure 7.3**). These results suggest that the protein content of a synbiotic contributes to its capacity to suppress *Salmonella* growth, either by exhibiting direct bactericidal or bacteriostatic effects on *Salmonella*, by indirectly interacting

with synbiotic metabolites to help them exert their functions, or by binding to and reducing the bioavailability of metabolites that may support *Salmonella* growth. The protein-free synbiotic supernatants were not capable of suppressing *Salmonella* growth at any time over 16h when examined over the 12%-25% v/v supernatant concentrations that were effective at suppressing *Salmonella* growth compared to the negative controls for the protein-intact cell-free supernatant. These dose analysis results suggest that in the absence of proteins, synbiotics may need to be applied at a higher dose overall to achieve *Salmonella* growth suppression compared to control treatments, a trend which could now additionally be considered during future synbiotic supernatant fractionation analyses for *Salmonella* growth suppression.

Another trend observed in the protein-free synbiotic supernatants was that protein-free *L. rhamnosus* + rice bran extract supernatant was more effective than both the *L. paracasei* and *L. fermentum* protein-free synbiotic supernatants. This effect, which wasn't observed in the protein-intact cell-free supernatants could suggest that *L. paracasei* and *L. fermentum* rice bran synbiotics rely more-heavily on their protein content to suppress *Salmonella* growth than *L. rhamnosus* synbiotics. One alternative interpretation could be that proteins in the intact *L. rhamnosus* synbiotic may bind to and reduce the bioavailability of antimicrobial metabolites within the supernatant, so that in the protein-free supernatant, antimicrobial metabolites present in the *L. rhamnosus* synbiotic supernatant are more bioavailable to drive *Salmonella* growth suppression. Moving forward, these preliminary analyses could be applied to additional synbiotics and probiotics and could be coupled with non-targeted and targeted proteomic analyses to further elucidate the mechanisms by which synbiotic proteins contribute to it overall bioactivity and antimicrobial effects on *Salmonella* and other pathogens.

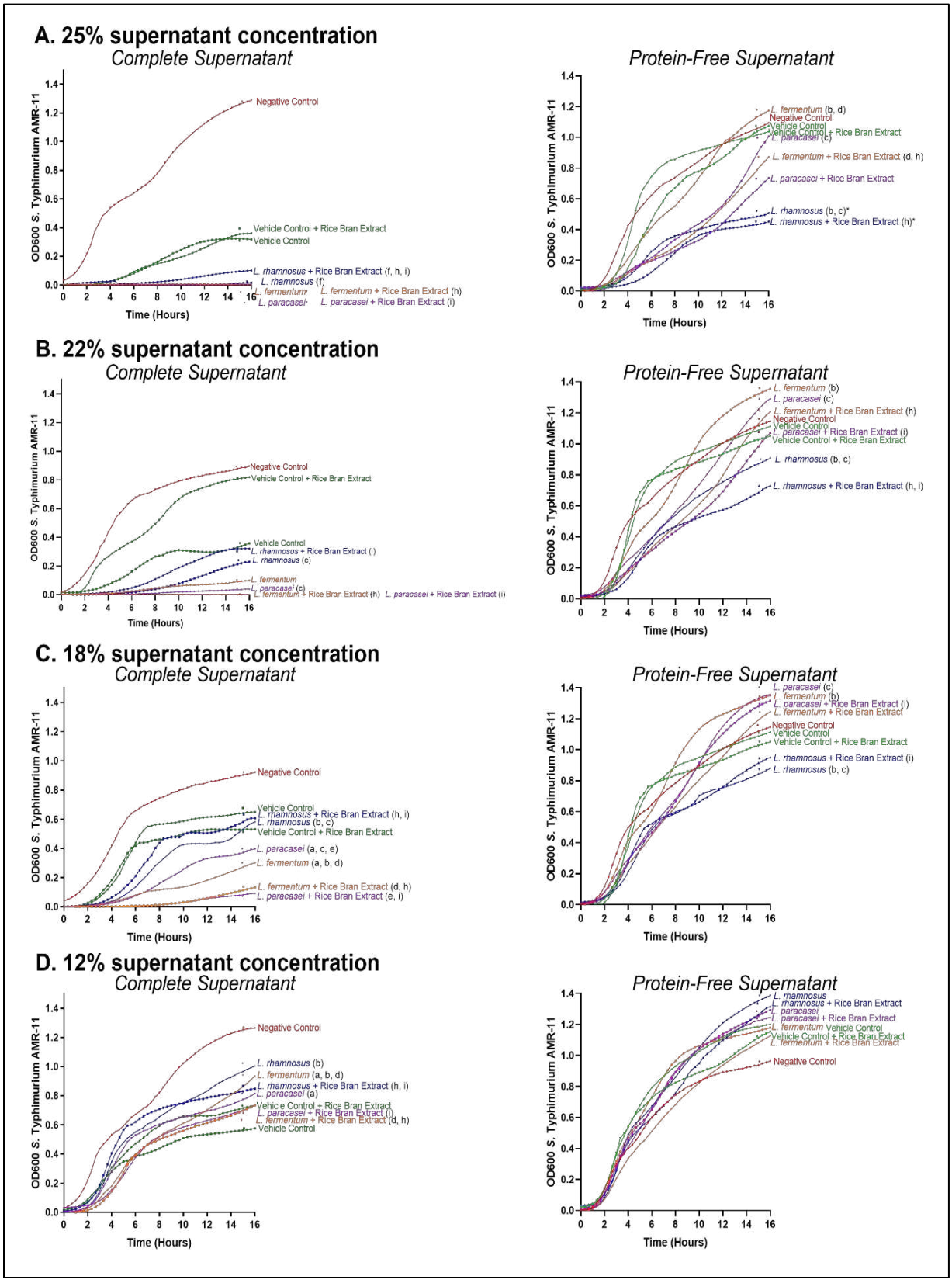
A. 25% supernatant concentration
Complete Supernatant
Protein-Free Supernatant
B. 22% supernatant concentration
Complete Supernatant
Protein-Free Supernatant
C. 18% supernatant concentration
Complete Supernatant
Protein-Free Supernatant
D. 12% supernatant concentration
Complete Supernatant
Protein-Free Supernatant
OD600 S. Typhimurium AMR-11
Time (Hours)
Negative Control
Vehicle Control + Rice Bran Extract
Vehicle Control
L. rhamnosus + Rice Bran Extract (f, h, i)
L. rhamnosus (f)
L. fermentum
L. fermentum + Rice Bran Extract (h)
L. paracasei
L. paracasei + Rice Bran Extract (i)
L. fermentum (b, d)
L. paracasei (c)
L. fermentum + Rice Bran Extract (d, h)
L. paracasei + Rice Bran Extract
L. rhamnosus (b, c)*
L. rhamnosus + Rice Bran Extract (h)*
L. rhamnosus + Rice Bran Extract (i)
L. rhamnosus (c)
L. fermentum + Rice Bran Extract (h)
L. paracasei + Rice Bran Extract (i)
L. rhamnosus (b, c)
L. rhamnosus + Rice Bran Extract (h, i)
L. rhamnosus + Rice Bran Extract (h, i)
L. rhamnosus (b, c)
L. fermentum + Rice Bran Extract (d, h)
L. paracasei + Rice Bran Extract (e, i)
L. paracasei (a, c, e)
L. fermentum (a, b, d)
L. rhamnosus (b)
L. fermentum (a, b, d)
L. paracasei (a)
L. paracasei + Rice Bran Extract (i)
L. fermentum + Rice Bran Extract (d, h)
L. rhamnosus
L. rhamnosus + Rice Bran Extract
L. paracasei
L. paracasei + Rice Bran Extract
L. fermentum Vehicle Control
L. fermentum + Rice Bran Extract

Figure 7.4. Protein-free synbiotic cell-free supernatant prepared with three *Lactobacillus* spp. enhances growth suppression of *Salmonella* Typhimurium compared to *Lactobacillus*-only protein-free supernatant.

*Four supernatant doses (percent supernatant per volume of treatment well) (**A-D**) were examined on non-resistant (**14028s**) antimicrobial-resistant (**AMR-11**) Salmonella. Letters indicate treatments had significantly-different ($p<0.05$) optical densities at 16h following a repeated-measures analysis of variance with a Tukey post-hoc adjustment: **a)** L. paracasei vs. L. fermentum; **b)** L. rhamnosus vs. L. fermentum; **c)** L. fermentum + rice bran extract vs. L. fermentum; **d)** L. paracasei + rice bran extract vs. L. paracasei; **e)** L. rhamnosus + rice bran extract vs. L. rhamnosus; **f)** L. paracasei + rice bran extract vs. L. fermentum + rice bran extract; **g)** L. rhamnosus + rice bran extract vs. L. fermentum + rice bran extract; **h)** L. rhamnosus + rice bran extract vs. L. paracasei + rice bran extract.*

REFERENCES

X

Adio AM, et al. Biosynthesis and defensive function of Ndelta-acetylornithine, a jasmonate-induced Arabidopsis metabolite. The Plant cell. 2011;23(9):3303-18.

Bottacini F, van Sinderen D, Ventura M. Omics of bifidobacteria: research and insights into their health-promoting activities. The Biochemical journal. 2017;474(24):4137-52.

Chung HJ, et al., Metabolomics and Lipidomics Approaches in the Science of Probiotics: A Review. Journal of medicinal food. 2018;21(11):1086-95.

e man, rogosa and sharpe (MRS) agar. In: Corry JEL, Curtis GDW, Baird RM, editors. Progress in Industrial Microbiology. 37: Elsevier; 2003. p. 511-3.

Dicks L.M.T., et al., A Review: The Fate of Bacteriocins in the Human Gastro-Intestinal Tract: Do They Cross the Gut-Blood Barrier? Frontiers in microbiology. 2018;9:2297.

Engevik M.A., Versalovic J., Biochemical Features of Beneficial Microbes: Foundations for Therapeutic Microbiology. Microbiology spectrum. 2017;5(5).

Ghazi I.A., et al., Rice Bran Extracts Inhibit Invasion and Intracellular Replication of Salmonella typhimurium in Mouse and Porcine Intestinal Epithelial Cells. Medicinal and Aromatic Plants. 2016;5(5):10.

Goldstein E.J., Tyrrell K.L., Citron D.M., Lactobacillus species: taxonomic complexity and controversial susceptibilities. Clinical infectious diseases : an official publication of the Infectious Diseases Society of America. 2015;60 Suppl 2:S98-107.

Greulich P., et al., Growth-dependent bacterial susceptibility to ribosome-targeting antibiotics. Molecular systems biology. 2015;11(3):796.

Hemalatha R., et al., Effect of probiotic supplementation on total lactobacilli, bifidobacteria and short chain fatty acids in 2-5-year-old children. Microbial ecology in health and disease. 2017;28(1):1298340.

Hidalgo-Cantabrana C., et al., Bifidobacteria and Their Health-Promoting Effects. Microbiology spectrum. 2017;5(3).

Hiippala K., et al. The Potential of Gut Commensals in Reinforcing Intestinal Barrier Function and Alleviating Inflammation. Nutrients. 2018;10(8).

Kite G.C., Ireland H., Non-protein amino acids of Bocoa (Leguminosae; Papilionoideae). Phytochemistry. 2002;59(2):163-8.

Klemashevich C., et al., Rational identification of diet-derived postbiotics for improving intestinal microbiota function. Current opinion in biotechnology. 2014;26:85-90.

LaRock D.L., Chaudhary A., Miller S.I., Salmonellae interactions with host processes. Nature reviews Microbiology. 2015;13(4):191-205.

Lemarie S., et al. Both the Jasmonic Acid and the Salicylic Acid Pathways Contribute to Resistance to the Biotrophic Clubroot Agent Plasmodiophora brassicae in Arabidopsis. Plant & cell physiology. 2015;56(11):2158-68.

Liang H., et al., Dietary l-Tryptophan Supplementation Enhances the Intestinal Mucosal Barrier Function in Weaned Piglets: Implication of Tryptophan-Metabolizing Microbiota. International journal of molecular sciences. 2018;20(1).

Mao X., et al. Dietary Lactobacillus rhamnosus GG Supplementation Improves the Mucosal Barrier Function in the Intestine of Weaned Piglets Challenged by Porcine Rotavirus. PloS one. 2016;11(1):e0146312.

Marianelli C., Cifani N., Pasquali P., Evaluation of antimicrobial activity of probiotic bacteria against Salmonella enterica subsp. enterica serovar typhimurium 1344 in a common medium under different environmental conditions. Research in microbiology. 2010;161(8):673-80.

Martin R., et al. The potential probiotic Lactobacillus rhamnosus CNCM I-3690 strain protects the intestinal barrier by stimulating both mucus production and cytoprotective response. Scientific reports. 2019;9(1):5398.

McLean I.C., et al., Powering ex vivo tissue models in microfluidic systems. Lab on a chip. 2018;18(10):1399-410.

Oka Y., Ogawa T., Sasaoka K., First evidence for the occurrence of N delta-acetyl-L-ornithine and quantification of the free amino acids in the cultivated mushroom, Pleurotus ostreatus. Journal of nutritional science and vitaminology. 1984;30(1):27-35.

Palmer J.D., et al., Engineered Probiotic for the Inhibition of Salmonella via Tetrathionate-Induced Production of Microcin H47. ACS infectious diseases. 2018;4(1):39-45.

Pessione E., Cirrincione S.,Bioactive Molecules Released in Food by Lactic Acid Bacteria: Encrypted Peptides and Biogenic Amines. Frontiers in microbiology. 2016;7:876.

Plaza-Diaz J., et al., Mechanisms of Action of Probiotics. Advances in nutrition (Bethesda, Md). 2019;10(suppl_1):S49-s66.

Shah P., et al., A microfluidics-based in vitro model of the gastrointestinal human-microbe interface. Nature communications. 2016;7:11535.

Sherman P.M., Ossa J.C., Johnson-Henry K., Unraveling mechanisms of action of probiotics. Nutrition in clinical practice: official publication of the American Society for Parenteral and Enteral Nutrition. 2009;24(1):10-4.

Talwalkar A, Kailasapathy K., The role of oxygen in the viability of probiotic bacteria with reference to L. acidophilus and Bifidobacterium spp. Current issues in intestinal microbiology. 2004;5(1):1-8.

van Baarlen P., Wells J.M., Kleerebezem M., Regulation of intestinal homeostasis and immunity with probiotic lactobacilli. Trends in immunology. 2013;34(5):208-15.

Wan L.Y., et al., Modulation of Intestinal Epithelial Defense Responses by Probiotic Bacteria. Critical reviews in food science and nutrition. 2016;56(16):2628-41.

Wang H., et al., Factors Derived From Escherichia Coli Nissle 1917, Grown in Different Growth Media, Enhance Cell Death in a Model of 5-Fluorouracil-Induced Caco-2 Intestinal Epithelial Cell Damage. Nutrition and Cancer. 2015;67(2):316-26.

Yousefi B., et al., Probiotics importance and their immunomodulatory properties. Journal of cellular physiology. 2019;234:8008-18.

BIBLIOGRAPHY

Aassalia, H. et al., Identification of Harman as the Antibiotic Compound Produced by a Tunicate-Associated Bacterium. Mar Biotechnol, 2003. 5(2): p.163-6.

Abe, M., et al., (2001). Adverse effects of excess lysine in calves. J Anim Sci, 79, 1337-45.

Adio, A.M., et al., Biosynthesis and defensive function of Ndelta-acetylornithine, a jasmonate-induced Arabidopsis metabolite. Plant Cell, 2011. 23(9): p. 3303-18.

Adler, A., N.D. Friedman, and D. Marchaim, Multidrug-Resistant Gram-Negative Bacilli: Infection Control Implications. Infect Dis Clin North Am, 2016. 30(4): p. 967-997.

Agarrwal, R., et al., (2016) Metabolic and transcriptomic changes induced in host during hypersensitive response mediated resistance in rice against the Asian rice gall midge. Rice 9, 5.

Ahmad, F., et al., (2016) Synergistic effect of (+)-pinitol from Saraca asoca with beta-lactam antibiotics and studies on the in silico possible mechanism. J Asian Nat Prod Res 18, 172-83.

Ahmed, I., et al., Microbiome, Metabolome and Inflammatory Bowel Disease. Microorganisms, 2016. 4(2).

Akula, M. K., et al., (2016). Control of the innate immune response by the mevalonate pathway. Nat Immunol, 17, 922-929.

Ali, S.M., R. Siddiqui, and N.A. Khan, Antimicrobial discovery from natural and unusual sources. J Pharm Pharmacol, 2018. 70(10): p. 1287-1300.

Alp Avci, G. (2016). Selection of superior bifidobacteria in the presence of rotavirus. Braz J Med Biol Res, 49, e5562.

Al-Shehri, S., et al., (2015) Breastmilk-saliva interactions boost innate immunity by regulating the oral microbiome in early infancy. PLoS ONE 10.

Aminov R. History of antimicrobial drug discovery: Major classes and health impact. Biochemical Pharmacology. 2017;133:4-19.

Aminnezhad, S., Kermanshahi, R. K. and Ranjbar, R. (2015) Evaluation of synergistic interactions between cell-free supernatant of lactobacillus strains and amikacin and genetamicin against Pseudomonas aeruginosa. Jundishapur J Microbiol, 8.

Antibiotic Resistant Threats in the United States, U.S.D.o.H.a.H. Services, Editor. 2013: Atlanta, Georgia.

Antibiotic/Antimicrobial Resistance (CDC): Biggest Threats and Data, D.o.H.Q.P. (CDC), Editor. 2018: Atlanta, Georgia.

Antibiotics Tested by NARMS, W. National Center for Emerging and Zoonotic Infectious Diseases (NCEZID): Division of Foodborne, and Environmental Diseases (DFWED), Editor. 2018, Centers for Disease Control and Prevention: Atlanta, Georgia. USA.

Borresen, E.C. and E.P. Ryan, Chapter 22 - Rice Bran: A Food Ingredient with Global Public Health Opportunities, in Wheat and Rice in Disease Prevention and Health, R.R. Watson, V.R. Preedy, and S. Zibadi, Editors. 2014, Academic Press: San Diego. p. 301-310.

Chen, Y.T., et al., A combination of Lactobacillus mali APS1 and dieting improved the efficacy of obesity treatment via manipulating gut microbiome in mice. Sci Rep, 2018. 8(1): p. 6153.

Chlebicz, A. and K. Slizewska, Campylobacteriosis, Salmonellosis, Yersiniosis, and Listeriosis as Zoonotic Foodborne Diseases: A Review. Int J Environ Res Public Health, 2018. 15(5).

Cortes-Penfield, N.W., et al., Prospects and Challenges in the Development of a Norovirus Vaccine. Clin Ther, 2017. 39(8): p. 1537-1549.

Arbulu, M., et al., (2015) Untargeted metabolomic analysis using liquid chromatography quadrupole time-of-flight mass spectrometry for non-volatile profiling of wines. Analytica Chimica Acta 858, 32-41.

Arshad, N., et al., (2008) Effect of Peganum harmala or its beta-carboline alkaloids on certain antibiotic resistant strains of bacteria and protozoa from poultry. Phytother Res 22, 1533-8.

Atlanta, Georgia. USA: Centers for Disease Control and Prevention; 2018.Baker KE, Ditullio KP, Neuhard J, Kelln RA. Utilization of orotate as a pyrimidine source by Salmonella typhimurium and Escherichia coli requires the dicarboxylate transport protein encoded by dctA. Journal of bacteriology. 1996;178(24):7099-105.

Atroshi F., Rizzo A., Westermarck T. and Ali-vehmas T. (1998) Effects of tamoxifen, melatonin, coenzyme Q10, and L-carnitine supplementation on bacterial growth in the presence of mycotoxins. Pharmacol Res 38, 289–295.

Auteri, M., Zizzo, M. G. and Serio, R. (2015). GABA and GABA receptors in the gastrointestinal tract: from motility to inflammation. Pharmacol Res. 93, 11-21.

Aviello, G., Romano, B., and Izzo, A. A. 2008. Cannabinoids and gastrointestinal motility: animal and human studies. Eur Rev Med Pharmacol Sci, 12 Suppl 1, 81-93.

Baquero F, Martínez J-L. Interventions on Metabolism: Making Antibiotic-Susceptible Bacteria. mBio. 2017;8(6):e01950-17.

Baraniuk, J.N., et al., Carnosine treatment for gulf war illness: a randomized, controlled trial. (2013). Glob J Health Sci. 5:3, 69-81.

Barcelo, A., et al., (2001). Effect of bile salts on colonic mucus secretion in isolated vascularly perfused rat colon. Dig Dis Sci, 46, 1223-31.

Barenholz, Y. (2004). Sphingomyelin and cholesterol: from membrane biophysics and rafts to potential medical applications. Subcell Biochem. 37, 167-215.

Bauchart-Thevret, C., et al., (2009). Sulfur amino acid deficiency upregulates intestinal methionine cycle activity and suppresses epithelial growth in neonatal pigs. Am J Physiol Endocrinol Metab. 296, E1239-50.

Bazanella, M., et al., D., 2017. Randomized controlled trial on the impact of early-life intervention with bifidobacteria on the healthy infant fecal microbiota and metabolome. Am J Clin Nutr 106: 1274-1286. 10.3945/ajcn.117.157529

Bibel, D.J., Aly, R. and Shinefield, H.R., 1992. Inhibition of microbial adherence by sphinganine. Can J Microbiol 38: 983-985.

Black, B. A., et al., (2013) Antifungal hydroxy fatty acids produced during sourdough fermentation: microbial and enzymatic pathways, and antifungal activity in bread. Appl Environ Microbiol 79, 1866-1873.

Bottacini F, van Sinderen D, Ventura M. Omics of bifidobacteria: research and insights into their health-promoting activities. The Biochemical journal. 2017;474(24):4137-52.

Böttcher, C., et al., (2014) The biosynthetic pathway of indole-3-carbaldehyde and indole-3-carboxylic acid derivatives in Arabidopsis. Plant Physiol 165, 841-853.

Bou Ghanem, E.N., et al., 2017. The Alpha-Tocopherol Form of Vitamin E Boosts Elastase Activity of Human PMNs and Their Ability to Kill Streptococcus pneumoniae. Front Cell Infect Microbiol 7: 161. 10.3389/fcimb.2017.00161

Boyd, J. M., Teoh, W. P. and Downs, D. M. (2012). Decreased transport restores growth of a Salmonella enterica apbC mutant on tricarballylate. J Bacteriol 194, 576-583.

Brocker, C., Thompson, D. C., and Vasiliou, V. (2012). The role of hyperosmotic stress in inflammation and disease. Biomolecular concepts, 3, 345-364.

Brown, D. G., et al., (2016) Metabolomics and metabolic pathway networks from human colorectal cancers, adjacent mucosa, and stool. Cancer Metab 4, 11.

Brown, D.G., et al., 2017. Heat-stabilised rice bran consumption by colorectal cancer survivors modulates stool metabolite profiles and metabolic networks: a randomised controlled trial. Br J Nutr 117: 1244-1256. 10.1017/s0007114517001106

Brundige, D. R., et al., (2010). Consumption of pasteurized human lysozyme transgenic goats' milk alters serum metabolite profile in young pigs. Transgenic Research, 19, 563-574.

Buccioni, A., et al., (2012). Lipid metabolism in the rumen: New insights on lipolysis and biohydrogenation with an emphasis on the role of endogenous plant factors. Anim Feed Sci and Technol. 174, 1-25.

Bunesova, V., Lacroix, C. and Schwab, C., 2016. Fucosyllactose and L-fucose utilization of infant Bifidobacterium longum and Bifidobacterium kashiwanohense. BMC Microbiol 16: 248-248. 10.1186/s12866-016-0867-4

Caridi, A. (2002) Selection of Escherichia coli-inhibiting strains of Lactobacillus paracasei subsp. paracasei. J Ind Microbiol Biotechnol 29, 303-8.

CDC, (DHQP). Atlanta, Georgia, USA.: Centers for Disease Control and Prevention; 2018.

CDC, Antibiotic/Antimicrobial Resistance (AR/AMR): Biggest Threats and Data, D.o.H.Q.P. (DHQP), 2018: Atlanta, Georgia.

CDC, Tracking antibiotic resistance in dangerous bacteria that affect people and cattle, D.o.F. National Center for Emerging and Zoonotic Infectious Diseases (NCEZID), Waterborne, and Environmental Diseases (DFWED), 2019, Centers for Disease Control: Atlanta, Georgia.

Celiberto, L.S., et al., 2017. Effect of a probiotic beverage consumption (Enterococcus faecium CRL 183 and Bifidobacterium longum ATCC 15707) in rats with chemically induced colitis. PLoS One 12: e0175935. 10.1371/journal.pone.0175935

Charnock, C., Brudeli, B. and Klaveness, J. (2004) Evaluation of the antibacterial efficacy of diesters of azelaic acid. Eur J Pharm Sci 21, 589-96.

Chemsa, A.E., et al., 2018. Chemical composition, antioxidant, anticholinesterase, antimicrobial and antibiofilm activities of essential oil and methanolic extract of Anthemis stiparum subsp. sabulicola (Pomel) Oberpr. Microb Pathog 119: 233-240. 10.1016/j.micpath.2018.04.033

Cheng X. and van deer Vort M. and Raaijmakers J.M., (2015) Gac-mediated changes in pyrroquinoline quinone biosynthesis enhance the antimicrobial activity of Pseudomonas fluorescens SBW25. Environ Microbiol Rep 7, 139–147.

Chenoll, E., et al., (2016). Identification of a Peptide Produced by Bifidobacterium longum CECT 7210 with Antirotaviral Activity. Front Microbiol. 7:655.

Chiang, S.S. and Pan, T.M. (2012) Beneficial effects of Lactobacillus paracasei subsp. paracasei NTU 101 and its fermented products. J Appl Microbiol and Biotechnol 93, 903-916.

Chin, Y.P., et al., (2012) Bactericidal activity of soymilk fermentation broth by in vitro and animal models. J Med Food 15, 520-526.

Chung HJ, et al., Metabolomics and Lipidomics Approaches in the Science of Probiotics: A Review. Journal of medicinal food. 2018;21(11):1086-95.

Clarke, E. and Desselberger, U. (2015). Correlates of protection against human rotavirus disease and the factors influencing protection in low-income settings. Mucosal Immunol. 8, 1-17.

Clarke, G., et al., (2014) Minireview: Gut microbiota: the neglected endocrine organ. Mol Endocrinol 28, 1221-38.

Collino, S., et al., (2013). Metabolic signatures of extreme longevity in northern Italian centenarians reveal a complex remodeling of lipids, amino acids, and gut microbiota metabolism. PLoS One, 8, e56564.

Consortium, T.U., 2018. UniProt: a worldwide hub of protein knowledge. Nucleic Acids Res 47: D506-D515. 10.1093/nar/gky1049

Cook, G. M., Wells, J. E. and Russell, J. B. (1994) Ability of Acidaminococcus fermentans to oxidize trans-aconitate and decrease the accumulation of tricarballylate, a toxic end product of ruminal fermentation. Appl Environ Microbiol 60, 2533-7.

Cordaro, M., et al., (2016). Adelmidrol, a Palmitoylethanolamide Analogue, as a New Pharmacological Treatment for the Management of Inflammatory Bowel Disease. Molec Pharmacol, 90, 549-561.

Cowan, M. M. (1999) Plant products as antimicrobial agents. Clin Microbiol Rev 12, 564-582.

Cowan, T.E., et al., 2014. Chronic coffee consumption in the diet-induced obese rat: impact on gut microbiota and serum metabolomics. J Nutr Biochem 25: 489-495. 10.1016/j.jnutbio.2013.12.009

D'Argenio, G., et al., (2005). Differential expression of multiple transglutaminases in human colon: impaired keratinocyte transglutaminase expression in ulcerative colitis. Gut, 54, 496-502.

De Jong, P. R., González-Navajas, J. M., and Jansen, N. J. G. (2016). The digestive tract as the origin of systemic inflammation. Crit Care, 20, 279.

Derkach, A., et al., 2017. Effects of dietary sodium on metabolites: the Dietary Approaches to Stop Hypertension (Maruyama *et al.*)-Sodium Feeding Study. Am J Clin Nutr 106: 1131-1141. 10.3945/ajcn.116.150136

Diarra, M.S., et al., Antibiotic resistance and diversity of Salmonella enterica serovars associated with broiler chickens. J Food Prot, 2014. 77(1): p. 40-9.

Diarrhoeal disease. [internet] 2013 Apr. 2013 [cited 2016 Dec. 3]; Available from: http://www.who.int/mediacentre/factsheets/fs330/en/.

Dieterich, W., M. Schink, and Y. Zopf, Microbiota in the Gastrointestinal Tract. Med Sci, 2018. 6(4).

Donado-Godoy, P., et al., Counts, serovars, and antimicrobial resistance phenotypes of Salmonella on raw chicken meat at retail in Colombia. J Food Prot, 2014. 77(2): p. 227-35.

Engevik, M.A. and J. Versalovic, Biochemical Features of Beneficial Microbes: Foundations for Therapeutic Microbiology. Microbiol Spectr, 2017. 5(5).

Dicks L.M.T., et al., A Review: The Fate of Bacteriocins in the Human Gastro-Intestinal Tract: Do They Cross the Gut-Blood Barrier? Frontiers in microbiology. 2018;9:2297.

Distrutti E, Monaldi L, Ricci P, Fiorucci S. Gut microbiota role in irritable bowel syndrome: New therapeutic strategies. World journal of gastroenterology. 2016;22(7):2219-41.

Druart, C., et al., (2014) Modulation of the gut microbiota by nutrients with prebiotic and probiotic properties. Adv Nutr 5, 624S-633S.

e man, rogosa and sharpe (MRS) agar. In: Corry JEL, Curtis GDW, Baird RM, editors. Progress in Industrial Microbiology. 37: Elsevier; 2003. p. 511-3.

Engels, F., et al., (1996). Preferential formation of 13-hydroxylinoleic acid by human peripheral blood eosinophils. Prostaglandins, 52, 117-24.

Engevik M.A., Versalovic J., Biochemical Features of Beneficial Microbes: Foundations for Therapeutic Microbiology. Microbiology spectrum. 2017;5(5).

Fabian, C. and Ju, Y.H., 2011. A review on rice bran protein: its properties and extraction methods. Crit Rev Food Sci Nutr 51: 816-827. 10.1080/10408398.2010.482678

FAO, (2006) Probiotics in food: Health and nutritional properties and guidelines for evaluation. FAO Food Nutr Pap 85, 50.

Florez-Cuadrado, D., et al., Antimicrobial Resistance in the Food Chain in the European Union. Adv Food Nutr Res, 2018. 86: p. 115-136.

Forster, G.M., et al., Rice varietal differences in bioactive bran components for inhibition of colorectal cancer cell growth. Food Chem, 2013. 141(2): p. 1545-52.

Founou, L.L., et al., Antibiotic Resistance in Food Animals in Africa: A Systematic Review and Meta-Analysis. Microb Drug Resist, 2018. 24(5): p. 648-665.

Ghazi, I.A., et al., Rice Bran Extracts Inhibit Invasion and Intracellular Replication of Salmonella typhimurium in Mouse and Porcine Intestinal Epithelial Cells. Medicinal and Aromatic Plants, 2016. 271(5).

Fernandez J, Guerra B, Rodicio MR. Resistance to Carbapenems in Non-Typhoidal Salmonella enterica Serovars from Humans, Animals and Food. Veterinary sciences. 2018;5(2).

Fischer, C.L., et al., 2013. Sphingoid Bases Are Taken Up by Escherichia coli and Staphylococcus aureus and Induce Ultrastructural Damage. Skin Pharmacology and Physiology 26: 36-44. 10.1159/000343175

Fix, J.A., et al., 1986. Acylcarnitines: drug absorption-enhancing agents in the gastrointestinal tract. Am J Physiol 251: G332-340. 10.1152/ajpgi.1986.251.3.G332

Frigolet, M. E. and Gutiérrez-Aguilar, R. (2017). The Role of the Novel Lipokine Palmitoleic Acid in Health and Disease. Adv in Nutr: An Internat Rev J, 8, 173S-181S.

Fujimura, K. E., et al., (2016). Neonatal gut microbiota associates with childhood multisensitized atopy and T cell differentiation. Nat Med, 22, 1187-1191.

Gadang, V. P., et al., (2008) Evaluation of antibacterial activity of whey protein isolate coating incorporated with nisin, grape seed extract, malic acid, and EDTA on a turkey frankfurter system. J Food Sci 73, M389-94.

Gagnon, M., et al., 2015. Bioaccessible antioxidants in milk fermented by Bifidobacterium longum subsp. longum strains. BioMed research international 2015: 169381-169381. 10.1155/2015/169381

Gao, C., Major et al., (2015). Histamine H2 Receptor-Mediated Suppression of Intestinal Inflammation by Probiotic Lactobacillus reuteri. MBio. 6:6.

Garvey MI, Rahman MM, Gibbons S, Piddock LJ. Medicinal plant extracts with efflux inhibitory activity against Gram-negative bacteria. International journal of antimicrobial agents. 2011;37(2):145-51.

Gertsch, J. (2017). Cannabimimetic phytochemicals in the diet – an evolutionary link to food selection and metabolic stress adaptation?. British J Pharmacol.

Ghazi I.A., et al., Rice Bran Extracts Inhibit Invasion and Intracellular Replication of Salmonella typhimurium in Mouse and Porcine Intestinal Epithelial Cells. Medicinal and Aromatic Plants. 2016;5(5):10.

Ghosal, A., Jellbauer, S., Kapadia, R., Raffatellu, M. and Said, H. M. (2015). Salmonella infection inhibits intestinal biotin transport: cellular and molecular mechanisms. Am J Physiol - Gastrointest Liver Physiol. 309:2.

Goldstein E.J., Tyrrell K.L., Citron D.M., Lactobacillus species: taxonomic complexity and controversial susceptibilities. Clinical infectious diseases : an official publication of the Infectious Diseases Society of America. 2015;60 Suppl 2:S98-107.

Goodgame, R. W. (1999). Viral infections of the gastrointestinal tract. Curr Gastroenterol Rep, 1, 292-300.

Goodyear, A., et al., (2015) Dietary rice bran supplementation prevents Salmonella colonization differentially across varieties and by priming intestinal immunity. J Funct Foods 18, Part A, 653-664.

Henderson, A.J., et al., Consumption of rice bran increases mucosal immunoglobulin A concentrations and numbers of intestinal Lactobacillus spp. J Med Food, 2012. 15(5): p. 469-75.

Goyal, N., et al., (2015). Effect of chenodeoxycholic acid and sodium hydrogen sulfide in dinitro benzene sulfonic acid (DNBS)-Induced ulcerative colitis in rats. Pharmacol Rep, 67, 616-23.

Greulich P., et al., Growth-dependent bacterial susceptibility to ribosome-targeting antibiotics. Molecular systems biology. 2015;11(3):796-.

Guttíerez, C., et al., (2007). Does an L-glutamine-containing, Glucose-free, Oral Rehydration Solution Reduce Stool Output and Time to Rehydrate in Children with Acute Diarrhoea? A Double-blind Randomized Clinical Trial. J Health, Popul, and Nutr, 25, 278-284.

Han F., et al. Effects of Whole-Grain Rice and Wheat on Composition of Gut Microbiota and Short-Chain Fatty Acids in Rats. Journal of agricultural and food chemistry. 2018;66(25):6326-35.

Han, B., et al., 2019. High doses of sodium ascorbate act as a prooxidant and protect gnotobiotic brine shrimp larvae (Artemia franciscana) against Vibrio harveyi infection coinciding with heat shock protein 70 activation. Dev Comp Immunol 92: 69-76. 10.1016/j.dci.2018.11.007

Han, X., et al. (2015). Apolipoprotein CIII regulates lipoprotein-associated phospholipase A2 expression via the MAPK and NFκB pathways. Biol. Open 4, 661–665. doi: 10.1242/bio.201410900

Harris H.M.B., et al., Draft Genome Sequence of Lactobacillus fermentum Lf2, an Exopolysaccharide-Producing Strain Isolated from Argentine Cheese. Microbiology resource announcements. 2018;7(18).

Hasobe, M., et al., (1989). Elucidation of the mechanism by which homocysteine potentiates the anti-vaccinia virus effects of the S-adenosylhomocysteine hydrolase inhibitor 9-(trans-2',trans-3'-dihydroxycyclopent4'-enyl)-adenine. Mol Pharmacol. 36:3, 490-96.

Hedrick, C.E., Separations by reversed-phase chromatography, in Chemistry. 1964, Iowa State University: Ames, Iowa.

Helmick, R.A., et al., Imidazole antibiotics inhibit the nitric oxide dioxygenase function of microbial flavohemoglobin. Antimicrob Agents Chemother, 2005. 49(5): p. 1837-43.

Hemalatha R., et al., Effect of probiotic supplementation on total lactobacilli, bifidobacteria and short chain fatty acids in 2-5-year-old children. Microbial ecology in health and disease. 2017;28(1):1298340.

Henderson, A.J., et al., 2012a. Consumption of rice bran increases mucosal immunoglobulin A concentrations and numbers of intestinal Lactobacillus spp. J Med Food 15: 469-475. 10.1089/jmf.2011.0213

Henderson, A.J., et al., 2012b. Chemopreventive properties of dietary rice bran: current status and future prospects. Adv Nutr 3: 643-653. 10.3945/an.112.002303

Hentchel, K. L. and Escalante-Semerena, J. C. (2015) In Salmonella enterica, the Gcn5-related acetyltransferase MddA (formerly YncA) acetylates methionine sulfoximine and methionine sulfone, blocking their toxic effects. J Bacteriol 197, 314-25.

Heredia-Castro, P. Y., et al., (2015) Antimicrobial activity and partial characterization of bacteriocin-like inhibitory substances produced by Lactobacillus spp. isolated from artisanal mexican cheese. J Dairy Sci 98, 8285-93.

Hernandez-Alonso, P., et al., 2017. Effect of pistachio consumption on the modulation of urinary gut microbiota-related metabolites in prediabetic subjects. J Nutr Biochem 45: 48-53. 10.1016/j.jnutbio.2017.04.002

Heuberger, A.L., et al., Metabolomic and functional genomic analyses reveal varietal differences in bioactive compounds of cooked rice. PLoS One, 2010. 5(9): p. e12915.

Hidalgo-Cantabrana C., et al., Bifidobacteria and Their Health-Promoting Effects. Microbiology spectrum. 2017;5(3).

Hiippala K., et al. The Potential of Gut Commensals in Reinforcing Intestinal Barrier Function and Alleviating Inflammation. Nutrients. 2018;10(8).

Hinton, A., Jr. and Ingram, K. D. (2000) Use of oleic acid to reduce the population of the bacterial flora of poultry skin. J Food Prot 63, 1282-6.

Hlavacek, J., et al., Inhibitors of N(alpha)-acetyl-L-ornithine deacetylase: synthesis, characterization and analysis of their inhibitory potency. Amino Acids, 2010. 38(4): p. 1155-64.

Holschbach, C.L. and S.F. Peek, Salmonella in Dairy Cattle. Vet Clin North Am Food Anim Pract, 2018. 34(1): p. 133-154.

Hoshi, T. and Heinemann, S. H. (2001) Regulation of cell function by methionine oxidation and reduction. J Physiol (Khanna et al.) 531, 1-11.

Hyser, J. M., et al., (2013). Activation of the Endoplasmic Reticulum Calcium Sensor STIM1 and Store-Operated Calcium Entry by Rotavirus Requires NSP4 Viroporin Activity. J Virol. 87, 13579-13588.

Iannino, F., et al., Development of a dual vaccine for prevention of Brucella abortus infection and Escherichia coli O157:H7 intestinal colonization. Vaccine, 2015. 33(19): p. 2248-53.

Ishida, T., et al., (2013). Linoleoyl ethanolamide reduces lipopolysaccharide-induced inflammation in macrophages and ameliorates 2,4-dinitrofluorobenzene-induced contact dermatitis in mice. Eur J Pharmacol, 699, 6-13.

J.M. Berg, J.L.T., and L. Stryer, Carbon Atoms of Degraded Amino Acids Emerge as Major Metabolic Intermediates. 5 ed. Biochemistry. 2002, New York: W. H. Freeman and Company.

Jensen K.F., Apparent involvement of purines in the control of expression of Salmonella typhimurium pyr genes: analysis of a leaky guaB mutant resistant to pyrimidine analogs. Journal of bacteriology. 1979;138(3):731-8.

Jones, S.E., et al., Cyclopropane fatty acid synthase mutants of probiotic human-derived Lactobacillus reuteri are defective in TNF inhibition. Gut Microbes, 2011. 2(2): p.69-79.

Jourdan, N., et al., (1998). Rotavirus Infection Reduces Sucrase-Isomaltase Expression in Human Intestinal Epithelial Cells by Perturbing Protein Targeting and Organization of Microvillar Cytoskeleton. J Virol, 72, 7228-7236.

Kandasamy, S., et al., Unraveling the Differences between Gram-Positive and Gram-Negative Probiotics in Modulating Protective Immunity to Enteric Infections. Front Immunol, 2017. 8: p. 334.

Kanehisa, M. and Goto, S., 2000., KEGG: kyoto encyclopedia of genes and genomes. Nucleic Acids Res 28: 27-30. 10.1093/nar/28.1.27

Kanehisa, M., et al., 2019. New approach for understanding genome variations in KEGG. Nucleic Acids Res 47: D590-d595. 10.1093/nar/gky962

Kanehisa, M., et al., KEGG: new perspectives on genomes, pathways, diseases and drugs. Nucleic Acids Res 45: D353-d361. 10.1093/nar/gkw1092

Kanjan P., Hongpattarakere T., Antibacterial metabolites secreted under glucose-limited environment of the mimicked proximal colon model by lactobacilli abundant in infant feces. Applied microbiology and biotechnology. 2016;100(17):7651-64.

Kanjan, P. and T. Hongpattarakere, Prebiotic efficacy and mechanism of inulin combined with inulin-degrading Lactobacillus paracasei I321 in competition with Salmonella. Carbohydr Polym, 2017. 169: p. 236-244.

Katyal, R., et al., (1999). Effect of rotavirus infection on small gut pathophysiology in a mouse model. J Gastroenterol Hepatol. 14, 779-84.

Kaur, A., Jassal, V., Thind, S. S. and Aggarwal, P. (2012) Rice bran oil an alternate bakery shortening. J Food Sci Technol 49, 110-4.

Kavitha, A., Prabhakar, P., Vijayalakshmi, M. and Venkateswarlu, Y. (2010) Purification and biological evaluation of the metabolites produced by Streptomyces sp. TK-VL_333. Res Microbiol 161, 335-45.

Kemppainen, K.M., et al., Factors that Increase Risk of Celiac Disease Autoimmunity Following a Gastrointestinal Infection in Early Life. Clinical Gastroenterology and Hepatology.

Keush, G.T., et al. (2016). “Diarrheal Diseases,” in Reproductive, Maternal, Newborn and Child Health: Disease Control Priorities, ed. Laxminarayan R., et al. (Washington DC: The World Bank).

Khan, M. T., Van Dijil, J. M., and Harmsen, H. J. M. (2014). Antioxidants Keep the Potentially Probiotic but Highly Oxygen-Sensitive Human Gut Bacterium Faecalibacterium prausnitzii Alive at Ambient Air. PLoS ONE, 9, e96097.

Kim, G. R., et al., (2014) Combined mass spectrometry-based metabolite profiling of different pigmented rice (Oryza sativa L.) seeds and correlation with antioxidant activities. Molecules 19, 15673-86.

Kim, J.M., et al., 2018. Safety Evaluations of Bifidobacterium bifidum BGN4 and Bifidobacterium longum BORI. Int J Mol Sci 19. 10.3390/ijms19051422

Kim, Y., et al., (2012). Novel triacsin C analogs as potential antivirals against rotavirus infections. Eur J Med Chem. 50, 311-8.

Kite G.C., Ireland H., Non-protein amino acids of Bocoa (Leguminosae; Papilionoideae). Phytochemistry. 2002;59(2):163-8.

Klemashevich C., et al., Rational identification of diet-derived postbiotics for improving intestinal microbiota function. Current opinion in biotechnology. 2014;26:85-90.

Kohanski MA, Dwyer DJ, Collins JJ. How antibiotics kill bacteria: from targets to networks. Nature reviews Microbiology. 2010;8(6):423-35.

Koistinen, V. M., et al., (2016) Changes in the phytochemical profile of rye bran induced by enzymatic bioprocessing and sourdough fermentation. Food Res Int [no pagination].

Kondo, N., M. Murata, and K. Isshiki, Efficiency of sodium hypochlorite, fumaric acid, and mild heat in killing native microflora and Escherichia coli O157:H7, Salmonella typhimurium DT104, and Staphylococcus aureus attached to fresh-cut lettuce. J Food Prot, 2006. 69(2): p. 323-9.

Kondoh, T., Mallick, H. N. and Torii, K. (2009). Activation of the gut-brain axis by dietary glutamate and physiologic significance in energy homeostasis. Am J Clin Nutr. 90, 832S-837S.

Kong, W., et al., (2015). Biomarkers for assessing mucosal barrier dysfunction induced by chemotherapy: Identifying a rapid and simple biomarker. Clin Lab, 61, 371-8.

Kosová, M., et al., (2015) Antimicrobial effect of 4-hydroxybenzoic acid ester with glycerol. J Clin Pharm Ther 40, 436-440.

Kumar A., et al. Dietary rice bran promotes resistance to Salmonella enterica serovar Typhimurium colonization in mice. BMC microbiology. 2012;12:71.

Kwon, D.H. and Lu, C. D. (2007) Polyamine Effects on antibiotic susceptibility in bacteria. Antimicrob Agents Chemother 51, 2070-2077.

Lakin SM, et al. MEGARes: an antimicrobial resistance database for high throughput sequencing. Nucleic acids research. 2017;45(D1):D574-D80.

Lamas A., et al., A comprehensive review of non-enterica subspecies of Salmonella enterica. Microbiological research. 2018;206:60-73.

Lan, R. and I. Kim, Effects of organic acid and medium chain fatty acid blends on the performance of sows and their piglets. Anim Sci J, 2018. 89(12): p. 1673-1679.

LaRock D.L., Chaudhary A., Miller S.I., Salmonellae interactions with host processes. Nature reviews Microbiology. 2015;13(4):191-205.

Lazar, V., et al., Gut Microbiota, Host Organism, and Diet Trialogue in Diabetes and Obesity. Front Nutr, 2019. 6: p. 21.

Lee, T., et al., (2017). Oral versus intravenous iron replacement therapy distinctly alters the gut microbiota and metabolome in patients with IBD. Gut 66: 863-871. 10.1136/gutjnl-2015-309940

Lee, Y., et al., (2016). Endocannabinoids in the gastrointestinal tract. Am J Physiol Gastrointest Liver Physiol, 311, G655-G666.

Lei, S., et al., (2016). High Protective Efficacy of Probiotics and Rice Bran against Human Norovirus Infection and Diarrhea in Gnotobiotic Pigs. Front Microbiol. 7:1699.

Lemarie S., et al. Both the Jasmonic Acid and the Salicylic Acid Pathways Contribute to Resistance to the Biotrophic Clubroot Agent Plasmodiophora brassicae in Arabidopsis. Plant & cell physiology. 2015;56(11):2158-68.

Lepine, A. and P. de Vos, Synbiotic Effects of the Dietary Fiber Long-Chain Inulin and Probiotic Lactobacillus acidophilus W37 Can be Caused by Direct, Synergistic Stimulation of Immune Toll-Like Receptors and Dendritic Cells. Mol Nutr Food Res, 2018: p. e1800251.

Li, S.A., et al., (2018), Dietary myo-inositol deficiency decreased intestinal immune function related to NF-kappaB and TOR signaling in the intestine of young grass carp (Ctenopharyngodon idella). Fish Shellfish Immunol 76: 333-346. 10.1016/j.fsi.2018.03.017

Li, Y., et al., (2012), A novel role of intestine epithelial GABAergic signaling in regulating intestinal fluid secretion. Am J Physiol Gastrointest Liver Physiol. 303, G453-60.

Liang H., et al., Dietary l-Tryptophan Supplementation Enhances the Intestinal Mucosal Barrier Function in Weaned Piglets: Implication of Tryptophan-Metabolizing Microbiota. International journal of molecular sciences. 2018;20(1).

Lievin-Le Moal, V., Amsellem, R. and Servin, A. L. (2011). Impairment of swimming motility by antidiarrheic Lactobacillus acidophilus strain LB retards internalization of Salmonella enterica serovar Typhimurium within human enterocyte-like cells. Antimicrob Agents Chemother 55, 4810-20.

Lin, H. C., et al., (2001). Slowing of gastrointestinal transit by oleic acid: a preliminary report of a novel, nutrient-based treatment in humans. Dig Dis Sci, 46, 223-9.

Liu, G., et al., (2014). Metabolomic Strategy for the Detection of Metabolic Effects of Spermine Supplementation in Weaned Rats. J Agr Food Chem, 62, 9035-9042.

Liu, G., et al., 2017. L-Glutamine and L-arginine protect against enterotoxigenic Escherichia coli infection via intestinal innate immunity in mice. Amino Acids 49: 1945-1954. 10.1007/s00726-017-2410-9

Lohan, S., et al., In vitro and in vivo antibacterial evaluation and mechanistic study of ornithine based small cationic lipopeptides against antibiotic resistant clinical isolates. Eur J Med Chem, 2014. 88: p. 19-27.

Luoma A, et al., Effect of synbiotic supplementation on layer production and cecal Salmonella load during a Salmonella challenge. Poultry science. 2017;96(12):4208-16.

Lustgarten, M. S., and Fielding, R. A. (2016). Metabolites Associated With Circulating Interleukin-6 in Older Adults. J Gerontol A Biol Sci Med Sci.

MandØe, J. M., et al., (2015). The 2-monoacylglycerol moiety of dietary fat appears to be responsible for the fat-induced release of GLP-1 in humans. Am J Clin Nutr, 102:3, 548-55.

Mao X., et al. Dietary Lactobacillus rhamnosus GG Supplementation Improves the Mucosal Barrier Function in the Intestine of Weaned Piglets Challenged by Porcine Rotavirus. PloS one. 2016;11(1):e0146312.

Marianelli C., Cifani N, Pasquali P. Evaluation of antimicrobial activity of probiotic bacteria against Salmonella enterica subsp. enterica serovar typhimurium 1344 in a common medium under different environmental conditions. Research in microbiology. 2010;161(8):673-80.

Markazi, A., et al., Effects of drinking water synbiotic supplementation in laying hens challenged with Salmonella. Poult Sci, 2018. 97(10): p. 3510-3518.

Markowiak P, Slizewska K. Effects of Probiotics, Prebiotics, and Synbiotics on Human Health. Nutrients. 2017;9(9).

Martin R., et al., The potential probiotic Lactobacillus rhamnosus CNCM I-3690 strain protects the intestinal barrier by stimulating both mucus production and cytoprotective response. Scientific reports. 2019;9(1):5398.

Martin-Arjol, I., et al., (2010) Identification of oxylipins with antifungal activity by LC-MS/MS from the supernatant of Pseudomonas 42A2. Chem Phys Lipids 163, 341-6.

Martinot, E., et al., (2017). Bile acids and their receptors. Mol Aspects Med. doi: 10.1016/j.mam.2017.01.006

Matty, A. J., and Seshardi, B. (1965), Effect of thyroxine on the isolated rat intestine. Gut, 6, 200-202.

Mcdevitt, J. and Goldman, P. (1991) Effect of the intestinal flora on the urinary organic acid profile of rats ingesting a chemically simplified diet. Food Chem Toxicol 29, 107-13.

Mcgavigan, A. K., et al., (2015). l-cysteine suppresses ghrelin and reduces appetite in rodents and humans. Internat J Obesity. 39, 447-455.

McIntosh, K., et al., 2017. FODMAPs alter symptoms and the metabolome of patients with IBS: a randomised controlled trial. Gut 66: 1241-1251. 10.1136/gutjnl-2015-311339

McLean I.C., et al., Powering ex vivo tissue models in microfluidic systems. Lab on a chip. 2018;18(10):1399-410.

Mechoulam, R., et al., (1995). Identification of an endogenous 2-monoglyceride, present in canine gut, that binds to cannabinoid receptors. Biochem Pharmacol. 50, 83-90.

Mehmood, M. H., et al., (2014). Pharmacological basis for the medicinal use of Carissa carandas in constipation and diarrhea. J Ethnopharmacol, 153, 359-67.

Mhongole, O.J., et al., Characterization of Salmonella spp. from wastewater used for food production in Morogoro, Tanzania. World J Microbiol Biotechnol, 2017. 33(3): p. 42.

Michael, G.B. and S. Schwarz, Antimicrobial resistance in zoonotic nontyphoidal Salmonella: an alarming trend? Clin Microbiol Infect, 2016. 22(12): p. 968-974.

Ming, T., et al., A metabolomics and proteomics study of the Lactobacillus plantarum in the grass carp fermentation. BMC Microbiol, 2018. 18(1): p. 216.

Mounce, B. C., et al., (2016). Inhibition of Polyamine Biosynthesis Is a Broad-Spectrum Strategy against RNA Viruses. J Virol, 90, 9683-9692.

Mozzi, F., et al., (2013) Metabolomics as a tool for the comprehensive understanding of fermented and functional foods with lactic acid bacteria. Food Res Int 54, 1152-1161.

Mukerji, S., et al., Development and transmission of antimicrobial resistance among Gram-negative bacteria in animals and their public health impact. Essays Biochem, 2017. 61(1): p. 23-35.

Muller-Loennies, S., L. Brade, and H. Brade, Neutralizing and cross-reactive antibodies against enterobacterial lipopolysaccharide. Int J Med Microbiol, 2007. 297(5): p. 321-40.

Murataeva, N. D. et al., (2016). Where's my entourage? The curious case of 2-oleoylglycerol, 2-linolenoylglycerol, and 2-palmitoylglycerol. Pharmacol Res, 110, 173-80.

Naouar, M. S., et al., (2016). Preventive and curative effect of Pistacia lentiscus oil in experimental colitis. Biomed Pharmacother, 83, 577-583.

NARMS. Antibiotics Tested by NARMS. In: National Center for Emerging and Zoonotic Infectious Diseases (NCEZID): Division of Foodborne W, and Environmental Diseases (DFWED).

Nealon, N.J., C.R. Worcester, and E.P. Ryan (2017a), Lactobacillus paracasei metabolism of rice bran reveals metabolome associated with Salmonella Typhimurium growth reduction. J Appl Microbiol, 2017. 122: p. 1639-1656.

Nealon N.J., et al. (2017b), Rice Bran and Probiotics Alter the Porcine Large Intestine and Serum Metabolomes for Protection against Human Rotavirus Diarrhea. Frontiers in microbiology. 2017;8:653.

Neis, E.P., Dejong, C.H. and Rensen, S.S. (2015). The role of microbial amino acid metabolism in host metabolism. Nutrients. 7, 2930-46.

Nie Y. F., Hu, J., and Yan, X. H. (2015). Cross-talk between bile acids and intestinal microbiota in host metabolism and health. J Zhejiang Univ Sci B, 16, 436-46.

Nielsch, A.S., et al., (1991). Influence of dietary protein and gut microflora on endogenous synthesis of nitrate induced by bacterial endotoxin in the rat. Food Chem Toxicol. 29:6, 387-90.

Nilsson, Å. (2016). Role of Sphingolipids in Infant Gut Health and Immunity. J Pediatr, 173, Supplement, S53-S59.

North, J.A., et al., (2017). Microbial pathway for anaerobic 5'-methylthioadenosine metabolism coupled to ethylene formation. Proc Natl Acad Sci U S A 114: E10455-e10464. 10.1073/pnas.1711625114

O'Gorman, A. and L. Brennan, (2015), Metabolomic applications in nutritional research: a perspective. J Sci Food Agric, 95(13): p. 2567-70.

Oka, Y., T. Ogawa, and K. Sasaoka, First evidence for the occurrence of N delta-acetyl-L-ornithine and quantification of the free amino acids in the cultivated mushroom, Pleurotus ostreatus. J Nutr Sci Vitaminol (Tokyo), 1984. 30(1): p. 27-35.

Olaya Galan, N. N., et al., (2016). In vitro antiviral activity of Lactobacillus casei and Bifidobacterium adolescentis against rotavirus infection monitored by NSP4 protein production. J Appl Microbiol. 120, 1041-51.

Oppezzo, O. J. and Anton, D. N. (1995) Involvement of cysB and cysE genes in the sensitivity of Salmonella Typhimurium to mecillinam. J Bacteriol 177, 4524-7.

Palmer J.D., et al., Engineered Probiotic for the Inhibition of Salmonella via Tetrathionate-Induced Production of Microcin H47. ACS infectious diseases. 2018;4(1):39-45.

Pandey, G., et al., (2016). Grilling enhances antidiarrheal activity of Terminalia bellerica Roxb. fruits. J Ethnopharmacol.

Parveen, N. and Cornell, K. A., (2011), Methylthioadenosine/S-adenosylhomocysteine nucleosidase, a critical enzyme for bacterial metabolism. Mol Microbiol 79, 7-20.

Patra, F.C., et al., (1989), Oral rehydration formula containing alanine and glucose for the treatment of diarrhoea: a controlled trial. Brit med J. 298:6684, 1353-6.

Patten, G., et al., (2002). Dietary fish oil increases acetylcholine- and eicosanoid-induced contractility of isolated rat ileum. J Nutr, 132, 2506-13.

Pearl, D. S., et al., (2014). Altered colonic mucosal availability of n-3 and n-6 polyunsaturated fatty acids in ulcerative colitis and the relationship to disease activity. J Crohns Colitis, 8, 70-9.

Peleman, C., et al., (2016). Colonic Transit and Bile Acid Synthesis or Excretion in Patients With Irritable Bowel Syndrome-Diarrhea Without Bile Acid Malabsorption. Clin Gastroenterol Hepatol.

Peng, M., et al., Prevalence and antibiotic resistance pattern of Salmonella serovars in integrated crop-livestock farms and their products sold in local markets. Environ Microbiol, 2016. 18(5): p. 1654-65.

Peng, X., et al., (2006) Discovery of a marine bacterium producing 4-Hydroxybenzoate and its alkyl esters, parabens. Appl Environ Microbiol 72, 5556-5561.

Pessione E., Cirrincione S., (2016), Bioactive Molecules Released in Food by Lactic Acid Bacteria: Encrypted Peptides and Biogenic Amines. Frontiers in microbiology, 7:876.

Pessione, E., (2012), Lactic acid bacteria contribution to gut microbiota complexity: lights and shadows. Front Cell Infect Microbiol 2, 86.

Phoem, A.N., Chanthachum, S. and Voravuthikunchai, S.P., 2015. Applications of microencapsulated Bifidobacterium longum with Eleutherine americana in fresh milk tofu and pineapple juice. Nutrients 7: 2469-2484. 10.3390/nu7042469

Piatek J., et al., Persistent infection by Salmonella enterica servovar Typhimurium: are synbiotics a therapeutic option? - a case report. Beneficial microbes. 2019;10(2):211-7.

Pimentel, G., et al., Metabolic Footprinting of Fermented Milk Consumption in Serum of Healthy Men. J Nutr, 2018. 148: p. 851-860.

Ryan, E.P., et al. (2013), Advances in Nutritional Metabolomics. Curr Metabolomics, 1(2): p. 109-120.

Plaza-Diaz J., et al., Mechanisms of Action of Probiotics. Advances in nutrition (Bethesda, Md). 2019;10(suppl_1):S49-s66.

Plaza-Zamora, J., et al., (2013). Polyamines in human breast milk for preterm and term infants. Brit J Nutr, 110, 524-528.

Rabbani, G. H., et al., (2005). Antidiarrheal effects of L-histidine-supplemented rice-based oral rehydration solution in the treatment of male adults with severe cholera in Bangladesh: a double-blind, randomized trial. J Infect Dis. 191, 1507-14.

Radenkovs, V., et al., (2018), Valorization of Wild Apple (Malus spp.) By-Products as a Source of Essential Fatty Acids, Tocopherols and Phytosterols with Antimicrobial Activity. Plants (Basel) 7. 10.3390/plants7040090

Radivojevic, J., et al., (2016), Polyhydroxyalkanoate-based 3-hydroxyoctanoic acid and its derivatives as a platform of bioactive compounds. Appl Microbiol Biotechnol 100, 161-72.

Ren, W., et al., (2013). Dietary supplementation with proline confers a positive effect in both porcine circovirus-infected pregnant and non-pregnant mice. Br J Nutr, 110, 1492-9.

Rezaei, R., et al., (2013). Dietary supplementation with monosodium glutamate is safe and improves growth performance in postweaning pigs. Amino Acids, 44, 911-23.

Rogers, A. C., et al., (2015). The effects of polyamines on human colonic mucosal function. Eur J Pharmacol. 764, 157-63.

Rojo F., Martínez JL., Metabolic regulation of antibiotic resistance. FEMS Microbiology Reviews. 2011;35(5):768-89.

Rubinelli P.M., et al., Differential effects of rice bran cultivars to limit Salmonella Typhimurium in chicken cecal in vitro incubations and impact on the cecal microbiome and metabolome. PLOS ONE. 2017;12(9):e0185002.

Ruth, M. R. and Field, C. J. (2013). The immune modifying effects of amino acids on gut-associated lymphoid tissue. J Anim Sci Biotechnol. 4:27.

Ryan E.P., et al. (2011), Rice bran fermented with saccharomyces boulardii generates novel metabolite profiles with bioactivity. Journal of agricultural and food chemistry. 59(5):1862-70.

Sabbatini, P., et al., (2013). Synthesis and Quantitative Structure-Property Relationships of Side Chain-Modified Hyodeoxycholic Acid Derivatives. Molecules, 18, 10497.

Sadiq, A., et al., Rotavirus: Genetics, pathogenesis and vaccine advances. Rev Med Virol, 2018. 28: p. e2003.

Sakko, M., et al., (2012) 2-Hydroxyisocaproic acid (HICA): a new potential topical antibacterial agent. Int J Antimicrob Agents 39, 539-540.

Schirmer, M., et al., (2016). Linking the Human Gut Microbiome to Inflammatory Cytokine Production Capacity. Cell, 167, 1125-1136.e8.

Schwartz, K.L. and S.K. Morris, Travel and the Spread of Drug-Resistant Bacteria. Curr Infect Dis Rep, 2018. 20(9): p. 29.

Settachaimongkon, S., et al., (2014) Influence of different proteolytic strains of Streptococcus thermophilus in co-culture with Lactobacillus delbrueckii subsp. bulgaricus on the metabolite profile of set-yoghurt. Int J Food Microbiol, 177, 29-36.

Shah P., et al., A microfluidics-based in vitro model of the gastrointestinal human-microbe interface. Nature communications. 2016;7:11535.

Sharif, M.K., et al., Rice bran: a novel functional ingredient. Crit Rev Food Sci Nutr, 2014. 54: p. 807-16.

Sheflin, A.M., et al., Pilot dietary intervention with heat-stabilized rice bran modulates stool microbiota and metabolites in healthy adults. Nutrients, 2015. 7(2): p. 1282-300.

Sheflin A.M., et al. Dietary supplementation with rice bran or navy bean alters gut bacterial metabolism in colorectal cancer survivors. Molecular nutrition & food research. 2017;61(1).

Sherman P.M., Ossa J.C., Johnson-Henry K., Unraveling mechanisms of action of probiotics. Nutrition in clinical practice: official publication of the American Society for Parenteral and Enteral Nutrition. 2009;24(1):10-4.

Shimizu, M., et al., (2009). Dietary taurine attenuates dextran sulfate sodium (DSS)-induced experimental colitis in mice. Adv Exp Med Biol, 643, 265-71.

Si, X., et al., 2018. Gamma-aminobutyric Acid Enriched Rice Bran Diet Attenuates Insulin Resistance and Balances Energy Expenditure via Modification of Gut Microbiota and Short-Chain Fatty Acids. J Agric Food Chem 66: 881-890. 10.1021/acs.jafc.7b04994

Simms, S. A. and Subbaramaiah, K. (1991) The kinetic mechanism of S-adenosyl-L-methionine: glutamylmethyltransferase from Salmonella Typhimurium. J Biol Chem 266, 12741-6.

Sinha, R., et al., (2016). Fecal Microbiota, Fecal Metabolome, and Colorectal Cancer Interrelations. PLoS One, 11, e0152126.

Smirnov K.S., et al., Challenges of metabolomics in human gut microbiota research. International journal of medical microbiology : IJMM. 2016;306(5):266-79.

Smolinska, S., et al., (2014). Histamine and gut mucosal immune regulation. Allergy. 69, 273-81.

So, W.K.W., et al., 2016. Current Hypothesis for the Relationship between Dietary Rice Bran Intake, the Intestinal Microbiota and Colorectal Cancer Prevention. Nutrients 8: 569. 10.3390/nu8090569

Soderholm, J.D., et al., (2002). Augmented increase in tight junction permeability by luminal stimuli in the non-inflamed ileum of Crohn's disease. Gut, 50, 307-13.

Sohail, M., et al., 2017. Rice bran nutraceutics: A comprehensive review. Crit Rev Food Sci Nutr 57: 3771-3780. 10.1080/10408398.2016.1164120

Somekawa, S., et al., (2012). Dietary free glutamate prevents diarrhoea during intra-gastric tube feeding in a rat model. Br J Nutr, 107, 20-3.

Sonnenborn, U., Escherichia coli strain Nissle 1917-from bench to bedside and back: history of a special Escherichia coli strain with probiotic properties. FEMS Microbiol Lett, 2016. 363(19).

Spinler, J.K., et al., Next-Generation Probiotics Targeting Clostridium difficile through Precursor-Directed Antimicrobial Biosynthesis. Infect Immun, 2017. 85(10).

Srnivias, S. R., et al., (2007). Transport of butyryl- carnitine, a potential prodrug, via the carnitine transporter OCTN2 and the amino acid transporter ATB. Am J Physiol - Gastrointest Liver Physiol, 293, G1046-G1053.

Staiano, N., et al., Mutagenicity of D- and L-azaserine, 6-diazo-5-oxo-L-norleucine and N-(N-methyl-N-nitroso-carbamyl)-L-ornithine in the Salmonella test system. Mutat Res, 1980. 79(4): p. 387-90.

Sugahara, H., et al., (2015). Probiotic Bifidobacterium longum alters gut luminal metabolism through modification of the gut microbial community. Sci Rep. 5:13548

Swami, U., Goel, S., and Mani, S. (2013). Therapeutic Targeting of CPT-11 Induced Diarrhea: A Case for Prophylaxis. Curr drug targets, 14, 777-797.

Talwalkar A, Kailasapathy K., The role of oxygen in the viability of probiotic bacteria with reference to L. acidophilus and Bifidobacterium spp. Current issues in intestinal microbiology. 2004;5(1):1-8.

Tango, C.N., et al., Synergetic effect of combined fumaric acid and slightly acidic electrolysed water on the inactivation of food-borne pathogens and extending the shelf life of fresh beef. J Appl Microbiol, 2014. 117: p. 1709-20.

Taschler, U., et al., (2017). Cannabinoid Receptors in Regulating the GI Tract: Experimental Evidence and Therapeutic Relevance. Handb Exp Pharmacol. doi: 10.1007/164_2016_105

Tazume, S., et al.,(1990). Ecological studies on intestinal microbial flora of Kenyan children with diarrhoea. J Trop Med Hyg. 93, 215-21.

Theriot, C. M., Bowman, A. A., and Young, V. B. Antibiotic-Induced Alterations of the Gut Microbiota Alter Secondary Bile Acid Production and Allow for Clostridium difficile Spore Germination and Outgrowth in the Large Intestine. (2016). mSphere. doi: 10.1128/mSphere.00045-15

Thomas M., et al., Whole genome sequencing-based detection of antimicrobial resistance and virulence in non-typhoidal Salmonella enterica isolated from wildlife. Gut pathogens. 2017;9:66.

Timmons, J., et al., (2012). Polyamines and Gut Mucosal Homeostasis. J gastrointest & digest syst, 2, 001.

Tovar, J., et al., 2017. Reduction in cardiometabolic risk factors by a multifunctional diet is mediated via several branches of metabolism as evidenced by nontargeted metabolite profiling approach. Mol Nutr Food Res 61. 10.1002/mnfr.201600552

Trabelsi, I., et al., (2016). Effect of a probiotic Lactobacillus plantarum TN8 strain on trinitrobenzene sulphonic acid-induced colitis in rats. J Anim Physiol Anim Nutr (Arumugam et al.).

Tremblay, S., et al., 2017. Bile Acid Administration Elicits an Intestinal Antimicrobial Program and Reduces the Bacterial Burden in Two Mouse Models of Enteric Infection. Infect Immun 85. 10.1128/iai.00942-16

Tsolis, R. M., et al., (1999) Identification of a putative Salmonella enterica serotype Typhimurium host range factor with homology to IpaH and YopM by signature-tagged mutagenesis. Infect Immun 67, 6385-93.

Tuncil, Y.E., et al., 2018. Fecal Microbiota Responses to Bran Particles Are Specific to Cereal Type and In Vitro Digestion Methods That Mimic Upper Gastrointestinal Tract Passage. J Agric Food Chem 66: 12580-12593. 10.1021/acs.jafc.8b03469

Turcotte, C., et al., (2015). Regulation of inflammation by cannabinoids, the endocannabinoids 2-arachidonoyl-glycerol and arachidonoyl-ethanolamide, and their metabolites. J Leukoc Biol. 97, 1049-70.

Turroni, F., et al., Bifidobacteria and the infant gut: an example of co-evolution and natural selection. Cell Mol Life Sci, 2018. 75(1): p. 103-118.

Valerio, F., et al., (2013) Bioprotection of ready-to-eat probiotic artichokes processed with Lactobacillus paracasei LMGP22043 against foodborne pathogens. J Food Sci 78, M1757-63.

van Baarlen P., Wells J.M., Kleerebezem M., Regulation of intestinal homeostasis and immunity with probiotic lactobacilli. Trends in immunology. 2013;34(5):208-15.

van der Hooft, J.J.J., et al., Substantial Extracellular Metabolic Differences Found Between Phylogenetically Closely Related Probiotic and Pathogenic Strains of Escherichia coli. Front Microbiol, 2019. 10: p. 252.

Vandeputte, D., et al., 2017. Prebiotic inulin-type fructans induce specific changes in the human gut microbiota. Gut 66: 1968-1974. 10.1136/gutjnl-2016-313271

Vitaglione P., et al., Whole-grain wheat consumption reduces inflammation in a randomized controlled trial on overweight and obese subjects with unhealthy dietary and lifestyle behaviors: role of polyphenols bound to cereal dietary fiber. The American journal of clinical nutrition. 2015;101(2):251-61.

Vitali, B., et al., (2010) Impact of a synbiotic food on the gut microbial ecology and metabolic profiles. BMC Microbiol 10, 4.

Vlasova, A. N., et al., (2016). Comparison of probiotic lactobacilli and bifidobacteria effects, immune responses and rotavirus vaccines and infection in different host species. Vet Immunol Immunopathol. 172, 72-84.

Wan L.Y., et al., Modulation of Intestinal Epithelial Defense Responses by Probiotic Bacteria. Critical reviews in food science and nutrition. 2016;56(16):2628-41.

Wang H., et al., Factors Derived From Escherichia Coli Nissle 1917, Grown in Different Growth Media, Enhance Cell Death in a Model of 5-Fluorouracil-Induced Caco-2 Intestinal Epithelial Cell Damage. Nutrition and Cancer. 2015;67(2):316-26.

Wang, A., et al., (2015). Gut microbial dysbiosis may predict diarrhea and fatigue in patients undergoing pelvic cancer radiotherapy: a pilot study. PLoS One, 10, e0126312.

Wang, H., et al., (2016). Lactobacillus rhamnosus GG modulates innate signaling pathway and cytokine responses to rotavirus vaccine in intestinal mononuclear cells of gnotobiotic pigs transplanted with human gut microbiota. BMC Microbiol, 16, 109.

Wang, Y., et al., (2012) Lactobacillus rhamnosus GG culture supernatant ameliorates acute alcohol-induced intestinal permeability and liver injury. Am J Physiol-Gastrointes Liver Physiol 303, G32-G41.

Watson, J.A., Fang, M. and Lowenstein, J.M., 1969. Tricarballylate and hydroxycitrate: Substrate and inhibitor of ATP: Citrate oxaloacetate lyase. Archives of Biochemistry and Biophysics 135: 209-217. https://doi.org/10.1016/0003-9861(69)90532-3

Wee, L. H., et al., (1988). Ethyl eicosapentaenoate restored the immunosuppression in mice fed fat-free diet. Res Commun Chem Pathol Pharmacol, 62, 49-66.

Weir, T. L., et al., (2013). Stool Microbiome and metabolome differences between colorectal cancer patients and healthy adults. PLoS ONE 8.

Wen, K., et al., (2015). Lactobacillus rhamnosus GG dosage affects the adjuvanticity and protection against rotavirus diarrhea in gnotobiotic pigs. J Pediatr Gastroenterol Nutr. 60, 834-843.

Whittemore, J.C., et al., Short and long-term effects of a synbiotic on clinical signs, the fecal microbiome, and metabolomic profiles in healthy research cats receiving clindamycin: a randomized, controlled trial. PeerJ, 2018. 6: p. e5130.

Willame, C., et al., Effectiveness of the Oral Human Attenuated Rotavirus Vaccine: A Systematic Review and Meta-analysis-2006-2016. Open Forum Infect Dis, 2018. 5(11): p. ofy292.

WHO, Salmonella (non-typhoidal). [Internet] 2016 December 2016 [cited 2017 July 30]; Available from: http://www.who.int/mediacentre/factsheets/fs139/en/.

Wishart, D.S., et al., 2009. HMDB: a knowledgebase for the human metabolome. Nucleic Acids Res 37: D603-610. 10.1093/nar/gkn810

Wishart, D.S., et al., 2013. HMDB 3.0--The Human Metabolome Database in 2013. Nucleic Acids Res 41: D801-807. 10.1093/nar/gks1065

Wishart, D.S., et al., 2018. HMDB 4.0: the human metabolome database for 2018. Nucleic Acids Res 46: D608-d617. 10.1093/nar/gkx1089

Wishart, D.S., et al., HMDB: the Human Metabolome Database. Nucleic Acids Res 35: D521-526. 10.1093/nar/gkl923

Wolffram, S., Badertscher, M. and Scharrer, E., 1994. Carrier-mediated transport is involved in mucosal succinate uptake by rat large intestine. Exp Physiol 79: 215-226.

Yang, X., 2015. Study of Infection, Immunity, Vaccine and Therapeutics Using Gnotobiotic Pig Models for Human Enteric Viruses, Virginia Polytechnic Institute and State University, Blacksburg, Virginia, 231 pp.

Yang, X., et al., (2015) High protective efficacy of rice bran against human rotavirus diarrhea via enhancing probiotic growth, gut barrier function, and innate immunity. Sci Rep 5, 15004.

Yang, X., et al., Dietary rice bran protects against rotavirus diarrhea and promotes Th1-type immune responses to human rotavirus vaccine in gnotobiotic pigs. Clin Vaccine Immunol, 2014. 21(10): p. 1396-403.

Yeh, K. Y., Yeh, M., and Holt, P. R. (1989). Differential effects of thyroxine and cortisone on jejunal sucrase expression in suckling rats. Am J Physiol, 256, G604-12.

Yen, C., et al., (2014). Rotavirus vaccines: Current status and future considerations. Human vaccines & immunotherapeutics. 10, 1436-1448.

Yoo W., et al., Fine-tuning of amino sugar homeostasis by EIIA(Ntr) in Salmonella Typhimurium. Scientific reports. 2016;6:33055-.

Yousefi B., et al., Probiotics importance and their immunomodulatory properties. Journal of cellular physiology. 2019;234:8008-18.

Yuan J., et al., (2018), Composition and antimicrobial activity of the essential oil from the branches of Jacaranda cuspidifolia Mart. growing in Sichuan, China. Natural product research, 32(12):1451-4.

Yuan, D., Wu, Z., and Wang, Y. (2016). Evolution of the diacylglycerol lipases. Progress in Lipid Research, 64, 85-97.

Zarei I., et al., Comparative Rice Bran Metabolomics across Diverse Cultivars and Functional Rice Gene(-)Bran Metabolite Relationships. Metabolites. 2018;8(4).

Zarei I., et al., Rice Bran Metabolome Contains Amino Acids, Vitamins & Cofactors, and Phytochemicals with Medicinal and Nutritional Properties. Rice (New York, NY). 2017;10(1):24.

Zavala-Mendoza, et al., (2013). Composition and Antidiarrheal Activity of Bidens odorata Cav. Evid Based Complement Alternat Med, 2013, 170290.

Zelante, T., et al., (2013) Tryptophan catabolites from microbiota engage aryl hydrocarbon receptor and balance mucosal reactivity via interleukin-22. Immunity 39, 372-85.

Zhang X., et al., Inactivation of Salmonella spp. and Listeria spp. by Palmitic, Stearic, and Oleic Acid Sophorolipids and Thiamine Dilauryl Sulfate. Frontiers in microbiology. 2016;7:2076

Abdel-Wareth, A.A.A., et al., Synbiotic as eco-friendly feed additive in diets of chickens under hot climatic conditions. Poult Sci, 2019.

Zhang, H., et al., (2014). Probiotics and virulent human rotavirus modulate the transplanted human gut microbiota in gnotobiotic pigs. Gut Pathog. 6:39

Zheng, C. J., et al., (2005) Fatty acid synthesis is a target for antibacterial activity of unsaturated fatty acids. FEBS Lett 579, 5157-62.

Zheng, H., et al., 2015. Metabolomics investigation to shed light on cheese as a possible piece in the French paradox puzzle. J Agric Food Chem 63: 2830-2839. 10.1021/jf505878a

Zheng, X., S. Wang, and W. Jia, Calorie restriction and its impact on gut microbial composition and global metabolism. Front Med, 2018. 12: p. 634-644.

Zhou, Y., et al., 2012. Intracellular ATP Levels Are a Pivotal Determinant of Chemoresistance in Colon Cancer Cells. Cancer Research 72: 304. 10.1158/0008-5472.CAN-11-1674

Zutz, C., et al., (2016) Valproic acid induces antimicrobial compound production in doratomyces microspores. Front Microbiol 7, 510.

APPENDIX

A1. NAVY AND BLACK BEAN-BASED DOG FOODS ARE DIGESTIBLE DURING WEIGHT LOSS IN OVERWEIGHT AND OBESE ADULT COMPANION DOGS[4]

A1.1. Summary:

Common beans (*Phaseolus vulgaris, L.)* are a nutrient-dense, low glycemic index food that supports healthy weight management in people and was examined for dogs. The objectives of this study were to evaluate the apparent total tract digestibility **(ATTD)** and nutrient utilization of navy **(NB)** and black **(BB)** bean-based diets in overweight or obese companion dogs undergoing a weight loss intervention. A nutritionally complete, dry extruded dog food was the control (**CON**) diet and two isocaloric, nutrient matched bean diets, containing either 25 % w/w cooked BB or NB powder comprised the test diets. Diets were fed to adult, overweight companion dogs for either four weeks (short-term study, n=30) or twenty-six weeks (long-term study, n=15) at 60% of maintenance calories for ideal weight. Apparent weight loss increased over time in the short- and long-term studies ($p < 0.001$) but was not different between the three study groups: apparent weight loss was between 4.05 % - 6.14 % for the short-term study and 14.00 % – 17.90 % in the long-term study. The ATTD was within expected ranges for all groups: total dry matter and crude protein ATTD was 7-8 % higher in the BB diet compared to CON ($p < 0.05$), crude fat ATTD was similar across all diets, and nitrogen free extract ATTD was 5-6 %

---

[4]Forster, G.M.*, **Nealon, N.J.***, Hill, D., Jensen, T.D., Stone, T.L., Bauer, J.E., and Ryan, E.P. *Navy bean and black bean-based dog foods are digestible during weight loss in overweight and obese companion dogs*. Journal of Applied Animal Nutrition. 4:e4. April 2016. ***Co-first authors.**

higher in both BB and NB compared to CON ($p < 0.05$). Metabolizable energy was similar for all diets and ranged from 3,434 – 3,632 kcal/kg. At the end of each study period, dogs had hemoglobin levels ≥ 12 g/dL, packed cell volume ≥ 36 %, albumin ≥ 2.4 g/dL, and ALP ≤ 300 IU/L: all median values for each group were within defined limits for nutritional adequacy. This investigation demonstrated that BB and NB diets were safe, digestible, and supported weight loss in calorically restricted, overweight or obese, adult companion dogs.

A1.2. Introduction:

Obesity is the primary nutritional disorder in companion dogs (German, 2010). Recent surveys estimate that 34-59% of pet dogs in the United States, Europe and China are overweight or obese (Linder *et al.*, 2013; Mao *et al.*, 2013; McGreevy *et al.*, 2005). Overweight dogs may have shorter, reduced-quality of life (German, 2010; Kealy *et al.*, 2002; Linder *et al.*, 2013) and increased risk for developing chronic diseases such as diabetes, cardiovascular and respiratory disease, urinary tract infections, pancreatitis, osteoarthritis, and some types of cancer (German, 2006; Linder, 2014).

For clinically healthy dogs, the primary treatment for obesity is nutritional therapy (NRC, 2006). Because excess adiposity is directly related to a positive energy balance, the most practical dietary approach for weight loss is caloric restriction. An adequate weight loss diet has a nutrient composition that supports lean mass retention, induces fat mass reduction, and increases satiety (Linder *et al.*, 2013). Diets high in protein and fiber have been shown in both humans and dogs to promote weight loss and maintain lean muscle mass (Butterwick and Markwell, 1997; German *et al.*, 2010), as well as reduce voluntary food intake in dogs (Weber *et al.*, 2007). Emerging research support that in addition to macronutrients, there are specific foods

and dietary patterns that may promote weight loss as a function of bioactive components and phytochemicals (Deibert *et al.*, 2004; Rayalam *et al.*, 2008; Shai *et al.*, 2008). For example, in people, consumption of non-soy legumes such as common beans (*Phaseolus vulgaris,* L.), split peas, lentils, and chickpeas, is associated with decreased risk for obesity, (Papanikolaou and Fulgoni, 2008), reduced adiposity without caloric restriction (Mollard *et al.*, 2012), voluntary reduction of caloric intake (Borresen *et al.*, 2014), increased satiety, and in some cases, resulted in higher levels of weight loss with 30% caloric restriction compared to an isocaloric, low legume or legume-free diet intervention (McCrory *et al.*, 2010).

Common beans, such as navy, black and pinto, are excellent candidates for a weight loss-promoting food because they contain high quality proteins, have a carbohydrate profile with a low glycemic index, are abundant in dietary fiber, and are rich sources of iron, zinc, folate and magnesium (Mudryj *et al.*, 2014). The high protein content and amino acid profiles of beans have been associated with increased energy expenditure during weight loss and the arginine and glutamine content in particular was associated with improved carbohydrate and fat oxidation (Rebello *et al.*, 2014). The fiber fraction from beans is abundant in resistant starch, which can augment weight loss via slower carbohydrate digestion and increased microbial fermentation (Hayat *et al.*, 2014; McCrory *et al.*, 2010). Furthermore, bean fiber provides prebiotics sources for the gut microbiome, which contribute to energy balance via production of short chain fatty acids (**SCFA**) that have been shown to regulate hormones involved in food intake regulation, such as glucose-like protein 1 (**GLP-1**) and leptin (Huazano-Garcia and Lopez, 2015). Common beans also contain a wide range of bioactive phytochemicals such as alpha-amylase inhibitors, phenolic compounds, and phytosterols which may modulate excess nutrient absorption, reduce dietary energy availability, promote satiety, and improve lipid metabolism (Barrett and Udani,

2011; Chávez-Santoscoy *et al.*, 2014; McCrory *et al.*, 2010; Ramírez-Jiménez *et al.*, 2015). Due to the fact that dry bean consumption promoted weight loss in humans and rodents, the potential of beans to promote weight loss in dogs merits investigation because dogs have similar digestive physiology, obesity related co-morbidities, and environmental exposures to people.

Common beans are safe and digestible in normal, healthy weight dogs (Forster *et al.*, 2012a). Bean-based diet formulations support short-term apparent weight loss and were reported effective at reducing low density lipoprotein **(LDL)**, high density lipoprotein **(HDL)**, and triglycerides **(TG)** when compared to a control, bean-free diet (Forster *et al.*, 2012b). Therefore, the objectives of this current study were to: 1) evaluate the apparent total tract digestibility (**ATTD**) of nutritionally complete, navy (**NB**) and black (**BB**) bean diets in overweight or obese dogs undergoing calorically restricted weight loss and 2) determine the nutritional adequacy and utilization bean-based diets compared to a no-bean, nutrient-matched control (**CON**) diet using the outcome measurements defined by the Association of American Feed Control Officials (AAFCO, 2010) compared to an isocaloric, nutrient matched, standard ingredient, control diet. We hypothesize that cooked bean powders added at 25% weight/weight **(w/w)** into a nutritionally complete extruded dog food formulation will be digestible, support weight loss, and maintain indices of nutritional adequacy as compared to no-bean control diet.

A1.3. Materials and Methods:

A1.3.1. Study Design:

The four-week short-term and twenty-six-week long-term studies were prospective, randomized, double-blinded, controlled, three-arm, dietary intervention clinical trials for calorically-restricted weight loss. The three study groups were CON, NB, or BB. The short-term

weight loss study was conducted at the Colorado State University Veterinary Teaching Hospital (Fort Collins, CO, USA) and the long-term study was conducted at the Wellington Veterinary Hospital (Wellington, CO, USA). Owners signed an informed consent form and provided a medical history before dogs were enrolled in the study. All dogs were transitioned to the study-provided diet (**CON**, **NB**, **BB**) over a 4-day period by increasing the proportion of the study-provided food mixed into the dog's regular food as previously described (Forster *et al.*, 2012a). At the end of the study period, all dogs were transitioned back to their regular food. Owners were instructed to exclusively feed the study kibble in the amounts prescribed. For the short-term study, owners were given pre-measured daily packets of food, and in the long-term study owners were given measuring cups with lines marked to indicate the appropriate amount of kibble to feed daily. All owners were instructed to feed only the prescribed dog food for the duration of the study. Water was provided *ad libitum* and no treats were allowed.

Body weights were assessed bi-weekly and caloric intake was adjusted as needed to achieve a target weight loss of 0.5% - 2% body weight per week. For the short-term study (n=30), a 96-hour faecal collection was performed at 2 weeks, after the dogs had been exclusively consuming the study food for 10 days. For the long-term study (n=15) a 96-hour faecal collection was performed at 12 weeks. Owners were instructed to collect the canine faecal samples within 5 hours of being voided. Samples were frozen and stored at -20° C until analysis. Compliance to the study protocol was determined by owner surveys, diet logs (short-term study only), number of faecal samples collected, and apparent weight loss.

A1.3.2. Eligibility Criteria for Companion Dog Participants:

The Colorado State University Institutional Animal Care and Use Committee approved all clinical trial operations, animal care procedures, and collection of biological samples for analysis before beginning the study (IACUC 13-4316A). Adult, male and female dogs between the ages of 2-7 years, with a body condition score (**BCS**) of at least 6 on a 9-point scale (Laflamme, 1997) and body weight of at least 10 kg, with no known health concerns were recruited for study participation. All dog owners provided written informed consent for participation. After enrollment, all dogs were evaluated by the study veterinarian, assessed for hematologic and biochemical anomalies, assigned a BCS, and screened for hypothyroidism with a total thyroxine **(T4)** test as previously described (Forster *et al.*, 2012b). Dogs were excluded from participation for hypothyroidism, abnormal blood results (unless determined by the veterinarian to be within normal limits for a specific dog), or a history or diagnosis of cancer, inflammatory disease, or current infection. Dogs were also excluded if they had been administered antibiotics or analgesics within 1 month of starting the study. The preventive use of anthelmintics was allowed. Dogs could be removed from the study at the discretion of the study veterinarian or request of owner. All dogs were monitored throughout the study for adverse changes in clinical blood, serum, or plasma analytes. At the end of each study period, hemoglobin, packed cell volume (**PCV**), albumin, and alkaline phosphatase (**ALP**) were compared to the AAFCO reference ranges for nutritionally adequacy (AAFCO, 2010). One dog (short-term study, CON) had chronically-elevated ALP (830 g/dl at baseline that decreased to 320 g/dl at 4 weeks) and participated at the discretion of the attending veterinarian. Hemoglobin and PCV values were not obtained from one dog at the end of study (long-term study, BB) due to clotted blood.

Fifty-six dogs were screened for participation in the short-term or long-term weight loss study and 49 were enrolled. Seven dogs failed the pre-screen exam for either renal or hepatic abnormalities (n=2), detection of previously undiagnosed cancer (n=2), hypothyroidism (n=1), urinary tract infection (n=1), or aggression and difficult handling (n=1). Thirty-three dogs were enrolled in the short-term study and randomized based on BCS to CON, BB, or NB study groups. Three dogs were withdrawn due to physical injury (n=1), owner unable to keep study-related appointments (n=1), and not consuming the study provided dog food (n=1) (Forster *et al.*, 2012b). Sixteen dogs were enrolled in the long-term study and randomized based on BCS to the CON, BB, or NB study groups. One dog was withdrawn from the long-term study after diagnosis with tapeworm and the owner's non-compliance to study protocol by feeding dog treats. Individual characteristics of each dog are presented in **Table A1.1** and summaries of the baseline characteristics are shown in **Table A1.2**. Breeds included dogs from retriever, terrier, herding, and working lineages, and spanned both purebred and mixed breeds. Dogs were equally distributed between study diet groups for age, weight, sex, and BCS. There was one dog in each of the short-term and long-term studies that was not neutered. One 8-year-old dog was included in the short-term study and one 10-year-old dog was included in the long-term study at the discretion of the study veterinarian.

Table A1.1. Baseline characteristics of dogs completing cooked bean powder-based calorically restricted weight loss study interventions

Characteristic		Control Group *Median (IQR)*	Black Bean Group *Median (IQR)*	Navy Bean Group *Median (IQR)*	*p-value*[4]
Age[1], yr					0.16
	Short-term	6.0 (4.7-7.0)	5.0 (2.8-5.3)	4.5 (3.5-6.0)	0.10
	Long-term	3.0 (2.0-8.5)	3.0 (3.0-4.5)	6.0 (4.5-7.0)	0.32
Body weight, kg					0.25
	Short-term	34.5 (20.7-39.6)	28.8 (16.5-34.1)	29.25 (20.4-38.1)	0.59

Table A1.1. Baseline characteristics of dogs completing cooked bean powder-based calorically restricted weight loss study interventions

	Long-term	36.5 (29.2-40.4)		37.7 (26.7-45.7)		39.5 (27.3-56.1)		0.59
		Number of Dogs						
Sex[2]		*Female*	*Male*	*Female*	*Male*	*Female*	*Male*	0.61
	Short-term	7	3	6	4	4	6	0.86
	Long-term	3	2	4	1	2	3	0.89
BCS[3]		*BCS 6-7*	*BCS 8-9*	*BCS 6-7*	*BCS 8-9*	*BCS 6-7*	*BCS 8-9*	0.33
	Short-term	7	3	4	6	7	3	0.77
	Long-term	2	3	2	3	1	4	0.99

Thirty dogs completed the short-term, 4-week study: Control Diet, N=10; Black Bean Diet, N=10; Navy Bean Diet, N=10. Fifteen dogs completed the long-term, 6-month study: Control Diet, N=5; Black Bean Diet, N=5; Navy Bean Diet, N=5.

[1]Age as reported by owner.

[2]All dogs were neutered with the exception of one female in the short-term study control group and 1 female in the long-term study black bean group.

[3]Body Condition Score (BCS) was determined using a 9-point scale (Laflamme, 1997).

[4]Continuous variables (age and weight) were evaluated for differences across groups using a Kruskal-Wallis test and categorical variables (sex and BCS) were evaluated using a Chi-square test. P values are shown across short-term and long-term studies and within study across diet. $P < 0.05$ was considered significant.

Table A1.2. Baseline characteristics of individual canine study participants[1].

Dog ID	Study	Diet	BCS	Weight	Age	Sex	Breed
O_C1	Short-Term	Control	6	27.4	6	F/S	Dalmatian
O_C2	Short-Term	Control	7	37.3	6	M/N	Labrador Retriever Mix
O_C3	Short-Term	Control	7	62.4	4	F/I	Saint Bernard
O_C4	Short-Term	Control	7	42.7	7	F/S	Labrador Retriever
O_C5	Short-Term	Control	7	14.7	7	M/N	Welsh Corgie
O_C6	Short-Term	Control	6	22.4	5	F/S	Australian Shepherd
O_C7	Short-Term	Control	7	15.4	3	M/N	Mixed - unknown
O_C8	Short-Term	Control	8	37.7	7	F/S	Labrador Retriever Mix
O_C9	Short-Term	Control	9	38.6	6	F/S	Golden Retriever
O_C10	Short-Term	Control	8	31.6	7	F/S	Border Collie
O_BB1	Short-Term	Black Bean	8	23.8	5	F/S	Keeshond
O_BB2	Short-Term	Black Bean	6	17.2	3	F/S	Basset Hound
O_BB3	Short-Term	Black Bean	8	40.8	7	M/N	Australian Cattle Dog
O_BB4	Short-Term	Black Bean	9	27	5	F/S	Border Collie Mix
O_BB5	Short-Term	Black Bean	7	14.2	2	F/S	Boston Terrier Mix
O_BB6	Short-Term	Black Bean	9	10.7	3	M/N	Shiz Tzu
O_BB7	Short-Term	Black Bean	7	31.8	5	F/S	Pit Bull
O_BB8	Short-Term	Black Bean	7	30.6	5	M/N	Australian Cattle Dog
O_BB9	Short-Term	Black Bean	8	32.8	6	F/S	Australian Cattle Dog
O_BB10	Short-Term	Black Bean	8	38.1	2	M/N	Australian Shepherd Mix
O_NB1	Short-Term	Navy Bean	7	32.6	6	M/N	Airdale mix
O_NB2	Short-Term	Navy Bean	7	36	2	M/N	Border Collie Mix
O_NB3	Short-Term	Navy Bean	7	17.8	4	F/S	Boston Terrier
O_NB4	Short-Term	Navy Bean	7	44.2	8	F/S	Labrador Retriever
O_NB5	Short-Term	Navy Bean	8	10	4	M/N	Dachshund
O_NB6	Short-Term	Navy Bean	9	21.2	4	M/N	Dachshund

Table A1.2. Baseline characteristics of individual canine study participants[1].							
O_NB7	Short-Term	Navy Bean	6	25.9	5	M/N	Australian shepherd
O_NB8	Short-Term	Navy Bean	7	21.2	6	F/S	Australian shepherd
O_NB9	Short-Term	Navy Bean	7	34.3	2	F/S	Boxer
O_NB10	Short-Term	Navy Bean	8	44.4	5	M/N	Karelian Bear Dog Mix
O_C11	Long-Term	Control	7	33.1	10	M/N	Cocker Spaniel
O_C12	Long-Term	Control	8	36.5	3	F/S	American Spaniel
O_C13	Long-Term	Control	8	42.2	2	M/N	German Shepherd Mix
O_C14	Long-Term	Control	7	25.2	2	F/S	Labrador Retriever Mix
O_C15	Long-Term	Control	9	38.5	7	F/S	Labrador Retriever
O_BB11	Long-Term	Black Bean	8	24.9	3	F/I	Labrador/Pit Bull Mix
O_BB12	Long-Term	Black Bean	8	44.5	3	M/N	Labrador/Pit Bull Mix
O_BB13	Long-Term	Black Bean	7	28.5	3	F/S	Pit Bull
O_BB14	Long-Term	Black Bean	7	46.8	3	F/S	Labrador Retriever
O_BB15	Long-Term	Black Bean	8	37.7	6	F/S	Labrador Retriever Mix
O_NB11	Long-Term	Navy Bean	9	16.2	7	M/N	Labrador Retriever
O_NB12	Long-Term	Navy Bean	7	63.7	3	M/N	Border Collie/Corgi Mix
O_NB13	Long-Term	Navy Bean	8	39.5	6	M/N	Golden Retriever
O_NB14	Long-Term	Navy Bean	8	38.3	6	F/S	Border Collie/New Foundland Mix
O_NB15	Long-Term	Navy Bean	9	48.5	7	F/S	Labrador Retriever
[1]Age, sex, and breed were reported by owners. **BCS**: body condition score on a 9-point scale; Weight: body weight in kg; **F/I**: intact female; **F/S**: spayed female; **M/N**: neutered male.							

A1.3.3. Dietary Formulations:

CON, BB, and NB dietary study groups were provided a dry, extruded, pelleted dog food that was formulated to meet nutritional recommendations for adult dog maintenance (AAFCO, 2010; NRC, 2006) and adjusted to consist of 27% protein and 8% fat (as-fed). The CON, BB, and NB diets were mixed and manufactured under the same conditions and location (ADM Alliance Nutrition Feed Research Pilot Plant, Quincy, IL; Applied Food Biotechnology Plant, St. Charles, MO) and formulated to be isocaloric and nutrient matched. The CON diet ingredients consisted of poultry meal, wheat, corn, brewer's rice, pork and bone meal, flaxseed, fishmeal, brewer's yeast, and added vitamins and minerals **(Table A1.3)**. The BB and NB diets contained identical ingredients as the CON diet with the inclusion of cooked BB or NB bean powder (ADM Bean Specialties, Decatur, IL) added at 25% w/w to the BB and NB diets. To account for the inclusion of the cooked bean powders, the wheat and corn ingredients were reduced to

achieve iso-nutrient formulations to the CON diet. The metabolizable energy (**ME**) of the diets was calculated using modified Atwater Factors and estimated at 3,314 kcal/kg (NRC, 2006).

Table A1.3. Diet Ingredient and Chemical Composition

Ingredient, % (as-fed)	**Control Diet**	**Black Bean Diet**	**Navy Bean Diet**
black bean (cooked powder)	-	25.00	-
cooked navy bean powder	-	-	25.00
poultry meal	19.53	19.00	19.61
wheat grain	19.00	2.66	3.62
wheat middlings	19.00	11.61	9.42
corn grain	16.11	17.67	19.00
brewer's rice	10.00	10.00	10.17
pork and bone meal	7.32	3.95	2.56
poultry fat	3.00	3.00	3.00
flaxseed	1.00	1.00	1.00
fish meal	1.00	1.00	1.00
brewer's yeast	1.00	1.00	1.00
digest	1.00	1.00	1.00
calcium carbonate	0.80	1.28	1.47
salt	0.50	0.50	0.50
vitamin-trace mineral premix [a, b, c, d]	0.50	0.50	0.50
potassium chloride	0.14	0.05	0.05
choline chloride	0.10	0.10	0.10
monocalcium phosphate	-	0.68	1.00
Analyzed Composition, % (as-fed)			
dry matter	95.02	95.59	94.96
moisture	4.98	4.41	5.04
crude protein	26.60	26.90	26.30
nitrogen free extract	47.82	47.99	48.96
acid hydrolyzed fat	8.40	8.10	8.00
crude fiber	3.90	4.30	3.70
total dietary fiber	16.98	17.96	18.65
soluble fiber	4.05	3.36	5.25
insoluble fiber	12.93	14.60	13.40
ash	8.30	8.30	8.00
Gross energy, kcal/kg	4,505	4,371	4,375
Est. metabolizable energy, kcal/kg	3,314	3,314	3,314

a. Provided per kilogram of control, black bean, and navy bean diets: vitamin A, 7,500 IU; vitamin D, 750 IU; vitamin E, 93.75 IU; thiamine 3.75 mg; riboflavin, 30 mg; pantothenic acid, 12 mg; niacin, 15 mg; pyridoxine, 1.88 mg; folic acid, 0.26 mg; vitamin B12, 37.5 µg; choline, 534.4 mg; Fe from ferrous sulfate, 282 mg; Cu from copper sulfate, 15 mg; I from calcium iodate, 2.025 mg.
b. Manganese from manganous oxide provided per kilogram: 10.125 mg (control, black bean), 32.01 mg (navy bean).
c. Zinc from zinc oxide provided per kilogram: 213.068 mg (control), 150 mg (black bean), 198.02 mg (navy bean).
d. Selenium from sodium selenite provided per kilogram: 0.6463 mg (control), 0.2250 mg (black bean, navy bean).

A1.3.4. Calculations for Energy Requirements and Caloric Restriction:

Body condition scoring **(BCS)** was used to estimate ideal bodyweight (**BW**) and determined using a 9-point scale (Laflamme, 1997). A score of less than 4 was considered underweight, a score of either 4 or 5 was considered ideal BW, a score of 6 or 7 was overweight, and a score of 8 or 9 was considered obese (Forster *et al.*, 2012b). For each point over 5, a dog was considered to be 10 % above his or her ideal body weight in kilograms (German *et al.*, 2009). Using ideal weights determined by BCS, daily ME requirements for weight maintenance were calculated for each dog using the following formula: ME (kcal/day) = 110 x (ideal BW, kg)$^{0.75}$ (Forster *et al.*, 2012a; NRC, 2006)**.** Dogs were calorically restricted to approximately 60% of their maintenance energy requirement. Apparent BW (Balmer *et al.*) was measured at least every two weeks throughout each study.

A1.3.5. Proximate Analysis, Apparent Total Tract Digestibility, and Bomb Calorimetry:

Proximate analysis was used to determine the crude nutrient profiles of the food and faecal samples as previously reported (Forster *et al.*, 2012a). Soluble and insoluble fiber fractions were determined as previously described (Prosky *et al.*, 1992). ATTD were evaluated at two weeks for the short-term study, and at twelve weeks for the long-term study and were calculated for total dry matter (**TDM**), crude protein (**CP**), crude fat (**CF**), and nitrogen free extract (**NFE**). The following formula was used to determine NFE: NFE % = TDM % – CP % – CF % - crude fiber % – ash %. For each nutrient component, the ATTD was calculated on a dry matter (**DM**) basis using the following formula (AAFCO, 2010): % ATTD = [(g of nutrient consumed – g of nutrient excreted) / (g of nutrient consumed)] × 100.

Total gross energy **(GE)** content was measured by bomb calorimetry for each diet, and in each faecal sample at two weeks for the short-term study and at twelve weeks for the long-term study. ME was determined at two weeks during the short-term study, and at twelve weeks during the long-term study and reported in kcal/kg using the following formula (AAFCO, 2010): ME (kcal/kg of food) = {GE of food consumed – GE of feces collected – [(g of protein consumed – g protein in feces) × 1.25]}/ grams of food consumed × 1,000, where GE was in kcal/g, 1.25 kcal/g was the correction factor for energy lost in urine, and both diet and faecal values were on a DM basis.

Dogs were excluded from the ATTD and ME analysis if owners reported dietary indiscretion during the faecal collection period, were unable to differentiate between samples from different dogs, or collected faecal samples for less than 3 days. CON group exclusions: short-term, n = 4 and long-term, n =1; BB group exclusions: short-term n=1 and long-term, n=1; and NB group exclusions: short-term, n=3 and long term, n=0.

Non-parametric analyses were performed on all measures. For percent apparent weight loss, a two-way ANOVA (repeated measures) was performed within each study. For ATTD, ME, and food intake/kg BW, a two-way ANOVA (non-repeated measures) was performed. Bonferroni post-hoc tests were applied to correct for multiple comparisons. Statistical analyses for all measurements were performed using GraphPad Prism, Version 5.03 (San Diego, CA, USA). Significance was reported at a p-value of $p < 0.05$.

A1.4. Results and Discussion:

A1.4.1. Nutrient Profiles of Bean-Based Dog Foods:

The primary objective of this study was to determine the digestibility of nutritionally complete, NB and BB based dog food when compared to a nutrient matched CON dog food in overweight or obese dogs undergoing calorically restricted weight loss. Proximate analysis and bomb calorimetry results confirmed that the CON, NB and BB dog food formulations were nutrient matched and isocaloric **(Table A1.3).** On an as-fed basis, for all diets, the estimated ME content of the diets was 3,314 kcal/kg, CP content was approximately 26 %, and CF was 8 %. Crude fiber was similar between the CON, BB, and NB diets (~4 %), while TDF was ~1 % higher in NB and BB diets when compared to CON. Compared to the CON diet, insoluble fiber was slightly increased in the BB diet (~1.5 %), while soluble fiber was slightly increased in the NB diet (~1 %).

A1.4.2. Companion Dog Characteristics, Dietary Intake, and Apparent Weight Loss:

Forty-five clinically healthy, adult, companion dogs, BCS classified as overweight or obese completed a short or long term calorically restricted weight loss trial and were assigned to either the NB, BB, or CON study groups. Caloric restriction continued for 12 weeks in all dogs in the long-term study: some dogs were transitioned to weight maintenance rations between 12 and 26 weeks at the discretion of the owner, study nurse, and clinician. There was no difference in sex, median age, or BCS between dietary treatment groups or studies **(Table A1.2)**. In both the short and long-term studies, percent apparent weight loss increased over time ($p < 0.0001$) and was similar between dietary treatments in each study; in the short-term study the median weight loss was 4.05 % in CON, 5.98 % in BB, and 6.14 % in NB; for the long-term study, the

median weight loss was 17.90 % in CON, 14.0 % in BB, and 12.21 % in NB (**Figure A1.1**). Daily nutrient intake (g/kg ideal BW) was not different between groups (**Table A1.4**) except for soluble fiber, which was significantly higher ($p < 0.001$) in NB group (~0.4 g/kg ideal BW) compared to BB (~0.25 g/kg ideal BW), but not different from CON (~0.3 g/kg ideal BW, $p > 0.05$). All dogs consumed approximately 2.5 g CP per kg ideal BW (medians ranged from 2.1 g – 2.7 g/kg ideal BW), and dogs within the BB and NB group consumed, on average, 2 g cooked bean powder per kg ideal body weight (**Table A1.4**).

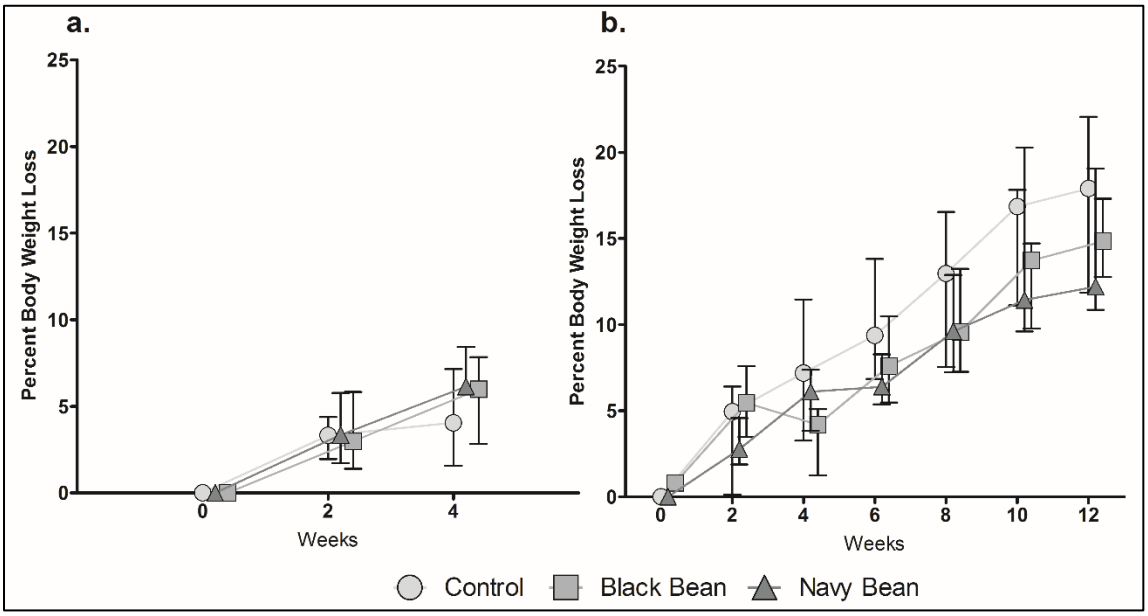

Figure A1.1. Percent apparent weight loss in dogs consuming a bean-based or control diet over (a) 4-weeks (short-term study, n =30) and (b) 12-weeks (long-term study, n = 15).
*In both **(a)** and **(b)** percent apparent weight loss increased over time ($p < 0.05$), but not between dietary treatments at any time point. Data are shown as median and interquartile range.*

Table A1.4. Daily nutrient intake of forty-five overweight or obese adult, companion dogs undergoing calorically restricted weight loss on nutritionally complete diets.

Daily Intake/kg ideal BW		Control Diet	Black Bean Diet	Navy Bean Diet	
		Median (IQR)	*Median (IQR)*	*Median (IQR)*	***p-value***
Total Dietary Intake, g (*As-fed basis*)					
	Short-Term	9.0 (8.5-9.7)	9.5 (8.8-10.2)	8.9 (8.6-10.3)	0.939
	Long-Term	8.8 (8.2-10.1)	8.8 (8.5-9.0)	8.7 (8.6-9.1)	
ME (Estimated) Intake, Kcal (*DM Basis*)					
	Short-Term	1.4 (1.4-1.7)	1.6 (1.5-2.0)	1.5 (1.5-1.8)	0.510
	Long-Term	1.3 (1.3-1.6)	1.3 (1.2-1.5)	1.5 (1.3-1.6)	
Total DM Intake g/kg ideal BW					
	Short-Term	8.7 (8.4-10.0)	9.5 (8.5-12.0)	8.5 (8.2-10.0)	0.900
	Long-Term	8.0 (7.8-10.0)	7.4 (7.1-8.9)	8.3 (7.3-9.0)	
Crude Protein, g (*DM Basis*)					
	Short-Term	2.4 (2.4-2.9)	2.7 (2.4-3.3)	2.4 (2.3-2.8)	0.808
	Long-Term	2.2 (2.2-2.8)	2.1 (2-2.5)	2.3 (2.0-2.5)	
Crude Fat, g (*DM Basis*)					
	Short-Term	0.8 (0.7-0.9)	0.8 (0.7-1.0)	0.7 (0.7-0.8)	0.729
	Long-Term	0.7 (0.7-0.9)	0.6 (0.6-0.8)	0.7 (0.6-0.8)	
NFE, g (*DM Basis*)					
	Short-Term	4.4 (4.2-5.2)	4.8 (4.3-5.9)	4.4 (4.2-5.2)	0.967
	Long-Term	4.0 (3.9-5.1)	3.7 (3.6-4.5)	4.3 (3.8-4.7)	
Crude Fiber, g (*DM Basis*)					
	Short-Term	0.4 (0.3-0.4)	0.4 (0.4-0.5)	0.3 (0.3-0.4)	0.087
	Long-Term	0.3 (0.3-0.4)	0.3 (0.3-0.4)	0.3 (0.3-0.4)	
TDF, g (*DM Basis*)					
	Short-Term	1.4 (1.4-1.7)	1.6 (1.5-2.0)	1.5 (1.5-1.8)	0.510
	Long-Term	1.3 (1.3-1.6)	1.3 (1.2-1.5)	1.5 (1.3-1.6)	
Soluble Fiber, g (*DM Basis*)					
	Short-Term	0.3 (0.3-0.4)^{ab}	0.3 (0.3-0.4)^{a}	0.4 (0.4-0.5)^{b}	< 0.001
	Long-Term	0.3 (0.3-0.4)^{ab}	0.2 (0.2-0.3)^{a}	0.4 (0.4-0.4)^{b}	
Insoluble Fiber, g (*DM Basis*)					
	Short-Term	1.1 (1.0-1.3)	1.3 (1.2-1.6)	1.1 (1.0-1.3)	0.133
	Long-Term	1.0 (1.0-1.2)	1.0 (1.0-1.2)	1.1 (1.0-1.1)	
Cooked Bean Powder, g (*DM Basis*)					
	Short-Term	0 (0-0)^{a}	2.4 (2.1-2.9)^{b}	2.1 (2.1-2.5)^{b}	< 0.001
	Long-Term	0 (0-0)^{a}	1.8 (1.8-2.2)^{b}	2.1 (1.8-2.3)^{b}	

To determine differences in daily intake between diets and studies, each nutrient was evaluated with 2-way ANOVA. There were no differences between studies or interactions terms. A Bonferroni post-test was used to determine the groups with significant differences. Groups not sharing the same letter superscript are significantly different from each other.

A1.4.3. Apparent Total Tract Digestibility and Metabolizable Energy of Black and Navy Bean-Based Dog Diets during Weight Loss:

In the CON, BB, and NB diets, nutrient ATTD was consistent with expected ranges for standard ingredient and bean-based extruded dog diets (Forster *et al.*, 2012a). TDM, CP, CF, and NFE ATTD are presented as median and range (min-max, **Table A1.5**). There were no differences in ATTD between each study group of the short and long-term study. In the short-term study, median TDM ATTD was higher ($p < 0.05$) for BB (83.0 %) than CON (74.6 %), while NB was similar to both (80.2 %); in the long-term study, TDM ATTD was similar for all three diets: CON (73.7 %), BB (79.6 %), and NB (77.5 %). For the NB diet, these results were consistent with previous studies demonstrating equal TDM ATTD compared to a nutrient matched CON diet (Forster *et al.*, 2012a). To our knowledge, this is the first report of a BB based canine diet ATTD. To verify that TDM ATTD was higher for the BB diet compared to CON, we performed a pooled analysis on the results from both trials. The differences in TDM ATTD between CON and BB remained significant (data not shown), further supporting that that the BB TDM was indeed more digestible than CON and may have not been significant in the long-term study due to the sample size.

Table A1.5. Apparent Total Tract Nutrient digestibility, metabolizable energy, and energy extraction efficiency of three nutritionally complete diets fed to overweight or obese adult companion dogs undergoing calorically restricted weight loss.

Digestibility[1], %		Control Diet[2] Median (IQR)	Black Bean Diet[3] Median (IQR)	Navy Bean Diet[4] Median (IQR)	*p-value*[5]
Total dry matter %					
	Short-term	74.6 (67.0-80.7)[a]	83.0 (75.8-89.0)[b]	80.2 (66.8-83.5)[ab]	0.015
	Long-term	73.7 (69.9-79.1)	79.6 (76.9-83.7)	77.5 (71.8-88.1)	
Crude protein					
	Short-term	78.6 (73.1-84.6)[a]	85.7 (80.4-91.4)[b]	83.5 (78.7-87.4)[ab]	0.040
	Long-term	80.9 (78.5-84.3)	82.5 (81.8-85.9)	79.4 (77.0-91.4)	
Crude fat					
	Short-term	89.8 (88.7-92.9)	95.2 (88.5-97.7)	92.9 (77. 3-96.4)	0.120
	Long-term	93.2 (90.7-93.5)	94.1 (90.5-96.1)	89.4 (87.1-95.9)	
Nitrogen free extract					
	Short-term	83.2 (76.9-86.8)[a]	89.3 (82.3-91.9)[b]	87.6 (84.1-89.8)[b]	0.002
	Long-term	82.1 (77.7-85.4)	86.5 (83.9-89.5)	85.1 (83.5-91.6)	
Metabolizable energy, kcal/kg					
	Short-term	3,446 (3,188-3,674)	3,632 (3,348-3,804)	3,571 (3,235-3,689)	0.617
	Long-term	3,519 (3,271-3,670)	3,507 (3,367-3.618)	3,434 (3,328-3,844)	

[1]Digestibility was calculated on a DM basis. [2-4]Five, two, and three dogs were excluded from analysis in the CON, BB, and NB groups, respectively. Total number of dogs analyzed: CON, n=6 (short-term), n=4 (long-term); BB, n=9 (short-term), n=4 (long-term); NB, n=7 (short-term), n=5 (long-term). [5]To determine differences in digestibilities between diets and studies, each nutrient was evaluated with 2-way ANOVA. There were no differences between studies or interactions terms (data not shown). A Bonferroni post-test was used to determine the groups with significant differences. Groups not sharing the same letter superscript are significantly different from each other.

In the short-term study, CP ATTD was higher in BB (85.7 %) compared to CON (78.6 %, $p < 0.01$), and NB was similar to both (83.5 %); in the long-term study, CP ATTD was similar between the CON (80.9 %), BB (82.5 %), and NB (79.4 %). Again, the difference in CP ATTD between CON and BB remained significant when data from both the long and short-term studies were pooled (data not shown). During the long-term study, the consistency of CP digestibility and cumulative weight loss between dietary treatments supports the use of common beans as a as a staple ingredient in weight loss dog food formulas. Past work with dogs has demonstrated that dietary protein intake is associated with lean mass retention and is central in facilitating a healthy

metabolism during weight loss (Laflamme, 2012). Given that cooked beans are both highly digestible and capable of supporting weight loss, the role of bean-based diets as a novel protein source in supporting canine lean mass retention warrants further investigation.

CF was equally digestible between all diets in the short-term study: CON (89.8 %), BB (95.2 %), and NB (92.9 %); and the long-term study: CON (93.2 %), BB (94.1 %), and NB (89.4 %). Carbohydrate ATTD, as measured by NFE, was higher in both the BB (89.3 %) and NB (87.6 %) diets compared to CON (83.2 %) in the short-term study, and similar between all diets in the long-term study: CON (82.1 %), BB (86.5 %), and NB (85.1 %). The NFE ATTD remained significantly higher in both bean groups when data from both the short and long-term studies were pooled (data not shown) supporting that the carbohydrates derived from the BB and NB were more digestible than those derived from corn and wheat-based diets. Recent metabolomic studies support that metabolism of carbohydrates may be modulated in normal weight dogs consuming bean-based diets (Forster *et al.*, 2015) even though carbohydrate digestibility was the same as the control diet (Forster *et al.*, 2012a). For dogs undergoing weight loss, BB diets did influence the relative NFE digestibility (**Table A1.5.**), which may be due to differential modulation of carbohydrate metabolism compared to the CON diet. Future metabolome investigations using samples from this study may reveal distinct carbohydrate compositions contributing to these effects in overweight and obese dogs consuming bean-based diets during weight loss.

ME was calculated for each group to determine the amount of utilizable energy provided by the CON, BB, and NB foods. Measured ME was similar between both the short and long-term studies and across all diets. Results are presented as a median (min-max, **Table A1.4**). The median ME for the CON diet was 3,446 kcal/kg for the short-term and 3,519 kcal/kg for the

long-term study. In the BB diet, ME was 3,632 kcal/kg for the short-term and 3,507 kcal/kg for long-term study. In the NB diet, ME was 3,571 kcal/kg for the short-term and 3,434 kcal/kg for the long-term study. ME was highest in in the BB short-term study (3,632 kcal/kg) and this was the only measured ME that was higher than the estimated ME of 3,314 kcal/kg ($p = 0.004$). These data support that the energy utilization from bean-based dog food was equivalent to standard ingredient dog food formulations in dogs undergoing calorically restricted weight loss.

A1.4.4. Whole Blood Analyses and Serum Biochemistry Reveal Safety of Bean Diets During Companion Dog Weight Loss:

To determine if dogs consuming the bean-based foods maintained indices of nutritional adequacy, comprehensive blood cell counts and serum biochemical analyses were performed for every dog at baseline and throughout the study as previously described (Forster *et al.*, 2012a; Forster *et al.*, 2012b). No negative physiological effects were observed in any analyte measured (data not shown). To demonstrate the nutritional adequacy of the dog food formulations, each dog's results were compared to AAFCO reference limits or hemoglobin, PCV, albumin, and ALP at the end of the study period. Results are presented as a median (min-max) along with the AAFCO limits for each analyte (**Table A1.6**). The median albumin for the CON group was 3.9 g/dL and 3.9 g/dL; 3.9 g/dL and 4.0 g/dL for the BB group: and 3.9 g/dL and 4.1 g/dL for the NB group, for the short and long-term studies respectively. The median ALP for the CON group was 40.5 IU/L and 41.0 IU/L; 51.0 IU/L and 31.0 IU/L in the BB group; and 27.5 IU/L and 47.0 IU/L in the NB group for the short and long-term studies, respectively. The median PCV for the CON group was 51.0 % and 51.0 %; 49.5% and 56.0% in the BB group; and 51.0% and 51.0% in the NB group for the short and long-term studies, respectively. The median hemoglobin for the CON

group was 17.7 g/dL and 18.0 g/dL; for BB was 17.7 g/dL and 20.0 g/dL; and for NB was 17.8 g/dL and 17.9 g/dL for the short and long-term studies, respectively. Serum analytes values fell within AAFCO established reference limits, supporting that the experimental NB and BB dog foods provided adequate nutrition and were safe to consume during short and long-term weight loss. This study applied AAFCO values for adult dog weight maintenance because there are no established values for dogs undergoing calorically restricted weight loss. Given that differences in canine serum analytes have been reported for overweight and obese dogs compared to normal weight dogs, and also that changes occur during weight loss (Forster *et al.*, 2012b; Yamka *et al.*, 2006), future studies will need to determine if AAFCO reference values should adjusted for diets targeting weight management.

Table A1.6. Plasma and serum biochemical analysis of three diets fed to overweight or obese adult companion dogs undergoing calorically restricted weight loss.

Analyte		Control Group *Median (Min-Max)*	Black Bean Group *Median (Min-Max)*	Navy Bean Group *Median (Min-Max)*	Reference Values *Group (Individual)*
Hemoglobin, g/dL					
	Short-term	17.7 (16.2-18.4)	17.7 (16.7-19.4)	17.75 (16.0-19.2)	≥ 14.0 g/dL
	Long-term	18.0 (16.7-19.0)	20.0 (17.1-20.4)	17.9 (15.1-19.2)	(≥12.0)
Packed Cell Volume, %					
	Short-term	51.0 (46.0-54.0)	49.5 (48.0-55.0)	51.0 (47.0-55.0)	≥ 42%
	Long-term	51.0 (47.0-51.0)	56.0 (50.0-59.0)	51.0 (42.0-53.0)	(≥ 36%)
Albumin, g/dL					
	Short-term	3.9 (3.6-4.2)	3.9 (3.6-4.3)	3.9 (3.3-4.4)	≥ 2.8 g/dL
	Long-term	3.9 (3.7-4.1)	4.0 (3.9-4.1)	4.1 (3.9-4.3)	(≥ 2.4)
Alkaline Phosphatase, IU/L					
	Short-term	40.5 (27.0-320.0)	51.0 (26.0-152.0)	27.5 (16.0-76.0)	≤ 150 IU/L
	Long-term	41.0 (23.0- 75.0)	31.0 (28.0-85.0)	47.0 (12.0-74.0)	(≤ 300)

Values for blood and serum analytes were determined at four weeks (short-term), and twenty-six weeks (long-term). Reference values were taken from AAFCO guidelines (AAFCO, 2010) for group means and individual dogs.

Conducting weight loss and digestibility studies with companion dogs, as opposed to colony dogs, presents new challenges because owner compliance in feeding and sample collection must be accounted for, as well as lapses in dietary discretion when feeding and

collecting samples in a multiple dog household. Although this study was successful in achieving weight loss, many dogs did not achieve ideal weight during or following completion of the long-term study. This investigative team appreciates that lapses in study compliance may complicate interpretation of the results. However, these challenges emphasize the need for effective communication and perhaps an accelerated translation of canine weight loss study findings to real-clinic settings for body weight management planning.

A1.5. Conclusions:

In this study, we showed that nutritionally complete dog foods containing cooked bean powders were digestible by overweight or obese, adult, companion dogs undergoing short or long-term calorically restricted weight loss. The dog foods supported apparent weight loss, provided utilizable energy, and the dogs maintained indices of nutritional adequacy when compared to a bean-free control dog food. Our findings of higher NFE ATTD in both the BB and NB diets compared to CON suggests that bean-based dog foods may differentially impact canine carbohydrate metabolism. This study concludes that cooked common beans are safe and digestible as a major food ingredient during canine weight loss, when fed in a nutritionally complete, extruded kibble, and provides rationale for the continued investigation of the potential for cooked beans to improve protein, lipid, and carbohydrate metabolism, which are important for overall canine health.

A1.6. Acknowledgements:

We would like to thank ADM Alliance Nutrition for providing the dog foods and Gordon Gregory at ADM Edible Bean Specialties for providing the cooked bean powder. We would also

like to thank the Wellington Veterinary Hospital and the Flint Animal Cancer Center Clinical Trials Core for providing companion dogs for participation in this study and clinical oversight. Additionally, we would like to thank Cadie Tillotson for technical assistance with study coordination. This research received no specific grant from any funding agency, commercial or not-for profit sectors.

A1.7. Declaration of Interests:

Bean powder was supplied by ADM Edible Bean Specialties and dog food formulations and proximate analysis were completed by ADM Alliance Nutrition labs. While these studies and analysis of results were completed at Colorado State University and should be considered free from any experimental bias, commercialization of bean-based dog foods are in early stages of development by members of this investigative team.

REFERENCES

AAFCO, (2010), 2010 Official Publication. Association of American Feed Control Officials Inc, West Lafayette, IN.

Barrett, M.L., and Udani, J.K., (2011), A proprietary alpha-amylase inhibitor from white bean (Phaseolus vulgaris): A review of clinical studies on weight loss and glycemic control. Nutrition Journal 10 (24) doi:10.1186/1475-2891-10-24

Borresen, E.C., et al., (2014), Feasibility of Increased Navy Bean Powder Consumption for Primary and Secondary Colorectal Cancer Prevention. Current Nutrition and Food Science 10 (2): 112–119. doi:10.2174/1573401310666140306005934

Butterwick, R., and Markwell, P., (1997), Effect of amount and type of dietary fiber on food intake in energy-restricted dogs. American Journal of Veterinary Research 58 (3): 272–276.

Chávez-Santoscoy, R.A., et al., (2014), Conjugated and free sterols from black bean (Phaseolus vulgaris L.) seed coats as cholesterol micelle disruptors and their effect on lipid metabolism and cholesterol transport in rat primary hepatocytes. Genes & Nutrition 9 (1): 367. doi:10.1007/s12263-013-0367-1

Deibert, P., et al., (2004), Weight loss without losing muscle mass in pre-obese and obese subjects induced by a high-soy-protein diet. International Journal of Obesity 28 (10): 1349–1352.

Forster, G.M., et al., (2015), Consumption of Cooked Navy Bean Powders Modulate the Canine Fecal and Urine Metabolome. Current Metabolomics 3 (2): 90–101. doi:10.2174/2213235X03666150519234354

Forster, G.M., et al., (2012a), Effects of cooked navy bean powder on apparent total tract nutrient digestibility and safety in healthy adult dogs. Journal of Animal Science 90 (8): 2631–2638. doi:10.2527/jas.2011-4324

Forster, G.M., (2012b), Nutritional weight loss therapy with cooked bean powders regulates serum lipids and biochemical analytes in overweight and obese dogs. Journal of Obesity & Weight Loss Therapy 2 (8): 149. doi:10.4172/2165-7904.1000149

German, A., (2010), Obesity in companion animals. In Practice 32 (2): 42–50. doi:10.1136/inp.b5665

German, A. J., (2006), The Growing Problem of Obesity in Dogs and Cats. The Journal of Nutrition 136 (7): 1940S–1946S.

German, A.J., et al., (2009), Use of starting condition score to estimate changes in body weight and composition during weight loss in obese dogs. Research in Veterinary Science 87 (2): 249–254.

German, A.J., et al., (2010), A high protein high fibre diet improves weight loss in obese dogs. The Veterinary Journal 183 (3): 294–297.

Hayat, I., et al., (2014), Nutritional and health perspectives of beans (Phaseolus vulgaris L.): an overview. Critical Reviews in Food Science and Nutrition 54 (5): 580–592.

Huazano-Garcia, A. and Lopez., M.G., (2015), Agavins reverse the metabolic disorders in overweight mice through the increment of short chain fatty acids and hormones. Food & Function. DOI: 10.1039/C5FO00830A

Kealy, R.D., et al., (2002), Effects of diet restriction on life span and age-related changes in dogs. Journal of the American Veterinary Medical Association 220 (9): 1315–1320.

Laflamme, D., (1997), Development and validation of a body condition score system for dogs. Canine Practice: 10–15.

Laflamme, D.P., (2012), Obesity in dogs and cats: What is wrong with being fat? Journal of Animal Science 90 (5): 1653–1662. doi:10.2527/jas.2011-4571

Linder, D.E., (2014), Top 5 Clincial Consequences of Obesity. Clinician's Brief http://www.cliniciansbrief.com/article/top-5-clinical-consequences-obesity

Linder, D.E., et al., (2013), Status of selected nutrients in obese dogs undergoing caloric restriction. BMC Veterinary Research 9: 219. doi:10.1186/1746-6148-9-219

Mao, J.F., et al., (2013), Prevalence and risk factors for canine obesity surveyed in veterinary practices in Beijing, China. Preventive Veterinary Medicine 112 (3–4): 438–442.

McCrory, M.A., et al., (2010), Pulse consumption, satiety, and weight management. Advances in Nutrition: An International Review Journal 1 (1): 17–30.

McGreevy, P., (2005), Prevalence of obesity in dogs examined by Australian veterinary practices and the risk factors involved. The Veterinary Record (156): 695–702.

Mollard, R., et al., (2012), Regular consumption of pulses for 8 weeks reduces metabolic syndrome risk factors in overweight and obese adults. British Journal of Nutrition 108 (S1): S111–S122.

Mudryj, A.N., Yu, N., and Aukema, H.M. (2014), Nutritional and health benefits of pulses. Applied Physiology, Nutrition, and Metabolism 39 (11): 1197–1204. doi:10.1139/apnm-2013-0557

NRC, (2006), Nutrient Requirements of Dogs and Cats. The National Academies Press, Washington, DC.

Papanikolaou, Y., and Fulgoni, V.L. (2008), Bean Consumption Is Associated with Greater Nutrient Intake, Reduced Systolic Blood Pressure, Lower Body Weight, and a Smaller Waist Circumference in Adults: Results from the National Health and Nutrition Examination Survey 1999–2002. Journal of the American College of Nutrition 27 (5): 569–576.

Prosky, L., et al., (1992), Determination of Insoluble and Soluble Dietary Fiber in Foods and Food-Products - Collaborative Study. Journal of AOAC International 75 (2): 360–367.

Ramírez-Jiménez, et al., (2015), Potential role of bioactive compounds of Phaseolus vulgaris L. on lipids-lowering mechanisms. Food Research International ahead-of-print doi:10.1016/j.foodres.2015.01.002

Rayalam, S., Della-Fera, M.A., and Baile, C.A., (2008), Phytochemicals and regulation of the adipocyte life cycle. The Journal of Nutritional Biochemistry 19 (11): 717–726. doi:http://dx.doi.org/10.1016/j.jnutbio.2007.12.007

Rebello, C., Greenway, F., and Finley, J., (2014), A review of the nutritional value of legumes and their effects on obesity and its related co-morbidities. Obesity Reviews 15 (5): 392–407.

Shai, I., et al., (2008), Weight Loss with a Low-Carbohydrate, Mediterranean, or Low-Fat Diet. New England Journal of Medicine 359 (3): 229–241. doi:10.1056/NEJMoa0708681

Weber, M., et al., (2007), A High-Protein, High-Fiber Diet Designed for Weight Loss Improves Satiety in Dogs. Journal of Veterinary Internal Medicine 21 (6): 1203–1208.

Yamka, R.M., Friesen, K.G., and Frantz, N.Z., (2006), Identification of Canine Markers Related to Obesity and the Effects of Weight Loss on the Markers of Interest. International Journal of Applied Research in Veterinary Medicine 4 (4): 10.

APPENDIX

A2. DIFFERENTIAL EFFECTS OF RICE BRAN CULTIVARS TO LIMIT *SALMONELLA* TYPHIMURIUM IN CHICKEN CECAL *IN VITRO* INCUBATIONS AND IMPACT ON CECAL MICROBIOME AND METABOLOME[5]

A2.1. Summary:

In this study, rice brans from different cultivars (Calrose, Jasmine, and Red Wells) were assessed for their ability to inhibit *Salmonella enterica* serovar Typhimurium using an *in vitro* mixed anaerobic culture system containing cecal microbiota obtained from broilers of different ages. *Salmonella* Typhimurium was added to controls (feed only, cecal only, and feed + cecal material) and treatments (feed + cecal + different rice brans) and *S*. Typhimurium populations were enumerated at 0, 24, and 48 h. Two experimental conditions were applied 1) un-adapted condition in which *S*. Typhimurium was added at the beginning of the culture incubation and 2) adapted condition in which *S*. Typhimurium was added after a 24-hour pre-incubation of the cecal bacteria with the feed and/or rice bran. Among the three rice brans, only Calrose exhibited a rapid inhibition of *S*. Typhimurium, which decreased to undetectable levels after 24 h under the adapted incubation. Changes in microbiological composition and metabolites by addition of Calrose bran were also investigated with an Illumina MiSeq platform and gas chromatography—mass spectrometry, respectively. Addition of Calrose bran resulted in significant changes including decreased Firmicutes phylum abundance and an increased number of metabolites

---

[5] Rubinelli, P.M., Kim, S.A., Park, S.H., Roto, S.M., **Nealon, N.J.**, Ryan, E.P., Ricke, S.C. *Differential effects of rice bran cultivars to limit Salmonella Typhimurium in chicken cecal in vitro incubations and impact on the cecal microbiome and metabolome*. PLoS One. 12(9):e0185002. September 2017.

associated with fatty acid metabolism. In summary, it appears that rice bran from specific rice cultivars may be effective as a means to reduce *Salmonella* in the chicken ceca. In addition, Calrose rice bran inclusion leads to changes in cecal microbiological composition and metabolite profile.

A2.2. Introduction:

Ensuring the microbiological safety of poultry products is a critical concern for the poultry industry. Traditional prebiotics were defined as "a non-digestible ingredient which beneficially influence the host by selectively stimulating the growth and/or activity of one or a limited number of bacteria in the colon" and promoted occasionally as effective alternatives to antimicrobials. More recently, the definition of a prebiotic has been modified and now includes a broader range of ingredients derived from multiple sources (Hutkins *et al.*, 2016; Roto *et al.*, 2015). Given the escalating global public health concern of antibiotic resistance (in *Salmonella*), prebiotics and their resultant modulation of gastrointestinal microbiota activity can thus be promoted as potential alternatives to antimicrobial therapy use in poultry (Gibson and Roberfroid, 1995; Patterson and Burkholder, 2003; Ricke, 2015; Roberfroid, 2007). Rice bran is an underutilized product of rice milling and contains a variety of components including proteins, amino acids, complex carbohydrates, minerals, vitamins, phytonutrients, phospholipids, essential fatty acids, and antioxidants that have nutritional value (Ryan *et al.*, 2011). Rice bran also possesses various components that exhibit prebiotic activities which can modulate microbiota in the intestine and potentially help to prevent chronic diseases (Sheflin *et al.*, 2015), and evidence supports that the antimicrobial activity of rice bran against *Salmonella* Typhimurium can vary across cultivars (Goodyear *et al.*, 2015). Rice bran has been investigated for its prebiotic

properties and several studies have demonstrated that *S*. Typhimurium colonization in the animal gastrointestinal tract can be reduced by inclusion of rice bran in the diet (Kim *et al.*, 2012a; Kim *et al.*, 2013; Kumar *et al.*, 2012).

There is no information on the general ability of rice bran to reduce *Salmonella* when fed to poultry, or on the relative potency of brans derived from different rice cultivars in specifically reducing *Salmonella* in the poultry gastrointestinal tract. The main site of *Salmonella* colonization poultry is the ceca (Hudault *et al.*, 1985). Poultry ceca contain a variety of bacteria which are characterized as strict anaerobes (Fan *et al.*, 1995; Ricke and Pillai, 1999; Salanitro *et al.*, 1974). To investigate the possible effects of prebiotics or prebiotic-like materials on these anaerobic bacteria and their interaction with prebiotics and *Salmonella*, an anaerobic mixed culture system has been employed as a screening tool (Rubinelli *et al.*, 2016).

Inhibition of *S*. Typhimurium by rice bran was previously investigated across rice varieties in mice (Ghazi *et al.*, 2016; Goodyear *et al.*, 2015), and these findings are relevant to the present study for chickens as the previous studies compared three different cultivars of rice: Jasmine, Red Wells, and Calrose that were examined as treatment candidates in the current study. The previous studies confirmed variation in secondary metabolite components such as total phenolics, γ-oryzanol, fatty acids and vitamin-E isoforms (Forster *et al.*, 2013; Ghazi *et al.*, 2016; Goodyear *et al.*, 2015). Jasmine rice has a brown bran layer and has significantly less total phenolic content compared to Red Wells, but is relatively rich compared to other varieties in γ-tocotrienol, a vitamin E isoform with anti-proliferative activity on Caco-2 cells, a human colon cancer cell line (Forster *et al.*, 2013). Red Wells is isogenic with the agronomically important Wells variety, except for a deletion mutation that restores the correct reading frame in the *Rd* gene (Brooks *et al.*, 2008), encoding a regulatory factor that activates synthesis of

proanthocyanidins, precursors of anthocyanins, flavonoids, and flavonoid derivatives (Furukawa *et al.*, 2007). The wild-type Rd restores the red pericarp color of wild type red rice, thus the name Red Wells. Calrose rice contains a brown bran and this bran has been shown to exhibit a synergistic effect with probiotics on the elimination of rotavirus and norovirus-induced diarrhea in orally-challenged gnotobiotic neonatal pigs (Lei *et al.*, 2016; Yang *et al.*, 2015).

In this study, we used cecal contents collected from broiler chickens, which possess a fairly diverse microbiota, to investigate empirical effects of different rice bran on reducing the *Salmonella* population. In addition, because the microbiota in ceca can change as the host matures (Roto *et al.*, 2015), cecal materials were obtained and analyzed for microbiome changes at two different chicken ages (28 and 42 days). Metabolomic analysis by gas chromatography-mass spectrometry (**GC-MS**) of 24 h anaerobic cultures with and without rice bran was also investigated to examine metabolites of rice bran or of rice bran fermentation that might have roles in reducing *Salmonella* growth. Together with Illumina MiSeq DNA sequencing of 16s ribosomal DNA from these cultures, we present a comprehensive view of rice bran effects in a controlled system that approximates the anaerobic conditions and microbiota of the chicken hindgut. The findings indicate the potential utility of rice bran or components thereof in the control of *Salmonella* in the preharvest broiler chicken and contribute to a better understanding of ecological and metabolic changes in the ceca upon exposure to rice bran.

A2.3. Materials and Methods:

A2.3.1. Bacterial strain:

Salmonella enterica serovar Typhimurium marker strain ST97, a nalidixic acid-resistant (**NA^{R}**) strain, was kindly provided by Dr. Billy Hargis, Department of Poultry Science,

University of Arkansas (Fayetteville, AR). The bacterial strain was grown in sterile tubes containing Luria-Bertani (**LB**) medium supplemented with 20 μg/ml nalidixic acid at 37°C for 16 h with agitation at 250 rpm.

A2.3.2. Rice bran cultivars:

Heat-stabilized rice bran of cultivars Jasmine, Red Wells, and Calrose were obtained from Dr. Elizabeth Ryan, Colorado State University. Rice bran isolation was performed following detailed described in previously published research (Forster *et al.*, 2013).

A2.3.3. Anaerobic culture medium:

The chicken cecal microbiota were inoculated from freshly harvested chicken ceca at a 1:3000 dilution into anaerobic dilution solution (**ADS**:,0.45g/L K_2HPO_4, 0.45 g/L KH_2PO_4, 0.45 g/L $(NH_4)_2SO_4$, 0.9 g/L NaCl, 0.1875 g/L $MgSO_4$-$7H_2O$, 0.12 g/L $CaCl_2$-$2H_2O$, 1 ml/L 0.1% resazurin, 0.05% cysteine-HCl, and 0.4% sodium carbonate) (Donalson *et al.*, 2008; Donalson *et al.*, 2007; Dunkley *et al.*, 2007; Fan *et al.*, 1995; Saengkerdsub *et al.*, 2006; Shermer *et al.*, 1998) with ground (25 mesh) Torres chick starter feed (1.25% w/v) as the carbon source. Prepared ADS was sparged with an anaerobic gas mixture consisting of 90% nitrogen/5% carbon dioxide/5% hydrogen in an anaerobic chamber for 30 minutes using an aquarium air pump and airstone before autoclaving. After autoclaving, the ADS was subsequently cooled to room temperature and placed in an anaerobic chamber overnight to remove all traces of oxygen. One bird was used as cecal donor in each of three independent experiments.

A2.3.3. Cecal inocula preparation:

Cecal contents were obtained from freshly killed 28-day and 42-day-old Cobb male broiler chickens (Cobb-Vantress, Siloam Springs, AR), killed by CO_2 asphyxiation, followed by aseptically removing the ceca using sterile tools, and the ceca were subsequently placed in sterile sample bags in a portable anaerobic box (Mitsubishi Gas Chemical Co., Japan) containing oxygen-scrubbing sachets. The use of chickens as a source for cecal inocula was approved by a University of Arkansas Institutional Animal Care and Use Committee (**IACUC**) to ensure humane treatment of the chickens. Immediately after harvest, ceca were transferred to an anaerobic chamber (Coy Laboratory Products, Grass Lake, MI) devoid of oxygen and containing an atmosphere of 90% nitrogen/5% CO_2/5% hydrogen. To maintain an anaerobic environment inside the chamber, two palladium catalyst scrubbers were maintained continuously.

A2.3.4. Anaerobic in vitro mixed cultures:

The overall experimental approach used in this study is shown in **Figure A2.1**. Briefly, a portion of the cecal contents were weighed within the aseptic chamber. The weights of 0.1-gram aliquots of cecal contents were measured and subsequently diluted 1:3000 by addition to 300 ml ADS. Prior to the experiment, the absence of NA resistant *S*. Typhimurium was confirmed by inoculation into tetrathionate (**TT**) enrichment broth (BD Biosciences) followed by streaking onto brilliant green agar plates (BD Biosciences). A 20 ml portion of the diluted cecal content was added to each sterile serum bottle and 0.25 g chicken feed and/or 0.2 g rice bran was added to the bottles as indicated in **Figure A2.1A**. Three control groups were used in this study: ADS containing 1) feed only, 2) cecal content only, and 3) feed and cecal content combined. Three types of rice bran cultivars (Jasmine, Red Wells, and Calrose) were added to the anaerobic mixed

cultures (1% w/v) as treatment groups.

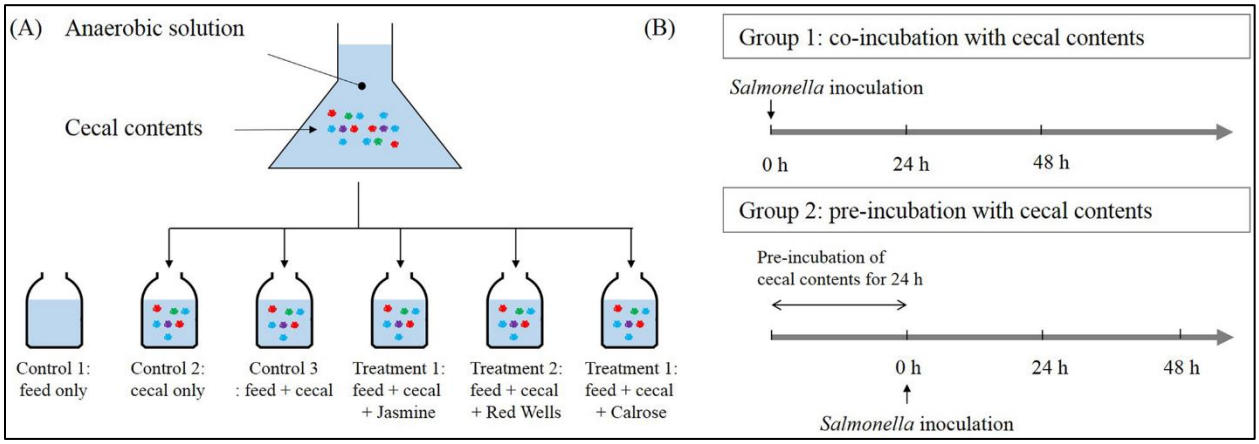

Figure A2.1. Experimental design of the anaerobic *in vitro* mixed cultures.
(A) *Controls contained 1) feed, 2) cecal content, and 3) feed and cecal contents without rice bran while treatments contained feed, cecal content, and different amounts of rice bran including Jasmine, Red Wells, and Calrose.* ***(B)*** *Experimental design used in this study. Unadapted condition: cultures receive Salmonella Typhimurium at the same time as cecal content (at 0 time). Adapted condition: cultures received* Salmonella *Typhimurium after a 24 h incubation of cecal content under anaerobic conditions. This figure was adapted and modified from Rubinelli et al. (2016).*

A2.3.5. Salmonella inoculation and enumeration of survivors:

The cell density of a 16 h culture of NA-resistant *S*. Typhimurium (strain ST97) was measured by spectrophotometry at 600 nm. Working in the anaerobic chamber, this culture was then added to each 20 mls of diluted cecal content in ADS to yield approximately 1 x 10^7 CFU/ml starting density of *S*. Typhimurium. A small portion of the culture was removed for plating, and the cultures were then stoppered with airtight rubber stoppers and aluminum crimps, removed from the anaerobic chamber, and incubated at 37°C for 48 h in a shaking incubator (Model G25, New Brunswick, Inc.) at 150 rpm. Two different experimental designs were established as shown in **Figure A2.1B**, referred to as Group 1 and Group 2. In Group 1 (unadapted incubation), *S*. Typhimurium was added at the beginning of the culture incubation

along with cecal bacteria and/or chicken feed and/or rice bran. In Group 2 (adapted incubation), *S*. Typhimurium was added after a 24 h pre-incubation of the cecal bacteria with the chicken feed and/or rice bran. After 0, 24, and 48 h incubation, an aliquot of each culture was removed and subsequently diluted with sterile phosphate-buffered saline (**PBS**). Undiluted and diluted aliquots of cultures were spread in duplicate on Brilliant Green agar plates (BD Biosciences) supplemented with 20 μg/ml NA for quantification of colony forming units (**CFU**) of *S*. Typhimurium. If no *S*. Typhimurium were detected at a particular time point in the undiluted culture, this culture was inoculated into tetrathionate (**TT**) enrichment broth in order to confirm that no *S*. Typhimurium survived. Experiments were performed in triplicate.

A2.3.6. Microbiome analysis:

Microbiome analysis was conducted in triplicate on two controls ("feed + cecal" and "cecal only" controls) and the Calrose treatment (feed + cecal + Calrose) in the adapted mixed culture condition described above at various time points (0, 6, 12, 24, and 48 h) using cecal contents from two different ages of broilers (28 and 42 days). Bacterial genomic DNA was extracted via a QIAamp Fast DNA Stool Mini Kit (Qiagen, Valencia, CA) following the manufacturer's instructions. Sequencing was performed by targeting the V4 hypervariable region of 16S rRNA using an Illumina MiSeq platform (Illumina, San Diego, CA) and sequence reads were analyzed with the Quantitative Insights into Microbial Ecology (**QIIME**) pipeline (version 1.9.0) as described previously (Park *et al.*, 2016).

A2.3.7. Extraction of metabolites:

Three replicate anaerobic cultures containing 1% Calrose rice bran, 1.25% chicken feed, and a 1:3000 dilution of chicken cecal contents in ADS were grown for 24 h at 37°C in airtight serum bottles with thick stoppers and crimps and contained a 5% H_2/5% CO_2/90% N_2 atmosphere. Control cultures were identical except that they did not contain rice bran. The cecal contents used were that of three 6-week-old broiler chickens (three biological replicates). After 24 h, each culture was centrifuged at 8000 x g for 6 minutes. The remainder of the metabolomics analysis was performed at the University of California Davis Genome Center, Metabolomics Core and Research Laboratories, as follows: A 30 µl portion of each supernatant was extracted with 1 ml of Extraction Solution (acetonitrile: isopropanol: water, 3:3:2, de-gassed with nitrogen for 5 minutes and pre-cooled to -20°C). This mixture was subsequently vortexed for 10 seconds and shaken for 5 minutes at 4°C using an orbital mixer. The resulting mixture was centrifuged 2 min, 14,000 x g. A 500 µl portion of supernatant was dried using a centrivap (Labconco). The dried sample was derivatized and analyzed by GC-MS as described in the following subsections.

A2.3.8. Injector conditions:

The Agilent 6890 GC was equipped with a Gerstel automatic liner exchange system (**ALEX**) that includes a multipurpose sample (**MPS2**) dual rail, and a Gerstel CIS cold injection system (Gerstel, Muehlheim, Germany) with a temperature program as follows: 50°C to 275°C final temperature at a rate of 12°C/s and held for 3 minutes. Injection volume was 0.5 µl with 10 µl/s injection speed on a splitless injector with purge time of 25 seconds. Liner (Gerstel #011711-010-00) was changed after every 10 samples, (using the Maestro1 Gerstel software vs.

1.1.4.18). Before and after each injection, the 10 µl injection syringe was washed three times with 10 µl ethyl acetate.

A2.3.9. Gas chromatography conditions:

A 30 m long, 0.25 mm i.d. Rtx-5Sil MS column (0.25 µm 95% dimethyl 5% diphenyl polysiloxane film) with an additional 10 m integrated guard column was used (Restek, Bellefonte PA). 99.9999% pure Helium with built-in purifier (Airgas, Radnor PA) was set at a constant flow of 1 ml/min. The oven temperature was held constant at 50°C for 1 min and then ramped at 20°C/min to 330°C and finally held constant for 5 min.

A2.3.10. Mass spectrometry:

A Leco Pegasus IV time of flight mass spectrometer was controlled by the Leco ChromaTOF software vs. 2.32 (St. Joseph, MI). The transfer line temperature between gas chromatograph and mass spectrometer was set to 280°C. Electron impact ionization at -70 eV was employed with an ion source temperature of 250°C. Acquisition rate was 17 spectra/second, with a scan mass range of 85 to 500 Da. The column was a Restek corporation Rtx-5Sil MS (30m x 0.25 mm I.D. with 0.25 µm 95% dimethyl/5% diphenylpolysiloxane film). The mobile phase was helium, column temperature 50 to 330°C, flow rate 1 ml/min. Injection volume was 0.5 ml, injection temperature 50°C ramped to 250°C at 12°C/s. Oven temperature program was 50°C 1 min, then ramped at 20°C/min to 330°C, and finally held for 5 min.

A2.3.11. Detection and identification of metabolites and metabolic pathway classification:

Raw data files were preprocessed directly after data acquisition and stored as ChromaTOF-specific *.peg files, as generic *.txt result files and additionally as generic ANDI MS *.cdf files. ChromaTOF vs. 2.32 was used for data preprocessing without smoothing, 3 s peak width, baseline subtraction just above the noise level, and automatic mass spectral deconvolution and peak detection at signal/noise levels of 5:1 throughout the chromatogram. Apex masses were reported for use in the BinBase algorithm. Result *.txt files were exported to a data server with absolute spectra intensities and further processed by a filtering algorithm implemented in the metabolomics BinBase database. The BinBase algorithm (**rtx5**) used the settings: validity of chromatogram (< 10 peaks with intensity $>10^7$ counts s^{-1}), unbiased retention index marker detection (MS similarity > 800, validity of intensity range for high m/z marker ions), retention index calculation by 5th order polynomial regression. Spectra were cut to 5% base peak abundance and matched to database entries from most to least abundant spectra using the following matching filters: retention index window ± 2,000 units (equivalent to approximately ± 2 s retention time), validation of unique ions and apex masses (unique ion must be included in apexing masses and present at greater than 3% of base peak abundance), mass spectrum similarity must fit criteria dependent on peak purity and signal/noise ratios and a final isomer filter. Metabolites were classified into possible pathways using the KEGG and PubChem databases.

A2.3.12. Statistical analysis:

The log CFU/ml for control (feed only, cecal only, feed + cecal) and experimental treatments (feed + cecal + Jasmine, Red Wells, or Calrose rice bran) were determined by

averaging all biological replicates and one way analysis of variance (Ly and Casanova) was conducted to compare differences of bacterial population or relative abundance among groups with JMP Genomics 7.0 (SAS Institute Inc., Cary, NC) at $P < 0.05$. A Student's t-test was also used to compare mean abundances of metabolites between Calrose and the "no rice bran" control (**NC**). $P < 0.05$ in a two-tailed test was considered significant.

A2.4. Results and Discussion:

A2.4.1. Calrose decreased Salmonella Typhimurium survival in anaerobic mixed culture during adapted incubation conditions.

This study investigated effect of rice brans within two different conditions including Group 1 (unadapted) and Group 2 (adapted condition). The survival of *S*. Typhimurium in the anaerobic mixed culture containing different rice brans (Jasmine, Red Wells, and Calrose) under unadapted and adapted incubation conditions is shown in **Table A2.1**. In the unadapted condition, neither of the controls or the experimental treatments significantly inhibited *S*. Typhimurium after either 24 or 48 h incubation. The population of *S*. Typhimurium was increased during incubation from 6.73 to 6.97 log CFU/ml (initial population) to 7.26 to 8.78 log CFU/ml after 24 h and 7.27 to 8.60 log CFU/ml after 48 h.

Table A2.1. Population of *Salmonella* Typhimurium (log CFU/ml) in an anaerobic *in vitro* mixed culture

Experimental Condition	**Treatment**	**Incubation time (hours)**		
		0	**24**	**48**
Unadapted condition	Control 1: feed only	6.97±0.09	8.25±0.09^{b}	8.02±0.26^{ab}
	Control 2: cecal only	6.78±0.15	7.26±0.12^{c}	7.27±0.07^{b}
	Control 3: feed + cecal	6.88±0.07	8.49±0.11^{ab}	8.51±0.09^{a}
	Treatment 1:feed + cecal + Jasmine	6.73±0.10	8.70±0.09^{a}	8.60±0.13^{a}
	Treatment 2: feed + cecal + Red Wells	6.86±0.07	8.61±0.10^{a}	8.55±0.09^{a}
	Treatment 3: feed + cecal + Calrose	6.92±0.12	8.78±0.08^{a}	7.76±0.64^{ab}
Adapted condition	Control 1: feed only	6.84±0.14	7.19±0.04^{a}	6.95±0.13^{a}
	Control 2: cecal only	6.65±0.12	6.35±0.30^{a}	5.78±0.91^{a}
	Control 3: feed + cecal	6.78±0.13	6.20±0.08^{a}	3.91±0.72^{b}

Table A2.1. Population of *Salmonella* Typhimurium (log CFU/ml) in an anaerobic *in vitro* mixed culture				
	Treatment 1:feed + cecal + Jasmine	6.75±0.14	5.17±1.24[a]	5.78±0.39[ab]
	Treatment 2: feed + cecal + Red Wells	6.65±0.07	5.11±1.20[a]	5.74±0.28[ab]
	Treatment 3: feed + cecal + Calrose	6.73±0.07	2.55±0.82[b]	ND[c*]

***** ND, not detected (detection limit: 10 CFU/mL).
[a-c] Mean values in the same column and experimental condition denoted by different superscript letters represent statistically significant differences *($P<0.05$)*.
Average log CFU data comes from 3 independent experiments using different cecal contents.

In contrast, *S*. Typhimurium survival was significantly reduced under the adapted incubation conditions (Group 2 treatments) by Calrose rice bran compared to the control with feed + cecal contents but no rice bran (**Table A2.1**). Calrose bran rapidly decreased *S*. Typhimurium levels when compared with the feed + cecal control at 24 h. The population of *S*. Typhimurium (initially 6.73 log CFU/ml) in the Calrose bran-containing cultures were significantly reduced to 2.55 log CFU/ml after 24 h ($P < 0.05$). However, the level in the feed + cecal control at this same timepoint was 6.20 log CFU/ml. The Calrose bran-containing cultures reached an undetectable level (below the limit of detection of the dilution plating less than 10 CFU/ml) after 48 h, while the feed + cecal control cultures and Jasmine- and Red Wells-containing cultures were not significantly different from each other and remained much higher (approx. 4 to 6 log CFU/ml, **Table A2.1**).

Cultures after 48 h in the presence of Calrose bran yielding no detectable colonies were inoculated into TT enrichment broth to determine if *S*. Typhimurium could be recovered from them and detected by subsequent streak plating from the enrichments. However, none of these cultures exhibited detectable growth after inoculation from TT enrichment broth, suggesting that *S*. Typhimurium was completely eradicated by adding Calrose to the anaerobic mixed culture. Calrose rice bran-treated anaerobic mixed cultures consistently and reproducibly exhibited a rapid killing of *S*. Typhimurium, but only under adapted cecal microbiota conditions. Different results between unadapted and adapted conditions suggest that the fermentation associated with

the cecal 24 h pre-incubation of cecal contents prior to addition of *S*. Typhimurium may play an important role in inhibiting *S*. Typhimurium in the anaerobic mixed culture. Collectively, these results suggest that incubation of the cecal microbiome in the presence of Calrose rice bran prior to inoculation of pathogen influences microbiota and/or fermentation profiles that work prophylactically to prevent *Salmonella* colonization after infections (Goodyear *et al.*, 2015; Kumar *et al.*, 2012). These results, which demonstrate that higher levels of *Salmonella* growth inhibition by Calrose are achieved in adapted conditions, are also in accordance with our previous study reporting that a commercial biological product derived from yeast fermentation showed significantly higher bactericidal effects in the adapted condition compared to the unadapted condition (Rubinelli *et al.*, 2016). This supports that under the adapted conditions, the yeast product and Calrose might have similar downstream effects on *Salmonella* growth.

A2.4.2. Microbial correlation among groups:

Rarefaction plots of average observed OTUs and Chao1 from alpha diversity analysis are shown in **Figure A2.2**. Samples containing cecal contents from 42-day old broiler chickens exhibited greater observed OTU numbers compared to the other samples containing cecal contents from 28-day old broiler chickens (**Figure A2.2A**). Samples after 6 h incubation exhibited greater numbers than the other samples (**Figure A2.2B**). There were no significant differences in OTU numbers among cecal only control, feed + cecal control, and Calrose treatment group (**Figure A2.2C**). The Chao 1 rarefaction plot estimating species richness revealed similar results with the observed OTU plot (**Figure A2.2D**).

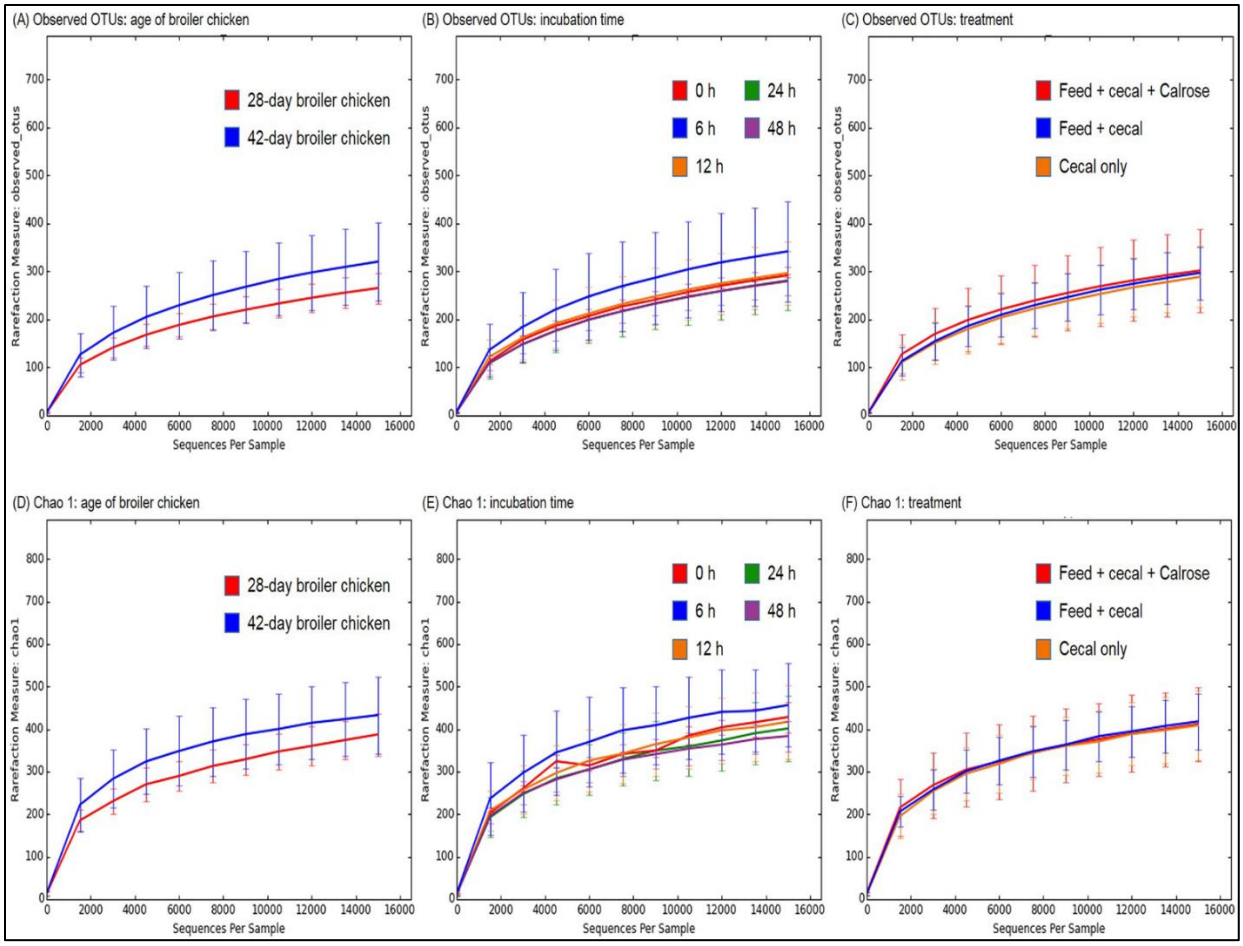

Figure A2.2. Alpha diversity analysis among groups.

Rarefaction curves of ***(A-C)*** *Observed_OTUs and* ***(D-F)*** *Chao 1.*

Figure A2.3 represents weighted (**A-C**) and unweighted (**D-F**) principal coordinated analysis (**PCoA**) UniFrac plots generated by the beta diversity analysis. In the PCoA UniFrac plot, each data point represents an individual sample. The P value indicates groups that are significantly different, and the R value indicates how strongly groups are different from each other. An R value near 0 meant no separation while the R value close to 1 was used to indicate that there was dissimilarity among groups. An R value from both weighted and unweighted PCoA plots categorized by age of the broiler chicken and incubation time (**Figure A2.3A**, **A2.3B**, **A2.3D**, **A2.3E**) was near 0 (0.011 to 0.114) which implied no significant dissimilarity among groups by these parameters. In both plots categorized by treatment (cecal only control,

cecal + feed control, and Calrose treatment), only the Calrose treatment group was slightly clustered but detectable patterns of obvious clustering were not observed (R value from weighted and unweighted plot: 0.437 and 0.322, respectively) **(Figure A2.3C** and **A2.3F).**

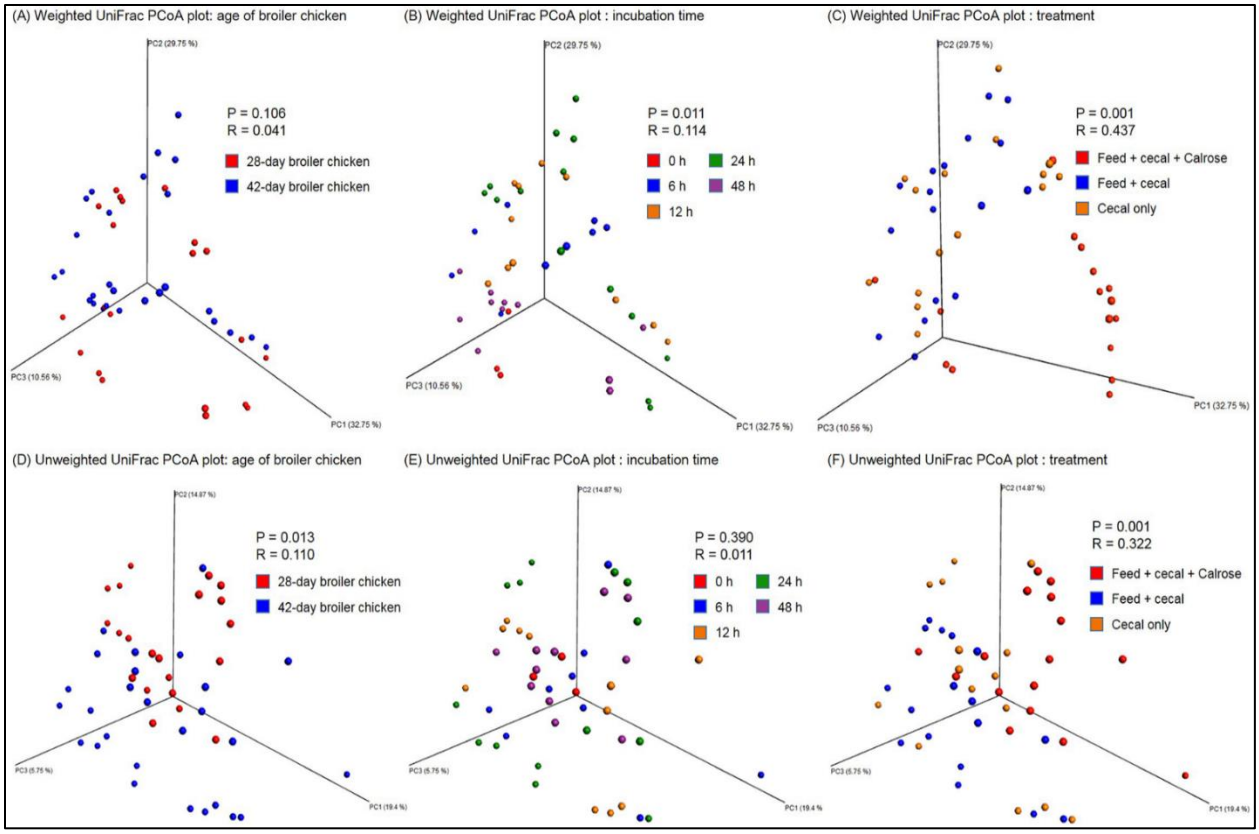

Figure A2.3. Beta diversity analysis among groups.

(A-C) *Weighted and* ***(D-F)*** *unweighted UniFrac PCoA plots of individual samples in each group.*

A2.4.3. Comparison of bacterial communities:

The overlap in microbial taxa at the genus level in control groups and Calrose treatment group are shown in **Figure A2.4A** as Venn diagrams. A 60.5% proportion of the bacterial genera were present in both control groups and the Calrose treatment group; indicating that controls and treatment groups shared similar bacterial communities. Only 3 and 2 genera were unique in cecal only control and feed + cecal control, respectively. In contrast, 22 unique genera were exclusively present in the Calrose treatment group but not in the control groups. This highlights the fact that Calrose treatment can significantly alter microbial communities. Venn diagram by

incubation time is also shown in **Figure A2.4B**. More than half of the genera (57.4%) were common among the four groups (6, 12, 24, and 48 h incubation groups).

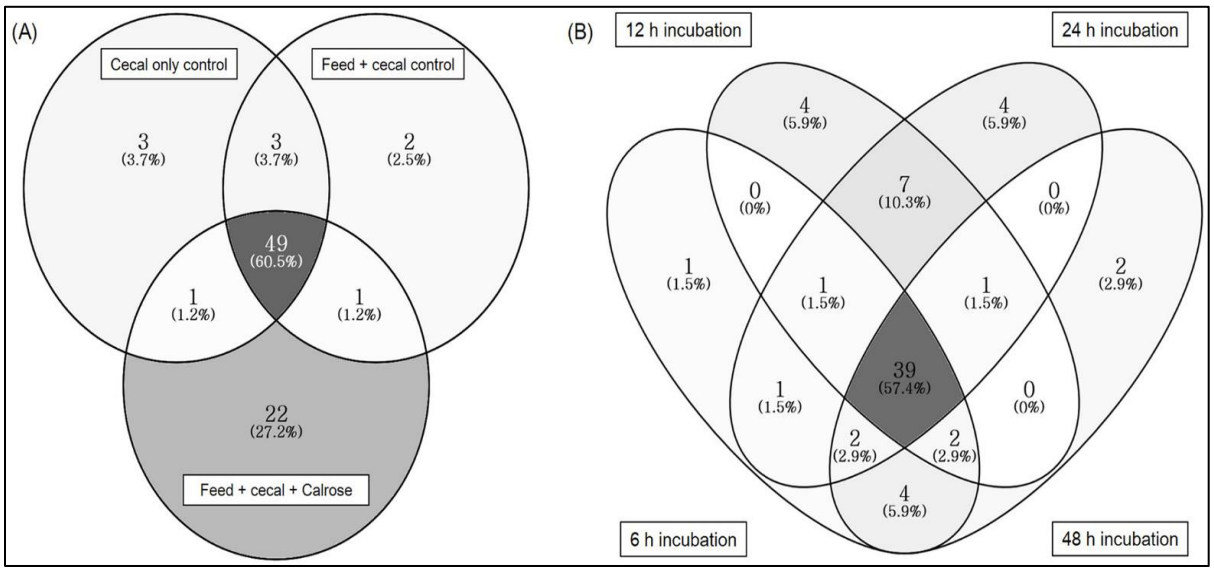

Figure A2.4. Distribution of bacterial taxa in genus level in sample groups.
A: *controls and treatment,* ***B:*** *incubation time.*

A2.4.4. Rice bran treatments and adaptation conditions are associated with phyla shifts in the microbiome profiles of incubated cecal contents originating from 28-day broiler chickens.

Microbiome analysis provides comprehensive information on bacterial composition changes in cecal microbiota when exposed to dietary changes or other factors that may influence microorganisms in the gastrointestinal tract. The relative abundance of major bacterial groups from phylum to genus level in an anaerobic mixed culture batch system containing cecal contents obtained from 28 days of broiler chickens is shown in **Figure A2.5.** Some data groups (e.g. cecal only control after 0, 6, and 24 h and feed + cecal control after 0, 12, 48 h) were removed since they yielded sequencing read numbers that were too low during sequencing and QIIME analysis.

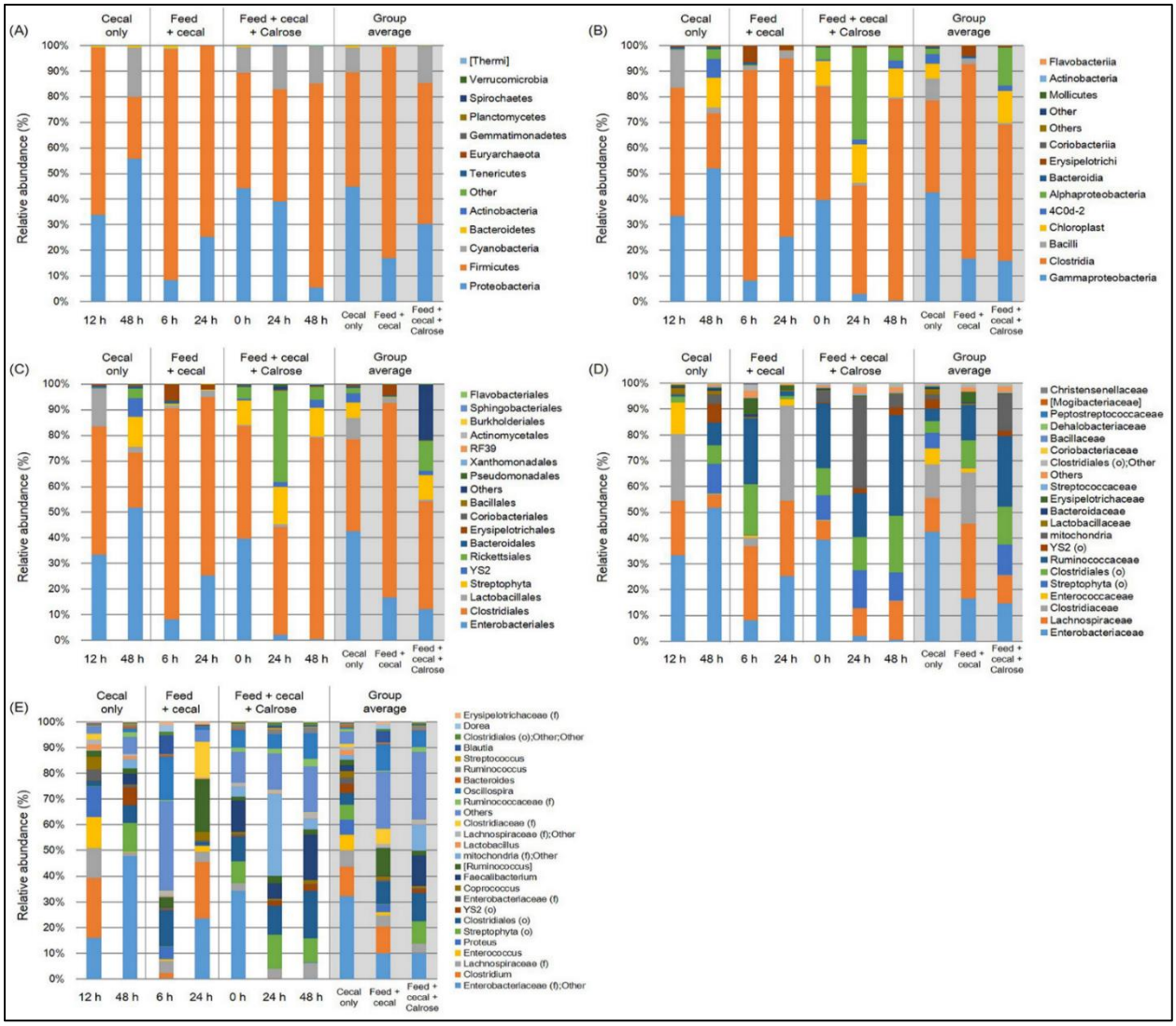

Figure A2.5. Relative abundance of major bacteria among different treatment groups at (A) phylum, (B) class, (C) order, (D) family, and (E) genus level in anaerobic mixed cultures (adapted condition) containing cecal contents.

*Microbiome analysis was conducted in triplicate on cecal contents only, feed and cecal contents, and feed + cecal + Calrose at various time points using cecal contents from 28-day-old broiler chickens. The bars represent the standard deviation. "**f**" and "**o**" in parentheses indicate family and order, respectively.*

The overall microbiota of each group revealed generally similar patterns; the top three dominant bacterial groups at the phylum level belonged to either Firmicutes, Proteobacteria, or Cyanobacteria (**Figure A2.5A**). The cecal only control group was dominated by Proteobacteria (group average value, 44.80%), Firmicutes (44.78%), and Cyanobacteria (9.62%) accounting for 99.20% of the entire phyla. However, the most predominant bacterial group in the feed + cecal control and Calrose treatment was Firmicutes with 82.37 and 42.93%, respectively. In the Calrose treatment group, the relative abundance of Firmicutes was significantly increased ($P < 0.05$) with increased incubation time from 44.88% (initial) and 43.90% (24 h) to 79.60% (48 h). Sequenced microbiota recovered from each group exhibited different class levels (**Figure A2.5B**). In the cecal only control, Clostridia (group average value, 35.80%), Gammaproteobacteria (42.71%), and Bacilli (8.48%) were relatively common accounting for 87.00%. In contrast, the Calrose treatment group harbored the greatest proportion of Clostridia constituting 42.14% and also contained Gammaproteobacteria and Alphaproteobacteria at 12.56 and 11.67%, respectively. In the Calrose treatment group, when the incubation time increased, the abundance of Clostridia significantly increased from 44.09% at initial time to 78.70% at 48 h incubation while that of Gammaproteobacteria decreased from 39.77% at the initial time to 0.58% at 48 h incubation.

At the order taxonomic level, overall microbial distributions via sequencing exhibited the most operational taxonomic units (**OTU**'s) belonging to Clostridiales and Enterobacteriales with 35.80 and 42.68% for the cecal only control group, 75.93 and 16.71% for the feed + cecal control, and 42.14 and 12.31% for the Calrose treatment group (**Figure A2.5C**). The Calrose treatment group revealed higher levels of Rickettsiales (11.61%) than the other control groups (2.07 and 0.13% for cecal only and feed + cecal control, respectively). Along with incubation

time, the proportion of Clostridiales in the Calrose treatment group generally increased (from 44.09 at 0 h to 78.70% at 48 h) while Enterobacteriales significantly decreased (from 39.69 at 0 h to 0.49% at 48 h).

Relative abundance of major bacterial groups at the family taxonomic level varied among different treatments. The top 5 bacterial groups of the cecal only control were Enterobacteriaceae (group average value 42.68%), Clostridiaceae (13.07%), Lachnospiraceae (13.10%), Enterococcaceae (6.21%), and Streptophya (order level) (5.97%). For the Calrose treatment groups, Ruminococcaceae, Clostridiales (order level), Enterobacteriaceae, Streptophyta (order level), and Lachnospiraceae accounted for the highest abundance level with 22.89, 12.40, 12.31, 9.82, and 8.99%, respectively. During prolonged incubation, the proportion of Lachnospiraceae, Ruminococcaceae, and Clostridiales (order level) increased (7.31 to 15.20%, 25.14 to 39.55%, and 10.76 to 22.23%, respectively) while that of Enterobacteriaceae decreased (39.63 to 0.49%).

Similar to the other taxonomic hierarchy, different treatments also exhibited variable proportions in the primary detectable bacterial genera. The top 5 genera were Enterobacteriaceae (family level); Other, Clostridium, Lachnospiraceae (family level), Enterococcus, and Proteus for the cecal control group and Ruminococcus, Clostridium, Oscillospira, Enterobacteriaceae (family level); Other, Clostridiales (order level) for feed + cecal control group. In contrast, Faecalibacterium (13.51%), Clostridiales (order level) (12.40%), Enterobacteriaceae (family level); Other (11.58%), Streptophyta (order level) (9.82%), and Oscillospira (7.18%) were apparently present in the Calrose treatment groups as the primary genera. There were significant increases in abundance level of Clostridiales (order level) and Faecalibacterium from 10.76 to 22.23% and 13.85 to 21.35%, respectively, along with incubation time.

A2.4.5. Microbiome profiles of incubated cecal contents originating from 42-day broiler chickens:

The relative abundance of major bacteria in different groups from phylum to genus level in an anaerobic mixed culture containing cecal contents obtained from 42-day old broiler chickens is shown in **Figure A2.6**. Firmicutes, Proteobacteria, Bacteroidetes, and Cyanobacteria were the major bacterial groups of the identified phyla (**Figure A2.6A**). Relative abundance of Proteobacteria in the Calrose treatment (group average value, 12.06%) was generally lower than that of feed + cecal control (39.74%) while abundance of Firmicutes was higher than feed + cecal control (79.93 versus 47.94%). In the Calrose treatment, the abundance of Firmicutes was increased (70.80% at 12 h to 83.06% at 24 h). The relative abundance of Proteobacteria in Calrose treatment was 18.71 after 12 h incubation and 5.41% after 24 h incubation, respectively. These changes (an increase in Firmicutes and decrease in Proteobacteria) are in accordance with the results from Calrose treatments using 28 days cecal contents.

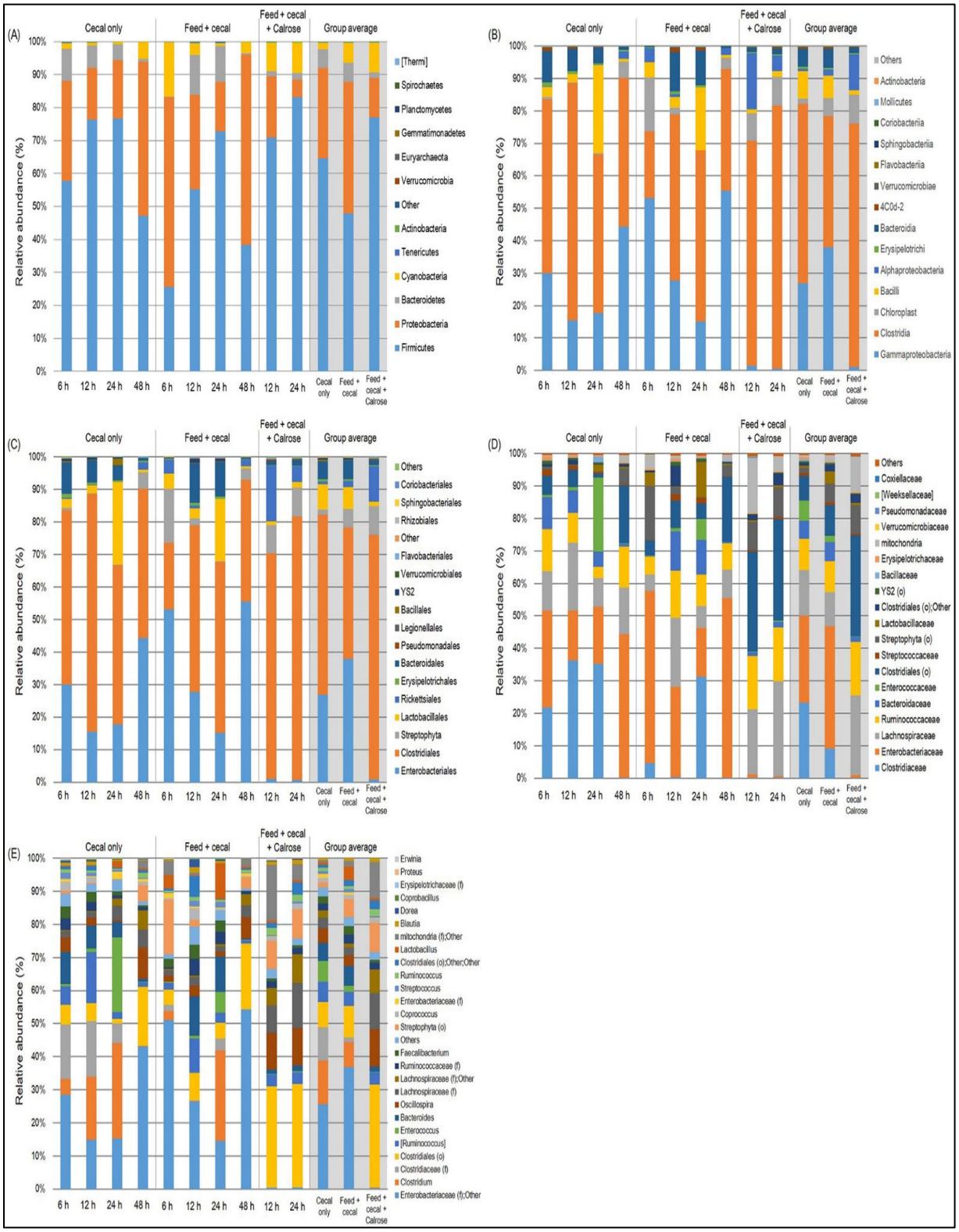
(A)
Cecal only
Feed + cecal
Feed + cecal + Calrose
Group average
Relative abundance (%)
6 h
12 h
24 h
48 h
Cecal only
Feed + cecal
Feed + cecal + Calrose
[Thermi]
Spirochaetes
Planctomycetes
Gemmatimonadetes
Euryarchaeota
Verrucomicrobia
Other
Actinobacteria
Tenericutes
Cyanobacteria
Bacteroidetes
Proteobacteria
Firmicutes
(B)
Others
Actinobacteria
Mollicutes
Coriobacteriia
Sphingobacteriia
Flavobacteriia
Verrucomicrobiae
4C0d-2
Bacteroidia
Erysipelotrichi
Alphaproteobacteria
Bacilli
Chloroplast
Clostridia
Gammaproteobacteria
(C)
Others
Coriobacteriales
Sphingobacteriales
Rhizobiales
Other
Flavobacteriales
Verrucomicrobiales
YS2
Bacillales
Legionellales
Pseudomonadales
Bacteroidales
Erysipelotrichales
Rickettsiales
Lactobacillales
Streptophyta
Clostridiales
Enterobacteriales
(D)
Others
Coxiellaceae
[Weeksellaceae]
Pseudomonadaceae
Verrucomicrobiaceae
mitochondria
Erysipelotrichaceae
Bacillaceae
YS2 (o)
Clostridiales (o);Other
Lactobacillaceae
Streptophyta (o)
Streptococcaceae
Clostridiales (o)
Enterococcaceae
Bacteroidaceae
Ruminococcaceae
Lachnospiraceae
Enterobacteriaceae
Clostridiaceae
(E)
Erwinia
Proteus
Erysipelotrichaceae (f)
Coprobacillus
Dorea
Blautia
mitochondria (f);Other
Lactobacillus
Clostridiales (o);Other;Other
Ruminococcus
Streptococcus
Enterobacteriaceae (f)
Coprococcus
Streptophyta (o)
Others
Faecalibacterium
Ruminococcaceae (f)
Lachnospiraceae (f);Other
Lachnospiraceae (f)
Oscillospira
Bacteroides
Enterococcus
[Ruminococcus]
Clostridiales (o)
Clostridiaceae (f)
Clostridium
Enterobacteriaceae (f);Other

Figure A2.6. Relative abundance of major bacteria among different treatment groups at (A) phylum, (B) class, (C) order, (D) family, and (E) genus level in anaerobic mixed cultures (adapted condition) containing cecal contents.

*Microbiome analysis was conducted in triplicate on cecal contents only, feed and cecal contents, and feed + cecal + Calrose at various time points using cecal contents from 48-day-old broiler chickens. The bars represent the standard deviation. "**f**" and "**o**" in parentheses indicate family and order, respectively.*

At the class taxonomic level, the top two dominant bacterial groups for the cecal only and feed + cecal control treatments were Clostridia and Gammaproteobacteria with 55.41 and 26.86% (group average value) for cecal only and 40.46 and 37.89% for feed + cecal control, respectively (**Figure A2.6B**). In the Calrose treatment group, the most predominant bacterial group was Clostridia accounting for 75.19% but the relative abundance of Gammaproteobacteria was significantly lower (1.01%) than the control groups. Bacilli were also relatively common in control groups (8.41 and 6.99%, respectively) while their abundance was significantly less in the Calrose treatment (1.45%). In contrast, the proportion of Alphaproteobacteria was higher in the Calrose treatment (11.02%) than the control groups (0.70 and 1.85%). During incubation, the proportion of Clostridia was maintained at a high level (69.32 and 81.05% at 12 and 24 h).

Sequenced microbiota recovered from each treatment exhibited proportionally different order taxonomic levels as well (**Figure A2.6C**). The top two dominant bacterial groups at the order level belonged to either Clostridiales or Enterobacteriales. The cecal only control and feed + cecal control treatments were dominated by Clostridiales (group average value, 55.41 and 4046%, respectively), Enterobacteriales (26.84 and 37.83%), and Lactobacillales (7.82 and 6.87%). However, the most predominant bacterial groups occurring in the Calrose treatment mixed cultures were Clostridiales (75.19%) and Rickettsiales (10.92%). The proportion of Clostridiales was significantly higher for the Calrose treatment than controls while the abundance of Enterobacteriales was significantly lower in the Calrose treatment (0.97%).

At the family taxonomic level, overall microbial distributions detected by sequencing revealed that most of the identified OTUs belonged to Clostridiaceae, Enterobacteriaceae, Lachnospiraceae, and Ruminococcaceae with 23.25, 26.84, 14.07, and 9.55% (group average value) for the cecal only control group and 9.03, 37.83, 10.50, and 9.45% for feed + cecal control, respectively (**Figure A2.6D**). In the Calrose treatment group, mixed culture incubations yielded a relatively high percentage of Clostridiales (39.19%), Lachnospiraceae (24.62%), and Ruminococcaceae (16.43%). The proportion of Enterobacteriaceae was significantly lower for the Calrose treatment (0.12%) than control groups (23.25% for cecal only control and 9.03% for feed + cecal control).

The different treatments also exhibited variable proportions in the primary bacterial genera. The top 5 genera were Enterobacteriaceae (family level); Other, Clostridium, Clostridiaceae (family level), Clostridiales (order level), and Ruminococcus for the cecal control group Enterobacteriaceae (family level); Other, Clostridium, Clostridiales (order level), Bacteroides, and Ruminococcus for feed + cecal control group (**Figure A2.6E**). For the Calrose treatment group, Clostridiales (order level), Oscillospira, Lachnospiraceae (family level), Lachnospiraceae (family level); Other, and Streptophyta (order level) were commonly present as the major genera. The Calrose treatment group yielded a significantly lower abundance of Enterobacteriaceae (family level) with 0.28% (group average value) compared to the other control groups (25.59 and 36.88% for cecal only and feed + cecal control, respectively). Since the *Salmonella* belongs to the family Enterobacteriaceae, the significant decreases in relative abundance of Enterobacteriaceae by Calrose treatment determined by microbiome analysis are in accordance with the results showing a significant reduction in *Salmonella* populations by Calrose treatment determined by bacterial culture method.

A2.4.6. Metabolite profiles reveal small molecules and metabolic pathways with potential anti-Salmonella activity.

Metabolite analysis was performed with only the Calrose supplemented incubations, since Calrose showed the most significant antimicrobial activity among the three cultivars of rice tested. Supernatants from the anaerobic cultures were collected at 0 and 24 h after initiating anaerobic incubation of the cecal contents with Calrose rice bran. Feed + cecal control cultures (negative control, **NC**) lacking rice bran were collected at the same time points. A total of 578 metabolites were detected, of which 211 were identified and 367 were unknown. A few metabolites related biochemically to short-chain fatty acids were increased in both NC and Calrose cultures (**Figure A2.7**). In addition, there were eight metabolites found to be reduced in Calrose cultures relative to the NC cultures (**Figure A2.8**). A 20-fold increase was chosen as an arbitrary cutoff for consideration of metabolites increased in the Calrose bran treatment. Those metabolites with a greater than 20-fold increase in the Calrose cultures and the corresponding levels in NC cultures are shown in **Figure A2.9**. Of these, a number of the metabolites were found to be statistically greater in abundance in the 24 h Calrose-containing cultures compared to the 24 h NC cultures (**Table A2.2**). Some of these metabolites can be explained as specific or predominant to rice, such as 1,2-anhydro-myo-inositol and inositol-4-monophosphate, which are components of phytate. Phytate, or phytic acid, is a highly substituted form of inositol, chemically designated as myo-inositol (1,2,3,4,5,6) hexakis phosphate, in which the hydroxyl groups have been esterified by addition of six phosphate groups. These phosphate groups chelate mineral cations, including calcium, and thus can reduce calcium uptake, leading to reduced bone minerals in chicks (Bohn *et al.*, 2008; Jang *et al.*, 2003). The high phosphorus content of the phytate in rice bran has also been shown to increase the phosphorous content of chicken waste

(Bohn *et al.*, 2008; Jang *et al.*, 2003; Ryan, 2011). The reduction of calcium uptake results in bone deficiency (Jang *et al.*, 2003), while the increased phosphate in manure emissions is detrimental to water quality and can contribute to eutrophication (Ryan, 2011). The presence of phytate in rice bran points out the value of differentiating between the components of rice bran that are beneficial and those such as phytate that could be detrimental. Thus, it will be necessary to separate the *Salmonella*-inhibiting component(s) from the phytate by chemical fractionation.

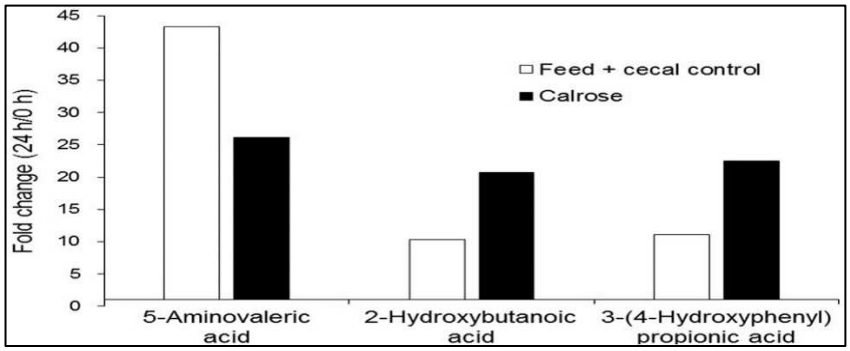

Figure A2.7. Metabolites that increased ≥ 10-fold over the course of the 24 h anaerobic culture, comparing the fold change (24 h/0 h) for feed + cecal control (negative control) and Calrose cultures.

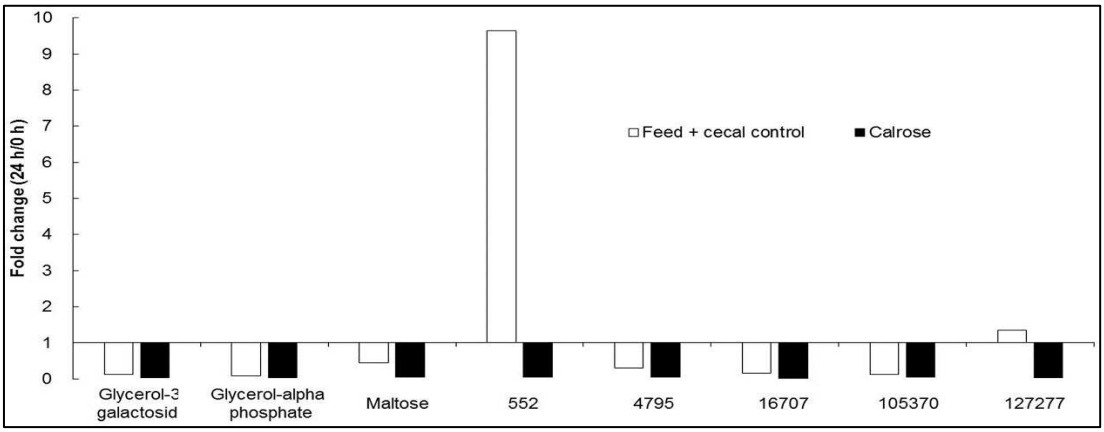

Figure A2.8. Metabolites that decreased ≥ 20-fold over the course of the 24 h anaerobic culture, comparing the fold change (24 h/0 h) for feed + cecal control (negative control) and Calrose cultures.

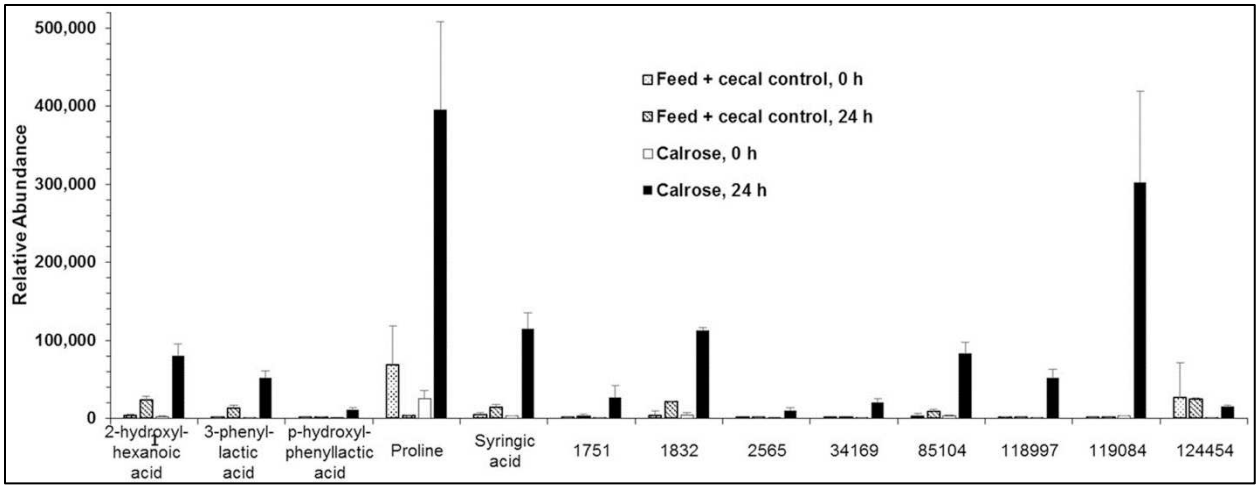

Figure A2.9. Metabolites that increased > 20-fold over the course of the 24 h Calrose anaerobic cultures, and the corresponding increases for the feed + cecal control (negative control) cultures.

Table A2.2. Identified metabolites with >10-fold greater abundance in Calrose-treated 24 h anaerobic cultures compared to negative control cultures.

Metabolite Name	**Mean Calrose RA***	**Mean Neg. Control RA**	**Fold Difference (Calrose/ Neg. control)****	***p-value***	**Possible metabolic pathways**
1,2,-Anhydro-myo-inositol	3,939±711	344±283	11.4	0.0484	Phytate metabolism
3-Hydroxy-3-methylglutaric acid	6,254±1,109	272±9	23.0	0.0324	Branched-chain amino acid metabolism
Allantoic acid	8,087±1,171	207±12	39.0	0.0210	Glycine biosynthesis, xylene degradation
Conduritol beta-epoxide	85,416±14,288	321±80	266.4	0.0272	Inhibitor of beta-glucosidases, free radical generation
Hexitol	5,060±981	137±41	36.8	0.0348	Osmoprotection, osmoregulation
Inositol-4-monophosphate	12,256±1,008	601±448	20.4	0.0130	Inositol phosphate, phytate metabolism, sugar alcohol metabolism
Malonic acid	2,577±75	156±14	16.5	0.0012	Beta-alanine biosynthesis, fatty acid biosynthesis, fatty acid beta-oxidation
Methionine	39,817±8,382	3,293±1,172	12.1	0.0423	Ethylene biosynthesis, methanethiol biosynthesis, homocysteine

Table A2.2. Identified metabolites with >10-fold greater abundance in Calrose-treated 24 h anaerobic cultures compared to negative control cultures.

Metabolite Name	Mean Calrose RA*	Mean Neg. Control RA	Fold Difference (Calrose/ Neg. control)**	*p-value*	Possible metabolic pathways
					metabolism, 1-carbon metabolism via conversion into S-adenosyl methionine
Ornithine	438,156±71,171	28,958±2,578	15.1	0.0309	Arginine catabolism, butyric acid synthesis, urea cycle
Pantothenic acid	2,594±203	182±49	14.3	0.0069	Fatty acid and B-vitamin metabolism
Phosphogluconic acid	21,927±2,018	1192±947	18.4	0.0152	Purine, pyrimidine and histidine metabolism
Pinitol	297,330±49,993	223±58	1335.3	0.0271	Inositol metabolism, inositol-phosphoglycan metabolism
Vanillic acid	7,071±806	491±126	14.4	0.0105	Aminobenzoate degradation
Xylitol	7,039±1448	482±37	14.6	0.0476	Pentose sugar metabolism

*RA, relative abundance ± standard error
**Fold difference was determined by dividing the relative abundance of Calrose by that of the Negative Control.

Other known metabolites found that may be rice-specific are conduritol beta-epoxide, hexitol, and pinitol. These possibly represent an inhibitor of beta-glucosidases and osmoprotectants, respectively. Numerous plant organs express beta-glucosidases during development, and inhibitors may be required to regulate their activity when they are no longer required as part of specific developmental events (Rubinelli *et al.*, 1998). Osmoprotectants are compatible solutes that accumulate within cells during periods of osmotic stress caused by high osmolarity (high solute concentration) of the environmental surroundings. This accumulation relieves the osmotic stress while avoiding passive, and often toxic, volume depletion within the cell in response to the high osmolarity (Csonka, 1989).

Of particular interest to the anti-*Salmonella* properties of rice bran is the increased abundance of malonic acid, ornithine, and pantothenic acid in Calrose cultures relative to the

control cultures (**Table A2.2**). These metabolites may be functioning in fatty acid synthesis, and catabolism (Sugino *et al.*, 2008). Previous studies have indicated that short-chain fatty acids (**SCFA**) can inhibit *Salmonella* through a mechanism of decoupling of ATP formation through membrane damage or by denaturation of acid-sensitive proteins (Ricke, 2003). Interestingly, butyric acid has also been observed to down-regulate pathogenicity island gene expression (Gantois *et al.*, 2006), suggesting that fatty acids can reduce the virulence of *Salmonella*. Thus, an increase in fatty acid synthesis in 24 h anaerobic cultures may have an inhibitory effect on *Salmonella* systemic infection by restricting host invasion or other functions. This can be further explored in live bird *Salmonella* challenge studies where organ invasion could be examined. A small number of fatty acid metabolites were increased in both Calrose and negative control cultures after 24 h of anaerobic growth compared to the 0 h culture supernatants (**Figure A2.8).** These appear consistent with the hypothesis that the anaerobic culturing promoted differences in fermentation. A potentially interesting metabolite of unknown structure, designated 552, was considerably reduced in Calrose cultures compared to control cultures at 24h (**Figure A2.9**).

In conclusion, the cultures containing Calrose bran had significantly less *Salmonella* recovered compared to control cultures without rice bran. Our results indicate that bran from Calrose rice is more effective at inhibiting *S.* Typhimurium in comparison to the two other rice brans tested, and this may be due in part to its effects on the metabolic profile. In addition, the microbiome results of this study obtained from in vitro poultry cecal incubations indicate that shifts in the cecal microbiota composition as well as metabolic and fermentation activities may also contribute to the reduction *S.* Typhimurium. One implication of these experiments is that Calrose rice bran or an extracted component thereof could have applications in poultry production as a feed component to reduce dependence on antibiotics, improving the

microbiological safety of chicken products. Chemical fractionation experiments to determine the specific biochemical component(s) responsible for the *Salmonella*-inhibitory effect observed also appear worthwhile. To achieve this, future feeding and challenge studies need to be conducted to examine the in vivo responses, including possible effects on bone density, immune response modulation, and the environmental implications of feeding rice bran. In addition, other foodborne disease-causing serovars, such as *S.* Enteritidis and *S.* Heidelberg, should be examined to gauge the spectrum of antimicrobial activity possessed by Calrose. Other factors needing more attention are the possible effects of Calrose bran on microbiome changes that in turn affect *Salmonella* colonization. Taken together, our data suggest that Calrose rice bran warrants further study as a practical prebiotic additive in poultry feed to limit cecal colonization with *Salmonella*.

A2.5. Author Contributions:

Peter M. Rubinelli:

Contributed equally to this work with: Peter M. Rubinelli, Sun Ae Kim

ROLES: Conceptualization, Data curation, Formal analysis, Investigation, Methodology, Project administration, Writing – original draft

‡ These authors are co-first authors on this work.

AFFILIATION: Center for Food Safety and Department of Food Science, University of Arkansas, Fayetteville, Arkansas, United States of America

Sun Ae Kim:

Contributed equally to this work with: Peter M. Rubinelli, Sun Ae Kim

ROLES: Data curation, Formal analysis, Methodology, Software, Validation, Visualization, Writing – original draft, Writing – review & editing

‡ These authors are co-first authors on this work.

AFFILIATION: Center for Food Safety and Department of Food Science, University of Arkansas, Fayetteville, Arkansas, United States of America

Si Hong Park:

ROLES: Conceptualization, Data curation, Formal analysis, Investigation, Project administration, Software, Supervision, Validation, Writing – review & editing

AFFILIATION: Department of Food Science and Technology, Oregon State University, Corvallis, Oregon, United States of America

Stephanie M. Roto:

ROLES: Data curation, Formal analysis, Investigation, Methodology

AFFILIATION: Center for Food Safety and Department of Food Science, University of Arkansas, Fayetteville, Arkansas, United States of America

Nora Jean Nealon:

ROLES: Data curation, Formal analysis, Investigation, Methodology, Writing – review & editing

AFFILIATION: Department of Environmental and Radiological Health Sciences, Colorado State University, Fort Collins, Colorado, United States of America

Elizabeth P. Ryan:

ROLES: Data curation, Formal analysis, Investigation, Methodology, Writing – review & editing

AFFILIATION: Department of Environmental and Radiological Health Sciences, Colorado State University, Fort Collins, Colorado, United States of America

Steven C. Ricke:

ROLES: Conceptualization, Data curation, Formal analysis, Funding acquisition, Investigation, Project administration, Resources, Supervision, Writing – review & editing

* E-mail: sricke@uark.edu

AFFILIATION: Center for Food Safety and Department of Food Science, University of Arkansas, Fayetteville, Arkansas, United States of America

A2.6. Competing Interests:

The authors have declared that no competing interests exist.

REFERENCES

Bohn L., Meyer A.S., Rasmussen, S.K., Phytate: impact on environment and human nutrition. A challenge for molecular breeding. J Zhejiang Univ Sci B. 2008; 9:165–191. pmid:18357620

Brooks S.A., et al., A natural mutation in rc reverts white-rice-pericarp to red and results in a new, dominant, wild-type allele: Rc-g. Theor Appl Genet. 2008; 117:575–580. pmid:18516586

Csonka L.N., Physiological and genetic responses of bacteria to osmotic stress. Microbiol Rev. 1989; 53:121–147. pmid:2651863

Donalson L., et al., In vitro fermentation response of laying hen cecal bacteria to combinations of fructooligosaccharide prebiotics with alfalfa or a layer ration. Poult Sci. 2008; 87:1263–1275. pmid:18577604

Donalson L.M., et al., In vitro anaerobic incubation of Salmonella enterica serotype Typhimurium and laying hen cecal bacteria in poultry feed substrates and a fructooligosaccharide prebiotic. Anaerobe. 2007; 13:208–214. pmid:17588782

Dunkley K.D., et al. Comparison of in vitro fermentation and molecular microbial profiles of high-fiber feed substrates incubated with chicken cecal inocula. Poult Sci. 2007; 86:801–810. pmid:17435012

Fan Y.Y., et al. Use of differential rumen fluid-based carbohydrate agar media for culturing lactose-selected cecal bacteria from chickens. J Food Prot. 1995; 58:361–367.

Forster G.M., et al. Rice varietal differences in bioactive bran components for inhibition of colorectal cancer cell growth. Food Chem. 2013; 141:1545–1552. pmid:23790950

Furukawa T., et al., The Rc and Rd genes are involved in proanthocyanidin synthesis in rice pericarp. Plant J. 2007; 49:91–102. pmid:17163879

Gantois I., et al., Butyrate specifically down-regulates Salmonella pathogenicity island 1 gene expression. Appl Environ Microbiol. 2006; 72:946–949. pmid:16391141

Ghazi I.A., et al., Rice bran extracts inhibit invasion and intracellular replication of Salmonella typhimurium in mouse and porcine intestinal epithelial cells. Med Aromat Plants. 2016; 5:271.

Gibson G.R., Roberfroid MB., Dietary modulation of the human colonic microbiota: introducing the concept of prebiotics. J Nutr. 1995; 125:1401–1412. pmid:7782892

Goodyear A., et al. Dietary rice bran supplementation prevents Salmonella colonization differentially across varieties and by priming intestinal immunity. J Funct Foods. 2015; 18, Part A:653–664.

Hudault S., et al., Efficiency of various bacterial suspensions derived from cecal floras of conventional chickens in reducing the population level of Salmonella typhimurium in gnotobiotic mice and chicken intestines. Can J Microbiol. 1985; 31:832–838. pmid:3910208

Hutkins R.W., et al. Prebiotics: why definitions matter. Curr Opin Biotechnol. 2016; 37:1–7. pmid:26431716

Jang D.A., et al. Evaluation of low-phytate corn and barley on broiler chick performance. Poult Sci. 2003; 82:1914–1924. pmid:14717549

Kim S.P., et al., Rice hull smoke extract inactivates Salmonella Typhimurium in laboratory media and protects infected mice against mortality. J Food Sci. 2012; 71:M80–M85. pmid:22132793

Kim S.P., et al., A polysaccharide isolated from the liquid culture of Lentinus edodes (Shiitake) mushroom mycelia containing black rice bran protects mice against a Salmonella lipopolysaccharide-induced endotoxemia. J Agric Food Chem. 2013; 61:10987–10994. pmid:24200110

Kumar A., et al., Dietary rice bran promotes resistance to Salmonella enterica serovar Typhimurium colonization in mice. BMC Microbiol. 2012; 12:71. pmid:22583915

Lei S., et al., High protective efficacy of probiotics and rice bran against human norovirus infection and diarrhea in gnotobiotic pigs. Front Microbiol. 2016; 7:1699. pmid:27853451

Park S.H., Lee S.I., Ricke S.C., Microbial populations in naked neck chicken ceca raised on pasture flock fed with commercial yeast cell wall prebiotics via an Illumina MiSeq platform. PloS ONE. 2016; 11:e0151944. pmid:26992104

Patterson J.A., Burkholder KM., Application of prebiotics and probiotics in poultry production. Poult Sci. 2003; 82:627–631. pmid:12710484.

Ricke S.C., Perspectives on the use of organic acids and short chain fatty acids as antimicrobials. Poult Sci. 2003; 82:632–639. pmid:12710485

Ricke S.C., Pillai SD., Conventional and molecular methods for understanding probiotic bacteria functionality in gastrointestinal tracts. Crit Rev Microbiol. 1999; 25:19–38. pmid:10342098

Ricke S.C., Potential of fructooligosaccharide prebiotics in alternative and nonconventional poultry production systems. Poult Sci. 2015; 94:1411–1418. pmid:25717086

Roberfroid M., Prebiotics: the concept revisited. J Nutr. 2007; 137:830S–837S. pmid:17311983

Roto S.M., Rubinelli PM, Ricke SC. An introduction to the avian gut microbiota and the effects of yeast-based prebiotic-type compounds as potential feed additives. Front Vet Sci. 2015; 2:28. pmid:26664957

Rubinelli P., Hu Y., Ma H., Identification, sequence analysis and expression studies of novel anther-specific genes of Arabidopsis thaliana. Plant Mol Biol. 1998; 37:607–619. pmid:9687065

Rubinelli P., et al., Reduction of Salmonella Typhimurium by fermentation metabolites of Diamond V Original XPC in an in vitro anaerobic mixed chicken cecal culture. Front Vet Sci. 2016; 3:83. pmid:27695699

Ryan E., Bioactive food components and health properties of rice bran. J Am Vet Med Assoc. 2011; 238:593–600. pmid:21355801

Ryan E.P., et al., Rice bran fermented with Saccharomyces boulardii generates novel metabolite profiles with bioactivity. J Agric Food Chem. 2011; 59:1862–1870. pmid:21306106

Saengkerdsub S., et al., Effects of nitrocompounds and feedstuffs on in vitro methane production in chicken cecal contents and rumen fluid. Anaerobe. 2006; 12:85–92. pmid:16701620

Salanitro J., Blake I., Muirhead P., Studies on the cecal microflora of commercial broiler chickens. Appl Microbiol. 1974; 28:439–447. pmid:4608322

Sheflin A.M., et al., Pilot dietary intervention with heat-stabilized rice bran modulates stool microbiota and metabolites in healthy adults. Nutrients. 2015; 7:1282–1300. pmid:25690418

Shermer C.L., et al., Caecal metabolites and microbial populations in chickens consuming diets containing a mined humate compound. J Sci Food Agric. 1998; 77:479–486.

Sugino T., et al., L-ornithine supplementation attenuates physical fatigue in healthy volunteers by modulating lipid and amino acid metabolism. Nutr Res. 2008; 28:738–743. pmid:19083482

Yang X., et al. High protective efficacy of rice bran against human rotavirus diarrhea via enhancing probiotic growth, gut barrier function, and innate immunity. Sci Rep. 2015; 5:15004. pmid:26459937

APPENDIX

A3. ANTIMICROBIAL RESISTANT *ESCHERICHIA COLI* FROM ENVIRONMENTAL WATERS IN NORTHERN COLORADO[6]

A3.1. Summary:

Waterborne *Escherichia coli* are a major reservoir of antimicrobial resistance (AMR), including but not limited to extended-spectrum beta-lactamase (**ESBL**) and *Klebsiella pneumoniae* carbapenemase (**KPC**) mechanisms. This study quantified and described ESBL and KPC producing *E. coli* in Northern Colorado from sewer water, surface water, and influent and effluent waste water treatment sources. Total detected bacteria and *E. coli* abundances, and the percentages that contain ESBL and/or KPC, were compared between water sources. Seventy *E. coli* isolates from the various waters had drug resistance validated with a panel of 17 antibiotics using a broth microdilution assay. The diverse drug-resistance observed across *E. coli* isolates was further documented by polymerase chain reaction of common ESBL genes and functional relatedness by PhenePlate assay-generated dendrograms (n=70). Total *E. coli* abundance decreased through the water treatment process as expected, yet the percentages of *E. coli* harboring ESBL resistance were highest (1.70%) in surface water. Whole-genome sequencing analysis was completed for 185 AMR genes in waste water *E. coli* isolates and confirmed the presence of diverse AMR gene classes (e.g. beta-lactams and efflux pumps) in isolate genomes. This study completed surveillance of AMR patterns in *E. coli* that reside in environmental water

---

[6] Haberecht, H.B.*, **Nealon, N.J**.*, Gilliand, J., Holder, A., Runyan, C., Oppel, R., Ibrahim, H., Mueller, L., Schrupp, F., Vilchez, S., Antony, L., Scaria, J., and Ryan, E.P. *Antimicrobial Resistant Escherichia coli from Environmental Waters in Northern Colorado*. Journal of Environmental and Public Health. January 2019. ***Co-first authors**

systems and suggests a role for integrating both phenotypic and genotypic profiling beyond ESBL and KPC mechanisms. AMR screening via multiple approaches may assist in the prevention of drug-resistant *E. coli* spread from waters to animals and humans.

A3.2. Introduction:

Antimicrobial resistant (**AMR**) bacteria are ubiquitous in environmental waters including oceans (Hatosy and Martiny, 2015; Moore *et al.*, 2008), rivers (Marti *et al.*, 2013; Ronald *et al.*, 2002), lakes (Pang *et al.*, 2015; Rosas *et al.*, 2015), sewer water (Blaak *et al.*, 2014; Rodriguez-Mozaz *et al.*, 2015), and have even been recorded in drinking water sources (Diab *et al.*, 2018; Li *et al.*, 2015; Martin *et al.*, 2018; Sharma *et al.*, 2017). Water systems harbor antibiotics, biocides, heavy metals, and other chemicals (Baquero *et al.*, 2008; Berendonk *et al.*, 2015) that naturally select for antimicrobial resistance within these waterborne microbial gene pools. *Escherichia coli* is abundant in water systems (Jang *et al.*, 2017) and is a concerning reservoir for AMR in these locations (Egervarn *et al.*, 2017; Li *et al.*, 2015; Osinska *et al.*, 2017). A survey of AMR *E. coli* in the Netherlands showed 17.1% of ESBL *E. coli* isolated from river water and waste water were reported as pathogenic, and of those pathogenic strains, approximately 84% exhibited resistance in up to three drug classes including beta-lactams, tetracyclines, and aminoglycosides (Franz *et al.*, 2015). In an estuary in Portugal, isolated *E. coli* was phylogenetically distributed into commensal and pathogenic groups, and bacteria in both groups were resistant to last resort antibiotics, including carbapenems (Pereira *et al.*, 2013). Given that antibiotics are conventionally used to treat *E. coli* infections in people and animals, improved AMR surveillance and a better understanding of how resistance spreads in environmental waters is warranted (EPA, 2012; WHO, 2011).

Two major types of beta-lactam resistance include microbial production of extended-spectrum beta-lactamase (**ESBL**) and *Klebsiella pneumoniae* carbapenemase (**KPC**) enzymes (Bush, 2010). These enzymes work via hydrolysis of the beta-lactam ring (ESBL) or via interference with antibiotic binding to penicillin binding proteins (KPC) (Page, 2012). The Centers for Disease Control and Prevention classifies ESBL as a serious threat and KPC as an urgent threat to public health (CDC, 2013). In the USA alone, ESBL resistance among Enterobacteriaceae, which includes *E. coli*, was reported to have caused approximately 1,700 deaths with medical costs per infection in excess of $40,000 US Dollars (CDC, 2013). KPC was attributed to 600 deaths in 2013 (CDC, 2013), and carbapenem drugs are considered a last resort antibiotic for severe bacterial infections (Hawkey and Livermore, 2012). Furthermore, *E. coli* that express ESBL and/or KPC genes have been frequently shown to harbor resistance to other antibiotic classes (Baudry *et al.*, 2008; Diab *et al.*, 2018). A thorough application of functional screening methods may be needed to comprehensively characterize the AMR phenotypes of waterborne *E. coli*.

There are multiple genes contributing to ESBL and KPC resistance, including $bla_{CTX\text{-}M}$, bla_{OXA}, bla_{SHV} and bla_{TEM}, and bla_{KPC}, bla_{VIM}, bla_{IMP} and bla_{NDM} (van Duin and Doi, 2017), all of which can be transferred to other species horizontally on plasmids (Paterson and Bonomo, 2005). Considering the potential of horizontal AMR gene transfer into reservoirs of human pathogens, increased attention is being given to the identification of AMR genes in bacteria isolated from environmental waters.

The objective of this study was to screen environmental water samples for AMR *E. coli*, to understand the phenotypic and genotypic resistance profiles of *E. coli* isolates, and to examine clonal relatedness of AMR *E. coli* strains across water systems. It was hypothesized that KPC

and ESBL screening of environmental *E. coli* would be predictive of additional multi-drug resistance mechanisms in these isolates, and that genotypic and phenotypic analysis would reveal patterns in drug resistance based on date and location of the water sources sampled. The cross-validation of the methodologies reported herein illustrates the depth by which multiple analysis platforms can be integrated to establish AMR profiles of *E. coli* across environmental waters.

A3.3. Materials and Methods:

A3.3.1. Environmental water sampling locations and collection procedures:

Water samples were collected from Larimer County, Colorado from May 2016 to April 2017. All water samples were collected with autoclaved Pyrex® wide mouth storage bottles, quantity of 1 liter. Following collection, all samples were immediately placed on ice and stored in a light-sensitive container until analysis, which occurred at least one-hour post collection. Remaining sample was then stored at -4 ºC. A map of sample collection locations is provided in **Figure A3.1**. Seventeen water samples were collected and classified as: sewer water, waste water treatment plant (**WWTP**) influent, WWTP-effluent, and surface water. Sewer water and WWTP-influent were grouped as waste water, and WWTP-effluent and surface water were grouped as ambient water. Sewer water (n=6) was collected from five manholes downstream from a human hospital and also from area residents, businesses and a university. WWTP-influent (n=3) and WWTP-effluent (n=2) samples were collected using the Hawk Composite Sampler (Hach, Loveland, CO) at the Drake Water Reclamation Facility, a conventional activated sludge treatment plant. WWTP-influent samples were collected before water treatment, and WWTP-effluent samples were collected post-sulfur dioxide and chlorine treatment and prior to discharge into the Cache la Poudre River. Surface water (n=6) was collected from five sources along the

Cache La Poudre River both upstream and downstream from the WWTP-effluent discharge with one site being upstream of the city limits. Storage bottles were submerged midstream in surface water for river samples and from covered manholes for sewer water samples. WWTP influent and WWTP effluent samples were collected mid-flow from the Hawk Composite Sampler.

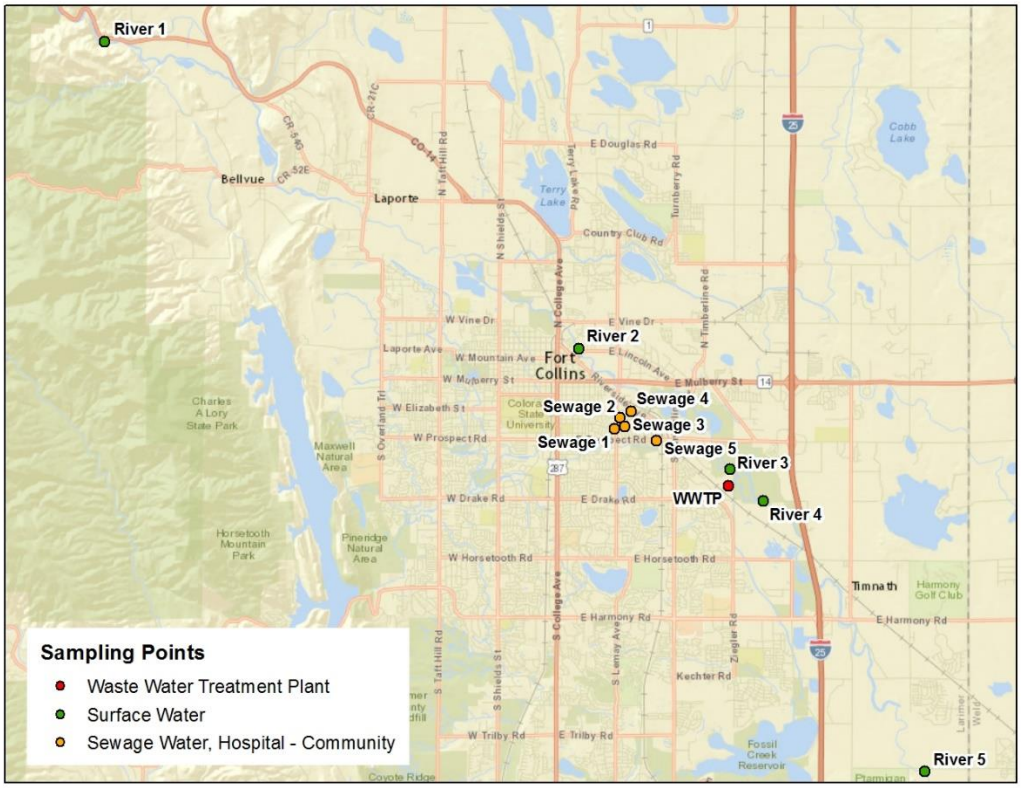

Figure A3.1. Environmental water sampling locations in and around Fort Collins, Colorado.

A3.3.2. Microbiological analysis of total detected bacteria and suspected E. coli from environmental water samples:

Seventeen independent sampling events between May 2016 and April 2017 were screened for total detected bacterial and *E. coli* abundance, as well as for ESBL and KPC resistance. Water samples were processed within 24 hours of acquisition. Samples were serially-diluted in

sterilized Phosphate Buffered Saline (**1X PBS**, pH 7.4, VWR, Radnor, PA) at room temperature (23ºC) and subjected to membrane filtration through cellulose nitrate filters (0.45 µm pore size; Millipore Sigma, Burlington, MA) for bacterial enumeration. With each sample, filtration was performed in triplicate at three different dilutions and membrane filters were placed on three different chromogenic agar types: ChromAgar Orientation™, ChromAgar ESBL™, which screens for ESBL producing isolates and ChromAgar KPC™ (DRG Diagnostics, Springfield, NJ), which screens for KPC producing isolates. All agars, broths and other liquid reagents were incubated for 24 hours and checked for sterility before use, and agar plates were stored along with inoculated plates to monitor for any contamination occurring during the filtering process. Additionally, contamination in sample dilutions were controlled using sterilized and filtered phosphate buffered saline (**PBS**) that was plated, incubated and assessed for colony growth along with inoculated plates. Although ChromAgar KPC plates have high sensitivity compared to other KPC-screening agars (Esther *et al.*, 2017; Garcia-Quintanilla *et al.*, 2018), bacterial growth on these plates is not an absolute conformation of KPC production (Bialvaei et al., 2016; Hinić et al., 2017). This is because resistance to carbapenems can be mediated by both KPC enzymes as well as efflux pumps (Arnold *et al.*, 2011) and consequently, a positive result will be referred to as "suspected KPC". ChromAgar Orientation quantified total detected bacterial abundance and total *E. coli*. ChromAgar ESBL quantified ESBL-producing total detected bacteria and ESBL *E. coli*, and ChromAgar KPC quantified suspected KPC-producing total detected bacteria and *E. coli*. Plates were incubated at 37º C at 2-5% CO_2 for 24-72 hours, until countable colonies were observed. Total colony forming units (**CFUs**) per plate within the range of 15-300 were included for descriptive analysis. Per manufacturer instructions, species identifications were made using CFU color and morphology, where *E. coli* colonies were pink with a faint halo (Al Anbgi, 2016;

Merlino et al., 1996). *E. coli* counts were included in the abundance calculation if they were counted on a plate with at least 15 (lowest countable detection limit) and at most 300 colonies (highest countable detection limit). To compare total detected AMR bacteria and total AMR *E. coli* abundances between sampling locations, relative percentages of ESBL and suspected KPC resistance were calculated by dividing the number of ESBL or suspected KPC-positive *E. coli* or total detected bacteria by *E. coli* or total detected bacteria in each water source.

A3.3.3. E. coli purification, isolation and species confirmation:

A spread-plate based screening of all water samples was used to collect *E. coli* isolates for more in-depth drug susceptibility and clonal relatedness analysis. *E. coli* isolates from each water sample were selected from 1 of the 3 ChromAgar-plates (Orientation, ESBL, or KPC) based on chromogenic appearance as pink colonies with a faint halo (Al Anbgi, 2016; Merlino *et al.*, 1996). Single colonies were isolated to MacConkey agar (Difco, BD Biosciences: Franklin Lakes, NJ) and incubated for 24-72 hours at 2-5% CO_2, until visible colonies were observed. Per manufacturer instructions, isolates that appeared bright pink on MacConkey agar were defined as *E. coli*, and were further isolated onto Tryptic Soy Agar (Remel™, Lenexa, KS) plates and incubated overnight at 37°C. Single colonies were selected and inoculated into sterile Tryptic Soy Broth (Remel™, Lenexa, KS) for 24-72 hours, until bacterial cell growth was observed. Blank Tryptic Soy Broth was incubated alongside isolated cultures as a negative control, and any growth in non-inoculated media blanks were addressed by repeating the assay by selecting new *E. coli* colonies from the original, agar plate and inoculating them into new sterile media.

Potential *E. coli* isolates in tryptic soy broth were species-confirmed using Matrix-Assisted Laser Desorption Ionization Time of Flight Mass Spectrometry (**MALDI-TOF**) at the Colorado

State University Proteomics and Metabolomics Facility (**CSU-PMF**). Briefly, isolates were dissolved in 1 µL 70% formic acid on a Biotyper plate (Bruker Daltonics Inc© Billerica, MA), and the dried spots were mixed with 1 µL of alpha-Cyano-4-hydroxycinnamic acid (**HCCA**) and analyzed in triplicate using the VITEK-MS™ (Biomerieux, USA). A 0.5 µL Bacterial Test Standard (Bruker Daltonics Inc© Billerica, MA) was added as an internal control. Protein identities were assigned using a CSU-PMF internal library, where a 70% match of total mass-spectral peaks (score of >2.0) identified an isolate as *E. coli*. Seventy total isolates were confirmed *E. coli* including: ESBL-producing (n=12), ESBL+ suspected KPC-producing (n=35), and neither ESBL nor KPC-producing (n=23).

A3.3.4. DNA isolation and PCR amplification of ESBL and KPC genes from E. coli isolates:

To further establish *E. coli* ESBL resistance profiles, polymerase chain reaction (**PCR**) was performed on the 70 confirmed *E. coli* isolates for 3 genes (*blaOXA*, *blaCTX-M* and *blaTEM*) representative of ESBL phenotypes. The following primer sequences were used during DNA amplification:

blaOXA (F: ACA CAA TAC ATA TCA ACT TCG C, R: AGT GTG TTT AGA ATG GTG ATC, 813bp), *blaCTX-M* (F: ATG TGC AGY ACC AGT AAR GTK ATG GC, R: TGG GTR AAR TAR GTS ACC AGA AYC AGC GG, 593 bp), and *blaTEM*. (F: CGC CGC ATA CAC TAT TCT CAG AAT GA, R: ACG CTC ACC GGC TCC AGA TTT AT, 445 bp).

E. coli isolates were lysed in 100 µL of Millipore water at 100°C for 1 hour using a BIO-RAD T100™ Thermocycler (Bio-Rad Laboratories, Inc, California). Amplification was carried out by 2 µL DNA, 10 pmol of each primer, and 12.5 µl Emerald Amp® GT PCR Master Mix (Takara Bio Inc., Clontech, Japan) under previously described conditions (Amaya *et al.*, 2012).

The PCR conditions were as followed: 15 minutes of denaturation at 95°C (1 cycle), 30 seconds of denaturation at 94°C, 90 seconds of annealing at 62°C, and 1 minute of polymerization at 72°C (34 cycles), with a final extension at 72°C for 10 minutes. PCR products were analyzed on a 1.5% agarose gel (BioRad, Hercules, CA) and visualized using 1 µL of Ethidium Bromide (Thermo-Fisher, Lafayette, CO). PCR-grade water or sterile autoclaved 1X PBS was used as a negative control. Bacterial isolates with confirmed presence of *blaOXA, blaCTX-M* and *blaTEM* were included as positive controls.

A3.3.5. Biochemical analysis to establish clonal-relatedness across E. coli isolates:

E. coli profiled with PCR were screened for clonal relatedness using a PhP-RE plate (PhP-RE, PhPlate AB, Microplate Techniques, Stockholm, Sweden) following manufacturer's instructions. The system consisted of a 96-well plate coated with 11 carbon sources: cellobiose, lactose, rhamnose, deoxyribose, sucrose, sorbose, tagatose, D-arabitol, raffinose, gal-Lacton, and ornithine. Three hundred µL of media containing a pH indicator (bromothymol blue 0.11%) and proteose peptone (Sigma-Aldrich: St. Louis, MO) was combined with ~1 mg of each bacterial isolate. After 1.5 hours, 12 µL of inoculum was transferred to each substrate well. One row of substrate was not inoculated, serving as a negative control. As an internal check for reproducibility, three replicate isolate pairs were also grown on separate 96-well plates and were determined to have correlation values of 0.94 and above. Plates were incubated at 37°C, covered with light-sensitive material and read at 620 nm on a BioTek Cytation™3 (BioTek Instruments: Winooski, VT) at 8h, 24h, and 48h. Clonal-relatedness was estimated using PhenePlate™ software (PhPlate AB), which examined variability in absorbance across each substrate and

presented relatedness as a dendrogram. A cutoff value of <97.5% similarity in functional profiles defined isolates as clonally-distinct from each other.

A3.3.6. E. coli isolates tested for antibiotic susceptibility to 17 antibiotics:

Thirty-four *E. coli* isolates were further screened for antimicrobial resistance using a broth microdilution assay at Colorado State University Veterinary Teaching Hospital-Diagnostic Medicine Center (**VTH-DMC**). The isolates were from sewer water (n=17), WWTP-influent (n=10), WWTP-effluent (n=2), and surface water (n=5) and were ESBL producing (n=10), suspected ESBL+KPC producing (n=1), or neither KPC nor ESBL producing (n=23). Given the higher abundance of ESBL/KPC-positive *E. coli* detected in waste water samples during membrane filtration analysis, this subset preferentially screened *E. coli* isolates from those water sources. The 17 antibiotics tested were: amoxicillin/clavulanic acid, ampicillin, cefalexin, cefovecin, ceftiofur, chloramphenicol, enrofloxacin, gentamicin, imipenem, marbofloxacin, nitrofurantoin, piperacillin, tetracycline, tobramycin, trimethoprim/sulfamethoxazole, amikacin, and cefpodoxime. Minimum inhibitory concentrations (**MIC**) were calculated and categorized as susceptible, intermediate, or resistant based on standards set by the Clinical and Laboratory Standards Institute guidelines (CLSI, 2010). For each drug, percent resistance was calculated by dividing the number of resistant isolates by the total number of isolates screened with that drug.

A3.4.7. Whole genome sequencing of E. coli isolates:

Whole genome sequencing was performed on a subset of *E. coli* isolated from WWTP-influent and sewer water samples. Twenty-five *E. coli* isolates were grown at 37°C at 2-5% CO_2 for 24-48 hours in sterile tryptic soy broth (**TSB**), centrifuged at 4000xg for 10 minutes

(Beckman Coulter Allegra X-14R, Indianapolis, IN, USA) and re-constituted in approximately 250 µL of TSB. DNA was extracted using a DNeasy Powersoil kit (Qiagen, Valenica, CA) following manufacturer protocols and stored at -20°C until quality-checking and quantification with a NanoDrop 2000 (Thermo Scientific, Lafayette, CO) Incubated sterile TSB media and sterile DNA extraction media were used as negative controls. Whole genome sequencing of DNA extracts was performed at the Animal Disease Research and Diagnostic Laboratory at South Dakota State University in Brookings, SD using previously-described methods (Thomas *et al.*, 2017). Briefly, 0.3 ng/µL of DNA from each isolate was processed using a Nextera XT DNA Sample Prep Kit (Illumina Inc., San Diego, CA), pooled together, and sequenced on an Illumina Miseq platform using a 2X250 paired end approach with V2 chemistry (Illumina Inc., San Diego, CA). Raw sequencing files were de-multiplexed and converted to FASTQ files using Casava version 1.8.2 (Illumina Inc., San Diego, CA). The CLC Genomics workbench version 9.4 (Qiagen bioinformatics, Valencia, CA) trimmed and assembled sequences, and for each isolate, AMR genes were **BLAST**-searched (basic local alignment search tool) against 185 distinct gene sequences from ResFinder (Zankari *et al.*, 2012) and the Comprehensive Antibiotic Resistance Database (Jia *et al.*, 2017). Gene identities were made based on a minimum 85% sample gene identity match over 50% of the gene sequence length, as compared to the database entry of the gene.

A3.3.8. Statistical Analysis:

Total bacteria and total *E. coli* abundances were compared across the four water sample types using a Kruskal-Wallis non-parametric analysis of variance test with a Dunn's post-test to adjust for multiple comparisons. Ambient and waste water were compared using a non-

parametric Mann-Whitney test. A p –value of $p<0.05$ was defined as a statistically-significant difference between treatments, and these values are reported alongside source abundance fold differences in the results below.

A3.5. Results and Discussion:

A3.4.1. Total detected bacterial and E. coli abundances through waste water treatment process:

Total detected bacterial and *E. coli* abundances across environmental waters tested in 17 sampling events are depicted in **Table A3.1**. The negative control plates included for each filtered sample did not contain microbial growth. Filter plates from each source had CFU counts between 15-300 and were included in source abundance. Of 460 total filter plates counted, a total of 216 plates were excluded from analysis, 34 of these exceeded a count of 300. To estimate relative bacterial density, total detected bacterial abundance and *E. coli* abundance were compared across sewer water, WWTP influent, WWTP-effluent and surface water locations. Total detected bacteria ranged from 2.1+04 CFU/100 mL in surface water to 3.4E+08 CFU/100 mL in WWTP-influent. Among waste water, WWTP-influent had 1.7-fold greater total detected bacterial abundance than sewer water (3.4E+08 CFU/100 mL and 2.1E+08 CFU/100 mL, respectively) though this difference was not significantly significant. Elevated levels of bacteria in WWTP-influent samples could be due to the convergence of different sewer water sources into a common WWTP (**Figure A3.1**).

Waste water (sewer and WWTP influent) had 3221-fold higher ($p < 0.0001$) total detected bacterial abundance than ambient water (WWTP effluent and surface water). Decreases in total detected bacterial abundance after waste water treatment have been previously reported in other microbial waste water treatment sampling investigations (Hendricks and Pool, 2012; Ma *et al.*,

2013; Morozzi *et al.*, 1988), suggesting that this studied wastewater treatment functions in a similar manner to previously-examined plants.

Table A3.1. Relative abundances of total detected bacteria and *E. coli* by water source and by ESBL and KPC production.

Source	Sampling Events	Total detected bacteria (CFU/100 mL)			*Escherichia coli* (CFU/100 mL)		
		All	ESBL	KPC	All	ESBL	KPC
Sewer Water	6	2.1E+08[b,c] (2.8E+08)	2.5E+06[b,c] (1.3E+06)	3.2E+06[b,c] (1.5E+06)	7.6E+07[b,c] (1.2E+08)	3.1E+05[b] (2.6E+05)	2.1E+05 (2.1E+05)
WWTP-Influent	3	3.5E+08[d,e] (3.2E+08)	3.5E+06[d,e] (1.9E+06)	3.6E+06[d,e] (1.3E+06)	7.7E+07[d,e] (1.5E+08)	2.3E+05[d] (1.1E+05)	7.8E+04 (7.0E+04)
WWTP-Effluent	2	1.5E+05[b,d] (2.2E+05)	1.4E+03[b,d] (1.4E+03)	1.6E+02[b,d] (1.3E+02)	3.6E+03[b,d] (4.3E+03)	100[d,b] (102)	BDL
Surface Water	6	2.1E+04[c,e] (3.8E+04)	1.4E+03[c,e] (1.9E+03)	5.8E+02[c,e] (5.5E+02)	2.9E+03[c,e] (4.7E+03)	500 (0)	BDL

Data represent colony counts collected during membrane filtration, all data are presented as mean (± standard deviation). Abundance was measured as colony-forming units/100 mL Plates with counts between 15 and 300 total CFU were considered for analysis.
CFU=colony forming unit
BDL= below detection limit
ESBL= extended-spectrum beta-lactamase
KPC= *Klebsiella pneumoniae* carbapenemase
WWTP= waste water treatment plant

Statistical differences ($p<0.05$) are noted between water sources with the following letters:
a= Sewer Water and WWTP-Influent
b= Sewer Water and WWTP-Effluent
c= Sewer Water and Surface Water
d= WWTP-Influent and WWTP-Effluent
e= WWTP-Influent and Surface Water
f= WWTP-Effluent and Surface Water

As a percentage of total detected bacterial content, *E. coli* was the highest in sewer water at 37%, detected at lower levels in WTTP-influent (22%) and surface water (14%), and was

lowest in WWTP effluent (2.4%) (**Table A3.1**). *E. coli* abundance followed similar trends to total detected bacterial abundance, with the greatest total *E. coli* found in waste water (averaging 1.5E+08 CFU/100 mL) compared to ambient water (averaging 3.3E+03 CFU/100 mL). The observed elevations in *E. coli* in sewer water and WWTP influent could be due to the proximity of fecal contamination from humans and animals, as reported previously (EPA, 2012; Ferguson *et al.*, 2012; Gilbert *et al.*, 2000; Gruber *et al.*, 2014; Levy *et al.*, 2009; WHO, 2011).

A3.4.2. Total and E. coli ESBL and KPC abundance varied across environmental water sources.

Each water sample was screened for total ESBL and KPC resistance to estimate levels in sampled bacteria. The abundances (absolute counts) and relative percentages (resistant *E. coli* or total detected bacteria divided by total *E. coli* or total detected bacteria) of ESBL and suspected-KPC bacteria are depicted by water source in **Table A3.1.** and **Figure A3.2**. ESBL and suspected-KPC resistance was present in all water sources tested for total detected bacteria. Sewer water (2.5E+06 CFU/100 mL) and WWTP-influent (3.5E+06 CFU/100 mL) together had a 2146-fold higher ($p<0.0001$) ESBL-positive bacterial abundance compared to the ambient sources, which were 1.4E+03 CFU/100 mL (WWTP-effluent) and 1.4E+03 CFU/100 mL (surface water). Suspected-KPC bacterial abundance in waste water was 8847-fold higher ($p<0.0001$) (3.4E+06 CFU/100 mL WWTP-influent, 3.2E+06 CFU/100 mL sewer water) than ambient water (5.8E+02 CFU/100 mL surface water, 1.7E+02 CFU/100 mL WWTP-effluent). The relative percentage of ESBL in total detected bacteria ranged from 0.93% (WWTP-effluent) to 6.6% (surface water), and the relative percentage of suspected KPC ranged from 0.11% (WWTP-effluent) to 2.7% (surface water) (**Figure A3.2A**).

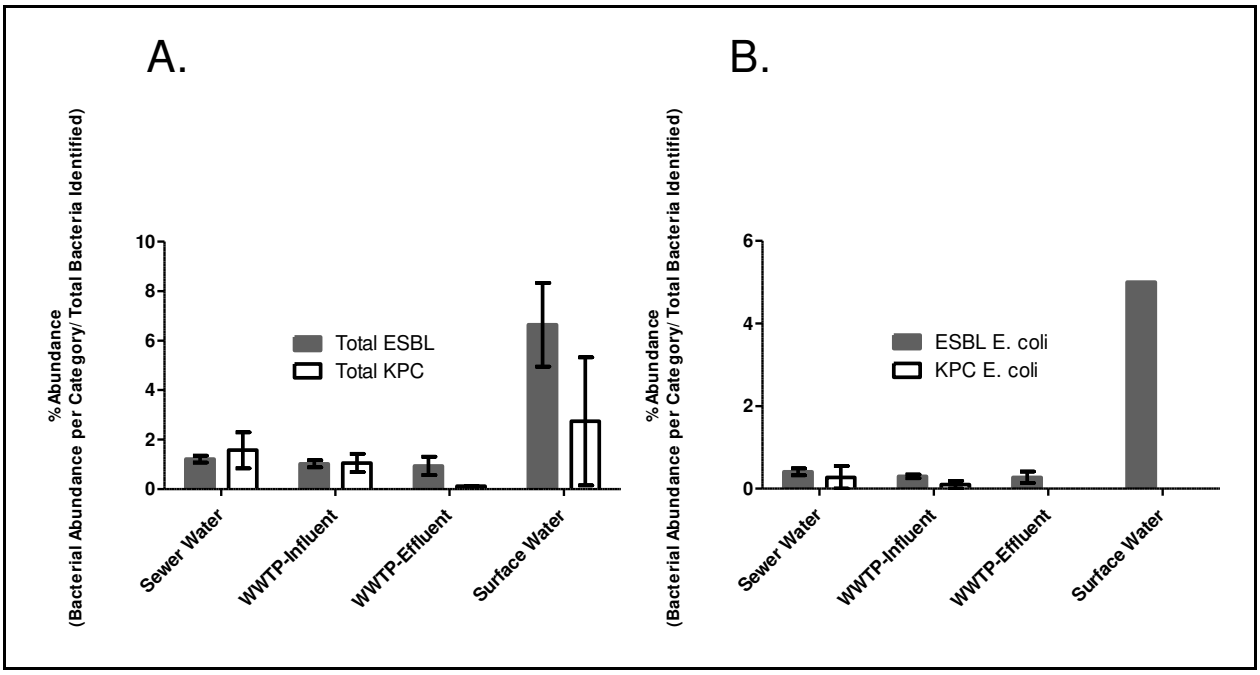

Figure A3.2. Relative percentages of ESBL and suspected KPC total detected bacteria and *E. coli* sampled from environmental waters.

Relative percentages of antimicrobial resistant bacteria from ***(A)*** *total detected bacterial colonies and* ***(B)*** *E. coli collected from membrane filtration across 17 respective environmental water sources. Error bars, representing standard deviation, were generated from each numerator value (individual ESBL/KPC bacterial abundance counts per source) divided by the average total detected non-AMR bacteria per source.* ***ESBL*** *= extended-spectrum beta-lactamase (Grey Bars);* ***KPC*** *= Klebsiella pneumoniae carbapenemase (White Bars); WWTP = waste water treatment plant.*

Abundance of ESBL *E. coli* in waste water (3.1E+05 CFU/100 mL sewer water, 2.3E+05 CFU/100 mL WWTP-influent) was 23318-fold higher ($p<0.01$) than ESBL *E. coli* abundance in ambient water, (1.0E+01 CFU/100 mL WWTP-effluent, 5.0E+01 CFU/100 mL surface water). Similarly, abundance of suspected KPC *E. coli* in waste water (2.1E+05 CFU/100 mL sewer

water, 7.8E+04 CFU/100 mL WWTP-influent) was higher, though not statistically significant compared to suspected KPC *E. coli* abundance in ambient water (*E. coli* in WWTP-effluent and surface water were below the limit of detection). Relative percentages of ESBL-positive *E. coli* ranged from 0.28% in WWTP effluent to 1.7% in surface water, and suspected KPC-positive *E. coli* was below detectable limits in WWTP-effluent and surface water and greatest in sewer water (0.28%) (**Figure A3.2B**). *E. coli* represented 8.9% of total ESBL and 4.2% of total suspected KPC abundance of all bacteria screened.

Abundance of drug-resistant total detected bacteria and *E. coli* decreased between waste water and ambient water samples and specifically between WWTP-influent and WWTP-effluent samples. The relative percentage of KPC also decreased between WWTP-influent and WWTP-effluent sources in both *E. coli* and total detected bacteria. It is noteworthy that other waste water treatment studies have reported increased relative percentage of KPC producing bacteria following waste water treatment (Atashgahi *et al.*, 2015; Gómez López *et al.*, 2010; Hrenovic *et al.*, 2017). The sludge found in many WWTPs are thought to be antibiotic resistance gene reservoirs (Da Costa *et al.*, 2006; Łuczkiewicz *et al.*, 2010; Novo *et al.*, 2013), and pressures put onto bacteria in the treatment process can include contact with residual antibiotics (Li *et al.*, 2013) driving transfer and development of resistance. Consequently, the factors contributing to the reduced abundances of suspected KPC *E. coli* between WWTP-influent and WWTP-effluent warrant investigation for application to other water treatment systems.

Surface water had the greatest relative percentage of ESBL *E. coli* and the greatest relative percentage of ESBL and suspected KPC-positive total detected bacteria. The proximity of surface water sampling sites to human recreational and agricultural inputs may explain this trend. Supporting this explanation, multiple studies have reported a transfer of ESBL and KPC-

expressing bacteria from people and animals into water systems (Atterby *et al.*, 2017; Diab *et al.*, 2018; Nuangmek, 2018).

A3.4.3. Phenotype and genotype profiles moderately separate E. coli isolates by source:

Previous studies have inspected ESBL and KPC gene reservoirs to understand their spread through environmental waters (Korzeniewska and Harnisz, 2013; Li *et al.*, 2015; Yao *et al.*, 2017) yet additional research is needed to elucidate patterns in *E.coli* resistance based on sampling location and date. 70 *E. coli* isolates with confirmed identity by MALDI-TOF were examined using a PhenePlate assay, which uses patterns in carbon-source metabolism to describe clonal relatedness across bacterial isolates. The dendrogram of clonal-relatedness for these selected *E. coli* isolates is shown in **Figure A3.3**.

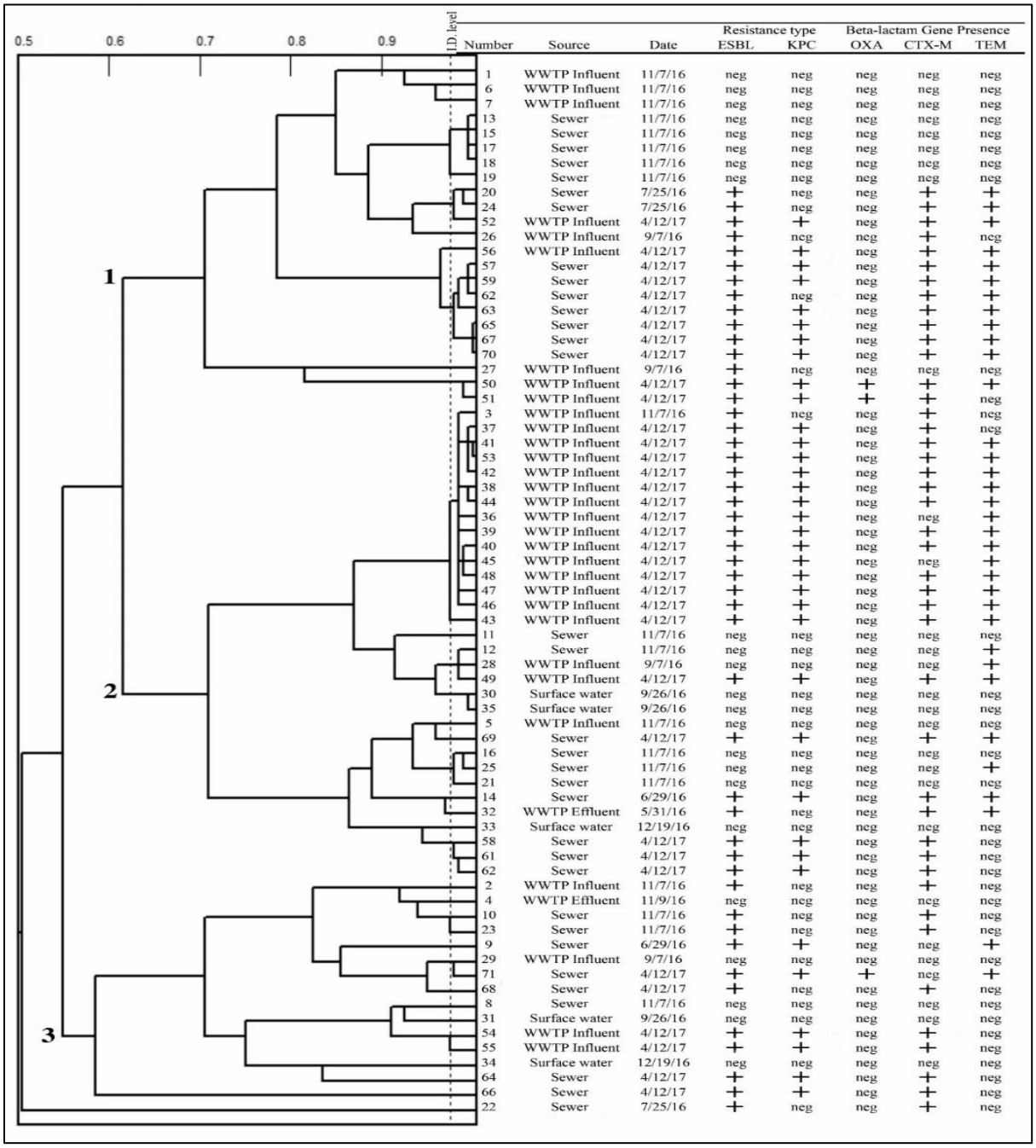

Number	Source	Date	Resistance type ESBL	Resistance type KPC	Beta-lactam Gene Presence OXA	Beta-lactam Gene Presence CTX-M	Beta-lactam Gene Presence TEM
1	WWTP Influent	11/7/16	neg	neg	neg	neg	neg
6	WWTP Influent	11/7/16	neg	neg	neg	neg	neg
7	WWTP Influent	11/7/16	neg	neg	neg	neg	neg
13	Sewer	11/7/16	neg	neg	neg	neg	neg
15	Sewer	11/7/16	neg	neg	neg	neg	neg
17	Sewer	11/7/16	neg	neg	neg	neg	neg
18	Sewer	11/7/16	neg	neg	neg	neg	neg
19	Sewer	11/7/16	neg	neg	neg	neg	neg
20	Sewer	7/25/16	+	neg	neg	+	+
24	Sewer	7/25/16	+	neg	neg	+	+
52	WWTP Influent	4/12/17	+	+	neg	+	+
26	WWTP Influent	9/7/16	+	neg	neg	+	neg
56	WWTP Influent	4/12/17	+	+	neg	+	+
57	Sewer	4/12/17	+	+	neg	+	+
59	Sewer	4/12/17	+	+	neg	+	+
62	Sewer	4/12/17	+	neg	neg	+	+
63	Sewer	4/12/17	+	+	neg	+	+
65	Sewer	4/12/17	+	+	neg	+	+
67	Sewer	4/12/17	+	+	neg	+	+
70	Sewer	4/12/17	+	+	neg	+	+
27	WWTP Influent	9/7/16	+	neg	neg	neg	neg
50	WWTP Influent	4/12/17	+	+	+	+	+
51	WWTP Influent	4/12/17	+	+	+	+	neg
3	WWTP Influent	11/7/16	+	neg	neg	+	neg
37	WWTP Influent	4/12/17	+	+	neg	+	neg
41	WWTP Influent	4/12/17	+	+	neg	+	+
53	WWTP Influent	4/12/17	+	+	neg	+	+
42	WWTP Influent	4/12/17	+	+	neg	+	+
38	WWTP Influent	4/12/17	+	+	neg	+	+
44	WWTP Influent	4/12/17	+	+	neg	+	+
36	WWTP Influent	4/12/17	+	+	neg	neg	+
39	WWTP Influent	4/12/17	+	+	neg	+	+
40	WWTP Influent	4/12/17	+	+	neg	+	+
45	WWTP Influent	4/12/17	+	+	neg	neg	+
48	WWTP Influent	4/12/17	+	+	neg	+	+
47	WWTP Influent	4/12/17	+	+	neg	+	+
46	WWTP Influent	4/12/17	+	+	neg	+	+
43	WWTP Influent	4/12/17	+	+	neg	+	+
11	Sewer	11/7/16	neg	neg	neg	neg	neg
12	Sewer	11/7/16	neg	neg	neg	neg	+
28	WWTP Influent	9/7/16	neg	neg	neg	neg	+
49	WWTP Influent	4/12/17	+	+	neg	+	+
30	Surface water	9/26/16	neg	neg	neg	neg	neg
35	Surface water	9/26/16	neg	neg	neg	neg	neg
5	WWTP Influent	11/7/16	neg	neg	neg	neg	neg
69	Sewer	4/12/17	+	+	neg	+	+
16	Sewer	11/7/16	neg	neg	neg	neg	neg
25	Sewer	11/7/16	neg	neg	neg	neg	+
21	Sewer	11/7/16	neg	neg	neg	neg	neg
14	Sewer	6/29/16	+	+	neg	+	+
32	WWTP Effluent	5/31/16	+	neg	neg	+	+
33	Surface water	12/19/16	neg	neg	neg	neg	neg
58	Sewer	4/12/17	+	+	neg	+	neg
61	Sewer	4/12/17	+	+	neg	+	neg
62	Sewer	4/12/17	+	+	neg	+	neg
2	WWTP Influent	11/7/16	+	neg	neg	+	neg
4	WWTP Effluent	11/9/16	neg	neg	neg	neg	neg
10	Sewer	11/7/16	+	neg	neg	+	neg
23	Sewer	11/7/16	+	neg	neg	+	neg
9	Sewer	6/29/16	+	+	neg	neg	+
29	WWTP Influent	9/7/16	neg	neg	neg	neg	neg
71	Sewer	4/12/17	+	+	+	neg	+
68	Sewer	4/12/17	+	neg	neg	+	neg
8	Sewer	11/7/16	neg	neg	neg	neg	neg
31	Surface water	9/26/16	neg	neg	neg	neg	neg
54	WWTP Influent	4/12/17	+	+	neg	+	neg
55	WWTP Influent	4/12/17	+	+	neg	+	neg
34	Surface water	12/19/16	neg	neg	neg	neg	neg
64	Sewer	4/12/17	+	+	neg	+	neg
66	Sewer	4/12/17	+	+	neg	+	neg
22	Sewer	7/25/16	+	neg	neg	+	neg

Figure A3.3. Clonal relatedness of *E. coli* isolates (n=70) from environmental sources using a functional biochemical analysis and PCR verification of beta-lactam resistance gene presence.

*Identity "**ID**" levels are to the left of the dotted line, which represents a sensitivity of 0.975. Branches to the right of this line represent isolates that are too similar to distinguish. Bold numbers on branches (**1**, **2**, **3**) refer to three major clusters of isolates identifiable from the Pheneplate assay. Isolate numbers represent the unique identifiers assigned to each E. coli*

isolate throughout this study. ***WWTP*** *= water treatment plant.* ***Date*** *= isolation date.* ***ESBL*** *= extended-spectrum beta-lactamase and* ***KPC****: Klebsiella pneumoniae carbapenemase. OXA, CTM-M and TEM were the three beta-lactamase genes assessed with PCR, where '***+***': gene present; '****neg****': gene absent.*

PhenePlate analysis was used to generate a dendrogram which shows 3 major branches of clonal-relatedness and was able to separate 38 functionally-distinct isolates (relatedness fell below the identity level (**I.D.**) of 97.5%). Branch 1 was composed of isolates exclusively from waste water sources and branches 2 and 3 included bacteria sourced from both waste and ambient locations. PhenePlate analysis was previously applied to separate *E. coli* by site, whereby this approach exhibited varying degrees of sensitivity (Ahmed *et al.*, 2005; Blanch *et al.*, 2006). Each branch in **Figure A3.3.** contained isolates collected from multiple sampling dates, though sample dates do show a small degree of clustering. These results suggest functional differences in carbon-source metabolism alone are not sensitive enough to clonally-distinguish environmental *E. coli* by collection site and date.

In an attempt to further distinguish the *E. coli*, each isolate examined with PhP-RE was profiled for the presence of three commonly expressed genes conferring ESBL and KPC resistance, *blaOXA*, *blaCTX-M*, and *blaTEM* through PCR (expression profiles across isolates are shown in **Figure A3.3**). All PCR negative controls were determined to be free of contamination, and all positive controls displayed the expected band size patterns (data not shown). High abundances of *blaOXA*, *blaCTX-M*, and *blaTEM* have been reported in clinically-resistant strains of *E. coli* in Colorado (Shaikh *et al.*, 2015). Dendrogram branching patterns show *blaCTX-M* and *blaTEM* across all sample types and collection dates. Other studies in Turkey and Austria, which examined AMR in waterborne *E. coli* before and after wastewater treatment, similarly observed that *blaCTX-M* was the most abundant ESBL-associated gene

among environmental *E. coli* (Yamasaki *et al.*, 2017; Zarfel *et al.*, 2017). Presence of *blaCTX-M* was independent of water source and was not indicative of clonal-relatedness among isolates (Bréchet *et al.*, 2014; Onnberg *et al.*, 2011). The apparent prevalence of *blaCTX-M* across 3 branch points and water sources may also be explained by the different variants of this gene, including *blaCTX-M-1*, *blaCTX-M-2*, *blaCTX-M-8*, *blaCTX-M-9*, and *blaCTX-M-25* which are present in environmental, human and animal sources (Canton *et al.*, 2012) but were not distinguished during PCR analysis herein. *blaOXA* was only detected in waste water isolates collected during April 2017, and thus merits further attention as a marker that could distinguish antimicrobial *E. coli* between waste waters and ambient waters. This is supported by previous investigations, where *blaOXA* presence was found to differentiate beta-lactam resistant *E. coli* across different water sources (Amaya *et al.*, 2012; Kappell *et al.*, 2015). A greater understanding of *E. coli* ESBL resistance distinctions could be valuable in WWTP design and could help to direct waste water treatment to continue elimination of *blaOXA* resistance from bacterial populations. Furthermore, despite some separation of ambient and waste water samples, the integrated PhenePlate and PCR analysis was not sensitive enough to distinguish waste-water *E. coli* from each other, suggesting that genotypic and phenotypic variables other than carbon source metabolism and presence of common beta-lactam genes is needed to better-characterize clonal relationships.

A3.4.4. Broth microdilution expanded E. coli resistance phenotypes from environmental waters.

To cross-validate the ESBL and suspected KPC-resistant phenotypes detected during spread-plating of *E. coli*, and to understand if screening for additional classes of AMR could better distinguish isolates, a broth microdilution assay was performed on a subset of the MALDI-

TOF confirmed *E. coli* isolates. Given the higher abundance of ESBL and suspected KPC *E. coli* detected in waste water compared to ambient water, sewer water (n=17) and WWTP-influent (n=10) samples were preferentially screened in this assay. Prior to broth microdilution testing, all of the negative control samples incubated along with the inoculated *E. coli* isolates were determined to be free of bacterial growth. Results from broth microdilution assay are shown in **Table A3.2**, which displays percent drug resistance of *E. coli* by sample source. **Table A3.3** provides a breakdown of resistance profiles for each isolate examined.

Table A3.2. Percent resistance by *E. coli* to a panel of different antibiotics and across different water sources.

		***E. coli* source**					
Drug Class	**Antibiotics**	Sewer Water n=17	WWTP Influent n=10	**Waste Water (Sewer+Influent) n=27**	WWTP Effluent n=2	Surface Water n=5	**Ambient Water (Effluent+Surface) n=7**
Aminoglycoside	Amikacin	0%	0%	0%	0%	0%	0%
	Gentamicin	11.7%	0%	7.40%	50.0%	0%	14.2%
	Tobramycin	5.88%	0%	3.70%	50.0%	0%	14.2%
Beta-Lactam	Amoxicillin/ Clavulanic Acid	29.4%	40.0%	33.3%	50.0%	0%	14.2%
	Ampicillin	41.1%	50.0%	44.4%	50.0%	0%	14.2%
	Cefalexin	35.2%	40.0%	37.0%	50.0%	0%	14.2%
	Cefovecin	35.2%	40.0%	37.0%	50.0%	0%	14.2%
	Cefpodoxine	35.2%	40.0%	37.0%	50.0%	0%	14.2%
	Ceftiofur	23.5%	40.0%	29.6%	50.0%	0%	14.2%
	Imipenem	29.4%	40.0%	33.3%	50.0%	0%	14.2%
	Piperacillin	41.1%	50.0%	44.4%	50.0%	0%	14.2%
Chloramphenicol	Chloram-phenicol	5.88%	10.0%	7.40%	0%	0%	0%
Fluoroquinolone	Marbo-floxacin	11.7%	0%	7.40%	0%	0%	0%
	Enrofloxacin	11.7%	10.0%	11.1%	0%	0%	0%
Nitrofuran	Nitrofurantoin	0%	0%	0%	0%	0%	0%
Tetracycline	Tetracycline	23.5%	10.0%	18.5%	50.0%	0%	14.2%
Sulfonamide	Trimethoprim / Sulfa-methoxazole	0%	20.0%	7.40%	0%	0%	0%

Table A3.2. Percent resistance by *E. coli* to a panel of different antibiotics and across different water sources.							
		***E. coli* source**					
Drug Class	**Antibiotics**	Sewer Water	WWTP Influent	**Waste Water (Sewer+Influent)**	WWTP Effluent	Surface Water	**Ambient Water (Effluent+Surface)**
		n=17	n=10	**n=27**	n=2	n=5	**n=7**
Percentage of *E. coli* isolates resistant to 17 drugs (5 drug classes) were calculated by dividing total *E. coli* resistant for a given drug by total *E. coli* examined in a source type. WWTP: waste water treatment plant.							

Diversity of drug resistance was seen between and within water sources (**Table A3.3**) A diverse array of resistance patterns across isolates may reflect multiple, independent horizontal gene transfers along isolate lineages (Burmeister, 2015). This reasoning is supported in past studies that reported an escalation in the rate of horizontal gene transfer among *E. coli* over the last few decades, including genes responsible for ESBL and other resistance mechanisms (von Wintersdorff *et al.*, 2016; Warnes *et al.*, 2012). Broth microdilution is the CLSI approved and conventional method used to screen for AMR in medical settings (Brook *et al.*, 2013). Broth microdilution results supported that screening *E. coli* for resistance to multiple drug classes can improve the capacity to distinguish closely-related isolates from each other. The successful application of this assay to environmental samples collected herein emphasizes its utility as part of a harmonized surveillance approach for identifying shared relatedness of AMR in people, animals and the environment.

Table A3.3. Antimicrobial resistance profiles of *E. coli* examined with broth microdilution.
R = Resistant; S = Susceptible; I = Intermediate

Location	Amikacin	Gentamicin	Tobramycin	Amoxicillin/ Clavulanic	Ampicillin	Cefalexin	Cefovecin	Cefpodoxime	Ceftiofur	Imipenem	Piperacillin	Chloram-	Marbof-loxacin	Enrofloxacin	Nitrofurantoin	Tetracycline	Trimethoprim/ Sulfameth-	oxazole
Sewage	S	S	S	S	S	S	S	S	S	S	S	S	S	S	S	S		S
	S	S	S	R	R	R	R	R	I	R	R	S	R	R	S	R		S
	S	S	S	S	S	S	S	S	S	S	S	S	S	S	S	S		S
	S	R	I	S	R	S	S	S	S	S	R	R	S	I	S	R		S
	S	S	S	S	S	S	S	S	S	S	S	I	S	S	S	S		S
	S	R	R	R	R	R	R	R	R	R	R	S	S	I	S	R		S
	S	S	S	S	S	S	S	S	S	S	S	S	S	S	S	S		S
	S	S	S	S	S	S	S	S	S	S	S	S	S	S	S	S		S
	S	S	S	S	S	S	S	S	S	S	S	I	S	S	S	S		S
	S	S	S	S	S	S	S	S	S	S	S	S	S	S	S	S		S
	S	S	S	S	S	S	S	S	S	S	S	S	S	S	S	S		S
	S	S	S	R	R	R	R	R	R	R	R	S	S	S	S	S		S
	S	S	S	S	S	S	S	S	S	S	S	S	S	S	S	S		S
	S	S	S	R	R	R	R	R	R	R	R	S	S	I	S	S		S
	S	S	S	S	R	R	R	R	I	S	R	S	R	R	S	R		S
	S	S	S	R	R	R	R	R	R	R	R	S	S	S	S	S		S
	S	S	S	S	S	S	S	S	S	S	S	S	S	S	S	S		S
WWTP Influent	S	S	S	S	S	S	S	S	S	S	S	S	S	S	S	R		S
	S	S	S	R	R	R	R	R	R	R	R	S	S	I	S	S		R
	S	S	S	R	R	R	R	R	R	R	R	S	S	I	S	S		S
	S	S	S	S	S	S	S	S	S	S	S	S	S	S	S	S		S
	S	S	S	S	S	S	S	S	S	S	S	S	S	S	S	S		S
	S	S	S	S	S	S	S	S	S	S	S	S	S	S	S	S		S
	S	S	S	R	R	R	R	R	R	R	R	S	S	S	I	S		R
	S	S	S	R	R	R	R	R	R	R	R	I	S	S	S	S		S
	S	S	S	I	R	S	S	S	S	S	R	R	R	R	S	S		S
	S	S	S	S	S	S	S	S	S	S	S	S	S	S	S	S		S
WWTP-Effluent	S	S	S	S	S	S	S	S	S	S	S	S	S	S	S	S		S
	S	R	R	R	R	R	R	R	R	R	R	S	S	I	S	R		S
Surface Water	S	S	S	S	S	S	S	S	S	S	S	S	S	S	S	S		S
	S	S	S	S	S	S	S	S	S	S	S	S	S	S	S	S		S
	S	S	S	S	S	S	S	S	S	S	S	S	S	S	S	S		S
	S	S	S	S	S	S	S	S	S	S	S	S	S	S	S	S		S
	S	S	S	S	S	S	S	S	S	S	S	S	S	S	S	S		S

A3.4.5. Whole genome sequencing for isolate resistance profiles and the spatial and temporal relationship of resistance genes:

While the integrated PhenePlate and PCR analysis supported differences in gene presence between waste water and ambient samples, it was not sensitive to distinguish many waste water

isolates from each other. Given the large variability in the antibiotic resistance profiles of waste water *E. coli* observed during broth microdilution, whole genome sequencing was performed on a subset (n=21) of waste water isolates, to evaluate if deeper sequencing could reveal spatial and temporal differences in resistance patterns among these closely-related *E. coli*. All blank media and DNA extraction reagents were confirmed to be free of contamination (data not shown), supporting that the downstream analysis was sensitive to differences across *E. coli* isolates. The results depicted in **Figure A3.4.** categorizes *E. coli* by sample type, date, and gene classes.

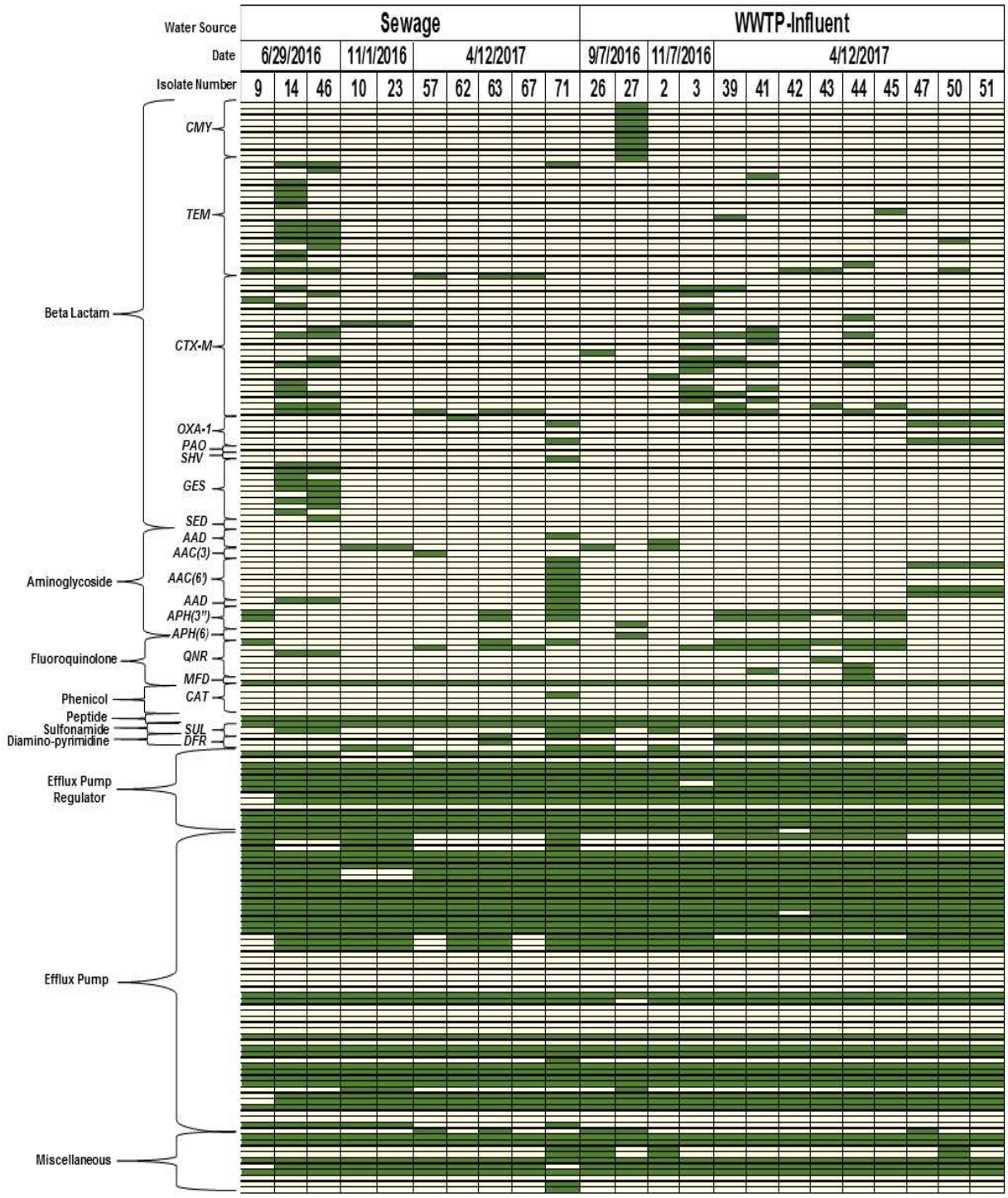

Figure A3.4. Whole genome sequencing distinguished sewer water and WWTP influent *E. coli* across sample type and collection date.

AMR profiles of (n=21) waste water *E. coli*. Isolates are organized by sample type (sewer water versus waste water treatment plant-influent) and are further categorized by sample collection date. Antimicrobial function and sub-class of gene family names were used to group resistance genes. For each isolate, green boxes indicate gene presence and beige boxes indicate

gene absence. **Isolate #:** the unique identifier assigned to each *E. coli* isolate with MALDI-TOF confirmation.

Of the 185 genes screened, 154 were identified across all isolates and included 66 that conferred resistance to beta-lactams, 18 to aminoglycosides, 7 to fluoroquinolones, 1 to chloramphenicol, 7 to peptides, 2 to sulfonamides, 2 to diaminopyrimidines, 12 to efflux pump regulators, 36 to efflux pumps, and 9 miscellaneous resistance genes involved in the inactivation and alternation of bacterial enzymes. This genetic profiling cross-validated and expanded the information available for *E. coli* isolates with AMR profiles established through ESBL/KPC spread plating and PCR.

Whole genome sequencing revealed differences across waste-water *E. coli* isolates, most notably in beta-lactam genes that were dependent on water sample source and collection date. Across water samples, 51 beta-lactam resistance genes (broken down as 29 sewer water and 22 WWTP-influent) distinguished sewer water and WWTP-influent isolates. These included multiple variants of *tem* and *ges* genes unique to sewer water isolates and *cmy* and *ctx-m* genes unique to WWTP-influent isolates. When examining sewer water *E. coli* across sampling dates, 43 beta-lactam genes were unique to one sampling date, including 37 among 6/29/16 isolates, 1 among isolates dated (11/7/16), and 5 among isolates dated (4/12/17), and included multiple *tem*, *ges* and *ctx-m* gene variants. For WWTP-influent *E. coli*, 25 beta-lactam resistance genes were specific to sample collection dates. There were 10 *cmy* variants in samples dated (9/7/16), 6 *ctx-m* variants in samples dated (11/7/16), and 9 genes, primarily *tem* variants, that were unique to *E. coli* dated (4/12/17). All of these gene variants have been associated with drug-resistant *E. coli* infections in people (Fernando *et al.*, 2016; Laffite *et al.*, 2016; Runcharoen, 2017), emphasizing that they should be closely-monitored. These results suggest the potential connection between

AMR gene presence and time of year and support that temporal screening of AMR genes should be considered in future surveillance programs.

Furthermore, whole genome sequencing provided additional insight into whether *E. coli* that grow on KPC plates were KPC-producing isolates. Although no carbapenemase-encoding genes, including *ndm-1*, *oxa-48*, and *vim* family genes (Lamba and Ahammad, 2017; Pfaller *et al.*, 2018; Saleh *et al.*, 2018), were detected in isolates, *E. coli* harbored multiple efflux pump genes. Efflux pump genes (35 sewer water, 31 WWTP-influent) and 12 efflux pump regulator genes (12 sewer water, 12 WWTP-influent) were detected across *E. coli*. Efflux pumps represent one mechanism of resistance to carbapenem drugs (van Duin and Doi, 2017), and provide supporting rational for why isolates may have tested positive for KPC despite the lack of carbapenemase-encoding genes. It is possible that these *E. coli* contained KPC gene variants that were not currently recognized by standard AMR gene databases, and therefore highlights the need for expanded KPC resistance gene indexing. This study provides a framework for analysis by which new investigations can enhance the statistical power of studies to characterize AMR in other geographic locations, and with potential utility across other matrices for testing, such as human and animal gastrointestinal tracts, agricultural systems, and food production systems. Screening samples for AMR via standardized detection and monitoring will improve needed comparisons between surveillance programs (O'Brien and Stelling, 2011).

A3.5. Conclusions:

This study illustrates the landscape of *E. coli* AMR across various water sources in Northern Colorado and utilizes an array of methodologies for AMR validation. Total detected bacteria and *E. coli* abundance was shown to decrease through the water reclamation process,

validating the effective clearance of microbes from human water sources by the WWTP. The decreased *E. coli* abundance in ambient water was coupled with an increased relative percentage of ESBL and suspected KPC-resistance in total detected bacteria and ESBL *E. coli* in surface water. The prevalence of ESBL/KPC resistant *E. coli* in surface water warrants deeper evaluation of potential antimicrobial inputs to rivers.

Broth microdilution further characterized drug resistance in isolates across water sources and validated *E. coli* ESBL/KPC phenotypes. Identification of beta-lactam resistance in *E. coli* that initially tested negative for ESBL/suspected KPC resistance supports that a multi-platform screening approach may be necessary for accurate characterization of AMR landscapes in environmental water sources. The increased prevalence of multi-drug resistant isolates in WWTP-influent as compared to sewer water illustrates how converging water sources can increase the level of drug-resistance in organisms entering waste-water treatment plants.

An integrated PhenePlate/PCR analysis was applied to understand the relationships between water types and diverse *E. coli* AMR profiles with respect to sampling location and date. PhenePlate analysis alone could not distinguish waste water and ambient water *E. coli* and suggests that this single measurement of carbon source metabolism is not sensitive to distinguish some environmental water *E. coli* from each other. However, the coupling of PCR for common beta-lactam resistance genes, such as *blaOXA, does support* the use as a potential marker to distinguish waste and ambient water *E. coli.*

Whole genome sequencing applied to waste water *E. coli* validated the resistance phenotypes and genotypes observed in the ESBL/ suspected KPC screening, broth microdilution, and PCR analyses and was effective at separating isolates both by sample type (sewage versus WWTP-influent) and by collection date. Sequencing results supported that resistance to beta-

lactam and aminoglycoside antimicrobials are major contributors to these geographic and temporal differences. Additionally, the clustering of isolates by source and collection date supports the integrity of bacterial samples, and the unlikelihood of sample contamination. These results warrant investigation into the development of applications and more sensitive screenings of beta-lactams and aminoglycosides that can both predict and understand how antimicrobial resistance landscapes can change within and across environments over time, as well as from waste and ambient water sources.

The sample sizes used to conduct research on these field isolates were small with respect to seasonality, yet the cross-validation of the methodologies reported herein illustrate the depth by which multiple analysis platforms could be integrated to establish AMR profiles of *E. coli* across environmental water types. This study provides a framework by which investigators can standardize analyses, in larger, statistically-powered studies, and specifically to characterize AMR landscapes across geographically diverse locations. The integrated use of these assays also has relevance to other matrices including human and animal gastrointestinal tracts, agriculture, and food production systems.

A3.6. Data Availability:

The whole-genome sequences of all 23 *E. coli* isolates were submitted to the NCBI Sequence Read Archive (NCBI SRA). However, only 22 of them have been assigned with SRA numbers. Isolate NCBI SRA identification numbers are presented in Supplementary Dataset 1 (not provided). Accession: PRJNA280335

A3.7. Disclosure:

Hannah B. Haberecht and Nora Jean Nealon are co-first authors.

A3.8. Conflicts of Interest:

The authors declare that they have no conflicts of interest.

A3.9. Author Contributions:

EPR, SV, and JS conceived the overall study design and secured funding support. LM and FS organized and coordinated water collection schemes and assisted in sample collection from the Drake Water Reclamation Facility and Poudre River. HBH, CR, JRG, AVH, and RCO performed field sampling in Northern Colorado waters and bacteria isolations. SV, HBH, JRG, AVH, HMI, and RCO performed data analysis and results interpretations for data in Tables 1 and 2 and Figures 1 and 2. Whole-genome sequencing and data analysis of isolates in Figure 3 were completed by HBH, NJN, LA, and JS. HBH, NJN, JRG, AVH, RCO, SV, and EPR wrote the manuscript. HBH and NJN contributed equally to the preparation of this manuscript.

A3.10. Acknowledgements:

The authors thank Megan Dietz and Adriana Romero for their contributions in project and protocol coordination for field sampling and Colette Worcester for technical laboratory support. This research was supported by awards and funding from the Colorado State University One Health Institute and the CSU Water Center and the National Institutes of Health (T32) Predoctoral Training Fellowship .

A3.11. Supplementary Materials:

Figure S1: a map of Fort Collins, Colorado, and the surrounding area with sampling locations of environmental waters. Table S1: AMR profiles of the individual *E. coli* isolates examined with broth microdilution. Table S2: an expanded whole-genome sequence table that details all genes detected across wastewater *E. coli* isolates.

REFERENCES

Ahmed, W., R. Neller, and M. Katouli, Host species-specific metabolic fingerprint database for enterococci and Escherichia coli and its application to identify sources of fecal contamination in surface waters. Appl Environ Microbiol, 2005. 71(8): p. 4461-8.

Al Anbgi, N., 360 Isolation and Identification Some Bacterial Causes of Lung Abscessesheep by Chromogenic Media. Basrah journal of veterinary research, 2016. 15(2).

Amaya, E., et al., Antibiotic resistance patterns of Escherichia coli isolates from different aquatic environmental sources in Leon, Nicaragua. Clin Microbiol Infect, 2012. 18(9): p. E347-54.

Arnold, R.S., et al., Emergence of Klebsiella pneumoniae Carbapenemase (KPC)-Producing Bacteria. Southern medical journal, 2011. 104(1): p. 40-45.

Atashgahi, S., et al., Impact of a wastewater treatment plant on microbial community composition and function in a hyporheic zone of a eutrophic river. Sci Rep, 2015. 5: p. 17284.

Atterby, C., et al., ESBL-producing Escherichia coli in Swedish gulls-A case of environmental pollution from humans? PLoS One, 2017. 12(12): p. e0190380.

Baquero, F., J.L. Martinez, and R. Canton, Antibiotics and antibiotic resistance in water environments. Curr Opin Biotechnol, 2008. 19(3): p. 260-5.

Baudry, P.J., et al., Comparison of antimicrobial resistance profiles among extended-spectrum-beta-lactamase-producing and acquired AmpC beta-lactamase-producing Escherichia coli isolates from Canadian intensive care units. Antimicrob Agents Chemother, 2008. 52(5): p. 1846-9.

Berendonk, T.U., et al., Tackling antibiotic resistance: the environmental framework. Nat Rev Micro, 2015. 13(5): p. 310-317.

Bialvaei, A.Z., et al., Current methods for the identification of carbapenemases. J Chemother, 2016. 28(1): p. 1-19.

Blaak, H., et al., Extended spectrum ß-lactamase- and constitutively AmpC-producing Enterobacteriaceae on fresh produce and in the agricultural environment. International Journal of Food Microbiology, 2014. 168–169: p. 8-16.

Blanch, A.R., et al., Integrated Analysis of Established and Novel Microbial and Chemical Methods for Microbial Source Tracking. Applied and Environmental Microbiology, 2006. 72(9): p. 5915-5926.

Bréchet, C., et al., Wastewater Treatment Plants Release Large Amounts of Extended-Spectrum β-Lactamase–Producing Escherichia coli Into the Environment. Clinical Infectious Diseases, 2014. 58(12): p. 1658-1665.

Brook, I., H.M. Wexler, and E.J.C. Goldstein, Antianaerobic Antimicrobials: Spectrum and Susceptibility Testing. Clinical Microbiology Reviews, 2013. 26(3): p. 526-546.

Burmeister, A.R., Horizontal Gene Transfer. Evolution, Medicine, and Public Health, 2015. 2015(1): p. 193-194.

Bush, K., Alarming β-lactamase-mediated resistance in multidrug-resistant Enterobacteriaceae. Current Opinion in Microbiology, 2010. 13(5): p. 558-564.

Canton, R., J.M. Gonzalez-Alba, and J.C. Galan, CTX-M Enzymes: Origin and Diffusion. Front Microbiol, 2012. 3: p. 110.

CDC, Antibiotic resistance threats in the United States, 2013. 2013: Atlanta.

CLSI, Performance Standards for Antimicrobial Susceptibility Testing: Nineteenth Informational Supplement, in M100-S1. 2010, Clinical and Laboratory Standards Institute: Wayne, PA.

Da Costa, P.M., P. Vaz-Pires, and F. Bernardo, Antimicrobial resistance in Enterococcus spp. isolated in inflow, effluent and sludge from municipal sewage water treatment plants. Water Research, 2006. 40(8): p. 1735-1740.

Diab, M., et al., Extended-spectrum beta-lactamase (ESBL)- and carbapenemase-producing Enterobacteriaceae in water sources in Lebanon. Vet Microbiol, 2018. 217: p. 97-103.

Egervarn, M., et al., Unexpected common occurrence of transferable extended spectrum cephalosporinase-producing Escherichia coli in Swedish surface waters used for drinking water supply. Sci Total Environ, 2017. 587-588: p. 466-472.

EPA, Recreational Water Quality Criteria O.o. Water, Editor. 2012.

Esther, J., D. Edwin, and Uma, Prevalence of Carbapenem Resistant Non-Fermenting Gram Negative Bacterial Infection and Identification of Carbapenemase Producing NFGNB Isolates by Simple Phenotypic Tests. J Clin Diagn Res, 2017. 11(3): p. DC10-DC13.

Ferguson, A.S., et al., Comparison of fecal indicators with pathogenic bacteria and rotavirus in groundwater. Science of The Total Environment, 2012. 431: p. 314-322.

Fernando, D.M., et al., Detection of Antibiotic Resistance Genes in Source and Drinking Water Samples from a First Nations Community in Canada. Appl Environ Microbiol, 2016. 82(15): p. 4767-75.

Franz, E., et al., Pathogenic Escherichia coli producing Extended-Spectrum beta-Lactamases isolated from surface water and wastewater. Sci Rep, 2015. 5: p. 14372.

Garcia-Quintanilla, M., L. Poirel, and P. Nordmann, CHROMagar mSuperCARBA and RAPIDEC(R) Carba NP test for detection of carbapenemase-producing Enterobacteriaceae. Diagn Microbiol Infect Dis, 2018. 90(2): p. 77-80.

Gilbert, R., et al., Guidelines for the microbiological quality of some ready-to-eat foods sampled at the point of sale. PHLS Advisory Committee for Food and Dairy Products. Communicable Disease and Public Health, 2000. 3(3): p. 163-167.

Gómez López, M.J., et al., Waste water treatment plants as redistributors of resistance genes in bacteria. Vol. 135. 2010. 83-94.

Gruber, J.S., A. Ercumen, and J.M. Colford, Jr, Coliform Bacteria as Indicators of Diarrheal Risk in Household Drinking Water: Systematic Review and Meta-Analysis. PLoS One 2014. 9(9): p. e107429.

Hatosy, S.M. and A.C. Martiny, The ocean as a global reservoir of antibiotic resistance genes. Appl Environ Microbiol, 2015. 81(21): p. 7593-9.

Hawkey, P.M. and D.M. Livermore, Carbapenem antibiotics for serious infections. BMJ, 2012. 344(7863): p. 43-47.

Hendricks, R. and E.J. Pool, The effectiveness of sewage treatment processes to remove faecal pathogens and antibiotic residues. Journal of Environmental Science and Health. Part A, Toxic/hazardous Substances & Environmental Engineering, 2012. 47(2): p. 289-297.

Hinić, V., et al., Comparison of two rapid biochemical tests and four chromogenic selective media for detection of carbapenemase-producing Gram-negative bacteria. Journal of Microbiological Methods, 2017. 135: p. 66-68.

Hrenovic, J., et al., The fate of carbapenem-resistant bacteria in a wastewater treatment plant. Water Research, 2017. 126: p. 232-239.

Institute, K., Manual for the Phene-Plate System 2012: Stockholm, Sweden p. 14.

Jang, J., et al., Environmental Escherichia coli: ecology and public health implications-a review. Journal of Applied Microbiology 2017. 123(3): p. 570-581.

Jia, B., et al., CARD 2017: expansion and model-centric curation of the comprehensive antibiotic resistance database. Nucleic Acids Res, 2017. 45(D1): p. D566-D573.

Kappell, A.D., et al., Detection of multi-drug resistant Escherichia coli in the urban waterways of Milwaukee, WI. Frontiers in Microbiology, 2015. 6(336).

Korzeniewska, E. and M. Harnisz, Extended-spectrum beta-lactamase (ESBL)-positive Enterobacteriaceae in municipal sewage and their emission to the environment. J Environ Manage, 2013. 128: p. 904-11.

Laffite, A., et al., Hospital Effluents Are One of Several Sources of Metal, Antibiotic Resistance Genes, and Bacterial Markers Disseminated in Sub-Saharan Urban Rivers. Front Microbiol, 2016. 7: p. 1128.

Lamba, M. and S.Z. Ahammad, Sewage treatment effluents in Delhi: A key contributor of β-lactam resistant bacteria and genes to the environment. Chemosphere, 2017. 188: p. 249-256.

Levy, K., et al., Drivers of water quality variability in northern coastal Ecuador. Environmental Science & Technology, 2009. 43: p. 1788-1797.

Li, S., et al., Prevalence and characterization of extended-spectrum beta-lactamase-producing Enterobacteriaceae in spring waters. Lett Appl Microbiol, 2015. 61: p. 544-8.

Li, W., et al., Occurrence, distribution and potential affecting factors of antibiotics in sewage sludge of wastewater treatment plants in China. Science of The Total Environment 2013. 445: p. 306-313.

Łuczkiewicz, A., et al., Antimicrobial resistance of fecal indicators in municipal wastewater treatment plant. Water Research, 2010. 44(17): p. 5089-5097.

Ma, L., et al., Rapid quantification of bacteria and viruses in influent, settled water, activated sludge and effluent from a wastewater treatment plant using flow cytometry. Water Sci Technol, 2013. 68(8): p. 1763-9.

Marti, E., J. Jofre, and J.L. Balcazar, Prevalence of Antibiotic Resistance Genes and Bacterial Community Composition in a River Influenced by a Wastewater Treatment Plant. PLOS ONE, 2013. 8(10): p. e78906.

Martin, M.S., et al., Characterization of bacterial diversity in contaminated groundwater using matrix-assisted laser desorption/ionization time-of-flight mass spectrometry. Sci Total Environ, 2018. 622-623: p. 1562-1571.

Merlino, J., et al., Evaluation of CHROMagar Orientation for Differentiation and Presumptive Identification of Gram-NegativeBacilli and Enterococcus Species. Journal of Clinical Microbiology, 1996. 34(7): p. 1788-1793.

Merlino, J., et al., Evaluation of CHROMagar Orientation for differentiation and presumptive identification of gram-negative bacilli and Enterococcus species. Journal of clinical microbiology, 1996. 34(7): p. 1788-1793.

Moore, D.F., J.A. Guzman, and C. McGee, Species distribution and antimicrobial resistance of enterococci isolated from surface and ocean water. Journal of Applied Microbiology, 2008. 105(4): p. 1017-1025.

Morozzi, G., et al., The effect of anaerobic and aerobic wastewater treatment on faecal coliforms and antibiotic-resistant faecal coliforms. Zentralbl Bakteriol Mikrobiol Hyg B, 1988. 185(4-5): p. 340-9.

Novo, A., et al., Antibiotic resistance, antimicrobial residues and bacterial community composition in urban wastewater. Water Research, 2013. 47(5): p. 1875-1887.

Nuangmek, A., et al., Antimicrobial Resistance in ESBL-Producing Escherichia coli Isolated from Layer and Pig Farms in Thailand. Acta Scientiae Veterinariae, 2018. 46(1).

O'Brien, T.F. and J. Stelling, Integrated Multilevel Surveillance of the World's Infecting Microbes and Their Resistance to Antimicrobial Agents. Clin Microbiol Rev, 2011. 24(2): p. 281-95.

Onnberg, A., et al., Molecular and phenotypic characterization of Escherichia coli and Klebsiella pneumoniae producing extended-spectrum beta-lactamases with focus on CTX-M in a low-endemic area in Sweden. APMIS, 2011. 119(4-5): p. 287-95.

Osinska, A., et al., The prevalence and characterization of antibiotic-resistant and virulent Escherichia coli strains in the municipal wastewater system and their environmental fate. Sci Total Environ, 2017. 577: p. 367-375.

Page, M.G., Beta-lactam antibiotics, in Antibiotic Discovery and Development. 2012, Springer. p. 79-117.

Pang, Y.-C., et al., Prevalence of antibiotic-resistant bacteria in a lake for the storage of reclaimed water before and after usage as cooling water. Environmental Science: Processes & Impacts, 2015. 17: p. 1182-1189.

Paterson, D.L. and R.A. Bonomo, Extended-spectrum β-lactamases: a clinical update. Clinical microbiology reviews, 2005. 18(4): p. 657-686.

Pereira, A., et al., Genetic diversity and antimicrobial resistance of Escherichia coli from Tagus estuary . Science of The Total Environment, 2013. 461–462: p. 65-71.

Pfaller, M.A., et al., In vitro activity of meropenem-vaborbactam and characterization of carbapenem resistance mechanisms among carbapenem-resistant Enterobacteriaceae from the 2015 meropenem-vaborbactam surveillance program. Int J Antimicrob Agents, 2018.

Rodriguez-Mozaz, S., et al., Occurrence of antibiotics and antibiotic resistance genes in hospital and urban wastewaters and their impact on the receiving river. Water research, 2015. 69: p. 234-242.

Ronald, J.A., M. Brena, and M. Melissa, Antibiotic Resistance of Gram-Negative Bacteria in Rivers, United States. Emerging Infectious Disease journal, 2002. 8(7): p. 713.

Rosas, I., et al., Characterization of Escherichia coli Isolates from an Urban Lake Receiving Water from a Wastewater Treatment Plant in Mexico City: Fecal Pollution and Antibiotic Resistance. Current Microbiology, 2015. 71(4): p. 490-495.

Runcharoen, C., et al., Whole genome sequencing of ESBL-producing Escherichia coli isolated from patients, farm waste and canals in Thailand. Genome Med, 2017. 9(1): p. 81.

Saleh, A., S. Gottig, and A. Hamprecht, Multiplex immunochromatographic detection of OXA-48, KPC and NDM carbapenemases: impact of the inoculum, antibiotics and agar. J Clin Microbiol, 2018.

Shaikh, S., et al., Antibiotic resistance and extended spectrum beta-lactamases: Types, epidemiology and treatment. Saudi Journal of Biological Sciences, 2015. 22(190-101).

Sharma, B., et al., Occurrence of multidrug resistant Escherichia coli in groundwater of Brij region (Uttar Pradesh) and its public health implications. Vet World, 2017. 10(3): p. 293-301.

Thomas, M., et al., Whole genome sequencing-based detection of antimicrobial resistance and virulence in non-typhoidal Salmonella enterica isolated from wildlife. Gut Pathog, 2017. 9: p. 66.

van Duin, D. and Y. Doi, The global epidemiology of carbapenemase-producing Enterobacteriaceae. Virulence, 2017. 8(4): p. 460-469.

von Wintersdorff, C.J.H., et al., Dissemination of Antimicrobial Resistance in Microbial Ecosystems through Horizontal Gene Transfer. Frontiers in Microbiology, 2016. 7: p. 173.

Warnes, S.L., C.J. Highmore, and C.W. Keevil, Horizontal Transfer of Antibiotic Resistance Genes on Abiotic Touch Surfaces: Implications for Public Health. mBio, 2012. 3: p. e00489-12.

WHO, Guidelines for Drinking-water Quality 2011: Geneva.

Yamasaki, S., et al., Prevalence of extended-spectrum beta-lactamase-producing Escherichia coli and residual antimicrobials in the environment in Vietnam. Anim Health Res Rev, 2017. 18(2): p. 128-135.

Yao, Y., et al., Insights into a Novel blaKPC-2-Encoding IncP-6 Plasmid Reveal Carbapenem-Resistance Circulation in Several Enterobacteriaceae Species from Wastewater and a Hospital Source in Spain. Front Microbiol, 2017. 8: p. 1143.

Zankari, E., et al., Identification of acquired antimicrobial resistance genes. J Antimicrob Chemother, 2012. 67(11): p. 2640-4.

Zarfel, G., et al., Troubled water under the bridge: Screening of River Mur water reveals dominance of CTX-M harboring Escherichia coli and for the first time an environmental VIM-1 producer in Austria. Sci Total Environ, 2017. 593-594: p. 399-405.